



UNIVERSIDADE ESTADUAL DE CAMPINAS
FACULDADE DE ENGENHARIA MECÂNICA
E INSTITUTO DE GEOCIÊNCIAS

ASHISH KUMAR LOOMBA

**RISK-INFORMED CLOSED-LOOP FIELD
DEVELOPMENT WORKFLOW FOR PRACTICAL
APPLICATIONS**

**FLUXO DE TRABALHO DE DESENVOLVIMENTO DE
CAMPO EM MALHA FECHADA INFORMADO DE
RISCO PARA APLICAÇÕES PRÁTICAS**

CAMPINAS

2022

ASHISH KUMAR LOOMBA

**RISK-INFORMED CLOSED-LOOP FIELD DEVELOPMENT
WORKFLOW FOR PRACTICAL APPLICATIONS**

**FLUXO DE TRABALHO DE DESENVOLVIMENTO DE CAMPO EM
MALHA FECHADA INFORMADO DE RISCO PARA APLICAÇÕES
PRÁTICAS**

A thesis presented to the Mechanical Engineering Faculty and Geosciences Institute of the University of Campinas in partial fulfillment of the requirements for the degree of Doctor of Philosophy in Petroleum Sciences and Engineering in the area of Reservoirs and Management.

Tese de doutorado apresentada à Faculdade de Engenharia Mecânica e Instituto de Geociências da Universidade Estadual de Campinas como parte dos requisitos exigidos para a obtenção do título de Doutor em Ciências e Engenharia de Petróleo na área de Reservatórios e Gestão.

Orientador: Prof. Dr. Denis José Schiozer

Este exemplar corresponde à versão final da Tese defendida pelo aluno Ashish Kumar Loomba e orientada pelo Prof. Dr. Denis José Schiozer.

Prof. Dr. Denis José Schiozer

CAMPINAS

2022

Ficha catalográfica
Universidade Estadual de Campinas
Biblioteca da Área de Engenharia e Arquitetura
Rose Meire da Silva - CRB 8/5974

L873r Loomba, Ashish Kumar, 1989-
Risk-informed closed-loop field development workflow for practical applications / Ashish Kumar Loomba. – Campinas, SP : [s.n.], 2022.

Orientador: Denis José Schiozer.
Tese (doutorado) – Universidade Estadual de Campinas, Faculdade de Engenharia Mecânica.
Em regime multiunidades com: Instituto de Geociências.

1. Reservatórios (Simulação). 2. Otimização. 3. Incerteza. 4. Avaliação de riscos. 5. Engenharia do petróleo. I. Schiozer, Denis José, 1963-. II. Universidade Estadual de Campinas. Faculdade de Engenharia Mecânica. III. Título.

Informações Complementares

Título em outro idioma: Fluxo de trabalho de desenvolvimento de campo em malha fechada informado de risco para aplicações práticas

Palavras-chave em inglês:

Reservoir simulation

Optimization

Uncertainty

Risk-assessment

Petroleum engineering

Área de concentração: Reservatórios e Gestão

Titulação: Doutor em Ciências e Engenharia de Petróleo

Banca examinadora:

Denis José Schiozer [Orientador]

Régis Kruel Romeu

José Sérgio de Araújo Cavalcante Filho

Ana Teresa Ferreira da Silva Gaspar

Susana Margarida da Graça Santos

Data de defesa: 21-12-2022

Programa de Pós-Graduação: Ciências e Engenharia de Petróleo

Identificação e informações acadêmicas do(a) aluno(a)

- ORCID do autor: <https://orcid.org/0000-0003-3951-1556>

- Currículo Lattes do autor: <http://lattes.cnpq.br/2685832574781110>

UNIVERSIDADE ESTADUAL DE CAMPINAS
FACULDADE DE ENGENHARIA MECÂNICA
E INSTITUTO DE GEOCIÊNCIAS

Ph.D. THESIS

**RISK-INFORMED CLOSED-LOOP FIELD DEVELOPMENT
WORKFLOW FOR PRACTICAL APPLICATIONS**

Author/Autor: Ashish Kumar Loomba

Advisor/Orientador: Prof. Dr. Denis José Schiozer

The Examining Committee composed of the members below approved this thesis:

A Banca Examinadora composta pelos membros abaixo aprovou esta tese:

Prof. Dr. Denis José Schiozer, President/Presidente
DE/FEM/UNICAMP

Prof. Dr. Régis Krueel Romeu
CONSULTOR

Prof. Dr. José Sérgio de Araújo Cavalcante Filho
PETROBRAS

Profª. Dra. Ana Teresa Ferreira da Silva Gaspar
UNISIM/CEPETRO/UNICAMP

Profª. Dra. Susana Margarida da Graça Santos
UNISIM/CEPETRO/UNICAMP

A Ata da Defesa com as respectivas assinaturas dos membros encontra-se no processo de vida acadêmica do aluno.

December 21, 2022
Campinas

DEDICATION

In fond and loving memories of my beloved father, grandfather and grandmother.

ACKNOWLEDGEMENTS

This thesis is an outcome of constructive criticism, encouragement, and contributions of countless people. I could not have undertaken this journey without Professor Dr. Denis José Schiozer, who provided this unique opportunity to work on an industry-relevant topic. Words cannot express my gratitude to Dr. Vinicius Eduardo Botechia for his constant support during all the work. Additionally, this endeavor would not have been possible without the generous support from the Libra consortium and Energi Simulation, who financed my research. I would also thank UNICAMP, CEPETRO, and UNISIM for providing a great platform to improve my skills during this research journey. Lastly, I would be remiss in not mentioning my family and friends. Their belief in me has kept my spirits and motivation high during this journey.

RESUMO

O desenvolvimento de um campo de petróleo e gás depende das informações descritas no plano de desenvolvimento do campo (FDP, *field development plan*) que rege a implementação de uma estratégia de produção ao longo do ciclo de vida do projeto. Entretanto, a escassez de informações e muitas incertezas técnicas e geológicas tornam o processo de tomada de decisão para seleção de FDP uma tarefa desafiadora. Dessa forma, uma equipe multidisciplinar é mandatória para tomar várias decisões de investimento para maximizar a função objetivo do projeto. Assim, um processo de desenvolvimento convencional de campos de petróleo pode oferecer um FDP abaixo do ideal devido a uma enorme lacuna de informações.

Tal configuração requer um processo de desenvolvimento de campo baseado em retroalimentação de informações para otimizar recorrentemente o FDP usando informações acumuladas ao longo do tempo para maximizar a função objetivo do projeto. O desenvolvimento de campo em malha fechada (CLFD, *Closed Loop Field Development*) é um fluxo de trabalho de desenvolvimento de campo baseado em retroalimentação com uma combinação exaustiva de tarefas multidisciplinares para usar dados adquiridos com frequência para otimizar a função objetivo do projeto. No entanto, estudos anteriores mostraram que o CLFD pode falhar por várias razões teóricas. Além disso, os fluxos de trabalho existentes dificilmente são adequados para revisar os FDPs para campos gigantes ou complexos que exigem modelos de simulação muito demorados.

Com base nesses fatos, este trabalho propõe um fluxo de trabalho CLFD eficiente e informado sobre o risco, utilizando quatro estudos científicos. No primeiro estudo, para entender melhor o CLFD, identificamos e enfatizamos o impacto de etapas individuais no CLFD para entender e mitigar possíveis problemas. Introduzimos um fluxo de trabalho CLFD informado sobre riscos no segundo trabalho e o testamos em dois estudos de caso com esse entendimento aprimorado. Um CLFD informado sobre riscos utiliza percepções de uma abordagem sistemática para avaliar os riscos associados ao desenvolvimento de campo para tomar decisões robustas para o campo real. No estudo subsequente, propomos e comparamos quatro métodos de otimização de FDP e suas vantagens e desvantagens do ponto de vista do fluxo de trabalho CLFD. No quarto trabalho, aplicamos um fluxo de trabalho CLFD eficiente e informado sobre riscos em um estudo de caso representando um campo gigante para destacar algumas preocupações práticas ao usar esses fluxos de trabalho.

Para resumir, a principal contribuição deste trabalho é apresentar dois fluxos de trabalho CLFD validados para promover um processo de tomada de decisão sólido, eficiente e informado sobre riscos sob incertezas geológicas para um campo de tamanho típico e gigante. Enquanto o primeiro fluxo de trabalho é abrangente e preparado para modelos mais rápidos, o último é mais eficiente e aplicável para aplicações práticas e demoradas. Sem um fluxo de trabalho eficiente, um ciclo do fluxo de trabalho CLFD pode consumir muito tempo e, portanto, pode ser impraticável desenvolver um campo com modelos de simulação baseados em física que demandam muito esforço computacional. Além disso, a aplicação dos fluxos de trabalho CLFD em todos os estudos de caso forneceu vários entendimentos interessantes sobre o tema. A tese também estabelece novas técnicas de otimização para uma otimização FDP mais rápida, ao mesmo tempo em que promove a probabilidade de sucesso da solução otimizada sobre o conjunto de cenários geológicos viáveis.

Para concluir, os estudos de reservatórios lutam para prever adequadamente o desempenho do reservatório devido às suas características inerentes de precisão, viés e erro. Apesar dessas características, um CLFD eficiente e informado sobre o risco oferece uma oportunidade ideal para assimilar novas informações em fases específicas e melhorar a compreensão do campo, que é visível na forma de decisões aprimoradas.

ABSTRACT

The development of an oil and gas field follows a field development plan (FDP) which governs the implementation of a production strategy throughout the project's lifespan. But, a dearth of information and copious technical and geological uncertainties makes the decision-making process very challenging. Thus, a multidisciplinary team is mandated to make several front-end investment decisions regarding infrastructure and wells to maximize the project's objective function. Consequently, such a conventional field development process may offer a suboptimal FDP due to a massive information gap.

Such a setup necessitates a feedback-based field development process to recurrently optimize FDP using accrued information over time for maximizing the project's objective function. Closed-loop field development (CLFD) is a feedback-based field development workflow with an exhaustive combination of multidisciplinary tasks to use frequently acquired data for optimizing the project's objective function. Nevertheless, previous studies have shown that CLFD could fail for several theoretical reasons. Furthermore, the existing workflows are hardly suitable for revising the FDPs for giant or complex fields that require extensively time-consuming simulation models.

Reasoning from these facts, this work proposes an efficient and risk-informed CLFD workflow utilizing four scientific studies. In the first study, we identify and emphasize the impact of individual steps in CLFD to recognize and mitigate potential problems. We introduce a risk-informed CLFD workflow in the second work and test it on two case studies with an improved understanding of CLFD. A risk-informed CLFD utilizes insights from a systematic approach for evaluating risks associated with field development to make well-informed decisions for the field. In the subsequent study, we propose and compare four FDP optimization methods and their advantages and disadvantages from the perspective of the CLFD workflow. In the fourth work, we apply an efficient and risk-informed CLFD workflow on a giant benchmark case study to highlight some practical concerns while using such workflows.

To summarize, the main contribution of this work is to introduce two validated CLFD workflows for promoting a deliberate, accelerated, and risk-informed decision-making process under geological uncertainties for typical-sized as well as giant fields. While the first workflow is comprehensive and equipped for faster models, the latter is more efficient and applicable for time-consuming and practical applications. Without an efficient workflow, a cycle of the CLFD workflow can be extensively time-intensive, and thus, it can be impractical to develop a field

with expensive physics-based simulation models. Furthermore, the application of the CLFD workflows on all the case studies provided several interesting insights on the topic. The thesis also establishes new optimization techniques for faster FDP optimization while promoting the likelihood of success of the optimized solution over the ensemble of geologically feasible scenarios.

To conclude, reservoir studies struggle to predict reservoir performance adequately due to their inherent characteristic of accuracy, bias, and error. Despite these characteristics, a risk-informed and efficient CLFD provides an ideal opportunity to assimilate new information over stipulated phases and improve the understanding of the field, which is visible in the form of improved decisions.

List of Figures

Figure 2-1: Generalized CLFD workflow.....	32
Figure 2-2: (a) Example of NQDS visualization for different objective functions (oil rate and BHP) for well W1 and W2 (adapted from Avansi et al., 2016) and (b) the corresponding NQDS values.	35
Figure 2-3: Initial PS (PS_1) based on the optimal strategy proposed by Schiozer et al. (2019).	37
Figure 2-4: Prior and posterior result of history matching is shown by graphs (a) to (f). The prior results are shown on the left while the posterior results are presented by the graphs on the right. The measured data from the reference case, P50 of the ensemble and the ensemble are represented by red dots, green line and blue lines, respectively.....	40
Figure 2-5: Prior and posterior histograms of uncertainty attribute (a) rock compressibility, (b) k_z -multiplier, (c) oil-water contact and (d) relative permeability curves.	41
Figure 2-6: Risk Curves prior and posterior to application of ICM.	42
Figure 2-7: Comparing the initial RMs selected using the lenient tolerance conditions of the ICM against the new RMs selected using the stricter tolerance conditions of the IAM.....	43
Figure 2-8: Comparing average reservoir pressure and cumulative water injection after implementing PS_1 and PS_{ICM} in the reference case.	44
Figure 2-9: Comparing cumulative oil and water production obtained after implementing PS_1 and PS_{ICM} in the reference case.....	45
Figure 2-10: Trajectory of INJ022 as proposed by PS_{ICM} in (a) the reference case and (b) the 9 RMs, which were used to obtain PS_{ICM} . Dashed orange box identifies better zones for the heel in the vicinity (FoD).....	46
Figure 3-1: Generalized CLFD workflow (adapted from Chapter 2).	58
Figure 3-2: The benchmark UNISIM-I case consists of a true field presented by the (a) reference case (UNISIM-I-R) and (b) lower fidelity models (UNISIM-I-D) for simulation (we present one of the scenarios here). Note how different the true field is to a random seed of UNISIM-I-D as the initial ensemble is devoid of important information.....	64
Figure 3-3: Initial FDP (FDP_1) based on the optimal strategy proposed by Schiozer et al. (2015) that was also used as the initial strategy by Morosov and Schiozer (2016).....	67
Figure 3-4: Obtained well logs for: (a) PROD023A horizontal section, (b) PROD023A vertical pilot hole, (c) INJ019 horizontal section and (d) INJ019 vertical pilot hole.....	68
Figure 3-5: Streamlines and localization volume for (a) PROD010 and (b) PROD024A during Cycle 1 of the case study I.	69
Figure 3-6: Prior and posterior histograms of uncertainty attribute (a) rock compressibility, (b) k_z -multiplier, (c) OWC and (d) relative permeability curves.	69
Figure 3-7: Reduction of average normalized data mismatch (\bar{O}) along multiple data assimilations (or iterations) to minimize the disparity between observed and simulated data.	70

Figure 3-8: NQDS analysis of M_{prior}^1 and (b) M_{post}^1 , presenting the percentage of models within acceptable range for individual well objective functions.....	70
Figure 3-9: NPV- N_p cross plot, (b) NPV risk curves and (c) rock compressibility probability distribution function showing the fitness of RMs in Cycle 1.	71
Figure 3-10: (a) Evolution of EMV of the 9 RMs with IDLHC iterations and (b) risk curves showing the result of optimization with approved scenarios (AS) and the reference case (without FoD).	72
Figure 3-11: Evolution of (a) NPV and cumulative oil production (N_p) and (b) cumulative water production (W_p) and water injection (W_i) in the reference case.....	74
Figure 3-12: From top left and in clockwise direction, the pictures illustrate the evolution of FDP (FDP ₁ to FDP ₄). The wells being completed, already producing and to-be-drilled, using the proposed FDP, are highlighted in black, gold, and red italic texts, respectively.	75
Figure 3-13: Proposed preliminary FDP (FDP ₀) used for the pre-CLFD optimization to obtain the benchmark initial FDP (FDP ₁).	76
Figure 3-14: From top left and in clockwise direction, the pictures illustrate the evolution of FDP (FDP ₁ to FDP ₄). The wells being completed, already producing and to-be-drilled, using the proposed FDP, are highlighted in black, gold, and red italic texts, respectively.	78
Figure 3-15: Evolution of (a) NPV and cumulative oil production (N_p) and (b) cumulative water production (W_p) and water injection (W_i) in the reference case.....	79
Figure 3-16: Risk curves of VOIP reflecting the reduction in uncertainty as new information from action phase is being implemented in case study (a) I and (b) II.....	80
Figure 3-17: Evolution of NPV in the reference case after implementing FoD approach on all the wells.	82
Figure 3-18: A 2D model showing different optimal locations for an injector in: (a) good history matched model (representing the “true field” in this case), and (b) poorly history matched model. The orange box represents the history matching area and all properties are the same outside this region..	84
Figure 3-19: Mean porosity for (a) the M_{post}^3 , (b) the approved 60 scenarios from M_{post}^3 and standard deviation of porosity for (c) the M_{post}^3 , (d) the approved 60 scenarios from M_{post}^3 for layer 3 of case study II.	85
Figure 3-20: Mean porosity for (a) the approved 315 scenarios from M_{post}^3 , (b) 9 RMs selected for optimization, and (c) 16 RMs selected for observation, and standard deviation of porosity for (d) the approved 315 scenarios from M_{post}^3 , (e) 9 RMs selected for optimization, and (f) 16 RMs selected for observation for layer 3 of case study I.	86
Figure 4-1: (a) Initial FDP in U3-22 (pink grid blocks highlight Sector-2) and (b) a simple topographic map of the field highlighting the fixed wells in Sector-2.....	104
Figure 4-2: Observed gas per unit area - total (meters) in one of the RMs within two years of opening well I24.	106

Figure 4-3: Evolution of the (a) EMV of the 10 RMs and (b) the minimum % improvement of individual RMs using the FFM-PBE workflow.....	106
Figure 4-4: Optimal FDP bred by the four workflows (a) FFM-PBE, (b) ISM, (c) FFM-PL-MR and (d) FFM-PL-TR. Note that P21, I21, P22, and I22 have exactly same locations as their positions were considered fixed along with the wells in the remaining sectors.	107
Figure 4-5: Evolution of the (a) EMV of the 10 RMs and (b) the minimum percentage improvement of individual RMs with isolated S2 using the ISM workflow.	109
Figure 4-6: Evolution of the (a) EMV of the 10 RMs and (b) the minimum percentage improvement of individual RMs with partially simulated FFMs using the FFM-PL-MR workflow.	110
Figure 4-7: An example of the (a) original and (b) discretized three-phase relative permeability diagram.	111
Figure 4-8: (a) An example of reducing problem space by evaluating the movable oil within 9 km ² of each grid block and (b) well-defined 230 eligible candidates for selecting producers with defined clusters and centroids.....	111
Figure 4-9: (a) Example of reducing problem space by evaluating the mean of horizontal permeabilities across the vertical depth and (b) well-defined 520 eligible candidates for selecting injectors with defined clusters and centroids.....	112
Figure 4-10: (a) Comparing the improvement in Field's EMV (nominal value and percentage) with the time consumption of the workflows and, (b) comparing the improvement in EMV (relative value) and approximating the role of isolated S2 and remaining sectors in entire field improvement.....	114
Figure 4-11: Two FDPs (Strategy 1 and Strategy 2) in a single FFM can yield contrasting total oil flow rate (influx) from all sectors surrounding S2. However, the ISM workflow assumes a constant 0 influx at all times as it ignores the boundary conditions.....	116
Figure 4-12: Cumulative oil production with the optimized FDPs yielded by the four workflows for (a) mid-term (~2 years before the partial life of 40%) and (b) long-term (5 years before the contractual life). The best FDP for the mid-term (obtained with FFM-PL-MR) becomes the poorest candidate in the long run.....	118
Figure 5-1: (a) UNISIM-III-2022 was divided into four sectors (pink blocks highlight Sector-2) and (b) grid-top map (in meters) of the UNISIM-III-2022 highlighting the field topography (adapted from Chapter 4).....	131
Figure 5-2: Chronology of the CLFD cycles (scaled to dates).....	134
Figure 5-3: Percentage change in cumulative oil production of respective wells at the end of Cycle 1 (the first and second numbers in the well's nomenclature refer to the sector and drilling sequence, respectively). Boxplot and red circles represent the expected and actual % change in cumulative oil production using M_{post}^1 , respectively.	135

Figure 5-4: For the same oil production, difference in gas production is almost double even after data assimilation (Red dots and blue lines denote the production data of true field and simulated models, respectively).	136
Figure 5-5: (a) Consideration of a thief zone connecting wells P17 and I17, without disturbing the neighboring well P12 and, (b) gas production rate of well P17 after revising data assimilation process.	137
Figure 5-6: From top left and in clockwise direction, the pictures illustrate the evolution of FDP: (a) FDP ₀ (initial strategy), (b) FDP ₁ (cycle 1), (c) FDP ₂ (cycle 2) and, (d) FDP ₃ (cycle 3). Faults (F4 and F6), producers and injectors are shown using bold pink, green, and blue, respectively. To-be-drilled wells are highlighted in red italics. Filled circles, squares, and triangles are used to segregate the existing wells and to-be-drilled wells in Cycle 1 and Cycle 2/3, respectively.	138
Figure 5-7: Graphs showing the evolution of (a) NPV (M_{post}^i) refers to the set of history-matched simulation models, where ‘ <i>i</i> ’ is the cycle number) and, (b) oil recovery factor (for each sector) over the cycles.	140
Figure 5-8: (a) FDP ₀ , (b) FDP ₁ , (c) FDP ₂ and, (d) FDP ₃ in M_{post}^1 , M_{post}^2 , M_{post}^3 and reference case.	147

List of Tables

Table 2-1: Activities performed: bottom-up analysis and application of FoD.	31
Table 2-2: Drilling chronology and acquired information during different cycles.....	38
Table 2-3: Economic parameters and their respective values for three economic scenarios.	39
Table 2-4: Comparing results obtained with ICM and IO.	42
Table 2-5: Comparing results obtained with ICM, IO and IAM activity.....	44
Table 2-6: Implementing different PS in the reference case.	47
Table 3-1: Drilling chronology and information acquisition.	66
Table 3-2: Economic parameters (adapted from Chapter 2).	67
Table 3-3: A detailed account of implementation of CLFD on case study I.....	73
Table 3-4: A detailed account of implementation of CLFD on case study II.....	77
Table 3-5: Observed differences between case study I and II.....	79
Table 3-6: Changing statistics of VOIP for case study I and II.....	81
Table 3-7: NQDS values obtained for the ensemble prior and posterior to the data assimilation process for both the case studies.	82
Table 3-8: Evaluating the performance of DA after removing the historical constraints reveals the existing discrepancy between the ensemble and the real field.	83
Table 3-9: Improving the minimum NPV improvement for each RM can potentially improve the chances of success of the FDP.	87
Table 3-10: An improved correlation between simulation models and the reference case as accrued information is utilized in case study II.....	87
Table 4-1: Relevant field activities and information.	104
Table 4-2: Summary of time consumed and results yielded by different workflows.	108
Table 4-3: Technical Results and their assigned weights for the simulations with PL = 40% of the contractual life.....	113
Table 4-4: Results obtained after implementing optimized strategies in M_{52}	119
Table 5-1: List of scalar and grid parameters extracted.....	128
Table 5-2: Relevant field activities and information.	133
Table 5-3: Estimated time consumed for Cycle 1 using the workflow in Chapter 3 and this article..	135
Table 5-4: A detailed account of implementation of CLFD.....	139
Table 5-5: Key differences between the workflow presented in Chapter 3 and this article.....	141
Table 5-6: Difference between growing RMs over iterations and Propagation of best experiments.	145

Table of Contents

1	INTRODUCTION	19
1.1	MOTIVATION.....	21
1.2	OBJECTIVES.....	22
1.3	DESCRIPTION OF THESIS	22
1.3.1	<i>Bottom-up analysis to unravel potential problems and emphasize the impact of individual steps in closed-loop field development (published work)</i>	<i>22</i>
1.3.2	<i>Application of risk-informed closed-loop field development workflow to elucidate the evolution of uncertainties (published work)</i>	<i>23</i>
1.3.3	<i>A comparative study to accelerate field development plan optimization (published work)</i>	<i>24</i>
1.3.4	<i>Revising field development plan of a giant field under uncertainty using accrued information (submitted for publication).....</i>	<i>24</i>
1.3.5	<i>Concept of risk-informed decision-making – Appendix A.....</i>	<i>25</i>
1.3.6	<i>Using “flux boundary option” for well location optimization: a feasibility study – Appendix B.....</i>	<i>25</i>
1.3.7	<i>Cluster-based learning and evolution algorithm for optimization (submitted for publication) – Appendix C.....</i>	<i>25</i>
2	BOTTOM-UP ANALYSIS TO UNRAVEL POTENTIAL PROBLEMS AND EMPHASIZE THE IMPACT OF INDIVIDUAL STEPS IN CLOSED-LOOP FIELD DEVELOPMENT	27
2.1	INTRODUCTION.....	28
2.2	METHODOLOGY	31
2.2.1	<i>Initial CLFD methodology (ICM).....</i>	<i>31</i>
2.2.2	<i>Improving optimization (IO)</i>	<i>33</i>
2.2.3	<i>Improving approved models (IAM)</i>	<i>34</i>
2.2.4	<i>Flexibility of drilling (FoD).....</i>	<i>35</i>
2.3	APPLICATION.....	36
2.4	RESULTS.....	39
2.4.1	<i>Initial CLFD methodology (ICM).....</i>	<i>39</i>
2.4.2	<i>Improving optimization (IO)</i>	<i>42</i>
2.4.3	<i>Improving approved models (IAM)</i>	<i>43</i>
2.4.4	<i>Flexibility of drilling (FoD).....</i>	<i>44</i>

2.5	DISCUSSION	47
2.6	CONCLUSIONS	49
	ACKNOWLEDGEMENTS.....	50
	NOMENCLATURE	50
3	APPLICATION OF RISK-INFORMED CLOSED-LOOP FIELD DEVELOPMENT WORKFLOW TO ELUCIDATE THE EVOLUTION OF UNCERTAINTIES	52
3.1	INTRODUCTION	53
3.2	OBJECTIVES.....	56
3.3	METHODOLOGY	57
3.4	APPLICATION.....	64
3.4.1	<i>Reference case (UNISIM-I-R)</i>	<i>64</i>
3.4.2	<i>Simulation models (UNISIM-I-D).....</i>	<i>65</i>
3.5	RESULTS.....	65
3.5.1	<i>Case study I: Repeating Morosov and Schiozer (2016)</i>	<i>67</i>
3.5.2	<i>Case study II: All vertical wells.....</i>	<i>75</i>
3.6	DISCUSSION	79
3.7	CONCLUSIONS	89
	ACKNOWLEDGEMENTS.....	91
	NOMENCLATURE	91
4	A COMPARATIVE STUDY TO ACCELERATE FIELD DEVELOPMENT PLAN OPTIMIZATION	95
4.1	INTRODUCTION	96
4.2	OBJECTIVES.....	98
4.3	METHODOLOGY	98
4.3.1	<i>Full-field model – Propagation of best experiments (FFM-PBE).....</i>	<i>99</i>
4.3.2	<i>Isolated sector model (ISM).....</i>	<i>101</i>
4.3.3	<i>Full-field model – partial life – monetary results (FFM-PL-MR).....</i>	<i>101</i>
4.3.4	<i>Full-field model – partial life – technical results (FFM-PL-TR)</i>	<i>102</i>
4.4	APPLICATION AND RESULTS	103
4.4.1	<i>Full-field model – Propagation of best experiments (FFM-PBE).....</i>	<i>105</i>
4.4.2	<i>Isolated sector model (ISM).....</i>	<i>106</i>
4.4.3	<i>Full-field model – partial life – monetary results (FFM-PL-MR).....</i>	<i>109</i>
4.4.4	<i>Full-field model – partial life – technical results (FFM-PL-TR)</i>	<i>110</i>
4.5	DISCUSSION	115

4.5.1	<i>Full-field model – Propagation of best experiments (FFM-PBE)</i>	115
4.5.2	<i>Isolated sector model (ISM)</i>	115
4.5.3	<i>Full-field model – partial life – monetary results (FFM-PL-MR)</i>	117
4.5.4	<i>Full-field model – partial life – technical results (FFM-PL-TR)</i>	118
4.6	CONCLUSIONS	120
	ACKNOWLEDGMENTS	122
	NOMENCLATURE	122
5	REVISING FIELD DEVELOPMENT PLAN OF A GIANT FIELD UNDER UNCERTAINTY USING	
	ACCRUED INFORMATION	124
5.1	INTRODUCTION	125
5.2	OBJECTIVES.....	126
5.3	METHODOLOGY	127
5.4	APPLICATION AND RESULTS	131
5.4.1	<i>Cycle 1 of CLFD</i>	133
5.4.2	<i>Practical problems in Cycle 3</i>	136
5.4.3	<i>Outcome</i>	137
5.5	DISCUSSION AND RECOMMENDATIONS	140
5.6	CONCLUSIONS	148
	ACKNOWLEDGMENTS	150
	NOMENCLATURE	150
6	CONCLUSIONS	152
7	SUGGESTIONS FOR FUTURE STUDIES.....	156
8	REFERENCES.....	159
	APPENDIX A : CONCEPT OF RISK-INFORMED DECISION-MAKING	170
	APPENDIX B : USING “FLUX BOUNDARY OPTION” FOR WELL LOCATION OPTIMIZATION: A	
	FEASIBILITY STUDY	173
	APPENDIX C : CLUSTER-BASED LEARNING AND EVOLUTION ALGORITHM FOR OPTIMIZATION .	182
	APPENDIX D : LICENSE AGREEMENTS	218

1 Introduction

A field development plan (FDP) is a mandated document that specifies the detailed actions, constraints, and processes required to develop an oil and gas field. It is a crucial document for a greenfield where a host of significant decisions must be made to bring the production online without delaying its plateau. A dearth of information and copious technical and geological uncertainties around the field renders the task even more complex. Despite these challenges, a multidisciplinary team makes several front-end investment decisions regarding infrastructure and wells to make the project as profitable as possible. Generally, this is performed by analyzing several hypothetical scenarios to forecast the long-term production of hydrocarbons and the corresponding monetary return. However, this conventional field development process may offer a suboptimal FDP due to a massive gap in information and a huge envelope of uncertainty.

Typically, only a few exploration wells and their production data over a couple of months are available for proposing the initial FDP. It is vital to assimilate new information over time to revise FDPs and make better decisions. Integrating new data with existing information can potentially aid the multidisciplinary team in understanding the field better for making well-informed decisions. Thus, optimizing updated models using the accrued information over time is critical for successfully developing an oil and gas field. This lacking is where the feedback-based field development process comes into play to mitigate a subpar FDP. Similar to the objective of drilling an appraisal well, a feedback-based field development process attempts to obtain information through new development well(s) for improving the project's objective function (for instance, net present value (NPV), recovery factor (RF)) by reviewing the decision variables (for example, number, type, and location of wells) in the FDP.

While there is an extensive list of studies on conventional field development optimization, minimal work has been done in the area of feedback-based field development. This concept was first successfully explored under the label of closed-loop field development (CLFD) as a cyclical process to utilize the intermittently acquired information to improve decisions with gradually increasing periods of field development.

CLFD is an exhaustive combination of multidisciplinary tasks for using frequently acquired data to optimize the pre-defined objective function of the project. The amount of information can vary from hours to years. Similarly, the quality and reliability of the data can

depend on the source of measurement. The acquired data can also range from two-dimensional (2D) production data, well-tests, and up-to-date inputs to three-dimensional (3D) well logs and geophysical surveys.

CLFD has been endorsed by all previous work as a simple concept that can help multidisciplinary teams to optimize objectives while dealing with uncertainty. Despite this, limited theoretical evidence exists to justify the use of this principle in practical applications. This lack of support is because theoretical studies involving 3D field development utilizing the CLFD workflow yielded both pessimistic and optimistic outcomes. Computational expense, a huge envelope of uncertainty, and heterogeneity, among other factors, can also render such workflows time-consuming. Furthermore, the existing workflows are slow, leading to a reasonably large delay in their implementation in actual field applications, limiting their true benefits.

Some of the Brazilian pre-salt reservoirs present a perfect example for testing practical workflows to enthruse confidence in the performance of such workflows. Among other reasons, this is chiefly due to their complexities in terms of heterogeneities and the size of the field. To test, learn and develop a robust workflow using such complex fields, we present this work in the form of five scientific articles. We begin this thesis by unraveling the potential problems in the CLFD workflow. Based on this learning, we propose a robust and risk-informed CLFD workflow to ensure that it improves the results in the reference case (which represents the "true field" behavior in a synthetic benchmark case). As the optimization process is sluggish for time-consuming models, we focus on this aspect in the subsequent research. Two of the scientific studies focus on improving the optimization step of the CLFD process to endorse an efficient CLFD methodology. Integrating the knowledge from all four works, we test the pragmatic workflow on a giant benchmark with typical characteristics of a pre-salt field in offshore Brazil. This final paper also focuses on the practical realization of the concept of CLFD, while establishing the impact of CLFD workflow.

Typically, reservoir studies struggle to predict reservoir performance adequately due to their inherent characteristic of accuracy, bias, and error. Despite these characteristics, a risk-informed and efficient CLFD provides an ideal opportunity to assimilate new information over specified phases and improve our understanding of the field. This improved understanding is best visible in the form of decisions made using CLFD.

This thesis focuses on learning the potential problems and using that knowledge to propose improved CLFD workflows. We introduce and validate two risk-informed CLFD

workflows for promoting robust decision-making under uncertainty for both typical and giant fields. The first workflow is comprehensive and equipped for faster simulation models. Without an efficient workflow, a CLFD cycle can be expensive in terms of time, rendering it impractical to develop a field with expensive physics-based simulation models. Hence, the second workflow is more efficient and applicable for time-consuming and practical applications. We addressed several research gaps in this niche subject while disclosing acute observations and enthusing confidence in applying the proposed workflows.

The research consists of seven chapters that include four chapters with scientific studies. The last two chapters of the work include the conclusion and likely future studies. The thesis also comprises four appendices which include a discussion on risk-informed decision-making, an additional scientific article on a novel optimization algorithm, a summarized report on using flux-boundary conditions in sectorized field development, and published manuscripts' license agreements.

1.1 Motivation

We derive our motivation from several well-established facts. Firstly, only limited research has been done in this niche area of the feedback-based field development process.

As endorsed by these limited studies, CLFD is an intuitive concept to assist multidisciplinary teams in maximizing the field's objective function while working with uncertainties. Despite this, none of the work supports the employment of this concept in the actual field. This impracticality arises because both negative and positive results were observed in the previous studies working on three-dimensional field development using CLFD workflow.

Furthermore, none of the previous work delved deeper and explained the impact of an individual step and all the steps of CLFD on uncertainties during field development. This description of the implicit working of steps is the key to highlighting the changes observed in the explicit objective function and revised FDP. Such descriptions are necessary to enthuse confidence in the effectiveness of CLFD and facilitate further improvements in the CLFD process.

Fourthly, all proposed workflows are highly time-consuming and infeasible for developing giant or complex fields requiring an elaborate physics-based simulation model to understand better the field's behavior. This shortcoming makes the CLFD workflows practical for only a theoretical application.

Finally, the limited work on the subject only focuses on improving the field's pre-defined objective function(s), disregarding practical concerns like associated delays, execution time, and limitations of CLFD workflows to improve decisions in certain reservoirs.

1.2 Objectives

The primary objective of this work is to delineate an efficient and risk-informed CLFD workflow for practical applications in the exploration and production industry. We systematically analyze and unravel the potential problems in the existing workflows to help us build a robust and methodical CLFD workflow. We attempt to bolster confidence in our workflow using a diverse group of controlled and systematic experiments with multiple benchmark case studies. Intending to make the workflow efficient for real field applications, we propose alternate approaches and apply them on a giant benchmark field.

1.3 Description of thesis

The thesis consists of a series of four scientific articles. Three additional work are discussed in the form of appendices. In this subsection, we summarize all these studies and their contribution towards the overall objectives of the thesis. We present the detailed articles in the subsequent chapters.

1.3.1 Bottom-up analysis to unravel potential problems and emphasize the impact of individual steps in closed-loop field development (published work)

Loomba, A.K., Botechia, V.E. and Schiozer, D.J. 2020. Bottom-up analysis to unravel potential problems and emphasize the impact of individual steps in closed-loop field development. Presented at the Offshore Technology Conference held in Houston, Texas, United States of America, 4-7 May. DOI: 10.4043/30776-MS.

We started this work using the hypothetical conclusions of one of the previous studies that yielded negative results using CLFD workflow and concluded that a higher fidelity model can mitigate such outcomes. However, using an ensemble of relatively higher fidelity models did not yield better results using the existing workflow. Considering this disagreeable result, we introduced a bottom-up assessment of the CLFD workflow to exhibit the impact of individual steps on the workflow and highlight associated potential problems. By performing three new activities and comparing them with the existing CLFD workflow, we expanded our understanding of the CLFD workflow and the importance of individual steps.

Based on these experiments, we were able to identify that the propagation of specious scenarios/outputs can lead to an overall bias in the results of CLFD. As CLFD is a cyclical

process, one needs to be cautious about the output of the preceding step to the input of the next step. We also introduced a bi-criterion objective function focusing on the ensemble as well as individual representative models (RMs) to improve the likelihood of success of the optimized FDP. Based on one set of experiments, we also learned that accepting poorly history-matched scenarios can lead to an inferior ensemble of RMs and, consequently, influence the optimization process. Given that we work with limited information during the field development process, we also introduced flexibility of drilling (FoD) as an alternative to incorporate pragmatic drilling and avoid “unrealistic” bias that may affect FDPs in some instances when working in a theoretical environment.

The main contribution of this work is to systematically analyze and unravel the potential problems in the existing workflows. The work explores the impact of individual steps on the CLFD workflow. This knowledge is crucial for building a robust and methodical CLFD workflow.

1.3.2 Application of risk-informed closed-loop field development workflow to elucidate the evolution of uncertainties (published work)

Loomba, A.K., Botechia, V.E. and Schiozer, D.J. 2021. Application of risk-informed closed-loop field development workflow to elucidate the evolution of uncertainties. Journal of Petroleum Science and Engineering, 197, 107960, DOI: 10.1016/j.petrol.2020.107960.

Learning from the first work, we propose an improved and risk-informed CLFD workflow for three-dimensional (3D) synthetic field applications. This article attempts to provide a diverse and all-inclusive perspective on the subject to address some of the previously unanswered questions. The specific objectives of this study include testing the proposed risk-informed workflow on two synthetic case studies while systematically investigating the individual steps to improve the CLFD workflow further. Unlike any previous work, we present a comprehensive discussion on the evolution of uncertainties as individual components of the risk-informed workflow are executed. As most of the previous work rarely focused on this aspect, we attempt to reinforce confidence in the feedback-based field development process by providing an intuition into the working of the methodology by contemplating our evolving ensemble of models. Most importantly, this work also introduces the value of closed-loop (VoCL) to quantify the impact of new decisions on the project's monetary objective function and analyze the bias related to model-based decisions.

The main contribution of this work is to delineate a comprehensive and risk-informed CLFD workflow and validate it using two field-scale examples. Unlike previous studies, we

strengthen the confidence in a CLFD workflow by providing a step-by-step analysis of the inputs and outputs of individual steps.

1.3.3 A comparative study to accelerate field development plan optimization (published work)

Loomba, A.K., Botechia, V.E. and Schiozer, D.J. 2022. A comparative study to accelerate field development plan optimization. Journal of Petroleum Science and Engineering, 208, 109708, DOI: 10.1016/j.petrol.2021.109708.

In this comparative study, we present and compare a few practical solutions to assist a complex/giant field's development while considering probabilistic scenarios to capture uncertainty. We define four workflows to expedite the process of FDP optimization. We implement and compare those workflows on a giant benchmark field. Based on a detailed investigation, we also present their advantages and disadvantages for establishing their applicability in different situations. Moreover, we show that the newly proposed methods and some fine-tuning exercises can make the FDP optimization process considerably efficient. With all research combined, we establish its usefulness in the CLFD workflow.

The focus of this work is to propose new techniques for making the optimization process highly efficient. As the model error is an inherent component within the simulation models, this research promotes the idea of developing a field with risk-averse techniques and selecting an appropriate FDP efficiently.

1.3.4 Revising field development plan of a giant field under uncertainty using accrued information (submitted for publication)

Stimulated by the high execution time for implementing a CLFD cycle in a complex oil and gas field with extensively time-consuming simulation models, we present an efficient CLFD workflow in this final work on CLFD. Without an efficient workflow, it can be time-intensive to develop such field-scale examples. Hence, we propose and validate an efficient workflow for practical applications. The proposed workflow in this article uses the essential knowledge from previous studies to make all the individual steps faster than the previously validated workflow.

We test this efficient workflow on a giant benchmark case created with typical heterogeneous characteristics of a pre-salt field in Brazil. This benchmark case manifests a challenging environment with spatial and temporal complexity. Consequently, it makes a perfect testing ground for investigating the proposed workflow. To study the effect of CLFD, we also work with fewer decision variables in a quarter of a giant field and consider practical

timelines. Unlike previous work, we also establish the benefit of the workflow by including its execution time and buffer period to stress that CLFD works in a delayed environment.

The main contribution of this work to the thesis is to validate an improved, risk-informed, and efficient CLFD workflow. Such a holistic workflow is indispensable for developing real field examples, which can be fraught with complexities. The article also stresses deliberately planning for the successful implementation of CLFD.

1.3.5 Concept of risk-informed decision-making – Appendix A

In 2008 and 2010, National Aeronautics and Space Administration (NASA) presented a risk-informed decision-making process as a deliberate workflow to mitigate the shortfalls in their outcomes. This appendix presents the difference between a risk-based and risk-informed decision-making process while highlighting the definition of risk-informed decision-making and how it was used in conjunction with CLFD workflow to yield robust results.

1.3.6 Using “flux boundary option” for well location optimization: a feasibility study – Appendix B

Computer Modelling Group Ltd. (CMG) introduced the “flux boundary option” in 2019 as a tool to simulate a section of the full-field model, without hampering the results as well as saving time. In this appendix, we assess the applicability of this newly introduced tool in terms of its function for performing production strategy (only well-location) optimization in a giant field.

1.3.7 Cluster-based learning and evolution algorithm for optimization (submitted for publication) – Appendix C

In this manuscript, we present cluster-based learning and evolution optimizer (CLEO) as an algorithm for solving optimization problems. The optimizer uses cluster-based manipulation of problem space during the exploration phase. The exploitation phase is executed using the updated knowledge of the problem space for fine-tuning. Using the concept of CLEO, we propose two approaches.

We validate the proposed approaches by optimizing the FDP for a simple and synthetic simulation model as well as a giant field-scale model. We perform both deterministic and probabilistic analyses with extensive as well as limited decision variables. In addition, we compared our proposed methods with four well-established optimizers (particle swarm optimization (PSO), differential evolution (DE), designed exploration controlled evolution (DECE), and iterative discrete Latin hypercube sampling method (IDLHC)).

The main contribution of this addendum work is to propose a new optimization algorithm. As this optimization algorithm explores the problem space more efficiently, we use it as the core optimization algorithm in the final study on CLFD. We adapted the concepts of the second approach presented in this work to optimize >90% faster in the final study.

2 Bottom-up Analysis to Unravel Potential Problems and Emphasize the Impact of individual steps in Closed-loop Field Development

Authors:

Ashish Kumar Loomba

Vinicius Eduardo Botechia

Denis José Schiozer

Abstract

Closed-loop field development (CLFD) is a feedback-based approach to optimize production strategy by utilizing new information iteratively during field development. Positive and negative results have been presented in previous work using CLFD, so this paper presents a bottom-up assessment of CLFD workflow to exhibit the impact of individual steps on the workflow, highlighting associated potential problems and, finally, proposing a methodology to tackle these problems.

Our CLFD workflow consists of updating static information, assimilating dynamic data to select an appropriate subset of models and, finally, selecting representative models to optimize the production strategy under uncertainties. We performed four activities to expand our understanding of CLFD by applying the workflow on UNISIM-I, a benchmark case study: (1) applying the aforementioned CLFD workflow, (2) applying the workflow after modifying objective function of optimization process, emphasizing the likelihood of success of optimized production strategy over the ensemble of simulation models, (3) applying the workflow after modifying the objective function, as well as the criteria for selecting the appropriate subset of models, post dynamic data assimilation, and (4) reanalyzing the results of activity 1 after using flexibility of drilling (FoD) - an approach proposed to partially imitate the real-time decision-making process to ensure that the heel of a well is not drilled in a non-reservoir zone, by utilizing the available information.

The application of the initial CLFD methodology (first activity) led to an increase in expected monetary value (EMV) based on simulation models, but we observed a decrease in EMV when we implemented this optimized strategy in the reference case UNISM-I-R (a very refined model that emulates a "true field"). This negative result formed the basis for our motivation to perform the bottom-up analysis. During the second activity, our attempt to improve the optimization process using a new objective-function, led to a significant improvement in EMV for the reference case, compared to the first activity. Re-applying the CLFD workflow using this newly tested objective function, while using stricter criteria for selecting approved models (third activity), provided an optimized production strategy for the reference case. Last activity provided a deeper insight into the CLFD workflow. Application of FoD, during the fourth activity, revealed that the poorer results during the first activity can be segregated into two separate components: (a) relatively poorer CLFD workflow and, (b) ignoring FoD to ineptly drill the wells in non-reservoir zones.

The bottom-up approach helped us systematically improve the CLFD workflow. Implementation of the improved workflow ensured that the optimized production strategy not only improved EMV for simulation models, but also the reference case.

2.1 Introduction

Optimization of a production strategy (PS) to improve pre-defined objective function(s) (expected monetary value (EMV), recovery factor (RF), etc.) of a field development plan is an arduous task. The lack of ample information and uncertainties revolving around geological and technical parameters renders the optimization process even more challenging. Acquiring information and reducing uncertainties to produce better geological and simulation models is, therefore, one of the key tasks for multidisciplinary teams working on the field development.

However, under the provided circumstances, decisions related to the design variables in a green field, i.e., the most crucial variables associated with the infrastructure and wells (Gaspar et.al 2016), need to be made under a large bracket of uncertainties. While most of these design variables, (e.g., platform and flowline system) cannot be modified after a concrete decision has been made, some of the other design variables (for e.g., well count, placement, etc.) can still be modified and optimized in an ad hoc manner by collecting and exploiting new information acquired during the development phase of the green field. This idea was first presented by Shirangi and Durlofsky (2015), under the broad label of closed-loop field development (CLFD) to optimize production strategy (PS) based on number, type, and

placement as well as operating constraints of wells by assimilating new information acquired by drilling new wells and using production data from the existing wells.

CLFD can be defined as a feedback-based approach to optimize PS by utilizing new information (production data, well-logs, etc.) iteratively during field development. According to Shirangi and Durlofsky (2015), CLFD consists of three cyclic steps; optimizing PS under the currently available geological information, drilling wells to obtain hard data as well as production data and finally, updating multiple geological models based on freshly available data. The authors used a hybrid particle swarm optimization-mesh adaptive direct search algorithm (Isebor et al., 2014) for optimizing the well type, location, and controls for the to-be-drilled wells and well controls for the existing wells. For history matching, they opted for randomized maximum likelihood procedure (Oliver et al., 1996) by obtaining gradients using the adjoint method. In addition, they introduced the concept of optimization with sample validation (OSV) to select an apt number of representative models (RMs) to provide efficiency to the process under geological uncertainties. When applied to different synthetic small-scale examples, they noted that CLFD could yield positive results. Furthermore, Shirangi and Durlofsky (2015) also concluded that simultaneous optimization provides a better result compared to sequential optimization in CLFD and lower number of RMs in CLFD can yield lower positive results compared to the case where OSV was used to select apt number of RMs.

Morosov and Schiozer (2016), however, stressed that history matching (HM) and optimization are the two critical components of the CLFD workflow, and implemented a repeated sequence of drilling, data acquisition, HM and optimization in their work. For optimization, they used designed exploration and controlled evolution algorithm (Yang et al., 2007). The authors used ensemble smoother with multiple data assimilation (ES-MDA), proposed by Emerick and Reynolds (2013), to perform HM and RMFinder, a software based on Meira et al. (2016), to select RMs. The authors implemented their CLFD methodology on UNISIM-I benchmark case (Gaspar et al., 2014 and Avansi and Schiozer, 2015), based on the Namorado field, Brazil. However, the authors obtained negative results after implementing CLFD. They highlighted that the optimized PS, obtained after implementing CLFD, yielded negative NPV in the “true-field” due to poor uncertainty assessment as a result of mainly three reasons: (1) upscaling process, (2) HM convergence to non-representative variables and (3) lack of geostatistical variability to account for uncertainties. Additionally, we believe that approving bad ensemble of scenarios, poor optimization process, bias caused by wells

representation, bad set of RMs or using too few RMs, poor uncertainty quantification, software/human error, etc. could also be potential causes for the failure.

Hidalgo et al. (2017) presented their custom-made workflow based on a sequence of four steps; HM, selection of representative models, optimization and acquisition of new production data and well-logs. Intrigued by the negative results of Morosov and Schiozer (2016), the authors tested their methodology on the same benchmark case to validate the advantages of implementing the CLFD workflow. The optimization was performed using a procedure based on the genetic algorithm with nonlinear constraints (Emerick et al., 2009), while ES-MDA was used to perform HM. The selection of RMs was performed using a genetic algorithm proposed by Armstrong et al. (2012). Although they worked with the same initial set of simulation models, the initial well count, trajectory, type, and drilling schedule were completely different than the one proposed by Morosov and Schiozer (2016). In contrast to the result presented by Morosov and Schiozer (2016), their workflow was able to exhibit a positive result with CLFD.

Kim et al. (2018) proposed a customized workflow and stressed that a combination of particle-swarm optimization and ensemble Kalman filter can find a reliable solution for real field development challenges. Schiozer et al. (2019) proposed a CLFD process divided into 12 steps, contemplating a complete procedure that ranges from reservoir characterization to the final decision analysis.

In this work, we initially propose our custom-made workflow, motivated by previous work. Since Morosov and Schiozer (2016) concluded upscaling as one of the reasons for the failure of CLFD in their work, we test their hypothesis by implementing CLFD on relatively finer-scale simulation models of the benchmark UNISIM-I field, compared to Morosov and Schiozer (2016), under similar controlled-environment as theirs. We evaluate the results of the first cycle of CLFD and, based on the results, attempt to perform a bottom-up analysis. A bottom-up analysis can be defined as a systematic procedure for analyzing and finding the weakest component of a workflow, starting with the last step and gradually moving up toward the top or the preferred step. Such an analysis provides the necessary information to improve the workflow by understanding the impact of the individual steps on the subsequent steps of the workflow. In this paper, we investigate how to improve the initial custom-made CLFD methodology by improving the optimization process and increasing the likelihood of success

of the optimized PS over the ensemble of models. Furthermore, we also investigate how to improve the selection of an apt set of history-matched scenarios for picking a better set of RMs.

Given that we work with limited information during field development process, we also propose a pragmatic drilling approach for the synthetic “true field” (reference case – very refined model representing the real response), to partially imitate the real-time decision-making process in practice. This is important because an automatic procedure for model-based optimization in CLFD may suggest a good region/layer to drill a well based on the representative models, but the same might not be a good region in the reference case (due to intrinsic failure to capture uncertainties entirely). As the CLFD procedure does not consider this, we propose flexibility of drilling (FoD) as a supplementary method to ensure that we don’t drill the heel of the wells in a non-reservoir zone, by utilizing the available information.

2.2 Methodology

In this section, we start by presenting the initial CLFD methodology (ICM), motivated by the work done by Shirangi and Durlofsky (2015) and Morosov and Schiozer (2016). In sequence, we present and describe three more subsequent activities; improving optimization (IO), improving approved models (IAM) and application of flexibility of drilling (FoD). **Table 2-1** presents a glimpse of the three activities performed to improve the workflow.

Table 2-1: Activities performed: bottom-up analysis and application of FoD.

Activity	Significant Feature
ICM	Applying CLFD using our initial methodology
IO	Applying CLFD after improving optimization process
IAM	Applying CLFD after improving approved subset of models
FoD	Applying flexibility of drilling

2.2.1 Initial CLFD methodology (ICM)

Based on the previous studies, we present the CLFD workflow centered on six components (**Figure 2-1**):

1. Action: This is the first step of the CLFD methodology. Within this step, the new hard data, in the form of well-logs, is acquired as the new wells are drilled. These new well-logs, along with the existing ones, are used to update the existing geological model and generate an updated ensemble of 500 petrophysical properties. This step also provides

an opportunity to acquire production data of the field. We add noise to this production data to make it similar to a real-life field data.

2. **Update Inputs:** The newly drilled wells or production data can provide valuable information for updating the uncertainty attributes. In this step, the uncertainty attributes are updated based on this information. For example, drilling the first well in the eastern reservoir of the field assures the presence or absence of hydrocarbon and this uncertainty attribute can consequently be updated for simulation models.

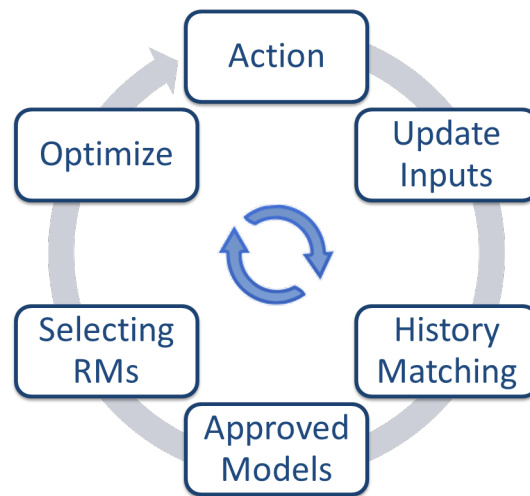


Figure 2-1: Generalized CLFD workflow.

3. **History Matching:** Computer-assisted history matching is an important component of CLFD. To utilize the information available in the form of production data and improve the simulation models, ensemble smoother - multiple data assimilation (ES-MDA) is used (Emerick and Reynolds, 2013). Furthermore, the Kalman-gain localization scheme (Soares, 2017) is used with ES-MDA to perform data assimilation by modifying the grid-properties in the pre-defined neighborhood of the producers and injectors only. In other words, only the localized areas influenced by respective wells are modified. In this study, we assume a standard localization circle of 2000 meters for all wells. Apart from the modification of grid-properties, this step also helps reduce the variability of scalar uncertainty attributes (e.g.: rock compressibility, oil-water contact, etc.).
4. **Approved Models:** To save computational time and exclude very bad scenarios, a smaller subset of scenarios is selected from the entire ensemble of 500 scenarios. Normalized quadratic distance with sign (NQDS) method (Avansi and Schiozer, 2015

and Avansi et al., 2016) is used to check the quality and exclude the bad scenarios. Based on a tolerance applied to the available production data, it provides a simple and yet sophisticated way to single out the bad scenarios.

5. Selecting RMs: Although a smaller subset is picked by the end of the previous step, using more than 100+ scenarios for optimization (next step) is unfeasible. One way to maintain the quality of the results and reduce the computational effort is by using representative models (RMs), which can represent the variability of the uncertainties in a small number of simulation models. Developed by Meira et al. (2017), RMFinder 2.0 is used to select nine RMs to represent the variability of the uncertain scenarios.
6. Optimize: Based on the chosen RMs, we optimize the PS by modifying the well locations of the undrilled wells only. Optimization is performed using designed exploration and controlled evolution (DECE) algorithm (Yang et al., 2007). The RMs are robustly optimized by applying the procedure of Silva (2018) with a slight modification of the objective function. Instead of assuming equiprobable RMs, we calculate the objective function based on the probability of occurrence of each RM (as provided by RMFinder 2.0). The objective function for the optimization process can be written as:

$$OF^i = \sum_{k=1}^n P(RM_k) * EMV_k^i \quad 2-1$$

where OF signifies objective function, i denotes the iteration, n signifies the total number of RMs and k denotes the index of RM.

Once an optimal strategy is obtained after using the freshly available information, the optimized strategy is finally applied to the reference case (very refined model that represents the real response – see Application Section) to evaluate the outcome of the six steps of CLFD. In this first activity, we use simulation models with a finer grid than Morosov and Schiozer (2016) with the objective to verify the impact of upscaling on negative results that the authors obtained.

2.2.2 Improving optimization (IO)

To improve the workflow using the bottom-up approach, we started with the last step of the workflow (**Figure 2-1**), i.e., optimization. Scrutinizing **Equation 2-1** revealed that the equation merely focuses on the EMV of RMs. As long as EMV with a new PS is higher than

the initial EMV (with the initial PS), **Equation 2-1** accepts the new PS as an optimized PS, even if one (or more) of the RMs observe an impaired EMV with this newly proposed PS. In short, **Equation 2-1** has a good tendency to provide an optimized PS that works for some RMs and fails for others. As such, to overcome this shortcoming, we decided to elaborate **Equation 2-1** to ensure that the optimized PS works for the maximum possible number of RMs, while improving the weighted EMV (**Equation 2-2**).

$$OF^i = \sum_{k=1}^n If (EMV_k^i - EMV_k^0 > 0, P(RM_k) * EMV_k^i, 0) \quad 2-2$$

As suggested by **Table 2-1**, only the last component of the CLFD workflow was modified in this activity by replacing **Equation 2-1** with **Equation 2-2** as the objective function. Leaving the other five steps unchanged, CLFD was re-implemented for us to understand the impact of the sixth step as well as **Equation 2-2**. It is noteworthy that, although we are modifying the equation for calculating the objective function of all RMs, the objective function of the field (EMV) remains the same. The modified equation only diverts the focus on improving the likelihood of success of the PS on the reference case, assuming that the prior steps can assess the reservoir uncertainties properly and we can capture a representative set of reservoir scenarios.

2.2.3 Improving approved models (IAM)

Based on the work of Meira et al. (2017), we assumed that RMFinder 2.0 performed its characteristic task of selecting a good set of representative models out of the approved set of history-matched scenarios that honored dynamic and static information. As such, for this work, we skipped investigating the penultimate component of the CLFD workflow (**Figure 2-1**) and decided to investigate the fourth component of CLFD, i.e., approved models.

At the end of the first cycle of CLFD, limited information is available, especially in terms of production data. Given that this data can be limited, one can be intrigued to use a lenient tolerance value for filtering the ensemble of history-matched scenarios. However, a lenient tolerance also indirectly implies that the selected scenarios might not have been history-matched very well. A badly history-matched model is not an acceptable scenario as it can always be associated with a bad forecasting scenario due to failure to even honor the past. One must note that, at the same time, we are not implying that an ensemble of excellent history-matched scenarios ensures a perfect forecast. We also emphasize that the adjectives associated

with the scenarios, i.e., “excellent”, “bad”, etc. are subjective and may depend on the available data points, the objective of the study, etc.

Therefore, in order to improve the fourth component of the workflow, we decided to impose a stricter filter to accept only good scenarios, instead of just excluding the bad scenarios (**Figure 2-2**). For the sake of completeness, a scenario was considered acceptable if simulated data was observed within a strict band of $\pm 30\%$ of observed data. As suggested by **Table 2-1**, leaving the other three previous components of CFLD workflow unchanged, this new strict criterion of selecting approved models was executed to select a new ensemble of history-matched models in this activity. Subsequently, a new subset of RMs is selected, based on the freshly selected ensemble of approved models and these RMs are optimized using **Equation 2-2** as the objective function. In short, with this experiment, we are able to seclude and understand the impact of the fourth step of CLFD individually, as well as its impact on the subsequent steps.

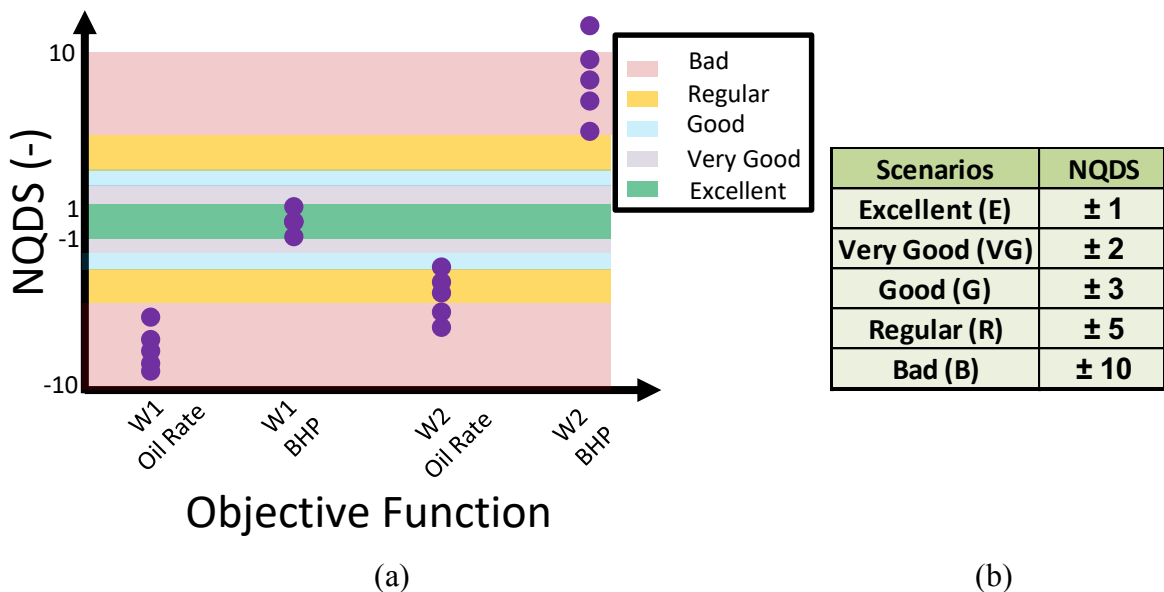


Figure 2-2: (a) Example of NQDS visualization for different objective functions (oil rate and BHP) for well W1 and W2 (adapted from Avansi et al., 2016) and (b) the corresponding NQDS values.

2.2.4 Flexibility of drilling (FoD)

CLFD workflow can also fail in exceptional cases due to a latent and untoward problem associated with “unrealistic” drilling in the “true field”. For example, in practice, one would not start drilling a well from a non-reservoir zone even if the simulation models suggested otherwise. To understand the impact of this problem on CLFD, we decided to use the option of the flexibility of drilling (FoD) with ICM. FoD is a proposed pragmatic drilling approach

for the reference case to partially imitate the real-time decision-making process in the actual world. The method ensures that we drill the heel of the wells in a good reservoir zone by using the available information.

To describe FoD further, since we drilled vertical pilot wells at the heel of all wells, we decided to investigate the petrophysical property using these logs before drilling at the pre-defined location, based on the simulation models. If the heel of a to-be-drilled well is located in a non-reservoir zone, we search for better zones in the vicinity with the help of the FoD approach. In our case, we tested FoD by looking at only the well-logs of the vertical pilot hole, drilled along the heel of the to-be-drilled well, and re-assessed the better locations for the heel of the to-be-drilled well. Porosity, permeability, depth of the reservoir and thickness of the reservoir zone are some of the properties that can be assessed to evaluate the better locations for the heel. Note that once the heel had been drilled, we did not modify the well locations even if the succeeding zones were non-reservoir.

2.3 Application

Motivated by the work of Morosov and Schiozer (2016), we implemented CLFD on UNISIM-I, a benchmark case based on the Namorado field in the Campos basin, Brazil (Gaspar et al., 2014 and Avansi and Schiozer, 2015). The benchmark case study consists of simulation models, built on a coarse-scale grid, as well as a “true field” with known properties in a fine-scale grid. However, taking a cue from the conclusion of Morosov and Schiozer (2016) about the upscaling effect, we decided to use simulation models with a slightly higher-resolution grid, compared to the ones they used. The new simulations models have an average grid-block volume of $75 \times 75 \times 5 \text{ m}^3$, discretized into a corner-point grid of $108 \times 77 \times 32$ cells with approximately 94k active cells, originating from a geological model built using data from 4 vertical exploratory wells (NA1A, NA2, NA3D and RJS19). Apart from the uncertainty associated with the grid properties, the ensemble attempts to quantify scalar uncertainties associated with rock compressibility, oil-water contact, existence and pressure/volume/temperature (PVT) tables of hydrocarbon in the eastern reservoir, vertical permeability multiplier, and relative permeability curves.

The reference case (UNISIM-I-R), on the other hand, is the fine-scale model epitomizing the “true field” in this controlled experiment with all known uncertainties. The average grid-block volume in the reference case is $25 \times 25 \times 1 \text{ m}^3$, with approximately 3.4 million active blocks. The geological model of UNISIM-I-R was built using the public

information of the field with data from 56 drilled wells in the Namorado field (Avansi and Schiozer, 2015).

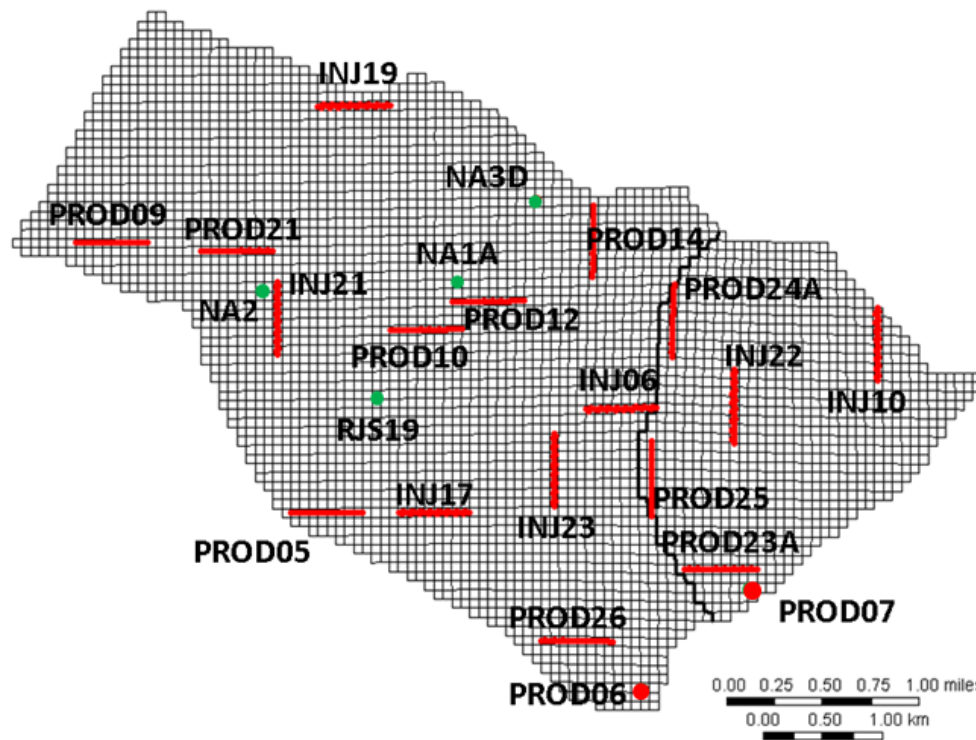


Figure 2-3: Initial PS (PS_1) based on the optimal strategy proposed by Schiozer et al. (2019).

A set of 500 scenarios constituted an ensemble for quantifying the geological uncertainties (permeability, porosity and net-to-gross) of the field, for each cycle of CLFD (**Table 2-2**). Additionally, unlike Shirangi and Durlofsky (2015), the reference case was not in itself at all close to the simulation models, as expected in real-life.

The first 4 vertical wells (shown using green dots in **Figure 2-3**), that provided the information for building the original simulation models, were under production until the 1461st day. Based on this initial production data and other initial inputs, Schiozer et al. (2019) presented the optimized production strategy with 13 producer and 7 injector wells. The same strategy was used as the initial strategy by Morosov and Schiozer (2016). To be consistent, we started with the same well placement strategy as our initial strategy for field development. **Table 2-2** highlights drilling chronology and **Table 2-3** shows the economic parameters for EMV calculation. **Figure 2-3** shows a top view of the initial well placement.

Table 2-2: Drilling chronology and acquired information during different cycles.

Cycle	Well	Opening (days)	Acquired Information
1	PROD023A	1857	East bloc + PVT + Updated OWC + Well-logs
	PROD024A	1887	
	INJ019	1918	
2	PROD010	1948	OWC + Well-logs
	PROD012	1979	
	INJ010	2009	
3	PROD009	2040	Well-logs
	INJ021	2071	
	PROD005	2099	
	INJ022	2130	
	PROD007	2160	
	INJ006	2191	
	PROD014	2221	
4	NA1A	2252	Well-logs
	INJ017	2283	
	PROD025A	2313	
	PROD026	2344	
	INJ023	2374	
	PROD021	2405	
	PROD006	2436	

Table 2-3: Economic parameters and their respective values for three economic scenarios.

Parameters	Units	Scenario 1	Scenario 2	Scenario 3
Oil price	USD/bbl.	50	70	40
Discount rate	%	9	9	9
Royalties	%	10	10	10
Special taxes on gross revenue	%	9.25	9.25	9.25
Corporate taxes	%	34	34	34
Cost of oil production	USD/bbl.	10	13	8
Cost of water production	USD/bbl.	1	1.3	0.8
Cost of water injection	USD/bbl.	1	1.3	0.8
Abandonment cost (% well investment)	%	7.4	9.2	6.5
Drilling, completion and connection of vertical well	USD Million	35	44	30.6
Drilling, completion and connection of horizontal well	USD Million	50	62.5	44.1
Probability	-	0.5	0.25	0.25

2.4 Results

2.4.1 Initial CLFD methodology (ICM)

Three new well-logs (PROD023A, PROD024A, and INJ019), along with the 4 previously existing logs, were used to update the existing geological model and generate a new ensemble of 500 petrophysical properties. Production data of the wells consisting of oil, water, and gas rates and bottom-hole pressure (BHP) were carefully documented after adding noise. PROD023A confirmed the presence and PVT of hydrocarbon in the eastern reservoir. Furthermore, PROD023A and PROD024A also provided vital information to update the oil-water contact in the eastern reservoir.

Similar to Morosov and Schiozer (2016), the new oil-water contact was considered to be at least 3163 meters deep. With the recorded production data and known locations of the 7 already drilled wells, the Kalman-gain localization scheme was used with ES-MDA (a circle of 2000 meters radius) to include the dynamic data to the existing static data of the ensemble. The liquid production rates and water injection rates were used for conditioning the simulation models for the historical period.

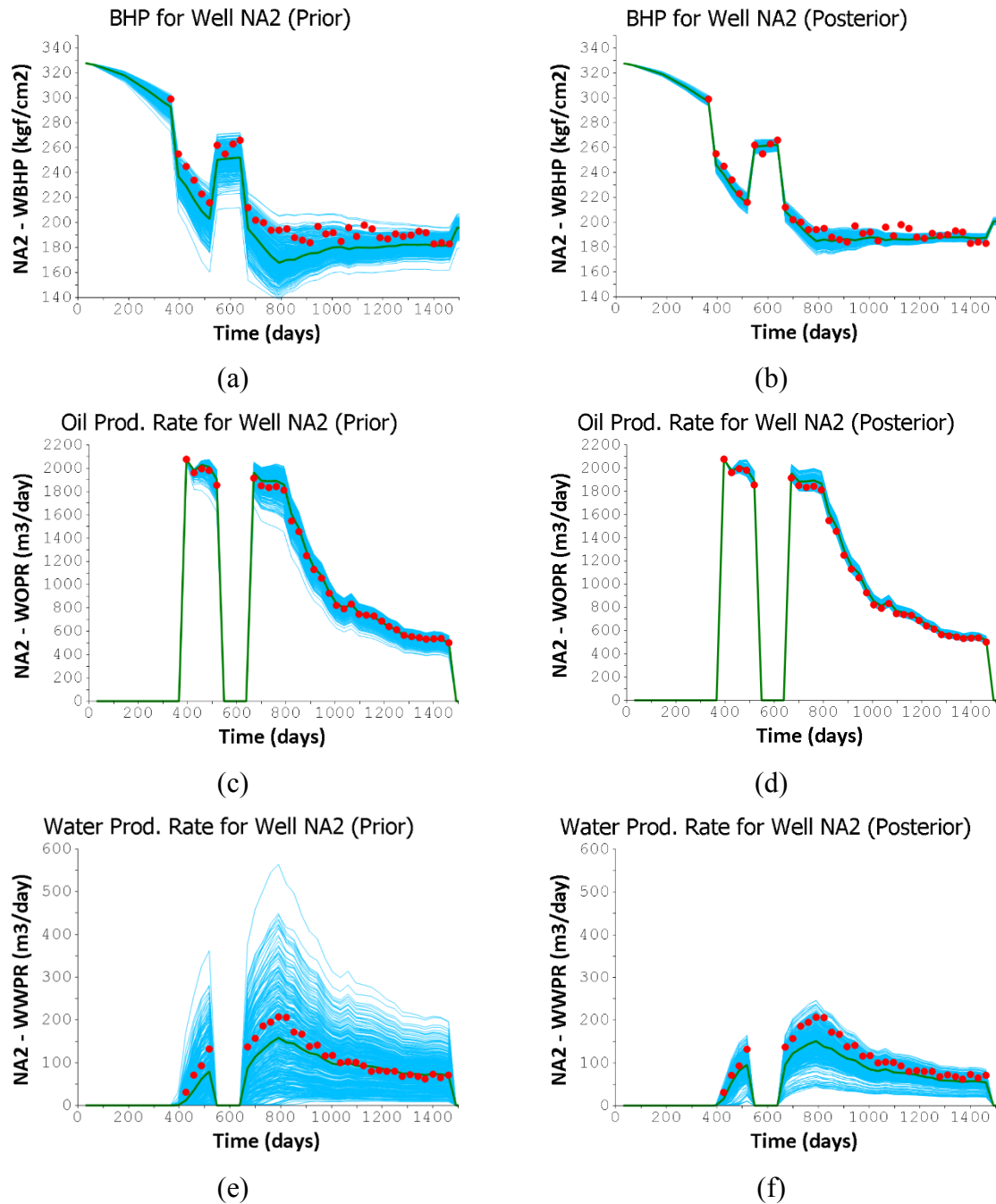


Figure 2-4: Prior and posterior result of history matching is shown by graphs (a) to (f). The prior results are shown on the left while the posterior results are presented by the graphs on the right. The measured data from the reference case, P50 of the ensemble and the ensemble are represented by red dots, green line and blue lines, respectively.

The results of computer-assisted history matching are presented in **Figure 2-4**. **Figure 2-5** shows the prior and posterior range and distribution of non-grid-based uncertainty attributes. The prior and posterior distribution remained unchanged for the oil-water contact (**Figure 2-5c**).

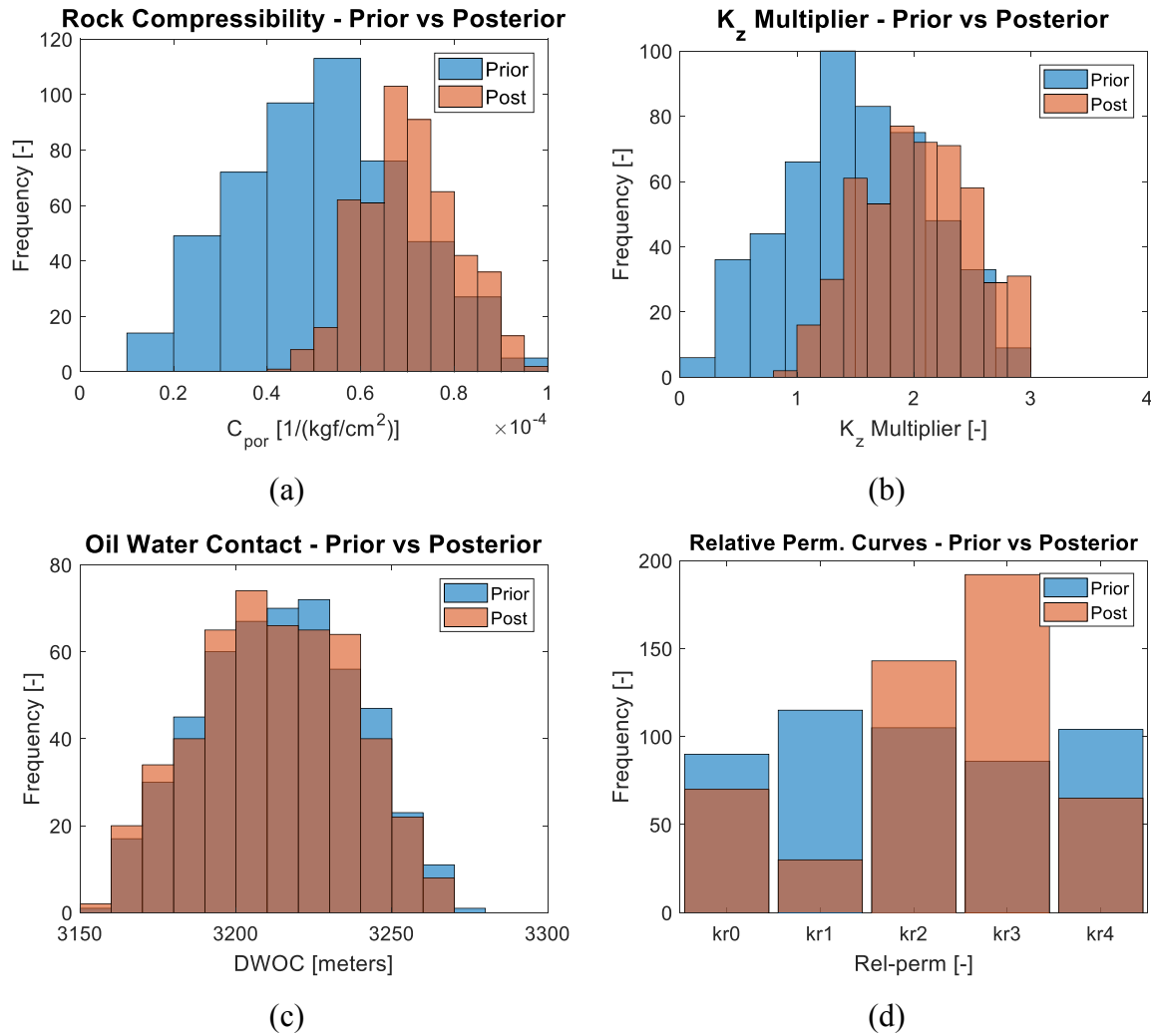


Figure 2-5: Prior and posterior histograms of uncertainty attribute (a) rock compressibility, (b) k_z -multiplier, (c) oil-water contact and (d) relative permeability curves.

Based on the production data for each well in the ensemble of history-matched scenarios, and using an acceptance range of ± 2 for NQDS, we selected a smaller subset of 112 approved models with 30% tolerance values for the 3 newly drilled wells. Successively, EMV, N_p , W_p , ORF of the 112 models, observed for the entire life of the reservoir, were used to select 9 RMs using RMFinder 2.0 software. Finally, PS_1 (**Figure 2-3**) was optimized over the chosen RMs using **Equation 2-1** as the objective function. Only the locations of the undrilled wells were modified to optimize the EMV via optimized PS (PS_{ICM}). We were able to improve the EMV of the 9 RMs by 3%, while the EMV of the whole ensemble was increased by 4%.

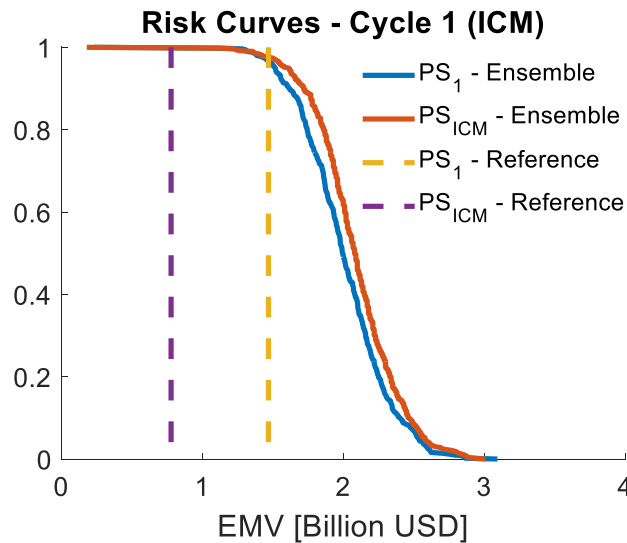


Figure 2-6: Risk Curves prior and posterior to application of ICM.

However, when this optimized PS_{ICM} strategy was implemented on UNISIM-I-R to evaluate the impact of CLFD, a -47% change in the EMV was observed (**Figure 2-6**). Similar to Morosov and Schiozer (2016), the contradictory result obtained by using simulation models and the real response highlights that perhaps the representative models did not depict the "true field", underscoring the need to observe the impact of individual steps of our methodology on the CLFD. This provided an excellent motivation to perform a bottom-up approach to understand the potential problems and propose solutions to improve the original CLFD workflow. As we used simulation models with a finer grid than Morosov and Schiozer (2016) and still attained negative results, we conclude that the upscaling, for this tested case, is not a critical factor for the bias encountered in the process.

2.4.2 Improving optimization (IO)

Based on the negative results obtained in the reference case with PS_{ICM} (obtained in ICM), we decided to test the IO and understand the impact of the optimization process on the overall CLFD workflow. To do that, **Equation 2-1** was replaced by **Equation 2-2** to obtain a new optimized PS (i.e., PS_{IO}) while using the same nine RMs selected during ICM.

Table 2-4: Comparing results obtained with ICM and IO.

Application of optimized strategy on	ICM		IO	
	Δ in EMV	Improved Scenarios	Δ in EMV	Improved Scenarios
RM s	3%	71%	2%	100%
Ensemble	4%	68%	6%	76%
Reference Model (UNISIM-I-R)	-47%	-	-12%	-

Table 2-4 shows the direct consequence of **Equation 2-2**. Given that it improves the likelihood of success of the PS_{IO} over the PS_{ICM} , as anticipated, we observe that for the same RMs used in ICM, the modified equation not only increased the total number of improved scenarios in the ensemble, but also provided better results after implementing the PS_{IO} in the reference case.

2.4.3 Improving approved models (IAM)

In this activity, we continued with the bottom-up approach to analyze and improve the selection of approved models. Instead of continuing with the lenient tolerance defined in ICM, a stricter and standardized tolerance value of 10% was used to filter the ensemble of history-matched scenarios to obtain a set of approved models. A history-matched scenario was considered good if the simulated data was observed within a strict band of $\pm 30\%$ of observed data (or ± 3 NQDS range). Using this criterion, 132 models were approved. Using RMFinder 2.0, 9 new RMs were re-selected out of the newly 132 approved models and re-optimized using **Equation 2-2** as the objective function.

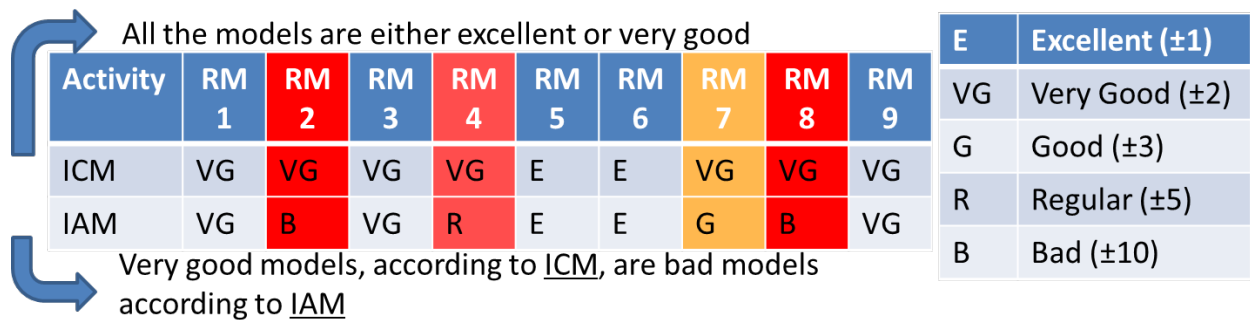


Figure 2-7: Comparing the initial RMs selected using the lenient tolerance conditions of the ICM against the new RMs selected using the stricter tolerance conditions of the IAM.

Figure 2-7 shows the significance of improving the approved set of scenarios, using a stricter tolerance. A brief analysis of the initial RMs selected using the lenient tolerance conditions of the ICM revealed that the inflated tolerance values were making the RMs seem very reasonable for the next step of the CLFD workflow. The original RMs, picked from the set of 112 approved models during ICM, were composed of a few bad models according to the new tolerance conditions specified in IAM.

The new set of RMs of IAM was optimized using **Equation 2-2** as the objective function. As shown in **Table 2-5**, using a better set of tolerance or, in other words, using a

better set of history-matched models, we were not just able to improve the results for simulation models but also the reference case.

Table 2-5: Comparing results obtained with ICM, IO and IAM activity.

Application of optimized strategy on	ICM		IO		IAM	
	Δ in EMV	Improved Scenarios	Δ in EMV	Improved Scenarios	Δ in EMV	Improved Scenarios
RMs	3%	71%	2%	100%	9%	100%
Ensemble	4%	68%	6%	76%	7%	80%
Reference Model (UNISIM-I-R)	-47%	-	-12%	-	+3%	-

As an interesting note, RM 1, RM 3 and, RM 6, which were adjudged as highly satisfactory models (**Figure 2-7**) by both lenient and strict tolerance conditions, were the RMs that ICM failed to optimize. As one would expect, failing to optimize highly satisfactory models while optimizing bad models can have a direct consequence on the optimized strategy (**Table 2-5**).

2.4.4 Flexibility of drilling (FoD)

In the face of negative result obtained during ICM activity, we analyzed the results obtained by implementing the original PS (PS₁) and the optimized PS_{ICM} in the reference case.

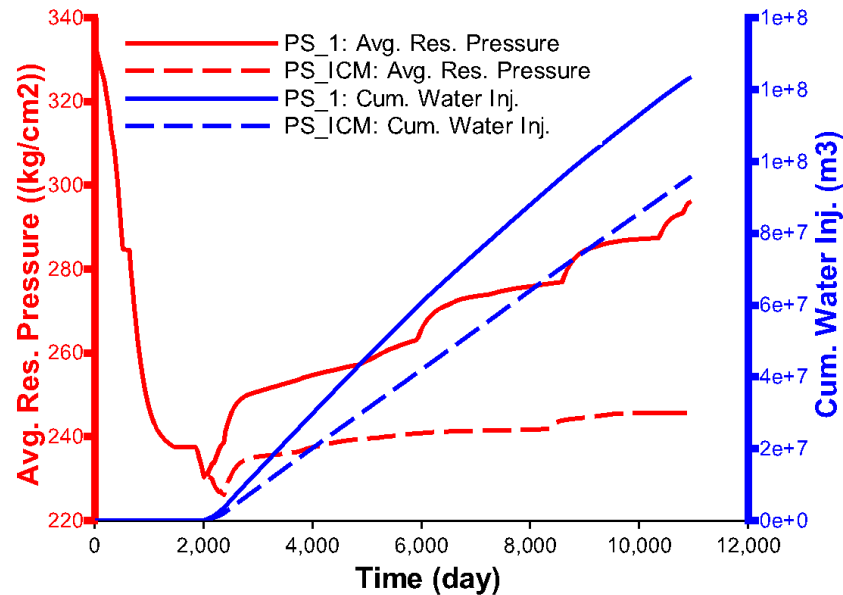


Figure 2-8: Comparing average reservoir pressure and cumulative water injection after implementing PS₁ and PS_{ICM} in the reference case.

One of the first inferences drawn from the analysis (**Figures 2-8** and **2-9**) was that the injectors were placed at poorer locations in such a way that either led to:

- Impeding the water injectivity and, consequently, affecting the average reservoir pressure maintenance and/or,
- A poorer connectivity between producers and injectors; an outcome of poor uncertainty assessment during ICM activity.

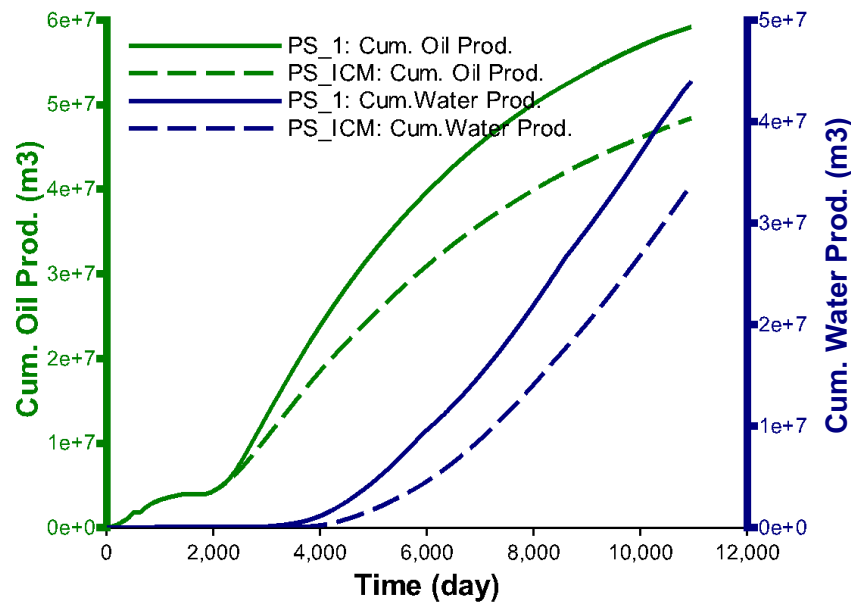


Figure 2-9: Comparing cumulative oil and water production obtained after implementing PS_1 and PS_{ICM} in the reference case.

Given that we were still able to improve the results during the IAM activity, we decided to attribute more significance to the first inference. Based on the first inference, we delved deeper into placement of injectors in PS_{ICM} . We observed that after the optimization process, the selected well locations indicated by the ensemble of RMs were adequate (**Figure 2-10b**). However, when the same well trajectories were drilled in the reference case, some of the wells were observed to be in non-reservoir region (**Figure 2-10a**). This can be attributed to the lack of proper geostatistical variability in relatively unknown and/or heterogeneous areas, as emphasized by the work of Morosov and Schiozer (2016). **Figure 2-10b** strengthens this statement by showing how all the RMs have a sufficiently variable but positively biased porosity map in the vicinity of INJ022. Although, only in terms of porosity map along the trajectory, RM 6 can be considered to be the closest to represent the reference case, it is noteworthy that the ICM failed to optimize the RM 6 due to lack of focus on the likelihood of success of all the RMs.

Due to a lack of perfect reservoir information, encountering unexpected regions while drilling a well is not an uncommon experience especially in a heterogeneous field. Generally,

a real-time decision-making process is a vital part of any drilling campaign. Also, the vertical pilot holes were drilled across the heel of all wells in our case study. Thus, we believe that ignoring this piece of information and continuing with the initial trajectory proposed by the optimization process, using a set of upscaled simulation models, is tantamount to rejecting a big chunk of important information.

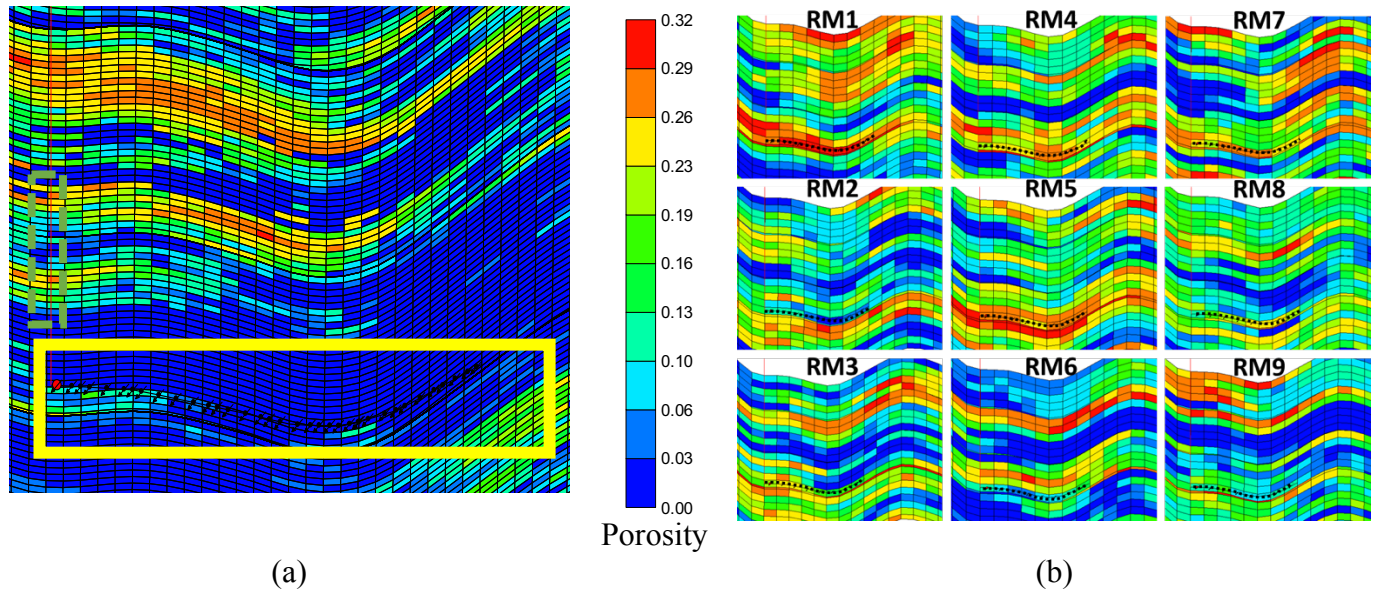


Figure 2-10: Trajectory of INJ022 as proposed by PS_{ICM} in (a) the reference case and (b) the 9 RMs, which were used to obtain PS_{ICM} . Dashed orange box identifies better zones for the heel in the vicinity (FoD).

To accommodate the unforeseen heterogeneities in our controlled experiment, we introduce an option to redress such situations. We propose flexibility of drilling (FoD) approach to deal with such situations. The idea behind FoD is to use the existing information (vertical well-logs in our case) to modify only the heel of the drilled well. Although drilling engineers would not restrict to simply modifying the heel of the well as they continuously avail new information while drilling, we believe it is sufficient to minimize the bias associated with “unrealistically” drilling in non-reservoir zones.

If the heel of a to-be-drilled well was in a non-reservoir zone, we examined the vertical logs for better porous zones in the vicinity and drilled the heel of the well at that superior location. **Table 2-6** shows the results obtained after implementing PS_1 and PS_{ICM} with and without FoD. As anticipated, FoD improves the results without modifying the x and y coordinates of the to-be-drilled well (only the depth is modified). As anticipated earlier, inferior

locations of the injectors played a major role in the negative result during ICM activity (**Table 2-6**).

Table 2-6: Implementing different PS in the reference case.

Implementation of PS in Reference Case	EMV (Billion USD)
PS _I	1.47 (0%)
PS _I (applying FoD for all wells)	1.62 (+ 10%)
PS _{ICM}	0.78 (- 47%)
PS _{ICM} (applying FoD only for injectors)	1.47 (+ 0%)
PS _{ICM} (applying FoD for all wells)	1.49 (+ 1%)
PS _{IO} (applying FoD for all wells)	1.54 (+5%)

2.5 Discussion

The application of closed-loop approach in the first activity led to an increase in EMV based on simulation models, but we observed a decrease in EMV when we implemented this optimized strategy in the reference case. This result, being alike the one presented by Morosov and Schiozer (2016), motivated us to perform bottom-up analysis to improve the workflow and understand the negative result. The bottom-up analysis exposed that the individual steps need to be tailored, understanding the requirements of CLFD as well as the possible consequences of each output on the subsequent process of the workflow.

First, we would like to reiterate that improving the likelihood of success of a PS over a subset of adequately history-matched models, while performing a good uncertainty assessment, can provide a robust strategy to improve the objective function of the project using CLFD. Nevertheless, developing a heterogenous field with or without CLFD comes with its own set of challenges. A lack of appropriate geostatistical variability in relatively unexplored areas brings a challenge that was one of the main factors for the extremely negative result obtained during the first activity (ICM). Because of that, some well locations selected after the optimization process were not adequate for the “true field”. We highlight that, for this study, the geostatistical variability was introduced using well-logs only. We believe that the geostatistical images could have been further improved if we had constrained the images to 3D seismic information to generate more coherent petrophysical images. An image conditioned to good 3D seismic data can always assist in capturing the lateral and longitudinal connectivity of the reservoir, within the resolution of the seismic survey, and thus reducing the chances of failure as observed in Figure 10 and improving the CLFD process.

However, one must note that we implemented the CLFD workflow on all the cases without conditioning our geostatistical uncertainties to 3D seismic data or any additional data that was acquired before drilling the first well. As CLFD implies developing a field using the information acquired in between the development cycles (**Table 2-2**), using any prior additional information that was not used to obtain the initial strategy (Schiozer et al., 2019) would have had created an artificial bias in the results affecting the evaluation of the CLFD workflow.

Nevertheless, while evaluating the graphs and well economic indicators for the "true field", it was quite evident that the exceedingly negative result during the first activity was unrealistic. It is an artifact, mainly due to drilling wells nonchalantly in the true field, and wrongly assuming that the well locations provided by upscaled simulation models are perfect.

Furthermore, considering that we have some operational flexibility to drill a horizontal well according to the information provided by pilot hole(s), we stress the importance of flexibility of drilling (FoD) approach as a way to redress the above described bias associated with drilling a well due to lack of information during field development. At the same time, one must note that FoD is a subjective assessment and better understanding of the reservoir can improve the sweep efficiency and drainage strategy. Seismic information is, generally, a commonly used source of information for improving the drilling decisions and thus, can improve FoD as well.

Whereas improving the optimization process and the process for approving history-matched models helped us develop a better understanding of CLFD, the study would be incomplete without a concise discussion of the significance and potential improvements for other components of the workflow:

1. Provided the uncertainty assessment is performed adequately, a better set of RMs can always improve the likelihood of success of a PS in the reference case. This is evident by a direct correlation between the number of scenarios being improved by a certain PS and change in EMV after implementing the same PS in the reference case. Based on the number of scenarios being improved (**Table 2-5**), we have ample indications that either the quality of RMs or the number of RMs need to be improved to increase the likelihood of success of the optimized strategy over the ensemble and consequently the reference case.
2. Computer-assisted history matching plays an important role in indirectly improving the objective function of a project while maintaining reliable models (Jansen, et al., 2009 and Pettan and Stromsvik, 2013). Based on the importance of streamlines in defining the

localization volume (Soares et al., 2018), using them can further improve the data assimilation process.

3. The first two steps in the CLFD are important for the quantification of uncertainties. Good uncertainty quantification forms a strong base for the next processes. Petrophysical models can be improved with better geological inputs. As mentioned before, other sources of information, such as seismic, could diminish the spatial variability in uncertainties and hence, could potentially decrease some of the biases of the closed-loop process. However, a discussion on this subject is out of the scope of this work. Updating inputs (range and probability distribution function of uncertainty attributes), for the simulation model, is solely based on the new information being provided and, at this moment, we consider this is to be perfect information.

2.6 Conclusions

This paper presents the framework of a systematic approach based on bottom-up analysis to improve workflow for model-based closed-loop field development, while evaluating the individual steps and asserting their significance. Some of the most important conclusions of our analysis are listed here:

- Propagation of specious scenarios/outputs from the output of the preceding step to the input of the following step can lead to an overall bias in the results of CLFD.
- Robustly optimized RMs, using a bi-criterion objective function focusing on EMV as well as improving EMVs of individual RMs, can improve the likelihood of success over the ensemble as well as the real response.
- Accepting poorly history-matched scenarios can lead to an inferior set of RMs and, consequently, influence the optimization process and the likelihood of success of a PS in the reference case.
- Similar to Morosov and Schiozer (2016), we obtained a negative result even when we used relatively fine-scaled simulation models compared to theirs. However, by improving the methodology, we were able to obtain a positive result with CLFD. Thus, upscaling, highlighted as one of the possible reasons for the pitfalls by Morosov and Schiozer (2016), was not a critical factor for the negative bias found in this case.
- Given that we work with limited information during the field development process, a pragmatic drilling approach in the reference case must be exercised to partially imitate the real-time decision-making process in the actual world. The proposed FoD is one

such method to ensure that we do not start drilling wells in the non-reservoir zone by utilizing the available information.

- Based on the different analyses conducted in this work, we improved the overall closed-loop field development methodology by improving individual steps.

Acknowledgements

This work was conducted with the support of Libra Consortium (Petrobras, Shell, Total, CNOOC, CNPC and PPSA) within the ANP R&D tax as "commitment to research and development investments" and Energi Simulation. The authors are grateful for the support of the Center of Petroleum Studies (CEPETRO-UNICAMP/Brazil), the Department of Energy (DE-FEM-UNICAMP/Brazil) and Research Group in Reservoir Simulation and Management (UNISIM-UNICAMP/Brazil). In addition, a special thanks to CMG and Schlumberger for software licenses. The authors would also like to thank Alexandre A. Emerick (Petrobras) for providing the EHM tool.

Nomenclature

List of Abbreviations

BHP	Bottom-hole pressure
CLFD	Closed-loop field development
DECE	Designed exploration and controlled evolution
EMV	Expected Monetary Value
ES-MDA	Ensemble smoother multiple data assimilation
FoD	Flexibility of drilling
HM	History matching
IAM	Improving approved models
ICM	Initial CLFD methodology
IO	Improving optimization
OF	Objective function
n	Total number of representative models
N_p	Cumulative Oil Production
NQDS	Normalized quadratic distance with sign
ORF	Oil recovery factor
OSV	Optimization with sample validation

P	Probability value
PS	Production strategy
PVT	Pressure, volume, temperature
RF	Recovery factor
RM(s)	Representative Model(s)
W_p	Cumulative water production
WBHP	Well bottom-hole pressure
WOPR	Well oil production rate
WWPR	Well water production rate

Superscript

0	Initial value
<i>i</i>	Iteration

Subscript

1	Initial production strategy
IAM	Optimized Production strategy after activity 3 (improving approved models)
ICM	Optimized Production strategy after activity 1 (initial CLFD methodology)
IO	Optimized Production strategy after activity 2 (improving optimization)
<i>k</i>	Index of RM

3 Application of Risk-informed Closed-loop Field Development Workflow to Elucidate the Evolution of Uncertainties

Authors:

Ashish Kumar Loomba

Vinicius Eduardo Botechia

Denis José Schiozer

Abstract

Closed-loop field development (CLFD) is an exhaustive combination of multidisciplinary tasks to use frequently acquired data for optimizing a pre-defined objective function of the field development plan (FDP). Although new information is bound to decrease the uncertainty around field development, previous studies have shown that CLFD could fail for several theoretical reasons. In this work, a risk-informed CLFD process is introduced to increase the chances of success of the optimized FDP in the true field. A risk-informed CLFD utilizes insights from a systematic approach for evaluating risks associated with field development to make robust decisions for the true field. We implemented the risk-informed CLFD methodology on two different case studies: (I) a scenario with mostly horizontal wells and, (II) a scenario with all vertical wells. While one of the previous studies has shown that CLFD can decrease the NPV by 2% for the presented case study I, our workflow validates the importance of the risk-informed CLFD by improving the net present value (NPV) of the project by 14%. Implementation of CLFD on case study II validates the workflow once again by improving the NPV by 40%. As with previous studies, we considered the project objective function (i.e., NPV) as the key performance indicator of the CLFD. While the performance indicator suffices the requirement of evaluating our methodology, in this work we delved deeper to understand how the intermittently acquired information influences the ensemble of simulation models and uncertainty assessment. We discuss that further fine-tuning the objective function of the optimization problem can improve the likelihood of success in the

true field. The paper presents two case studies that are based on a field-scale benchmark model in an attempt to answer the questions about the purport of a field development process with multiple phases while acquiring and utilizing information intermittently. Also, the work validates the risk-informed CLFD methodology to encourage tests on more complex fields. Some key observations to improve the CLFD methodology further are also discussed in the work.

Keywords

Field development; Optimization; Data assimilation; Reservoir simulation; Uncertainties; Decision-making

3.1 Introduction

A field development plan (FDP) for a greenfield is fraught with numerous critical decision-making processes (Schiozer and Mezzomo, 2003; Ahmed and Meehan, 2012). A dearth of information and copious technical and geological uncertainties around the field renders the task even more arduous. Despite these challenges, a multidisciplinary team is mandated to make several front-end investment decisions regarding infrastructure and wells to make the project as profitable as possible. Generally, this is performed by analyzing several hypothetical scenarios to forecast the long-term production of hydrocarbons and the corresponding monetary return.

However, this conventional field development process offers a suboptimal FDP due to a huge gap in information as well as uncertainties. To avoid such subpar FDP, this is where the feedback-based field development process comes into play. Similar to the objective of drilling an appraisal well, a feedback-based field development process attempts to obtain information through newly drilled development well(s) for improving the project objective function (net present value (NPV), recovery factor (RF), etc.) by modifying the flexible decision variables (number, type, and location of wells, etc.) in the FDP. Integrating new data with the existing information can potentially aid the multidisciplinary team to better understand the field for making well-informed decisions (Jansen et al., 2009).

While there is an extensive list of studies on conventional field development optimization (see Bittencourt, 1994; Beckner and Song, 1995; Nesvold et al., 1996; Cullick et al., 2005; Isebor et al., 2014a; Schiozer et al., 2015), very limited work has been done in the area of feedback-based field development. Although the concept of economically improving

reservoir performance with feedback-based field development and management process has existed for a long time (see Chierici, 1992), Shirangi and Durlofsky (2015) first successfully explored this idea under the label of closed-loop field development (CLFD).

Shirangi and Durlofsky (2015) defined CLFD as a cyclical process, based on three steps, starting with the optimization of FDP under the existing geological information, followed by drilling wells to obtain logs and production data and, eventually, using this new information to amend the ensemble of simulation models. The authors optimized FDP (controls for the existing wells and type, location, and controls for the to-be-drilled wells) using a hybrid particle swarm optimization-mesh adaptive direct search algorithm (Isebor et al., 2014b). They performed data assimilation (DA) using the adjoint method alongside the randomized likelihood procedure (Oliver et al., 1996) to update the ensemble in the third step. The authors also employed multilevel optimization with sample validation to test if the selected representative models (RMs) were representative of the entire ensemble. They tested their methodology on 2D synthetic field examples to prove that CLFD can help boost the project's objective function. Even though the reference case (or “true field”) was one of the models within the initial ensemble, they observed both positive and negative results.

On the other hand, Morosov and Schiozer (2016) identified data assimilation and optimization as the two critical components of the CLFD process. They performed history matching (HM) and FDP optimization (well location) using ensemble smoother with multiple data assimilation, ES-MDA (Emerick and Reynolds, 2013), and designed exploration and controlled evolution algorithm (Yang et al., 2007), respectively. The authors applied their workflow to the three-dimensional UNISIM-I benchmark case (Gaspar et al., 2015; Avansi and Schiozer, 2015). It is based on the Namorado Field in the Campos Basin, Brazil. Negative results obtained during the process prompted the authors to postulate the pitfalls associated with CLFD. Convergence of HM parameters to non-representative values, upscaled or low fidelity simulation models and lack of variability in petrophysical properties were hypothesized as the main reasons for the observed discrepancy. While the authors presented negative results with lesser information, we point out that they achieved positive results in the final cycle, which is in line with the idea that information plays a critical role in CLFD.

In their work, Hidalgo et al. (2017) presented a workflow based on four cyclical steps: HM, selection of RMs, optimization, and acquisition of new logs and production data. While the authors used ES-MDA to perform HM, they employed a genetic algorithm with nonlinear constraints-based method (Emerick et al., 2009) for optimizing the FDP (number, type, and

location of wells). The RMs were also selected using a genetic algorithm (Armstrong et al., 2013). The application of the CLFD process on the UNISIM-I benchmark case provided an improved project objective function. However, they did not work under the same controlled-environment as Morosov and Schiozer (2016). Additionally, while the observed monetary gain reached an optimal value after a certain number of cycles, it decreased towards the end cycles, contrasting the basic notion of CLFD (i.e., an increasing amount of information can reduce uncertainties to improve results). Although the number of wells is an important variable, it can create bias in evaluating a CLFD process. A strong correlation between the decreasing number of wells and the increasing monetary gains in Hidalgo et al. (2017) is a good example of such bias. This correlation makes it difficult to separate the overall monetary gain between the improvement caused by the decreasing wells and CLFD workflow. It is also interesting to note that the difference between the well locations in optimized FDP of cycle 0 and cycle 1 is minimal, even after performing more than 1000 experiments. These observations raise some important concerns about the methodology.

Instead of optimizing the complete FDP, Hanea et al. (2017) proposed a “drill and learn” workflow to optimize a strict drilling order for wells using the entire ensemble of simulation models. The latter part, however, was in direct contrast with the implied conclusions of Shirangi and Durlofsky (2015), who showed that using a large ensemble for FDP optimization could yield suboptimal results. Stochastic simplex approximate gradient (StoSAG) and ES-MDA were used for optimization and DA, respectively. To simplify further, the authors limited the scope of work by using production data assimilation as the only means of updating the simulation models. They observed a positive effect of the frequency of new information on the monetary gains using two different scenarios for the truth model. It is also noteworthy that the authors obtained a negative result in one of the case studies. The authors hypothesized that some realizations might be yielding negative results even when the mean of the ensemble was being optimized, leading to a negative result in such a case. Given that they worked with a simple 3D model while reducing the challenges of field development and working only with DA, the observed negative result raises the concern about the application of their methodology in a real field. Furthermore, it is interesting to note that although they introduced the “value of learning” as a new concept of evaluating the benefits of newly assimilated information, they presented four ambivalent measures to quantify it.

Kim et al. (2018) proposed a new CLFD workflow using ensemble Kalman filter for HM and particle-swarm optimization for optimizing the FDP. Apart from other FDP variables,

the authors proposed the conversion of suboptimal production wells to injection wells as a way to optimize FDP with the newly available information. Similar to Hanea et al. (2017), the study emphasized HM as the only way of introducing new information to the existing simulation models. The authors demonstrated the workability of CLFD results using a 2D synthetic case.

Prompted by the pitfalls postulated by Morosov and Schiozer (2016), Loomba et al. (2020) implemented their workflow on the benchmark case study (UNISIM-I). They worked with a higher fidelity of models, when compared to Morosov and Schiozer (2016), to minimize any bias associated with upscaling. However, their workflow yielded negative results, resounding with the conclusion of Botechia et al. (2018), i.e., the upscaling process had minimal impact on the adverse results reported by Morosov and Schiozer (2016). The authors performed three more activities to unravel other potential problems inherent in the workflow using a bottom-up approach. The authors introduced the concept of flexibility of drilling (FoD) to overcome the negative and unrealistic bias associated with well representation. With the FoD approach, they ensured that the heel of a well was not drilled in the non-reservoir zone, an unbiased and pragmatic attempt to replicate real-time decision-making processes. Nonetheless, the proposed ideas were not tested on a complete cycle, which begs the question of its applicability in field applications.

As endorsed by all previous studies, CLFD is an intuitive concept to assist multidisciplinary teams to maximize field objective function while working with uncertainties. Despite this, none of the work supports the employment of this concept in the real field. This is simply because both negative and positive results were observed in all the studies working on 3D field development using CLFD workflow. Furthermore, none of the previous work delved deeper and explained the impact of an individual step as well as all the steps of CLFD on uncertainties during the field development. We believe this description of the implicit working of steps is the key to highlight the changes observed in the explicit objective function being observed and optimized. Such descriptions would enthuse more confidence in the significance of CLFD and enable further improvements in the CLFD process.

3.2 Objectives

Understanding the gaps in the literature, the paper endeavors to discuss an improved and risk-informed CLFD workflow for real-field applications. In this work, we attempt to provide a diverse and all-inclusive perspective on the subject to address some of the previously unanswered questions. The specific objectives of the work include:

1. Bearing in mind that Morosov and Schiozer (2016) presented disagreeing results with a benchmark representative of a real field, repeat the same field development scenario to analyze the risk-informed workflow as well as systematically investigate the steps to further improve the CLFD workflow.
2. Employ the CLFD workflow on another case study with only vertical wells to validate the applicability of the newly improved workflow in an alternative case and stressing any key differences while implementing CLFD for a field with vertical versus horizontal wells.
3. Present the significance of using the flexibility of drilling (FoD) in a closed-loop workflow by avoiding “unrealistic” results obtained via knowingly completing the heel of a well in a non-reservoir zone.
4. Present a comprehensive discussion on the evolution of uncertainties as individual components of the risk-informed workflow are being realized. As most of the previous work rarely focused on this aspect, we attempt to reinforce confidence in the feedback-based field development process by providing an intuition into the working of the methodology by contemplating our evolving ensemble of models.
5. Introduce the concept of the value of closed-loop (VoCL) as a way of quantifying the impact of new decisions on the monetary objective function of the project as well as analyzing the bias related to model-based decisions.

3.3 Methodology

As discussed in the previous sections, the main objective of implementing CLFD is to maximize the field’s objective function. Thus, the final decision based on the outcome of the CLFD process must be made wisely while considering the huge envelope of uncertainty. A poor decision will still improve the objective function for the simulation models but will fail to improve the true field, rendering the CLFD process futile. Therefore, it is vital to have a methodology that makes robust decisions under uncertainty, and in this section, we endeavor to elaborate on our risk-informed CLFD workflow to assist in making such robust decisions.

A risk-informed CLFD is a cyclical process that utilizes insights from a systematic approach for evaluating risks associated with field development to make robust decisions for the true field. Assuming the uncertainties are quantified properly, the process meticulously assesses the uncertainties and expels the scenarios that might hamper the optimization process. The FDP is optimized while maximizing the likelihood of success by using an ample set of RMs honoring the uncertainties. The workflow also uses different performance measurement

tools to make deliberate decisions. In the subsequent section, we present one cycle of the risk-informed CLFD workflow as follows (**Figure 3-1**):

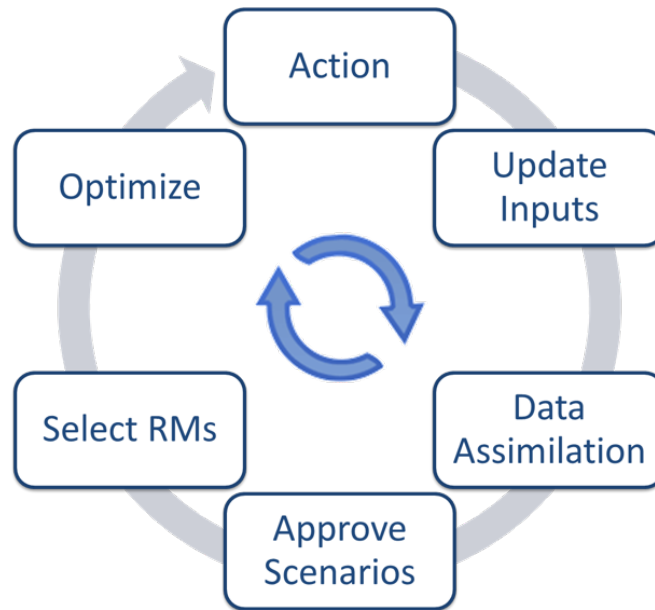


Figure 3-1: Generalized CLFD workflow (adapted from Chapter 2).

1. **Action:** The first step of CLFD workflow entails acquiring new hard data in the form of well logs, seismic interpretation, near-wellbore analysis, etc. using newly drilled wells, 3D and/or 4D seismic acquisition, well test and/or other forms of reservoir surveillance techniques. This newly acquired information can be used to build a new or update the existing geological model.

In this work, however, we restricted ourselves to using only new well logs as the source of information to update the initial ensemble of petrophysical inputs for reservoir simulation. We generated a set of 500 equiprobable and geologically consistent petrophysical properties using random seeds to capture the geological uncertainties. We also registered the field production data during this phase. Assuming that we do not have accurate measurement gauges on the field, we added noise to the production data to make it imperfect, which is similar to a real field data.

2. **Update Inputs:** Aside from improving the geological model, the hard data acquired during the previous step can also provide supplemental information for updating the known and/or previously unknown uncertainty attribute (UA). This information can be either direct (existence and PVT of the hydrocarbon in the neighboring reservoir, the true vertical depth of oil-water contact, etc.) or indirect information (interpreted skin-factor, interpreted oil-water contact, etc.). Updating the probability distribution

function of UAs, based on direct and/or indirect information, is a critical aspect for reducing uncertainty by updating the simulation models.

At the end of this stage of work, we used discretized Latin hypercube combined with geostatistical realizations (DLHG), and this was used together with updated inputs of UAs and petrophysical images, to generate a new ensemble of 500 scenarios to capture the field uncertainties (Schiozer et al., 2017).

3. Data Assimilation: Assimilation of available production, seismic, RFT/PLT data is the third component of the workflow. The main idea behind this step is to integrate the static knowledge of the field with dynamic information. To systematically integrate information, scalar uncertainty attributes (e.g., rock compressibility, oil-water contact, etc.), as well as grid-based petrophysical properties (e.g., porosity, permeability, etc.), are modified to minimize the mismatch between the measured field data and the simulated data of the ensemble.

The computer-assisted DA process enables expressing the mismatch between measured field data and simulated data as an optimization problem with the mismatch itself being the objective function of the problem (Evensen, 2007; Oliver et al., 2008). Ensemble smoother with multiple data assimilation (ES-MDA), an ensemble-based method introduced by Emerick and Reynolds (2013), is used to perform production data assimilation in this work. The objective function (\bar{O}) of the ES-MDA is the average normalized data mismatch, which can be written as:

$$\bar{O} = \frac{1}{2N_d N_e} \sum_{i=1}^{N_e} (d_i - d_{obs,i})^T C_e^{-1} (d_i - d_{obs,i}) \quad 3-1$$

where N_d is the number of production data observations, N_e denotes the size of the ensemble, d_i denotes the vector of predicted production data of the i^{th} simulation scenario, $d_{obs,i}$ is the vector of perturbed observations corresponding to the i^{th} simulation scenario, and C_e is the covariance matrix of the measurement errors. In this work, C_e was built by assuming BHP measurement error as a constant value of 10 kgf/cm². In parallel, we consider the rate measurement error to be the maximum value between 10% of the measured rate and the constant value of 10 m³/day.

Furthermore, the Kalman gain localization scheme is used with ES-MDA (Soares et al., 2018) to perform data assimilation by modifying the grid-properties in

the pre-defined neighborhood of producers and injectors. In other words, only the localized areas influenced by respective wells are modified, while the rest of the grid properties are left unchanged. Unlike Chapter 2, the geometry of the localization volume is selected, based on the streamlines obtained by simulating with averaged grid-properties of the complete ensemble (Soares et al., 2018), and average normalized data mismatch (\bar{O}) was used as a performance measurement tool.

4. Approve Scenarios: A smaller subset of scenarios ought to be selected from the entire ensemble to save costs associated with expensive simulations and exclude very bad scenarios. In this work, we used the normalized quadratic distance with sign (NQDS) method (Avansi et al., 2016) to filter the scenarios, which is ratio of the quadratic distance with signal (QDS) and acceptable quadratic distance (AQD):

$$NQDS = \frac{QDS}{AQD} \quad 3-2$$

$$QDS = \frac{SD}{|SD|} \times \sum_{j=1}^n (obs_j - sim_j)^2 \quad 3-3$$

$$AQD = \sum_{j=1}^n (obs_j \times \gamma + \delta)^2 \quad 3-4$$

$$SD = \sum_{j=1}^n (obs_j - sim_j) \quad 3-5$$

where sim_j and obs_j are the simulated and measured field data at time j , respectively; n denotes the total number of time-steps for which field data was recorded; γ is the tolerance value, while δ denotes the constant to avoid a division by 0. SD stands for simple distance (Avansi et al., 2016) and calculates the difference between measured and simulated field data summed over the n time-steps.

Selecting bad or implausible scenarios for the optimization process can have a direct and, potentially, undesirable impact on the optimization of the FDP (see Chapter 2). As such, a tolerance value of 10% was deemed appropriate in our work to account for errors in the simulation model.

5. Select RMs: Even though a smaller subset is picked by the end of the previous step, it is infeasible to work with a large number of approved scenarios (AS) for further analysis, especially in the optimization process. Schiozer et al. (2004), Armstrong et al.

(2013), and Sarma et al. (2013) presented different methods for selecting a smaller subset from the original ensemble of scenarios while ensuring a good representation of the original set.

In this work, we use RMFinder 2.0 software developed by Meira et al. (2017) which provides a set of RMs with the individual probability of each RM. To obtain a set of RMs, firstly, the approved models were simulated for the entire lifetime of the field to obtain the net present value (NPV), cumulative oil production (N_p), cumulative water production (W_p), and oil recovery factor (ORF). RMFinder 2.0 selects RMs and their probabilities to represent the NQDS approved models by expending the above-mentioned objective functions. Since the main idea is to represent the uncertainties with RMs as adequately as possible, the number of RMs can be deliberately increased or reduced based on engineering judgement. In this work, we selected nine RMs based on the work of Meira et al. (2017) and Schiozer et al. (2019).

6. Optimize: One of the main purposes of integrating multiple and non-additive information sources is to optimize FDP. CLFD provides ample opportunity to update flexible decision-variables, including but not limited to: number, type, location, opening schedule, control and trajectory of to-be-drilled wells, and control and conversion of existing wells. Furthermore, there are several gradient-based (Wang et al., 2007; Zandvliet et al., 2008; Sarma et al., 2008; Loomba, 2015) and gradient-free algorithms (Yeten et al., 2002; Badru and Kabir, 2003; Emerick et al., 2009) to optimize FDP. Moreover, optimization of decision variables can be performed either simultaneously or sequentially (Shirangi and Durlofsky, 2015).

Based on the selected RMs, in this work, we optimize the FDP by modifying the well locations of the undrilled wells only. We perform the optimization using a gradient-free algorithm based on iterative discrete Latin hypercube (IDLHC), proposed by Hohendorff Filho et al. (2016). The algorithm uses the correlation between prior frequency distribution of discrete variables (e.g., location of the heel of a well, direction, etc.) and the objective function to update the posterior frequency distribution of the variables to maximize the objective function. The RMs, selected in the prior step, were robustly optimized (van Essen et al., 2009; Silva, 2018) utilizing a new bi-criterion objective function, which focuses on improving the likelihood of success of the optimized FDP over the ensemble and, consequently, the “true field”:

$$OF^i = \sum_{k=1}^n If (NPV_k^i - f_c * NPV_k^0 > 0, P(RM_k) * NPV_k^i, 0) \quad 3-6$$

where NPV_k^i and NPV_k^0 stand for the NPV of the i^{th} scenario and the initial scenario of the k^{th} RM, which has a probability of occurrence $P(RM_k)$. Unlike Chapter 2, we added f_c as the cut-off frequency to ensure that the OF is non-zero. This provides a good set-up to penalize the scenarios in which all the RMs are not being improved above the cut-off NPV. In our work, we ensured that f_c was close to 1 by the end of the optimization process to pick the best scenario in which all the RMs were being improved.

To make the process even more risk-informed, we test the economic viability of the individual systems of the FDP at the end of the optimization. Based on Botechia et al. (2013), we calculate the economic viability of the wells by re-calculating the NPV without the to-be-drilled well, one at a time, and comparing it with the optimized NPV of the field. If an increase in NPV is observed when removing a given to-be-drilled well, we modify the well type and/or location of that well to further improve the NPV while still considering uncertainties revolving around the selected RMs. Although one could simply delete the economically unreasonable wells in such a case and continue with a reduced well count, we wanted to ensure that the final NPV improvement in the “true field” is not biased by this decreasing well count.

Finally, we apply the optimized strategy to the reference case UNISIM-I-R (the model emulating “true field”), to evaluate the CLFD workflow. However, given that we work with imperfect information during field development, Chapter 2 suggested exercising a pragmatic drilling approach in the reference case to partially imitate the real-time decision-making process in the real world. An automatic procedure for optimization may suggest a good region to drill a well based on the RMs, but the same might not be a good region in the reference case due to intrinsic failure to capture uncertainties entirely. Therefore, unlike the original methodology, we include the flexibility of drilling (FoD) as a supplementary tool to ensure that we do not drill the heel of the wells in a non-reservoir zone using the available information. Furthermore, to restrict unconscious bias, we implemented the FoD approach on the to-be-drilled wells during the subsequent cycle of CLFD only.

In this work, we also introduce the value of closed-loop ($VoCL$) as a new performance indicator tool to empirically evaluate the significance of a CLFD workflow. Since we acquire, include, and utilize new information during each cycle and these steps account for improved

understanding of the field, the value of closed-loop workflow also represents the maximum amount of resources a decision-maker would be willing to invest before applying the closed-loop workflow.

To quantify the value of improved understanding of our project, based on updated FDP, we present two definitions:

1. The expected value of closed-loop ($EVoCL$) provides a projected improvement in the project's objective function (POF) when an optimized FDP is implemented on simulation models. This value is always positive, as the main objective of any field development is to optimize the FDP:

$$EVoCL_i = \sum_{k=1}^n P(S_k) * \{POF_{FDP_{i+1}} - POF_{FDP_i}\}_k \quad 3-7$$

In **Equation 3-7**, $EVoCL_i$ represents the expected POF value improvement during cycle i alone. $P(S_k)$ represents the probability of the k^{th} simulation scenario. FDP_{i+1} and FDP_i denote the optimized strategy (FDP) for the given cycle i and optimized strategy for the prior cycle, respectively. We calculate the $EVoCL$ for each cycle independently as the ensemble keeps evolving for each cycle i . $EVoCL$ also provides an excellent criterion to assist in deciding the application of optimized FDP in the true model.

2. The actual value of closed-loop ($\overline{\overline{VoCL}}$) measures the true impact of the updated decisions (optimized FDP) on the project NPV. As seen in the previous work, $\overline{\overline{VoCL}}$ can be negative for several reasons. Such results are, however, good indications to either improve the methodology or include more information to improve the essential value of CLFD.

$$\overline{\overline{VoCL}}_{(Cy2-Cy1)} = POF_{FDP_{Cy2}}^{Ref} - POF_{FDP_{Cy1}}^{Ref} \quad 3-8$$

In **Equation 3-8**, $\overline{\overline{VoCL}}_{(Cy2-Cy1)}$ represents the value of closed-loop in between two cycles, $Cy1$ and $Cy2$ ($Cy2 > Cy1$), by comparing the value of the project's objective function POF attained by implementing the optimized decision for $Cy2$ (i.e. FDP_{Cy2}), against the value of POF using the best decision for $Cy1$ (i.e. FDP_{Cy1}). One must note that **Equation 3-8** only applies to the reference case (Ref).

3.4 Application

We used the UNISIM-I benchmark model (**Figure 3-2**) to build our case studies. This synthetic benchmark case is based on the Namorado Field in the Campos Basin of Brazil. It was prepared for oil field management and development applications (Gaspar et al., 2015; Avansi and Schiozer, 2015) and it consists of a reference case UNISIM-I-R and an ensemble of simulation models UNISIM-I-D.

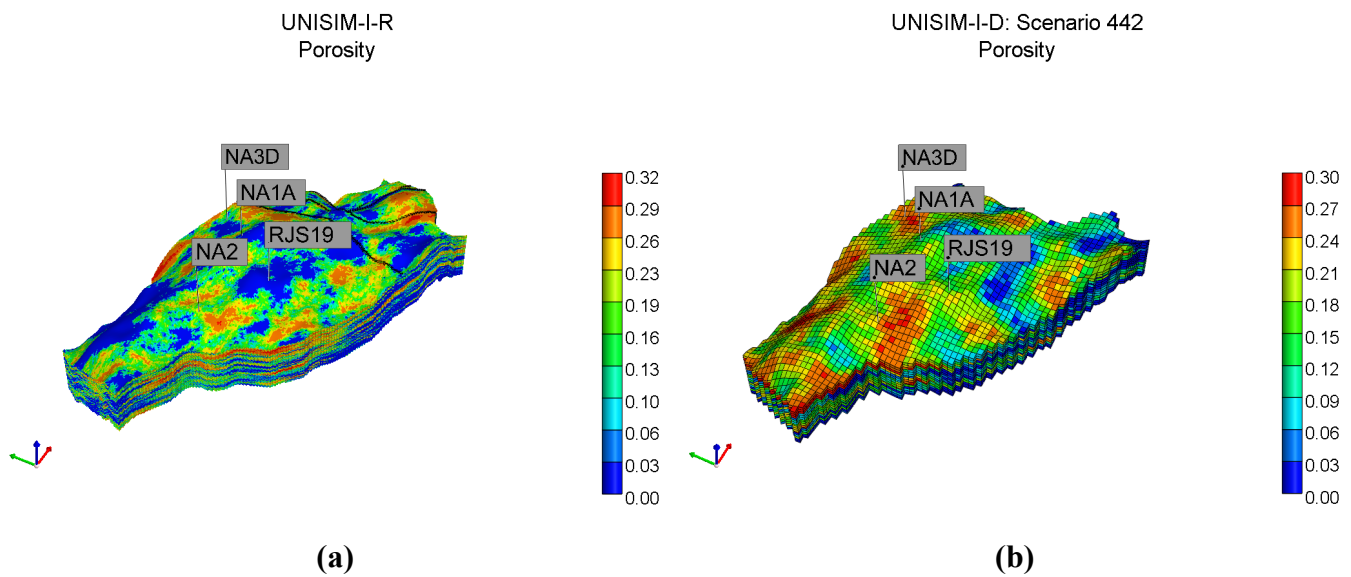


Figure 3-2: The benchmark UNISIM-I case consists of a true field presented by the (a) reference case (UNISIM-I-R) and (b) lower fidelity models (UNISIM-I-D) for simulation (we present one of the scenarios here). Note how different the true field is to a random seed of UNISIM-I-D as the initial ensemble is devoid of important information.

3.4.1 Reference case (UNISIM-I-R)

UNISIM-I-R, or the reference case, was built with the primary objective of emulating a “true field” scenario. The geological model of the reference case was created using publicly available information on the Namorado Field, using as many as 56 logs from wells drilled on-site. This fine-scaled simulation model for the reference case consists of approximately 3.4 million active grid-blocks with an average block volume of 25 x 25 x 1 m³. As the reference case represents the “true field”, the model defines the true geological and petrophysical properties. One must also note that production data, in addition to new well logs, were obtained using UNISIM-I-R simulation and geological model, respectively.

3.4.2 Simulation models (UNISIM-I-D)

The ensemble of simulation models, UNISIM-I-D are built on a coarse-scale grid with an average grid-block volume of $100 \times 100 \times 8 \text{ m}^3$. Discretized into a corner-point grid with 37k active grid-blocks, the geological model of UNISIM-I-D was built regardless of any influence from UNISIM-I-R. Assuming a greenfield development process, only exploration wells, namely NA1A, NA2, NA3D, and RJS19 were used to populate the geostatistical properties. These four vertical wells also provided production data until the 1461st day. Furthermore, depth of oil-water contact (OWC), pressure-volume-temperature (PVT) of hydrocarbon (HC) as well as its existence in the eastern reservoir, rock compressibility, relative-permeability curves, and vertical permeability (k_z) multiplier all characterize the major uncertainties related to developing this synthetic model. Apart from the uncertainty associated with the scalar properties, each simulation model consists of distinct facies, porosity, permeability, and net-to-gross rock volume map in an endeavor to also capture the geostatistical variability. Finally, we used an ensemble of 500 scenarios combining all the scalar and grid uncertainties (Schiozer et al., 2017) to represent the field.

Table 3-1 depicts the drilling schedule and the information acquired within each cycle of CLFD. **Table 3-2** highlights the economic scenario used for calculating the objective function of the project, i.e., NPV. The NPV of the project is being calculated with the help of **Equation 3-9** (Schiozer et al., 2019):

$$NPV = \sum_{t=1}^n \frac{[(R - RT - ST - OPEX) \times (1 - T)] - CAPEX - AC}{(1 + i)^t} \quad 3-9$$

where R is the gross revenue, T stands for corporate tax rate and, RT and ST denote the amount paid toward royalties and social taxes, respectively. $OPEX$ and $CAPEX$ are operational expenditure and investment in infrastructure, respectively, and AC stands for the abandonment costs. The net cash flow computed is discounted with the rate i and t denotes the time period.

3.5 Results

In this section, we start by presenting the implementation of the CLFD workflow on the same case study presented by Morosov and Schiozer (2016), under a similar controlled environment, to validate our methodology. In sequence, we also present the results obtained after the implementation of the workflow on a second case study with all vertical wells. Apart

from validation, both studies provide a better insight into the CLFD workflow to improve it further and realize the impact of FoD.

Table 3-1: Drilling chronology and information acquisition.

Cycle	Well	Opening (Days)	Acquired Information
1	PROD023A	1857	Existence of HC in the eastern reservoir + PVT of HC in the eastern reservoir + Revised OWC in the eastern reservoir + logs from 5 wells*
	PROD024A	1887	
	INJ019	1918	
	PROD010	1948	
	PROD012	1979	
2	INJ010	2009	OWC in the eastern reservoir + logs from 5 wells*
	PROD009	2040	
	INJ021	2071	
	PROD005	2099	
	INJ022	2130	
3	PROD007	2160	Logs from 4 wells (previously drilled well NA1A was reopened in this cycle) *
	INJ006	2191	
	PROD014	2221	
	NA1A	2252	
	INJ017	2283	
4	PROD025A	2313	Logs from 5 wells*
	PROD026	2344	
	INJ023	2374	
	PROD021	2405	
	PROD006	2436	

* The number of logs depended on the trajectory of the wells. For each horizontal well, we acquired one vertical pilot hole log and one horizontal log.

Table 3-2: Economic parameters (adapted from Chapter 2).

Parameters	Values
Oil price	50 USD/bbl.
Discount rate	9%
Royalties	10%
Special taxes on gross revenue	9.25%
Corporate taxes	34%
Cost of oil production	10 USD/bbl.
Cost of water production	1 USD/bbl.
Cost of water injection	1 USD/bbl.
Abandonment cost (% well investment)	7.4%
Drilling, completion and connection of vertical well	35 USD Million
Drilling, completion and connection of horizontal well	50 USD Million

3.5.1 Case study I: Repeating Morosov and Schiozer (2016)

The initial FDP (FDP_1) consists of seven horizontal water-injection wells and thirteen producers (ten horizontal and three vertical). **Figure 3-3** provides a glimpse of the top view of initial FDP.

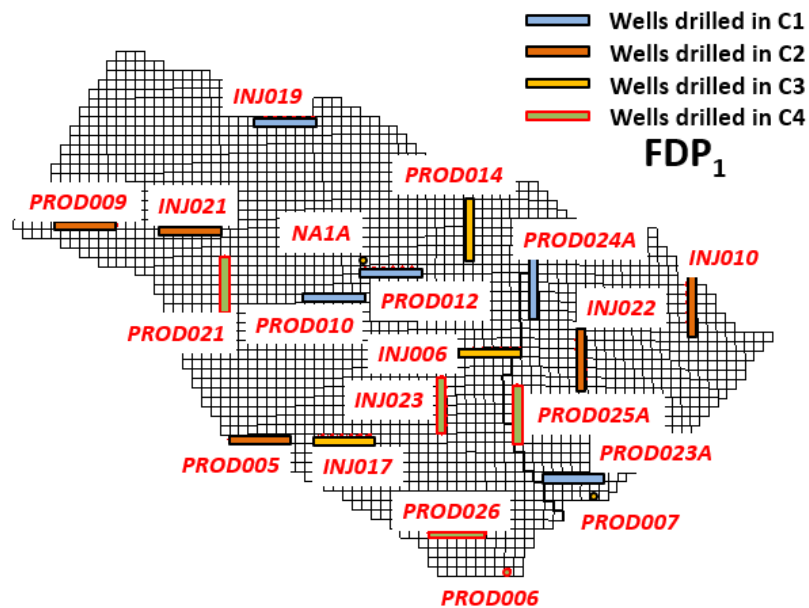


Figure 3-3: Initial FDP (FDP_1) based on the optimal strategy proposed by Schiozer et al. (2015) that was also used as the initial strategy by Morosov and Schiozer (2016).

We drilled and obtained horizontal and vertical well logs for the first five wells (**Table 3-1**) in the action phase of Cycle 1. **Figure 3-4** shows some examples of well logs that were extracted from the UNISIM-I-R geological model (or true field) and used to update the geological model of the UNISIM-I-D so that improved petrophysical images could be generated.

On top of that, we also obtained new information during the next phase of Cycle 1 (C1). PROD023A confirmed the presence of HC and PVT in the eastern reservoir. PROD023A and PROD024A, newly drilled wells in the eastern reservoir, also provided sufficient information to update the uncertainty related to the depth of OWC. Similar to Morosov and Schiozer (2016), we updated the OWC to at least 3163 meters.

Once we updated the uncertainties and their probabilities of occurrence, we performed DA with Kalman gain localization scheme. **Figure 3-5** provides a preview of the localization volume for two of the five wells that were used during DA.

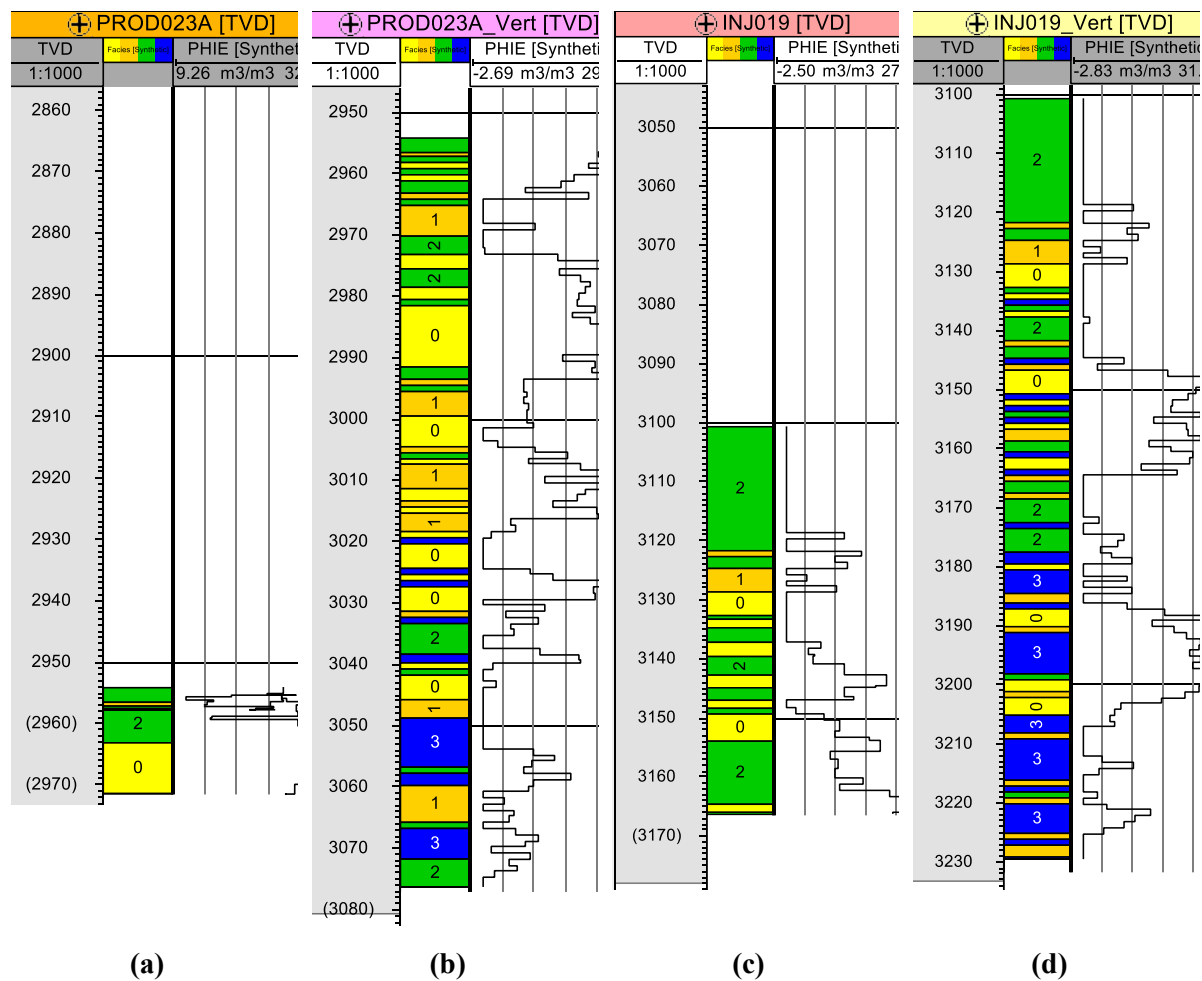


Figure 3-4: Obtained well logs for: (a) PROD023A horizontal section, (b) PROD023A vertical pilot hole, (c) INJ019 horizontal section and (d) INJ019 vertical pilot hole.

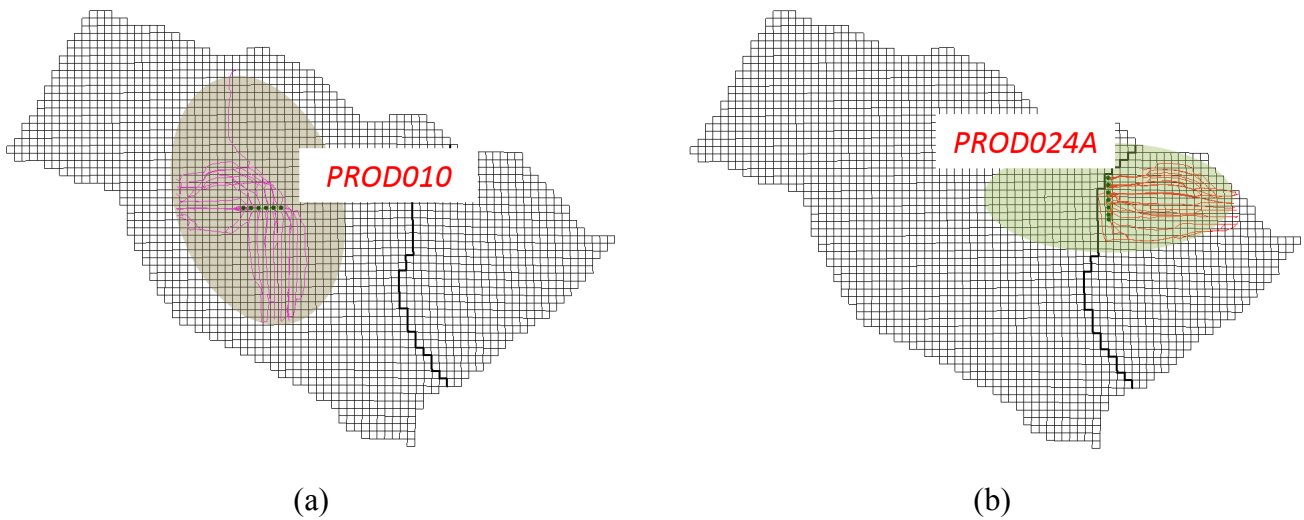


Figure 3-5: Streamlines and localization volume for (a) PROD010 and (b) PROD024A during Cycle 1 of the case study I.

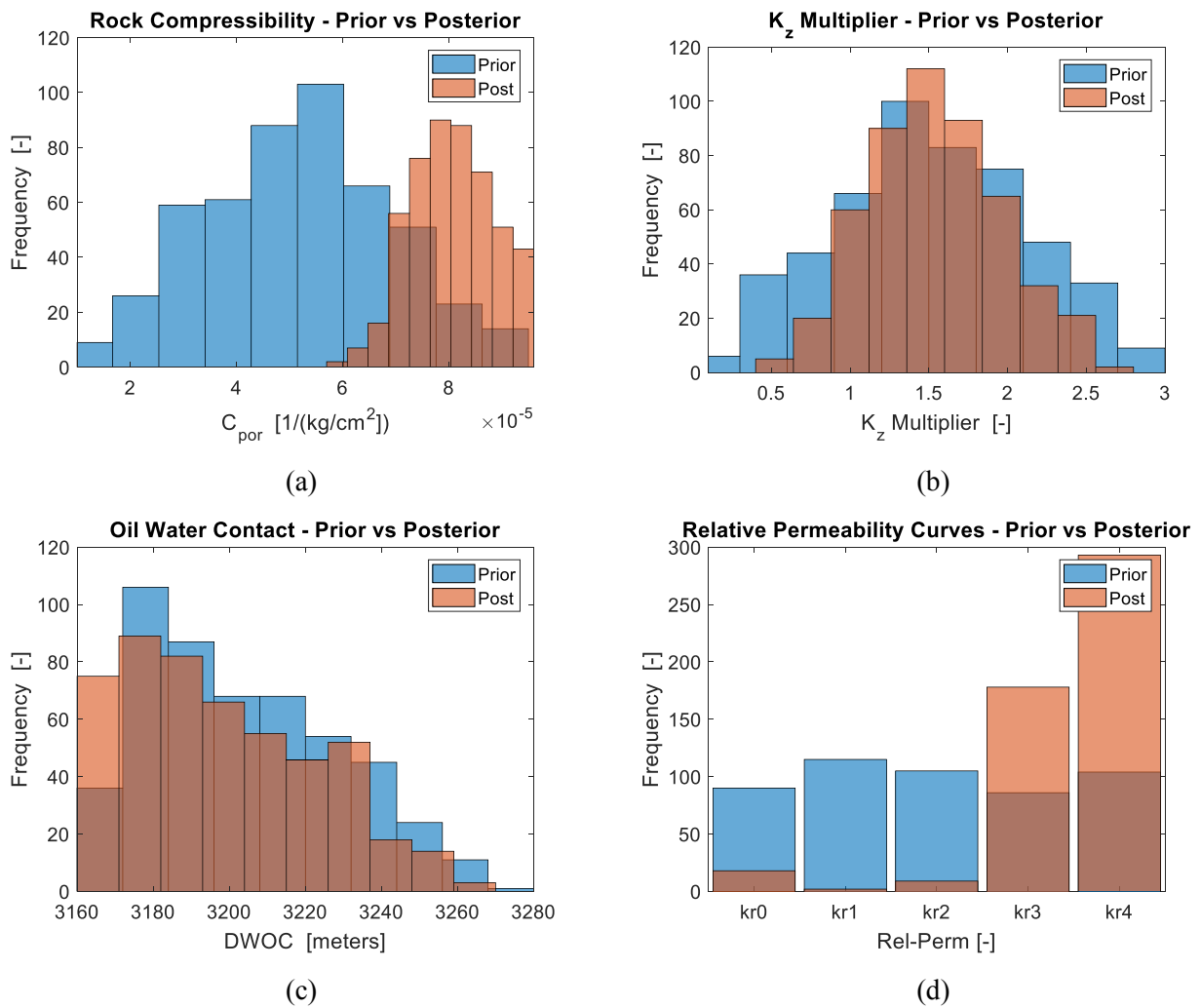


Figure 3-6: Prior and posterior histograms of uncertainty attribute (a) rock compressibility, (b) k_z -multiplier, (c) OWC and (d) relative permeability curves.

ES-MDA provided a revised ensemble of simulation models (prior ensemble, M_{prior}^1 was updated to posterior ensemble, M_{post}^1) by coherently updating the grid-based and scalar uncertainties (**Figure 3-6**) to reduce the average normalized data mismatch, \bar{O} (**Figure 3-7**). **Figure 3-8** provides a secondary analysis to confirm the functioning of DA, showing an improvement in well and total objective function posterior to DA (M_{prior}^1 to M_{post}^1).

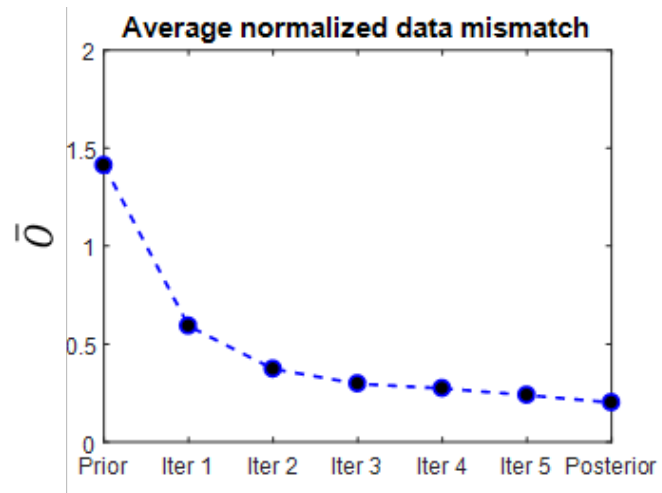


Figure 3-7: Reduction of average normalized data mismatch (\bar{O}) along multiple data assimilations (or iterations) to minimize the disparity between observed and simulated data.

Well	BHP	Q_g	Q_o	Q_w	Q_{wi}	Total
INJ019	32.8	-	-	-	94.6	27.4
NA1A	80.2	100	100	100	-	80.2
NA2	88.8	93.6	99.8	25	-	23.2
NA3D	86.6	98.4	98.4	97	-	85.4
PROD010	100	25.4	22.4	100	-	22.4
PROD012	100	-	-	100	-	100
PROD023A	0	100	100	100	-	0
PROD024A	61.8	100	100	100	-	61.8
RJS19	99.6	100	100	100	-	99.6
Total	0	21.6	22	24	94.6	0

(a)

Well	BHP	Q_g	Q_o	Q_w	Q_{wi}	Total
INJ019	79.2	-	-	-	99	78.2
NA1A	100	100	100	100	-	100
NA2	100	99.8	100	86	-	86
NA3D	100	100	100	100	-	100
PROD010	100	97.6	94	100	-	94
PROD012	100	-	-	100	-	100
PROD023A	62.2	100	100	100	-	62.2
PROD024A	99.8	100	100	100	-	99.8
RJS19	100	100	100	100	-	100
Total	49.8	97.4	94	86	99	39.6

(b)

Figure 3-8: NQDS analysis of (a) M_{prior}^1 and (b) M_{post}^1 , presenting the percentage of models within acceptable range for individual well objective functions.

Subsequently, with the help of NQDS, we approved 198 models from M_{post}^1 (**Figure 3-8**) while preserving the grid-based and scalar UAs. Unlike Morosov and Schiozer (2016), we used a stricter tolerance and constant values of 10% and 0 for all the well objective functions, respectively. We made an exception for the constant value for the entire well water production rate (Q_w) objective functions, which was set to 20. As Q_w was almost zero for all the wells, we assumed this exception to be fair enough for ensuring NQDS values are finite.

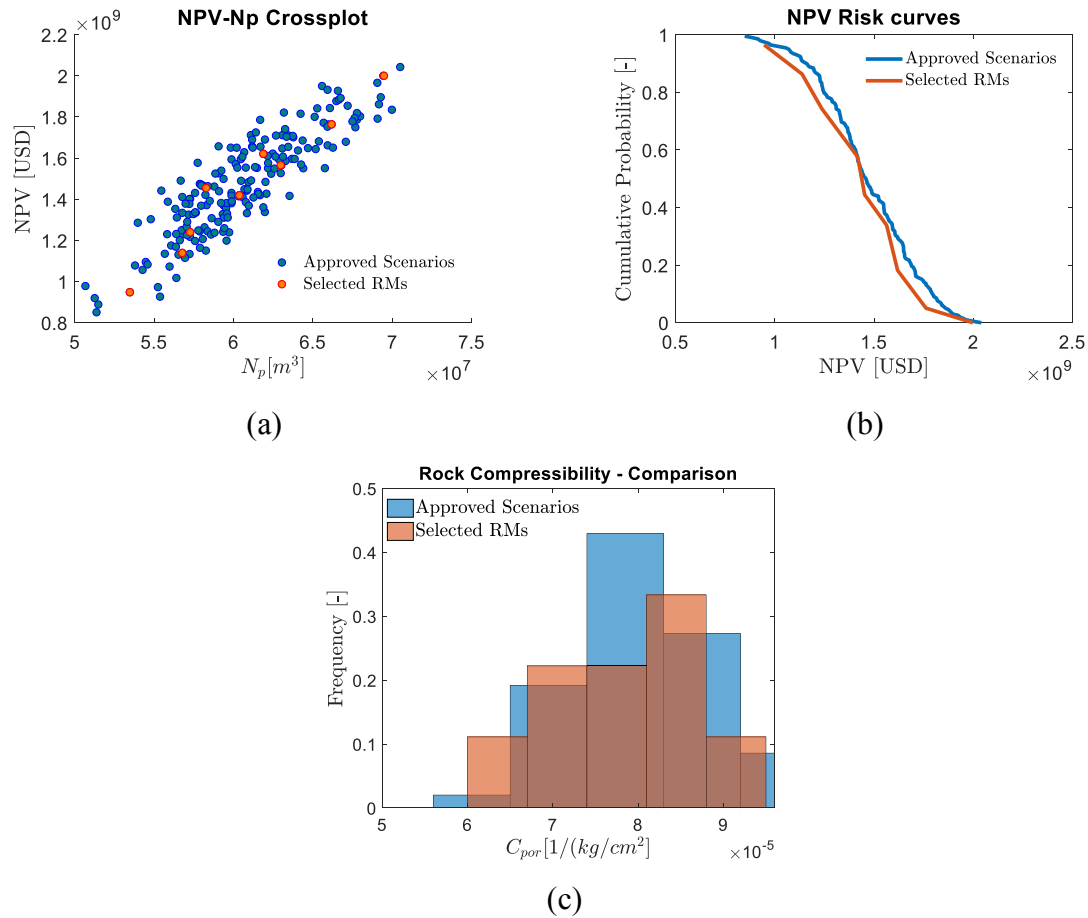


Figure 3-9: NPV- N_p cross plot, (b) NPV risk curves and (c) rock compressibility probability distribution function showing the fitness of RMs in Cycle 1.

Next, in order to work efficiently with optimization, nine RMs were obtained from the smaller subset of approved scenarios (AS). **Figure 3-9** attempts to show the suitability of the selected RMs, based on one of the cross-plots, risk curves and uncertainty attribute distributions that we used for getting RMs.

Finally, we optimized FDP using **Equation 3-6** as the objective function, aiming on improving the likelihood of success of the optimized FDP over the ensemble and, consequently, the “true field” (or the reference case). **Figure 3-10** provides a preview of the

optimization result. After robust optimization, we also tested the economic viability of all the wells. During C1, we observed that all the RMs were individually improved and all the wells were also observed to be economically viable for the collective set of RMs.

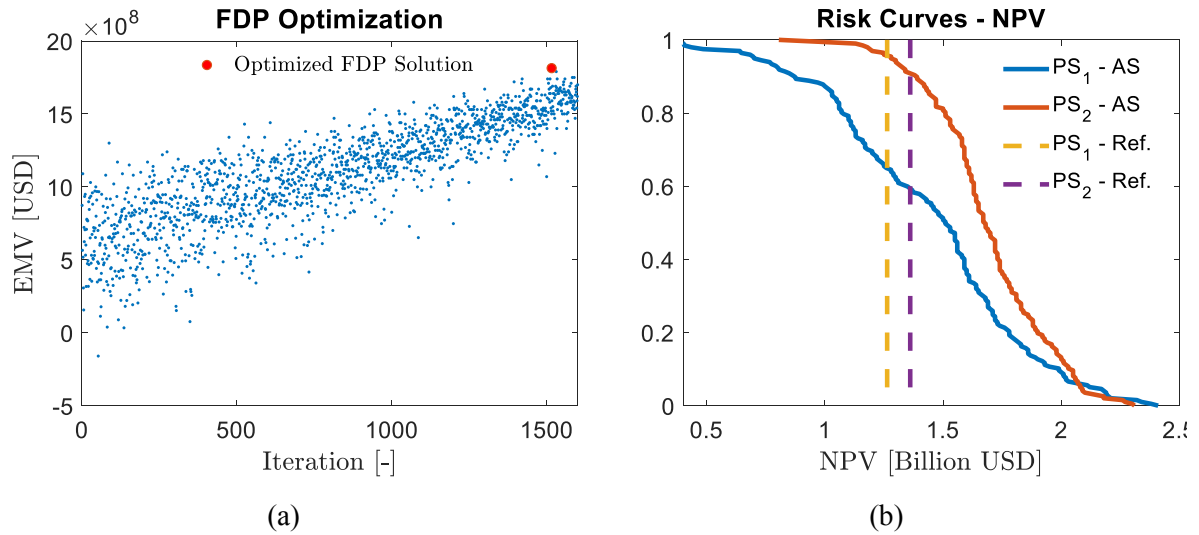


Figure 3-10: (a) Evolution of EMV of the 9 RMs with IDLHC iterations and (b) risk curves showing the result of optimization with approved scenarios (AS) and the reference case (without FoD).

In succession, we implemented the optimized FDP (FDP₂) on the reference case to evaluate the impact of the revised decision on the objective function of the project (**Figure 3-10b**). Altogether, new well logs, updated probabilities of inputs and computer-assisted history matching process increased the NPV by 8% and 1%, without and with the FoD approach, respectively.

Alike C1, two more cycles, namely Cycle 2 (C2) and Cycle 3 (C3), were executed using the CLFD workflow. With the help of **Table 3-3**, we present comprehensive results of all the cycles of CLFD in detail as well as \overline{EVoCL} and \overline{VoCL} for consecutive cycles.

Table 3-3: A detailed account of implementation of CLFD on case study I.

	Cycle 1 (C1)	Cycle 2 (C2)	Cycle 3 (C3)
Results obtained using simulation models			
Action	Drilled 5 new wells; Used a total of 14 well logs (9 vertical + 5 horizontal) for generating updated petrophysical images for M_{prior}^1	Drilled 5 new wells; Used a total of 24 well logs (14 vertical + 10 horizontal) for generating updated petrophysical images for M_{prior}^2	Drilled 4 new wells; Used a total of 31 well logs (18 vertical + 13 horizontal) for generating updated petrophysical images for M_{prior}^3
Updating inputs	PROD023A confirmed the existence of HC and PVT in the eastern bloc. OWC was updated for the eastern bloc ≥ 3163 meters	OWC (≈ 3174 meters)	-
Data assimilation¹	4 months of data was used to obtain M_{post}^1	9 months of data was used to obtain M_{post}^2	14 months of data was used to obtain M_{post}^3
Approving scenarios	198	239	315
Selecting RMs	9 RMs ($\sim 5\%$ of the AS)	9 RMs ($\sim 4\%$ of the AS)	9 RMs ($\sim 3\%$ of the AS)
Optimization	All RMs were improved; FDP ₁ was optimized to obtain FDP ₂	All RMs were improved; FDP ₂ was optimized to obtain FDP ₃	All RMs were improved; FDP ₃ was optimized to obtain FDP ₄
Range of <i>EVoCL</i> (considering RMs individually)	+0.1 to 0.73 Billion USD (10 to 77 ² %)	+0.01 to +0.16 Billion USD (1 to 14%)	0.01 to +0.28 Billion USD (5 to 20%)
<i>EVoCL</i> (based on RMs)	+0.36 Billion USD (25%)	+0.08 Billion USD (+6%)	+0.16 Billion USD (+10%)
<i>EVoCL</i> (based on AS)	+0.22 Billion USD (15%)	+0.05 Billion USD (+3%)	+0.14 Billion USD (+8%)
Results obtained using the reference case (true field)			
\overline{VoCL} (without FoD)	+ 0.1 Billion USD (+8%)	+ 0.13 Billion USD (+10%)	- 0.17 Billion USD (-11%)
\overline{VoCL} (FoD applied on to-be-drilled wells)	+0.06 Billion USD (+1%)	+0.17 Billion USD (+12%)	+0.01 Billion USD (+1%)

¹ Unlike Morosov and Schiozer (2016), production data was collected every month

² Inflated values exist where the initial FDP yielded very low NPVs

The evolution of FDP, a consequence of CLFD, can be best interpreted by studying the evolution of the project's objective function, i.e., NPV. **Figure 3-11** shows the changing NPV and corresponding parameters as new information is acquired and exploited within each cycle. **Figure 3-12** shows the evolution of FDP. C3 is the only cycle where the FoD approach played an important role in ensuring positive results by revising the location of heels for the wells drilled in the non-reservoir region. Despite this, one must note that the NPV obtained by the end of the C3, even without FoD, is 5% better than the benchmark, which exhibits two things: firstly, CLFD is beneficial and secondly, placement of a well in a non-reservoir zone by CLFD is an erratic error (and an inevitable element of developing a heterogeneous field). To be fair, one must note that we implemented FoD on all the wells of our initial FDP (FDP₁) to make it a benchmark for statistical comparisons like the one above. 1.399 Billion USD was the benchmark NPV with FoD implemented on all the wells (see **Figure 3-17** in the discussion section).

Major changes in well placement can already be seen between FDP₂ and FDP₁. We also point out that the PROD025A, initially drilled in the eastern reservoir, was deemed beneficial if drilled in the western reservoir (illustrated by FDP₄).

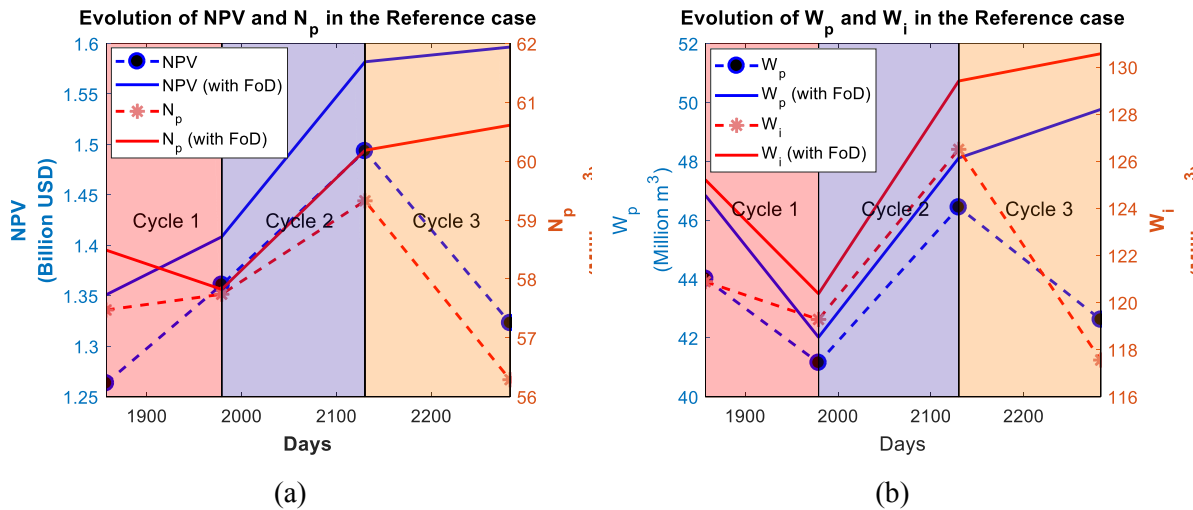


Figure 3-11: Evolution of (a) NPV and cumulative oil production (N_p) and (b) cumulative water production (W_p) and water injection (W_i) in the reference case.

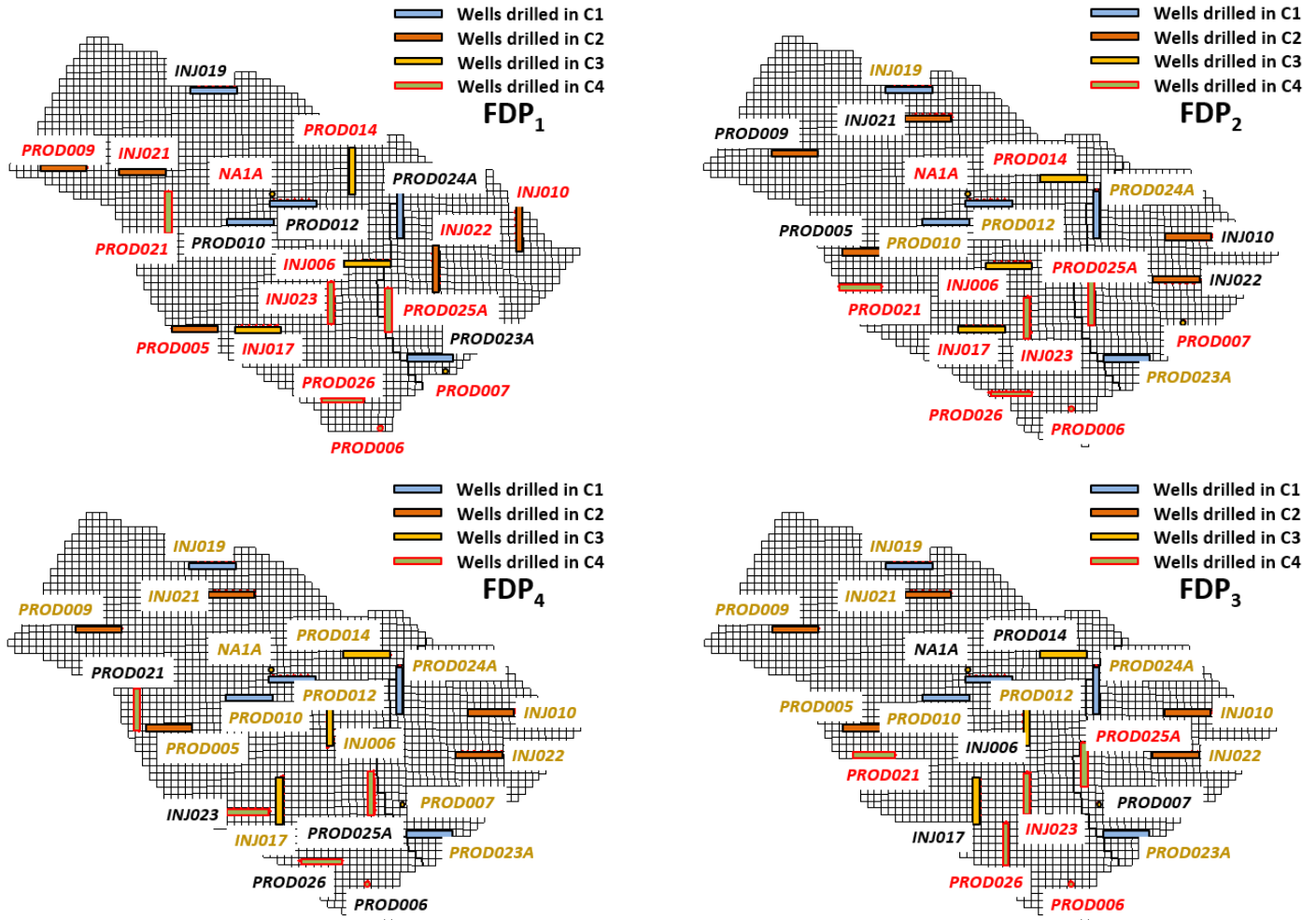


Figure 3-12: From top left and in clockwise direction, the pictures illustrate the evolution of FDP (FDP₁ to FDP₄). The wells being completed, already producing and to-be-drilled, using the proposed FDP, are highlighted in black, gold, and red italic texts, respectively.

3.5.2 Case study II: All vertical wells

Unlike case study I, we did not have an optimized FDP for case study II. As such, the initial well trajectories (**Figure 3-3**) proposed by Morosov and Schiozer (2016) were used to define an engineering estimation of the vertical well placement (**Figure 3-13**). We optimized the FDP defined by this well-placement using the concepts of Schiozer et al. (2019) to obtain the benchmark initial FDP, i.e., the reference strategy for evaluating the CLFD implementation in case study II.

The initial ensemble of petrophysical images, generated with the help of the existing 4 wells (NA1A, NA2, NA3D, and RJS19), were used with the initial probability density function of the uncertainties to generate 500 scenarios using DLHG. With the known historical

production data and using a strict tolerance of 10%, we approved 105 scenarios within ± 2 range of NQDS. We used RMFinder 2.0 to obtain a set of nine RMs along with their probabilities.

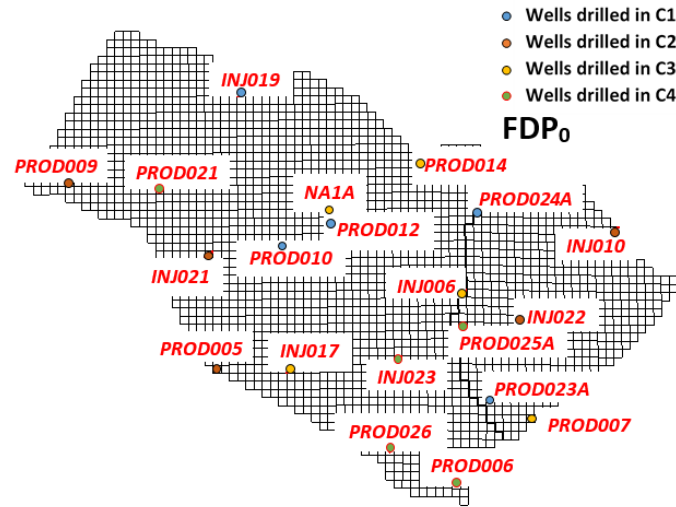


Figure 3-13: Proposed preliminary FDP (FDP_0) used for the pre-CLFD optimization to obtain the benchmark initial FDP (FDP_1).

We also used the selected RMs to perform robust optimization of the FDP (well placement only) using IDLHC algorithm with bi-criterion objective function (**Equation 3-6**). The optimization yielded a 24% (1.35 to 1.67 billion USD), 20% (1.34 to 1.61 billion USD), and 17% (1.32 to 1.54 billion USD) increase in expected monetary value (EMV) of the RMs, the 105 approved scenarios and the ensemble, respectively. Apart from that, the improved percentage scenarios were 100%, 97% and 94% for the RMs, the approved scenarios and the ensemble, respectively, stressing that the initial strategy was good enough based on the available knowledge at the given moment.

Similar to Cycle 1 of case study I, we implemented all the three cycles in case study II. With the help of **Table 3-4**, we present comprehensive results of all the cycles as well as EV_{oCL} and \overline{VoCL} for consecutive cycles.

Figure 3-14 provides a glimpse of the evolution of FDP within each cycle of CLFD. We emphasize the conversion of producer PROD014 to injector INJ014 during the optimization process of Cycle 1, as we observed that PROD014 was economically unviable. During Cycle 2, we observed that INJ014 was shifted to the western reservoir, modifying the producer to injector ratio again. By the end of Cycle 3, only four wells were deemed adequate for the eastern reservoir.

Table 3-4: A detailed account of implementation of CLFD on case study II.

	Cycle 1 (C1)	Cycle 2 (C2)	Cycle 3 (C3)
Results obtained using simulation models			
Action	Drilled 5 new wells; Used a total of 9 vertical well-logs for generating updated petrophysical images for M_{prior}^1	Drilled 5 new wells; Used a total of 14 vertical well-logs for generating updated petrophysical images for M_{prior}^2	Drilled 4 new wells; Used a total of 18 vertical well-logs for generating updated petrophysical images for M_{prior}^3
Updating inputs	PROD023A confirmed the existence of HC and PVT in the eastern bloc. OWC was updated for the eastern bloc ≥ 3163 meters (similar to case study I)	OWC (≈ 3174 meters)	-
Data assimilation¹	4 months of data was used to obtain M_{post}^1	9 months of data was used to obtain M_{post}^2	14 months of data was used to obtain M_{post}^3
Approving scenarios	370	240 ²	60 ²
Selecting RMs	9 RMs ($\sim 2\%$ of the AS)	9 RMs ($\sim 4\%$ of the AS)	9 RMs ($\sim 15\%$ of the AS)
Optimization	All RMs were improved; FDP ₁ was optimized to obtain FDP ₂ . A producer was converted to an injector while ensuring economic viability.	All RMs were improved; FDP ₂ was optimized to obtain FDP ₃	8 of 9 RMs were improved; FDP ₃ was optimized to obtain FDP ₄
Range of EV_{oCL} (considering RMs individually)	0.11 to 0.65 Billion USD (10 to 80 ³ %)	0 to 0.15 Billion USD (0 to 10%)	-0.01 to 0.24 Billion USD (-1 to 19%)
EV_{oCL} (over RMs)	+ 0.38 Billion USD (32%)	+ 0.06 Billion USD (+4%)	+ 0.05 Billion USD (+3%)
EV_{oCL} (based on AS)	+ 0.36 Billion USD (30%)	+ 0.08 Billion USD (+5%)	+ 0.04 Billion USD (+3%)
Results obtained using the reference case (true field)			
\overline{VoCL}	+ 0.41 Billion USD (37%)	0 Billion USD (0%)	+ 0.03 Billion USD (+2%)

¹ Alike Morosov and Schiozer (2016), new production data was collected every 5th day;

² A stricter tolerance value of 5% was used for the BHP to improve the efficiency;

³ Inflated values exist for those RMs where the initial FDP yielded very low NPVs

Figure 3-15 shows how the project's objective function increases as we acquire and utilize the new information using the CLFD framework.

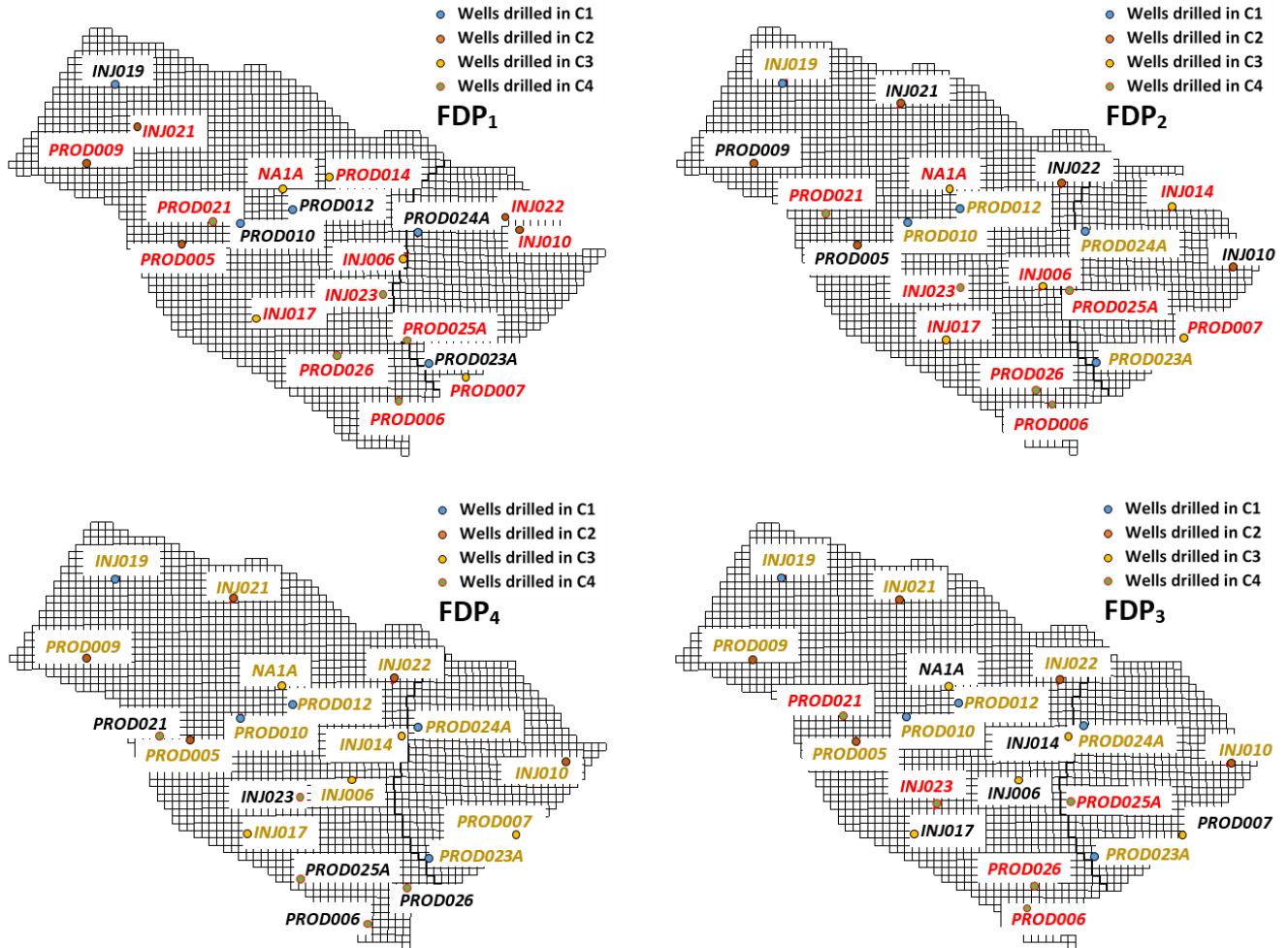


Figure 3-14: From top left and in clockwise direction, the pictures illustrate the evolution of FDP (FDP₁ to FDP₄). The wells being completed, already producing and to-be-drilled, using the proposed FDP, are highlighted in black, gold, and red italic texts, respectively.

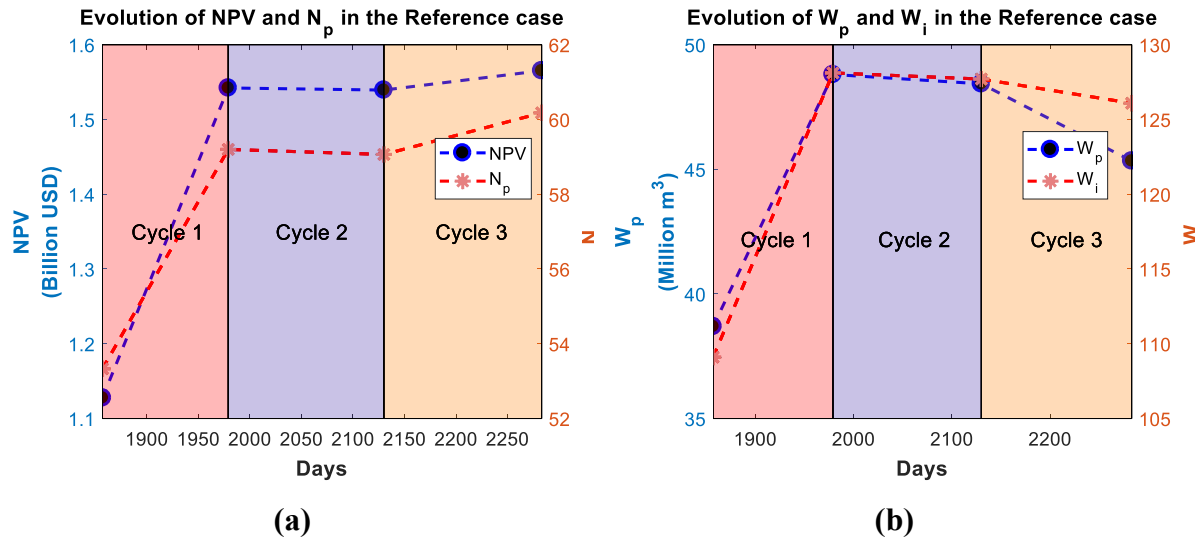


Figure 3-15: Evolution of (a) NPV and cumulative oil production (N_p) and (b) cumulative water production (W_p) and water injection (W_i) in the reference case.

3.6 Discussion

One of the primary objectives of working on case study I was to reacquaint ourselves with the pitfalls addressed by Morosov and Schiozer (2016) to improve the CLFD methodology. However, a contrarily positive result, both with and without FoD, and under the same controlled environment as theirs, promoted our confidence in the workflow. We validated this confidence by testing the workflow on case study II, where once again we observed a positive result. Some of the key differences between these two case studies are mentioned in **Table 3-5**.

Table 3-5: Observed differences between case study I and II.

	Case study I (with horizontal wells)	Case study II (all vertical wells)
Action	1 Horizontal + 1 Vertical log per well	1 Vertical well log for each well
Update Inputs	No difference	
Data Assimilation	Fewer scenarios were observed to be history matched aptly within acceptable range	More scenarios were observed to be history matched aptly within acceptable range
Approve Scenarios	No difference	
Select RMs	No difference	
Optimize	More variables for optimization	Fewer variables for optimization

Alike previous work, we considered the project objective function (NPV) as the key performance indicator of the CLFD. While the performance indicator suffices the requirement of evaluating our methodology, in this work we delved deeper to understand how the intermittently acquired information influences the ensemble of simulation models and uncertainty assessment. Following a typical cycle, we start our analysis from the action phase:

1. Action: A first and direct influence of the new well logs on the reduction of uncertainty can be observed in **Figure 3-16**. As anticipated, the well logs shift the volume of oil in place (VOIP) towards the true VOIP (from "true field") while reducing the range of P10-P90. **Table 3-6** provides a detailed analysis of the subject.

Concerned with the huge reduction of VOIP uncertainty range (at least 65% in both cases) with increasing number of wells, while still falling short of true VOIP by the end of CLFD ($\approx 9\%$), we tried to test the impact of additional wells on the VOIP reduction. The first 54 well-logs, which were used to build the "true field" geological model, were used with the 36 well-logs extracted until Cycle 3 of case study I to generate M_{prior}^{test} (**Figure 3-16a**). Not surprisingly, we obtained an almost deterministic VOIP, while still being 6% away from true VOIP.

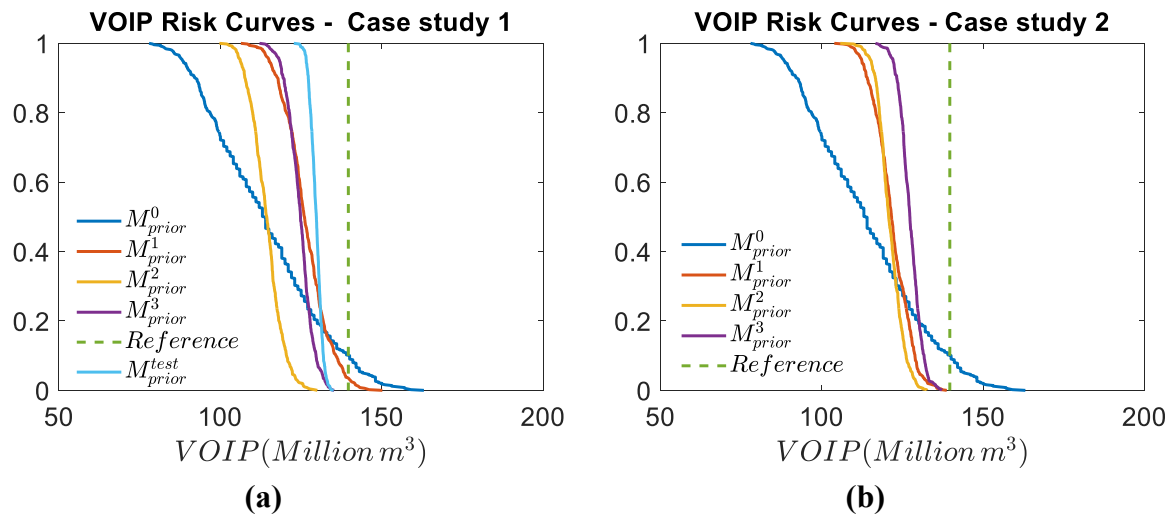


Figure 3-16: Risk curves of VOIP reflecting the reduction in uncertainty as new information from action phase is being implemented in case study (a) I and (b) II.

Table 3-6: Changing statistics of VOIP for case study I and II.

VOIP	Pre-CLFD	Case Study I			Case Study II		
		C1	C2	C3	C1	C2	C3
Minimum (Million m ³)	78	106	100	112	104	106	117
Maximum (Million m ³)	163	150	130	135	139	133	137
Range (Million m ³)	85	44	30	23	35	27	21
Median (Million m ³)	114	126	114	125	122	121	127
P90 (Million m ³)	92	118	108	119	114	117	123
P10 (Million m ³)	140	136	120	130	129	126	132
P90-P10 (Million m ³)	48	18	13	10	15	10	8

We also observed the VOIP shifting away and then towards the true VOIP during C2 and C3, respectively, in case study I (**Figure 3-16a**). This behavior is in line with our expectation as the quality of the well logs also has a dominant and direct influence on geostatistical properties. To affirm this hypothesis, we investigated case study I again and reproduced M_{prior}^1 using the well logs obtained during Cycle 3. Anticipated improvement in the VOIP ($\approx 12\%$) confirmed that the new geostatistical images are more optimistic as better-quality regions were encountered by the wells drilled in Cycle 3.

These observations revealed two things: Firstly, the geostatistical images must be generated while maintaining larger variability, especially when the ratio between the explored spatial volume to the extensively unexplored volume of the field is small. Secondly, well logs alone are not sufficient to determine the uncertainties (e.g., porosity and NTG for VOIP). We believe that constraining the geostatistical images to 3D seismic data can reduce the variability of the images while ensuring geological consistency so that the uncertainties shift more towards the “true field” value. Better usage of variograms can also improve the quality of petrophysical images. However, a comprehensive investigation on these subjects and their direct impact on the field development process is out of the scope for this study.

2. Update Inputs: **Figures 3-15a** and **3-17** reveal the impact of up-to-date inputs on the outcome of CLFD. Whereas, we obtained **Figure 3-11** by implementing FoD for the wells to-be-drilled during the subsequent cycle of CLFD only (to avoid unconscious bias) and **Figure 3-17** was obtained by applying FoD for all the wells. A strong correlation between

NPV and updated information in both cases shows that including vital and definite information can help reduce uncertainty to promote our understanding of the "true field" and, consequently, the FDP. Apart from this, similitude in the NPV evolution pattern, corresponding to the similar magnitude of updated inputs, reveals that new and substantial information could be the most important parameter for the success of CLFD. A study on this subject will be performed in the future to confirm the premise.

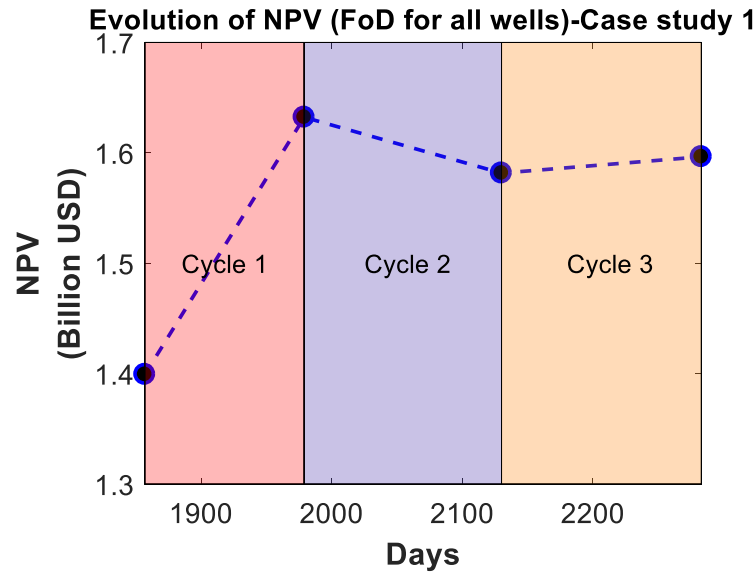


Figure 3-17: Evolution of NPV in the reference case after implementing FoD approach on all the wells.

Table 3-7: NQDS values obtained for the ensemble prior and posterior to the data assimilation process for both the case studies.

NQDS	Case study I						Case study II					
	Before DA (Prior)			After DA (Posterior)			Before DA (Prior)			After DA		
	M_{prior}^1	M_{prior}^2	M_{prior}^3	M_{post}^1	M_{post}^2	M_{post}^3	M_{prior}^1	M_{prior}^2	M_{prior}^3	M_{post}^1	M_{post}^2	M_{post}^3
±1	0	0	0	198	239	315	12	1	0	370	328	483
±2	0	0	0	368	399	431	80	50	6	456	429	492
±3	0	0	0	438	460	456	166	145	47	484	472	498
±5	0	0	2	489	488	485	243	241	136	493	492	500
±10	43	12	74	499	493	497	423	338	283	496	500	500

3. Data Assimilation: **Table 3-7** shows the number of scenarios within different NQDS ranges, before and after the computer-assisted history matching. As observed in case study I, having 0 scenarios within the ±10 range of NQDS already signifies that the scenarios

were not good enough. Despite this complication, ES-MDA, a popular data assimilation technique, assimilated data satisfactorily to generate cogent scenarios (**Table 3-7**).

It is fair to assume that all the post DA scenarios are comparable to the real field when history matching has been performed effectively. Given that our prior ensembles were adequately history matched (**Table 3-7**), we performed a simple test to evaluate how representative they were of the “true field” in case study I. In other words, we presumed that each scenario represents the real field and we ran simulations for each scenario the same way as for the “true field” model by removing the constraints (i.e., liquid production rate and water injection rate) that conditioned the scenarios during the historical period. **Table 3-8** provides the first glimpse of the result.

Failure to even predict the history period properly (**Table 3-8**) reveals that good history matched scenarios (with conditions) do not necessarily mean that the scenarios “represent” the field. This result should not come as a surprise as all models are imperfect, according to Oliver and Alfonzo, 2018, Rammay et. al., 2019 and Neto et al., 2020.

However, the important takeaway is that CLFD could be improved further by refining the DA process. Even if the historical period can be naturally stimulated (without history conditions) within a decent acceptable range, this will already ensure that we do not have fallible scenarios. Consequently, such models can significantly improve our understanding of the field. We will limit our discussion on this topic as improving imperfect models with DA is out of the scope for this study.

Table 3-8: Evaluating the performance of DA after removing the historical constraints reveals the existing discrepancy between the ensemble and the real field.

Case study I						
NQDS	Before DA (Prior)			After DA (without historical constraints)		
	M^1_{prior}	M^2_{prior}	M^3_{prior}	M^1_{post}	M^2_{post}	M^3_{post}
±1	0	0	0	0	0	0
±2	0	0	0	0	0	0
±3	0	0	0	0	0	0
±5	0	0	2	0	0	0
±10	0	0	74	117	3	3

4. Approve Scenarios: In order to appreciate this step, one must refer to **Figure 3-18** to understand how the quality of the history-matched model sways the FDP. As shown, not excluding bad scenarios, prior to selecting RMs, can yield a suboptimal FDP.

Another advantage of this step is that it reduces the number of expensive simulations while maintaining the average and standard deviation of geological UAs. Since as little as 60 scenarios were selected during the second case study, we randomly selected a layer and evaluated the statistics around porosity and permeability. **Figure 3-19** provides a preview of the qualitative comparison of porosity and how similar the history-matched scenarios are to the AS.

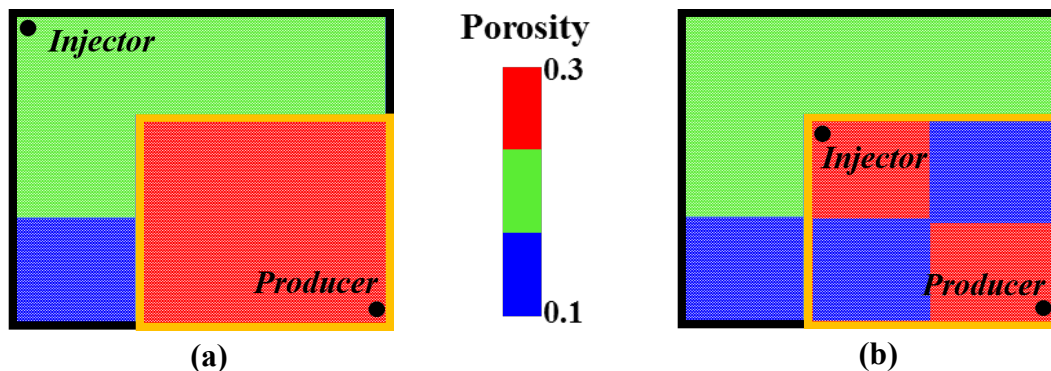


Figure 3-18: A 2D model showing different optimal locations for an injector in: (a) good history matched model (representing the “true field” in this case), and (b) poorly history matched model. The orange box represents the history matching area and all properties are the same outside this region.

5. Select RMs: Since Meira et al. (2017) allows the selection of RMs based on quantitative data alone, the RMs were observed to have a qualitative bias as shown by **Figure 3-20 (a, b, d, e)**. Assuming that AS represent the field well, ignoring their standard deviation can potentially lead to a negative bias towards risk-informed decision making.

Furthermore, **Figure 3-20 (c, f)** demonstrates the impact of increasing the number of RMs to overcome this bias and maintain the qualitative uncertainty attributes. Based on empirical pieces of evidence, we believe that maintaining good quality RMs becomes a necessity, especially when drilling in a previously unexplored area. However, one must note two things when considering increasing the number of RMs: (a) its trade-off with the number of simulations and, (b) its relative impact on the decision-making process (e.g., it may be more advantageous in the early phase of field development only). Select RMs: Since Meira et al. (2017) allows the selection of RMs based on quantitative data alone, the

RMs were observed to have a qualitative bias as shown by **Figure 3-20 (a, b, d, e)**. Assuming that AS represent the field well, ignoring their standard deviation can potentially lead to a negative bias towards risk-informed decision making.

Furthermore, **Figure 3-20 (c, f)** demonstrates the impact of increasing the number of RMs to overcome this bias and maintain the qualitative uncertainty attributes. Based on empirical pieces of evidence, we believe that maintaining good quality RMs becomes a necessity, especially when drilling in a previously unexplored area. However, one must note two things when considering increasing the number of RMs: (a) its trade-off with the number of simulations and, (b) its relative impact on the decision-making process (e.g., it may be more advantageous in the early phase of field development only).

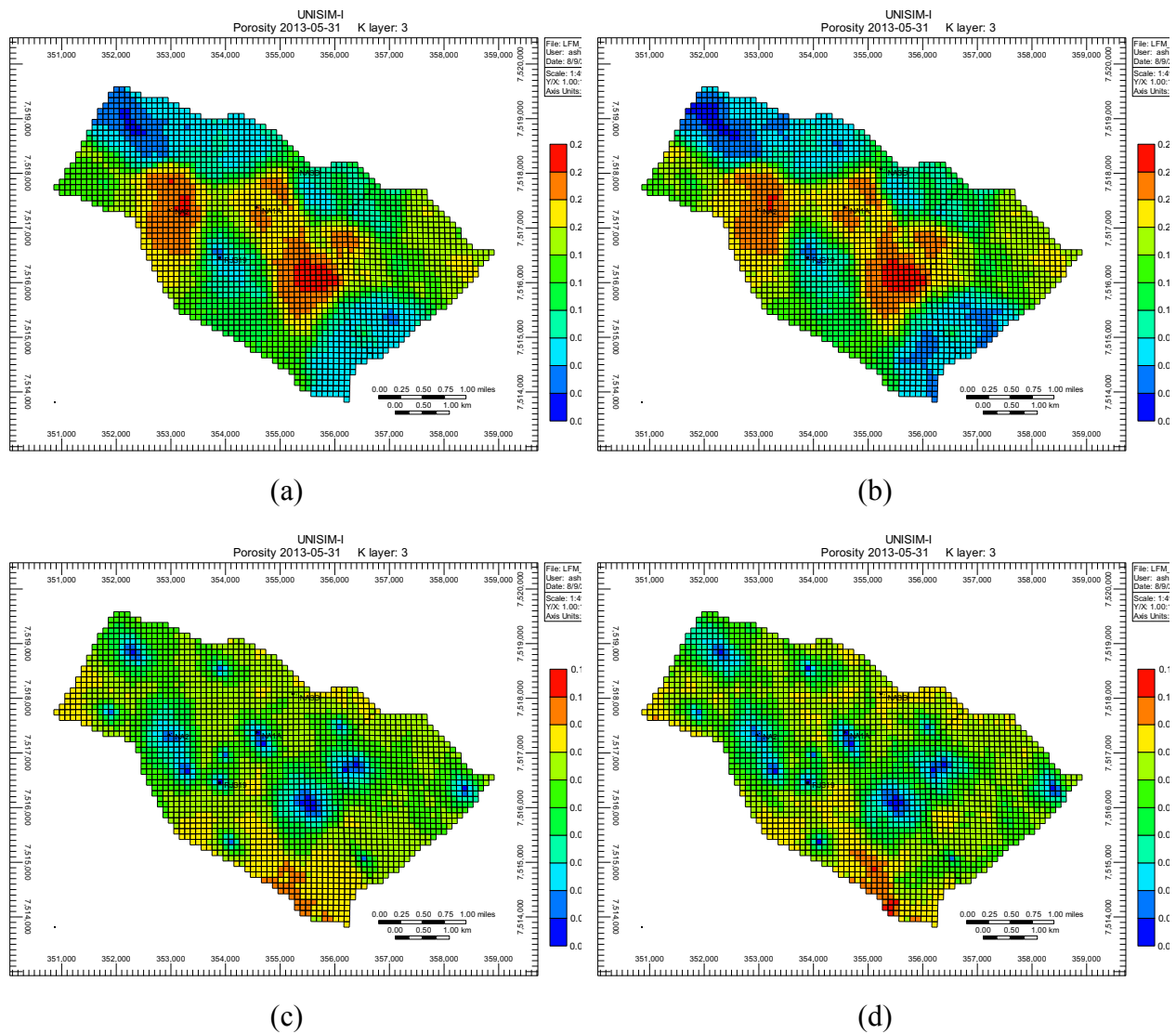


Figure 3-19: Mean porosity for (a) the M^3_{post} , (b) the approved 60 scenarios from M^3_{post} and standard deviation of porosity for (c) the M^3_{post} , (d) the approved 60 scenarios from M^3_{post} for layer 3 of case study II.

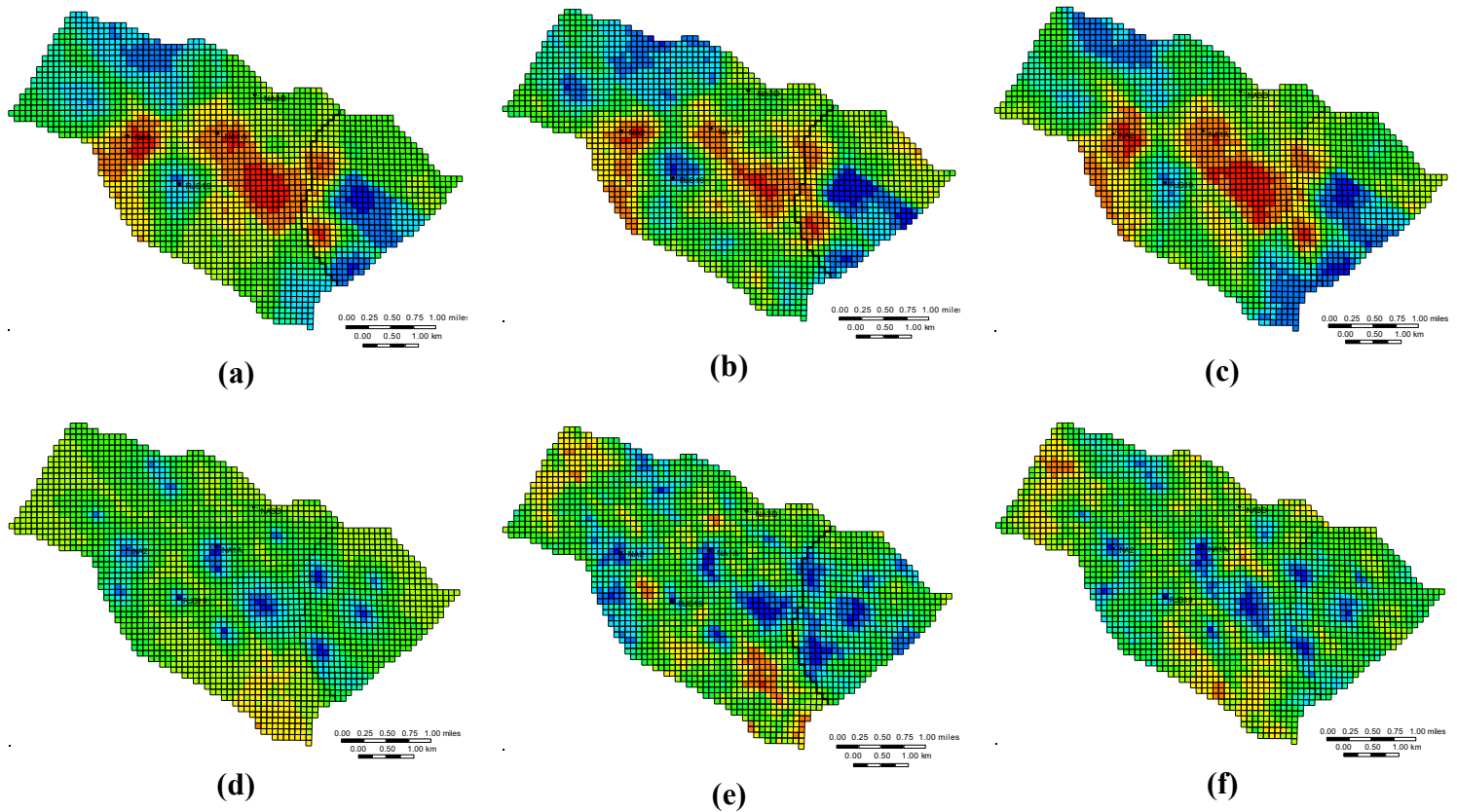


Figure 3-20: Mean porosity for (a) the approved 315 scenarios from M_{post}^3 , (b) 9 RMs selected for optimization, and (c) 16 RMs selected for observation, and standard deviation of porosity for (d) the approved 315 scenarios from M_{post}^3 , (e) 9 RMs selected for optimization, and (f) 16 RMs selected for observation for layer 3 of case study I.

6. Optimize: Given that the models explicitly represent the UAs, robust optimization of the RMs is an appropriate way to optimize FDP with regard to improving decisions. It also ensures easy applicability of the bi-criterion function to enhance the likelihood of success of an FDP. To understand the scope of improving this step, from the perspective of the feedback-based field development process, we conducted a small test using the optimization results of Cycle 2 of case study II as we had the lowest improvement (0%) in that case (**Figure 3-15a**). For that case, we examined our best solution (FDP_3) with an alternative solution ($FDP_{3,alt}$) for that cycle. The main difference between these two solutions is that, while our best solution tends to be more focused on the EMV of the RMs, the second-best solution is focused on both the objective function and maximizing the minimum NPV improvement for each RM. **Table 3-9** presents a comparison of the two alternative solutions, showing the benefit of the latter approach.

Table 3-9: Improving the minimum NPV improvement for each RM can potentially improve the chances of success of the FDP.

RMs	#1	#2	#3	#4	#5	#6	#7	#8	#9	All	True Field
$(FDP_3 - FDP_2)/FDP_2$ (%)	9	6	1	10	9	3	0.12	0.27	1	4.3	-0.2
$(FDP_{3,alt} - FDP_2)/FDP_2$ (%)	5	4	1	9	8	2	0.34	2	3	3.6	1.7

A good decision-making process, in general, would discuss the potential alternative solutions to overcome any technical hitches (e.g., non-existence of HC in the eastern reservoir) in the field development process. Although it might seem that the robust optimization can fall short in this area, using specific scenarios (e.g., using 3/9 RMs showing no HC in the eastern reservoir) for developing alternative solutions side-by-side can come in handy in such vulnerable situations. Therefore, an obvious extension of this work would be to include such scenarios in order to devise better alternatives and demonstrate the benefit of risk-informed workflow.

Finally, a stricter criterion for checking the economic viability of all the decision variables must be employed to improve the chances of success of the FDP. All decision variables must contribute sufficiently to be of practical significance in the FDP.

At this stage of understanding, we believe that it would be more appropriate to say that all models have a certain degree of accuracy, bias, and error. In our work, we observe these traits in different forms. For example, a good correlation between $EVoCL$ and \overline{VoCL} in both case studies represented the accuracy of the representation. However, this correlation was imperfect due to several model errors, including but not limited to the error in pay-zone representation, which necessitated the application of FoD. The bias of the model is the third important attribute that is best illustrated by the improvement in NPV even when the VOIP was negatively biased. As our analyses show, the proportion of these three traits constantly vary from initial until the end of the field development, as new information is acquired and utilized.

Table 3-10: An improved correlation between simulation models and the reference case as accrued information is utilized in case study II.

Application of strategy on	$(FDP_4 - FDP_1)/FDP_1$ (%)	RMs Improved
Pre-CLFD models, M_{prior}^0	-1%	41%
Cycle 1 models, M_{post}^1	+30%	All
True field (UNISIM-I-R)	+39%	-

As far as we are concerned with observing positive results with our process, we attribute it to three important aspects: (1) actual and assumed similarity between the simulation models and the reference case (**Table 3-10**), (2) the large subset of models to envelope the reservoir uncertainty, and (3) the increased likelihood of success in FDP with the bi-criterion objective function. This can be best illustrated by comparing our original models (prior to CLFD) with the C1 models and their performance with a randomly selected FDP strategy (FDP₄ in this case). Furthermore, one must note that FoD accommodates for the error related to placing a well in a non-reservoir zone and improves the chances of success of the FDP. While we stress the importance of FoD, the associated error with the process is quite inconsistent in nature. This statement is further bolstered by examining the first case study (**Figure 3-11**). Only Cycle 3 demonstrates differing results with and without FoD. One must note that we did not execute FoD for the vertical wells, as we believe that FoD plays an important role in planning a horizontal well only for the discussed case studies. This is also reflected in our results.

To enthruse confidence in the workflow, we aptly chose the initial FDP before executing the three cycles of CLFD using the limited first-hand information at the early stage of development. In case study I, we used carefully optimized FDP by Schiozer et al. (2015, 2019). In case study II, we again used the well-informed methodology of Schiozer et al. (2015, 2019) to optimize and obtain the initial strategy for the CLFD cycles. To reiterate that it was adequate at that stage, we underscore that 100%, 97%, and 94% for the RMs, the approved scenarios, and the ensemble, respectively, were improved using this optimized strategy using their workflow. Combining this evidence with the results observed in **Table 3-10**, one can appreciate that the CLFD cycles do not suffer from any optimization bias. With minimal knowledge in the early stage of field development, it is unlikely to obtain a significant improvement in the reference case in that stage. However, supposing we start with a higher objective function of the reference case prior to CLFD, a robust CLFD workflow must still ensure an improvement by the end of cycles.

The outcome of the CLFD process (or its sub-processes) solely depends on two factors; reliability of the input and robustness of the methodology to quantify and assess uncertainty, followed by reduction of scenarios and optimization. It can be improved further by ensuring that the prior ensemble (M_{prior}) is robust, with a good endeavor to represent the geology of the field. A thorough probabilistic risk assessment of the simulation inputs can help make the process more risk-informed. While there is a huge scope of improvement in the DA process, alternative HM approaches like the one presented by Zakirov et al. (2015) are quite interesting

ways to perform the DA while maintaining geological consistency, by adjusting the anisotropic variogram and petrophysical parameters simultaneously. In addition, Toledo et al. (2017) also suggested that assimilating well test data can further improve the reservoir models. Prudently eliminating irrelevant scenarios to select an appropriate subset of RMs forms the penultimate segment to make the CLFD process feasible for industry applications. Finally, a robust optimization technique offering alternative solutions for unforeseen circumstances must be adapted to boast a risk-mitigating decision. We recommend that CLFD must be implemented with emphasis to improve the project's objective while reducing the chances of failure.

3.7 Conclusions

In this paper, we provide a comprehensive and improved closed-loop field development workflow to obtain risk-informed decisions. The application of the risk-informed CLFD workflow on both the case studies provided several interesting insights on the topic. Some of the most significant conclusions of our study are listed here:

- We present and validate the functioning of CLFD in an actual field-scale benchmark model, based on the risk-informed CLFD methodology. We successfully implemented the workflow in two different case studies:
 - Case study I (Morosov and Schiozer, 2016):
 - Contrary to their results, we were able to improve the initial NPV, both with and without FoD, by 5% and 14%, respectively.
 - Given that we worked with the same level of fidelity (grid size) of models as Morosov and Schiozer (2016), this work shows that upscaling was not a critical factor for their contrasting result.
 - While Morosov and Schiozer (2016) concluded that one possible pitfall was a lack of geostatistical variability in the representative models, we demonstrate an improvement in the result, even without including FoD, under similar controlled environment as theirs.
 - Comparing the results of our first cycle with Morosov and Schiozer (2016), we also revealed that convergence to non-representative parameters during data assimilation was not a source of their negative result during the first cycle as we had similar trends in uncertainty reduction.
 - We observe a good correlation between the expected and the actual value of the closed-loop for all the cycles.

- We stress flexibility of drilling (FoD) as an important component to minimize the chances of “unrealistic drilling”, as bolstered by the results of Cycle 3. Pragmatic implementation of CLFD is important to avoid drilling “unrealistic wells” as the engineers would not drill in non-reservoir zones in a real-life situation, despite the output of simulation models suggesting otherwise.
- Case study II (all vertical wells):
 - We were able to improve the initial NPV by 40%.
 - We performed this to illustrate that the CLFD also works in the vertical-wells scenario, where the flexibility of drilling cannot be practiced as conveniently as for horizontal wells.
 - We observe a good correlation between the expected and the actual value of the closed-loop for all the cycles.
- Amending the conclusion of Morosov and Schiozer (2016), we assert that a large set of geologically consistent models is a vital component to attempt a reliable coverage of geological uncertainty as the field develops.
- The quality of initially drilled wells (in terms of well-bore logs) can sway the optimism or pessimism in an ensemble. To safeguard a good variability of the uncertainties in the ensemble, one must pay attention to these factors as well.
- As observed in both the case-studies, we exhibit that the amount of new and significant inputs to update the uncertainty attributes plays a critical role in the field development process.
- We identify the need for a better data assimilation process to improve assessment of uncertainties, while appreciating the existing bias and error in simulation models.
- While reservoir studies struggle to predict the reservoir performance adequately due to their inherent characteristic of accuracy, bias, and error, a risk-informed CLFD provides an ideal opportunity to include new information from time to time and improve the understanding of the field, which is visible in the form of improved decisions.
- Among other things, the work also exhibits the significance of expelling the relatively poor scenarios and improved optimization process to maximize the likelihood of success. Further improvements in this section, as well as a selection of a better ensemble of RMs, can improve the workflow.
- The introduced VoCL is a good way to quantify the value of a closed-loop based workflow as well as biases related to model-based decisions. While the expected VoCL is always

positive due to the optimization process, actual VoCL can be negative due to bad decision(s).

The work affirms the potential benefits of a CLFD methodology based on the different analyses conducted. We also provide a systematic analysis of the complete workflow to elucidate the evolution of uncertainties and enthuse more confidence in the implementation of such workflows in field applications. To conclude, we present a validated risk-informed closed-loop field development workflow for testing in more complex field development challenges.

Acknowledgements

This work was conducted with the support of Libra Consortium (Petrobras, Shell, Total, CNOOC, CNPC) and PPSA within the ANP R&D tax as "commitment to research and development investments", and Energi Simulation. The authors are grateful for the support of the Center of Petroleum Studies (CEPETRO-UNICAMP/Brazil), the Department of Energy (DE-FEM-UNICAMP/Brazil), and Research Group in Reservoir Simulation and Management (UNISIM-UNICAMP/Brazil). In addition, a special thanks to CMG and Schlumberger for software licenses. The authors would also like to thank Alexandre A. Emerick (Petrobras) for providing the EHM tool. Also, the authors would like to acknowledge the contribution of Celio Maschio (CEPETRO-UNICAMP/Brazil) for providing fundamental codes for the IDLHC optimization process.

Nomenclature

List of Abbreviations

2D	Two-dimensional space
3D	Three-dimensional space
AC	Abandonment costs
AQD	Acceptable quadratic distance
AS	Approved scenarios
BHP	Bottom-hole pressure
C1	Cycle 1
C2	Cycle 2
C3	Cycle 3
$CAPEX$	Capital expenditure
C_e	Covariance matrix of the measurement errors

CLFD	Closed-loop field development
d_i	Vector of predicted production data of the i^{th} simulation scenario
$d_{obs,i}$	Vector of perturbed observations corresponding to the i^{th} simulation scenario
DA	Data assimilation
DECE	Designed exploration and controlled evolution
DLHG	Discretized Latin hypercube combined with geostatistical realizations
EMV	Expected monetary value
ES-MDA	Ensemble smoother with multiple data assimilation
EV_{oCL}	Expected value of closed-loop
f_c	Cut-off frequency
FDP	Field development plan
FoD	Flexibility of drilling
HC	Hydrocarbon
HM	History matching
i	Discount rate
IDLHC	Iterative discrete Latin hypercube
k	Permeability
M	Ensemble of scenarios
OF	Objective function
\bar{O}	Average normalized data mismatch
obs_j	Measured field data at time j
OWC	Oil-water contact
n	Total number (time-steps, representative models, etc.)
N_d	Number of production data observations
N_e	Size of the ensemble
N_p	Cumulative oil production
NPV	Net present value
NQDS	Normalized quadratic distance with sign
NTG	Net-to-gross ratio
OF	Objective function
$OPEX$	Operational expenditure

ORF	Oil recovery factor
OWC	Oil-water contact
P	Probability value
PLT	Production logging tool
<i>POF</i>	Project's objective function
PVT	Pressure-volume-temperature
<i>Q</i>	Rate
QDS	Quadratic distance with signal
<i>R</i>	Gross revenue
RF	Recovery factor
RFT	Repeat formation tester
RM(s)	Representative model(s)
<i>RT</i>	Amount paid in royalties
<i>S</i>	Simulation scenario
SD	Simple distance
<i>sim_j</i>	Simulated field data at time <i>j</i>
<i>ST</i>	Amount paid in special taxes
StoSAG	Stochastic simplex approximate gradient
<i>t</i>	Time period
<i>T</i>	Corporate tax rate
UA(s)	Uncertainty attribute(s)
<i>VoCL</i>	Value of closed-loop
$\overline{\overline{VoCL}}$	Actual value of closed-loop
VOIP	Volume of oil in place
W_i	Cumulative water injection
W_p	Cumulative water production
γ	Tolerance value
δ	Constant

Superscript

0	Initial value
i	Iteration/Cycle
Ref	Reference case (or true field)

Subscript

FDP_{cyx}	Optimized FDP for Cycle x
FDP_{i+1}	Optimized FDP for i^{th} cycle
i (1,2,3..etc.)	# of FDP
k	Index of RM
g	Produced gas
o	Produced oil
$post$	Ensemble posterior to DA
$prior$	Ensemble prior to DA
w	Produced water
wi	Injected water
z	z-direction

4 A Comparative Study to Accelerate Field Development Plan Optimization

Authors:

Ashish Kumar Loomba

Vinicius Eduardo Botechia

Denis José Schiozer

Abstract

Rigorous and continual advancement in the computational domain have drastically reduced the time consumed for simulations. Despite this, the heterogeneity and requirement to use compositional models, among constraints such as field size, can still thwart the optimization of the field development plan (FDP) in terms of time spent. To address this, we proposed and compared different techniques to underscore how to optimize FDP efficiently under uncertainty using an example of a giant benchmark field. We compared four workflows to improve the efficiency of the optimization process. Method 1 uses a full-field model (FFM) approach with an intelligent selection process to eliminate the poorest FDPs. As it is usual to divide a field into sectors for risk-aversion and strategic purposes, Method 2 uses an isolated-sector approach to reduce average simulation time. Method 3 employs the FFM approach to perform the optimization using only the monetary value of the partial life of the field. Method 4 uses a cluster-based search space reduction technique for a predictive analysis from the technical results obtained with partial simulations, which are similar to Method 3. To ensure good decisions, the optimized FDP was always implemented in the FFM with complete field-life at the end of all methods. All proposed workflows are promising in terms of efficiency, acknowledge the entire envelope of uncertainty, and consider multiple scenarios to improve the chances of success of the optimized FDP in the real field. Aside from obtaining good results when compared to traditional methods, we also saved 80–93% of the computational time with these methods. Thus, one can reduce exorbitant costs and delays in performing the FDP optimization. As anticipated, we observed a generic trade-off between decreasing

computational time and increasing field objective function. Despite this, using a new algorithm with predictive analytics in Method 4 produced the best improvement within the shortest timespan, which demonstrates that one can use shorter-term data to understand a field's non-linear response. Numerous authors have already presented various algorithms to optimize an FDP. Despite the existing computational capabilities, these algorithms are still inept at developing a field with time-consuming simulation models. Unlike previous studies, this work presents practical solutions to assist field development, considering probabilistic scenarios to capture associated uncertainty. We also discuss the advantages and disadvantages of the methods to establish their application in different situations.

Keywords

Distributed Computing; Efficiency; Field development plan; Giant field; Isolated sector; Optimization; Partial simulations; Predictive analytics; Propagation of best experiments; Reservoir simulation; Time-consuming models; Uncertainties

4.1 Introduction

Development decisions are a critical component of any oil and gas project. The advent of numerical simulation models, continuously evolving seismic and well-testing procedures, systematic workflows, and perpetually improving computational capabilities, among other technologies, has enabled multidisciplinary teams to appraise a field more efficiently. A subsequently proposed field development plan (FDP) will impact the field's contractual life, with a vast number of significant decision variables. These variables include (but are not limited to) the number, type, location, schedule, and operational settings of wells, as well as the platform capacity and inflow control valves (ICVs). In summary, advancing technologies have been very helpful for the development of oil and gas fields.

Developing a complex and giant field, on the other hand, is still fraught with challenges. Rigorous and continual advancement in the computational domain has drastically reduced the time to simulate a full-field model (FFM) of such fields. Despite this feat, the numerical simulations can become demanding and impractical due to various constraints and boundary conditions. In addition, the requirement of using a compositional model, operation of ICVs, and enhanced oil recovery techniques are potential reasons that can perturb the convergence of the physics-based mathematical models. Consequently, a substantial simulation time combined

with a giant field renders the use of multiple representative FFMs impractical for the FDP optimization.

Volz et al. (2008) presented a workflow for optimizing such fields using multiple FFMs. The authors optimized a clastic reservoir in Siberia. Despite working with a giant field, the FFMs only consumed ~2.5 hours (Litvak and Angert, 2009). Such modest simulation time for FFMs allowed the authors to explore an extensive range of field development options using six equally probable FFMs. One of the authors' focus was on the optimum water injection pattern to assist with the injectors' placement. However, considerable heterogeneity would misplace the injectors in a more inferior location in such an optimization problem. Also, such an objective leaves the producers vulnerable to suboptimal sites. Even if the producers were placed optimally, this would have required a very high number of simulations. In short, the workflow focused on dealing with the extensive amount of decision variables but failed to reduce the number of simulations and total time consumption.

Azoug and Patel (2014) also presented the above-mentioned problem in their real-field example. Drastically contrasting with Volz et al. (2008), their FFMs consumed 5–6 days for a relatively small field (0.6 times Volz et al., 2008). Due to time-consuming simulation models, they revised the FDP of a mature giant field located offshore Abu Dhabi using a combination of 2D and 3D sector models. The models were extracted from a single history-matched and base-case FFM, making the process deterministic in geological uncertainty. The authors studied the impact of injecting water in 2D models. They then used these results to test 3D models for extending the plateau production. However, deterministic sector models come at the cost of ignoring subsurface uncertainty and boundary conditions, which can misguide FDP optimization.

To improve efficiency of an optimization process, Wang et al. (2012) introduced a retrospective optimization framework for optimizing the location of new wells using all the geological realizations. This intelligent procedure addresses consecutive subproblems at each step. In their work, the authors increased the number of realizations in each successive iteration. The authors also demonstrated that using k-means rather than a random clustering procedure could further improve the performance of their proposed method. They validated their work by optimizing the well placement in a 3D synthetic model. A total of 104 realizations were used with an average simulation time of 3 minutes. As the models were swift, the authors ran approximately 200,000 simulations with all realizations. They subsequently ran 20 times lesser simulations with their method and proved its worth. One must note that only five producers

were optimized using as many as 10,000 simulations with their new method. However, with time-consuming models, even 2000 FFMs can be too expensive, as we will present in this work.

Numerous authors have already presented various algorithms to optimize an FDP. Despite the existing computational capabilities, these algorithms are still inept at developing a field with time-consuming FFMs using multiple geological realizations. As previous studies high- lighted, FFMs are an asset but only serve their purpose when they are not time-consuming. Using a single model is unequivocally damaging for the FDP as it assumes that there are no geological and reservoir un- certainties. Thus, using a deterministic model to optimize an FDP, fraught with uncertainty, may still leave vast room for improvement.

Considering this, we propose new workflows to improve the efficiency of the optimization process using multiple representative models (RMs). We compare the efficiency of the proposed workflows with an iterative discrete Latin hypercube (IDLHC) based method (Hohendorff Filho and Schiozer, 2018) as this method was concluded to be as good but faster than the well-established methods (like genetic algorithm). Most importantly, this research introduces two novel concepts; (a) a cluster-based search space reduction for optimization and (b) use of partial simulations for evaluating a field's response over contractual life.

4.2 Objectives

This work presents a number of practical solutions to assist a complex/giant field development while also considering probabilistic scenarios to capture and reproduce uncertainty. The specific objectives of this work are:

1. Define workflows to expedite the process of FDP optimization.
2. Implement and compare these workflows in a giant benchmark field.
3. Discuss the advantages and disadvantages of all workflows to establish their applicability in different situations.
4. Underscore that intermediate results can be used to make the optimization process efficient.

4.3 Methodology

This section presents the four workflows created to optimize FDP under the broad scope of uncertainties. Firstly, we propose a two-step iterative discrete Latin hypercube (2S-IDLHC) algorithm for performing robust optimization (**Algorithm 4-1**). The proposed algorithm is based on Latin hypercube sampling (LHS) to optimize decision variables (Hohendorff Filho

and Schiozer, 2018). We introduced 2S-IDLHC to make the process more efficient. Typically, the lower iterations in an optimization process fall short of delivering an optimal solution. This stems from the fact that the frequency distribution of the decision variables is still amorphous during the early set of iterations. As a consequence, we observe a monotonous trend with evolving iterations. Considering this cue, 2S-IDLHC seeks to solve an optimization problem by breaking it into two steps (**Algorithm 4-1**).

Algorithm 4-1: Two-step iterative discrete Latin hypercube (2S-IDLHC)

Input: : Objective function (f), decision variables with PMF, LHS method
Output : Optimized decision variables
Define $i_1, n_1, r_1, i_2, n_2, r_2$
/* i_1 and i_2 : max. no. of iterations for the 1st and 2nd steps of 2S-IDLHC, respectively */
/* n_1 and n_2 : sample size for the 1st and 2nd steps of 2S-IDLHC, respectively */
/* r_1 and r_2 are total no. of RMs for the 1st and 2nd steps of 2S-IDLHC, respectively */
begin
 $iter \leftarrow 0$
 while $iter < i_1$ **do**
 Run all $n_1 * r_1$ simulations
 Select best x_1 experiments
 Update PMF of the decision variables to generate n_1 FDPs using LHS
 $iter \leftarrow iter + 1$
 end do
 while $iter < i_2$ **do**
 Run all $n_2 * r_2$ simulations
 Select best x_2 experiments
 Update PMF of the decision variables to generate n_2 FDPs using LHS
 $iter \leftarrow iter + 1$
 end do
end

In the first step, we use fewer realizations to build a pragmatic probability mass function (PMF). Next, this updated PMF of decision variables is robustly used with all the RMs to obtain the best solutions.

The four workflows are developed on the groundwork of 2S-IDLHC to expedite the FDP optimization process. Accordingly, the proposed workflows are presented here in descending order of time-consumption:

4.3.1 Full-field model – Propagation of best experiments (FFM-PBE)

Due to demanding FFMs, this workflow consists of the following stages to reduce the dissipated time without affecting the optimized solution:

1. The initial FDPs designed by a stochastic optimization method are more chaotic than those in later stages. As such, we execute the first step of the 2S-IDLHC with FFMs

using partial life as the proxy. One must note that the partial life must be a practical one that lowers the elapsed time and tries to capture a significant part of the field's monetary value, or other objective functions.

We used a bi-criterion objective function to evaluate the FDPs (see Chapter 3) to improve the likelihood of success of the optimized strategy within the ensemble of FFMs:

$$OF^i = \sum_{k=1}^n \begin{cases} P(RM_k) * NPV_k^i & , NPV_k^i \geq f_c * NPV_k^0 \\ 0 & , NPV_k^i < f_c * NPV_k^0 \end{cases} \quad 4-1$$

where NPV_k^0 and NPV_k^i are net present value (NPV) with the initial and the i^{th} FDP for the k^{th} RM, which has a probability of occurrence $P(RM_k)$. To ensure a non-zero objective function (OF) while penalizing the RMs, a cut-off frequency (f_c) is used with each RM to calculate their contributions.

2. In the second step, we simulate the FFMs for the contractual life. However, we introduce the concept of “propagation of best experiments” to limit the number of simulations intelligently. The idea is to select the best FDPs over a gradually incrementing subset of RMs (**Algorithm 4-2**). Therefore, it improves the likelihood of success of the optimized FDP over the ensemble, while drastically reducing the total number of simulations.

Algorithm 4-2: Propagation of best experiments

Input : Objective function (f), Experiments (n_1)
Output : A subset of experiments and their objective functions
/* r_i : RMs that will be evaluated in iteration i of PBE */
Define r_i and cut-off for selecting the best experiments for each iteration i of PBE
begin
 $i \leftarrow 1$
 $r \leftarrow r + r_i$
 while $r.length \leq (\text{Total RMs})$ **do**
 Obtain $f(n_i, r_i)$
 Select the best experiments (n_{i+1}) from $f(n_i, r)$
 $i \leftarrow i + 1$
 Update $r \leftarrow r + r_i$
 end do
 Select final subset of best experiments with their objective functions
end

After completing the optimization process, we recommend performing an intuitive evaluation of the FDP over the ensemble of RMs to extract the most of the proposed FDP. If necessary, one can also use the wells' economic viability test (Botechia et al., 2013) to improve the FDP further.

4.3.2 Isolated sector model (ISM)

It is a usual practice to divide a field into sectors, as it is a risky venture to develop the complete greenfield forthrightly (Volz et al., 2008; Litvak and Angert, 2009; Azoug and Patel, 2014). This approach is more common and appealing for developing giant fields due to their magnitude and concomitant risks. Such an approach is also necessary for offshore fields to strategize the location, number and type of wells, as well as the production systems' capacity.

The underlying theory behind the isolated sector model (ISM) workflow is that the optimal FDP in a sector can improve the complete field's response to a reasonable extent. This sector-based field development provides a direct and indirect approach to optimize the sector and the entire field, respectively. In other words, improving the to-be-optimized sector's economic response can improve the field's economic response.

Following this idea, we use **Algorithm 4-1** to optimize the FDP in the isolated and to-be-optimized sector with **Equation 4-1** as the objective function in the proposed ISM workflow. Due to a shorter simulation time for the sector, we test all the wells' economic viability after obtaining the best possible FDP from the optimization process. A subsequently proposed final strategy is imposed on the FFM to observe its response and evaluate its applicability in the real field.

4.3.3 Full-field model – partial life – monetary results (FFM-PL-MR)

While “time” is an inevitable part of the optimization process, this workflow questions the necessity of the entire contractual period for optimizing an FDP. The FFM-PL-MR workflow is based on the principle that improving the economic response of the FFMs over a sufficiently long partial life can, in turn, help approximate a good FDP for the field's contractual life.

Like the previous workflow, FFM-PL-MR also uses **Algorithm 4-1** to perform the FDP optimization. As the name indicates, we partially simulate the FFMs in this workflow over a shorter and pre-defined field life. We use **Equation 4-1** to calculate the objective function at the end of this period with the partial simulations' financial results. At the end of the process, the optimized FDP is imposed on the FFMs with complete life. Based on the outcome, we implement the FDP in the real field.

4.3.4 Full-field model – partial life – technical results (FFM-PL-TR)

The workflow's basic premise is that relevant technical results can help approximate the field's non-linear behavior. A multi-objective function optimization (MOFO) is performed in this workflow using the technical results (e.g., three-dimensional saturation/flux maps and production data) obtained at the end of the partially simulated FFM. This partial knowledge of the field can then be used to execute a predictive analysis and estimate a good FDP for the field's contractual life. With efficiency in mind, we also introduce an iterative cluster-based search space reduction technique, with the following sequential steps:

1. **Define search space and constraints:** Due quantification and assessment of the initial problem space (\mathbb{X}) can eliminate unnecessary solution candidates (x) to define search space (\mathbb{G}) with eligible candidates (g). We propose using reservoir engineering insights to define the search space and logical constraints. For example, one can define search space for producers by eliminating all grid blocks with statistically low drainage volume in the neighbourhood.
2. **Define clusters and centroids:** Even when using the 2S-IDLHC algorithm and the comparatively smaller search space (\mathbb{G}), one is compelled to test many permutations to find an optimal solution (Volz et al., 2008; Litvak and Angert, 2009). To overcome this issue without affecting the optimal solution, we cluster the search space and only the centroids of these clusters are investigated during the first exploratory phase.
3. **Employ Algorithms 4-1 and 4-2:** We perform MOFO using the 2S-IDLHC algorithm (**Algorithm 4-1**) with selective FDPs (**Algorithm 4-2**). The multi-objective function is calculated using:

$$OF^i = \sum_{k=1}^n P(RM_k) * (\mathbf{W}^T * \mathbf{TR}_k^i) \quad 4-2$$

where \mathbf{TR}_k^i is a vector of normalized technical results for the i^{th} FDP of the k^{th} RM and \mathbf{W}^T is the transposed weight matrix.

4. **Fine Tuning:** With the gradually increasing iterations of 2S-IDLHC, the number of clusters starts decreasing. At this stage, fine-tuning becomes an inevitable component of the cluster-based search space reduction and optimization technique. We gradually increase the number of centroids within the pre-defined clusters. This step ensures the reduction of the eligible candidates (g) while slowly fine-tuning around the best values

of the decision variables. We recommend repeating this process until all the eligible candidates of the search space are duly explored.

One of the main objectives of this work is to present four alternative workflows to accelerate the FDP optimization process. To estimate the efficiency of the workflows, we compare them against the IDLHC method proposed by Hohendorff Filho and Schiozer, 2018. The authors concluded that the IDLHC method yields comparable but faster results than a well-established genetic algorithm-based optimization method. As such, this comparison validates the benefit of using the presented workflows to accelerate the process, especially when working with time-consuming physics-based simulation models.

4.4 Application and Results

In this section, we discuss the results obtained after employing the methodologies. We used a giant-field benchmark case study (UNISIM-III) to test them. The benchmark consists of simulation models under the label of UNISIM-III-2022 (U3-22) and a reference model (UNISIM-III-R) with a high level of geological details emulating the actual field. Correia et al. (2020) created the models using typical reservoir characteristics of Brazilian pre-salt fields. The karstic reservoir models with a carbonate-depositional environment provide a suitable heterogeneous giant-field for testing our methodologies as the FFM's consume ~8 hours for simulations. These also require a compositional model due to high CO₂ content. Additionally, the plateau oil production rate is constrained by the gas production rate at all times.

Given its magnitude, Correia et al. (2020) divided the field into four sectors to streamline the surface and subsurface operations. They also defined water alternating gas (WAG) as the enhanced oil recovery (EOR) mechanism. To promote sustainable development, the gas produced has to be completely re-injected. **Figure 4-1a** shows the initial FDP in U3-22 with 33 producers and 32 injectors scattered across the field.

In this work, we focus on improving the “true” field’s NPV using a single sector of the field to identify the advantages and disadvantages of all four workflows. **Table 4-1** includes the chronological activities.

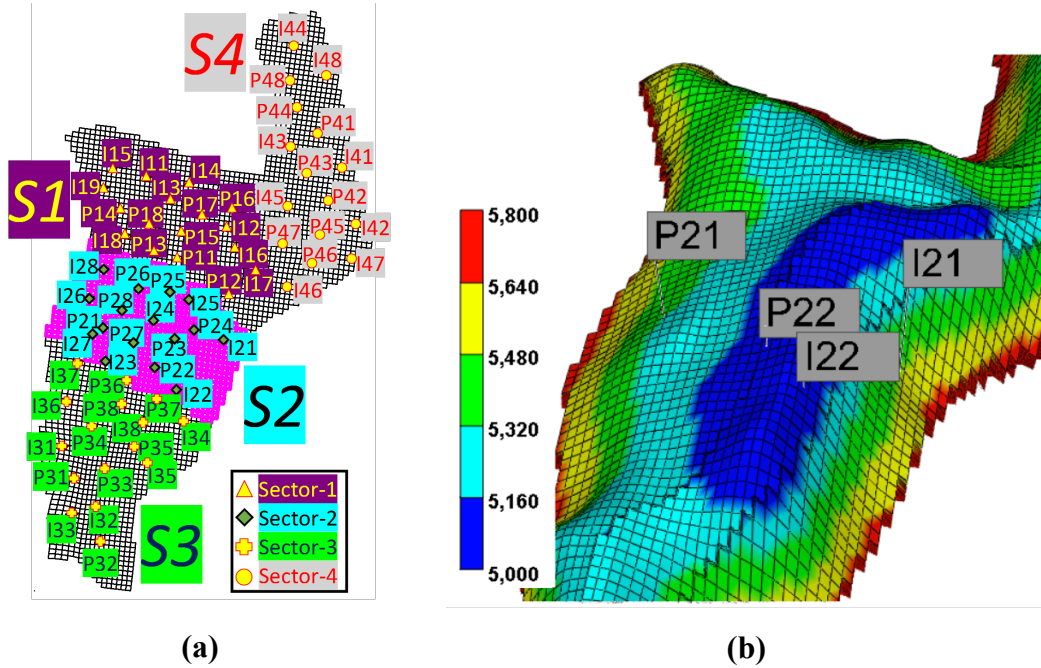


Figure 4-1: (a) Initial FDP in U3-22 (pink grid blocks highlight Sector-2) and (b) a simple topographic map of the field highlighting the fixed wells in Sector-2.

Table 4-1: Relevant field activities and information.

Period (days)	Drilling, completion and connection activity	Remarks
0-1219	6 producers (P11 ... P16) and 7 injectors (I11 ... I17) in S1	Extended well test
1765-1887	2 producers (P21 and P22) and 2 injectors (I21 and I22) in S2	End of history
1887-2131	4 producers (P23 ... P26) and 4 injectors (I23 ... I26) in S2	
2131-2496	6 producers and 6 injectors in both S3 and S4	
3014-3134	2 producers and 2 injectors in S1	All wells drilled in S1
3835-3957	2 producers (P27 and P28) and 2 injectors (I27 and I28) in S2	All wells drilled in S2
4200-4444	2 producers and 2 injectors in both S3 and S4	~40% contractual life
5540	-	~50% contractual life
6636	-	~60% contractual life
11019	-	Field Abandonment

At the end of the history period (i.e., 1887 days), 52 of 100 scenarios for U3-22 could be adequately history-matched. We used those scenarios (M^{52}) to select a set of 10 RMs (M^{10}) using RMFinder 2.0 (Meira et al., 2017). Also, three scenarios (M^3) were selected using the min-mean-max of the selected M^{10} for working with the first step of 2S-IDLHC. The same RMs and scenarios were used throughout this work to focus entirely on comparing the proposed

workflows. Furthermore, all simulations were executed using parallel solvers in a distributed simulations environment. A total of 100 processors were allotted for the optimization process, with ten processors for each simultaneous simulation.

The optimization problem can be defined as maximizing the EMV of the 10 RMs (**Equation 4-1**) at the end of the field's contractual life using 24 decision variables. These variables are positive integers and represent the (i,j) block of the twelve to-be-drilled wells in Sector 2 (S2). Four of the sixteen vertical wells have already been drilled in S2 by the end of the history period (**Table 4-1**). All wells are subject to shut down after reaching a maximum gas-oil ratio of $1600 \text{ m}^3/\text{m}^3$ at surface conditions. Although one can use all the four presented workflows with any underlying optimization algorithm, we only used IDLHC in this work. Furthermore, all decision variables are constrained to be within S2, and all grid blocks within S2 compose the problem space for the optimization process.

4.4.1 Full-field model – Propagation of best experiments (FFM-PBE)

FFM-PBE is initiated by partially simulating the M^3 during the first step of the 2S-IDLHC. We considered 40% of the field's contractual life adequate for this purpose due to four reasons:

1. It makes the process efficient by saving ~46 days.
2. It encapsulates all significant events (**Table 4-1**).
3. It contributes a sizeable portion to field NPV (>50%).
4. It acts as a suitable proxy in the early phase of the stochastic-based 2S-IDLHC algorithm.

Using the PMF obtained at the end of the first step of 2S-IDLHC, we continued with the second step of 2S-IDLHC by completely simulating the M^{10} .

At the end of the optimization, we reviewed the optimized FDP for any potential discrepancy to make necessary adjustments. Gas production is a limiting factor in the model and increased gas production further lowers the oil production rate. As the time value of money is much higher in the initial production phase, higher gas production in the early phase can thus lower the EMV. The optimization process placed three injectors close to P21 (**Figure 4-4a**). Such a scenario would lead to an early shutdown of P21 due to increasing gas production in the early phase (**Figure 4-2**). Hence, P21 was shut down to deliver a better alternative. Otherwise, P21 would have been shut down in a couple of years while depreciating the EMV.

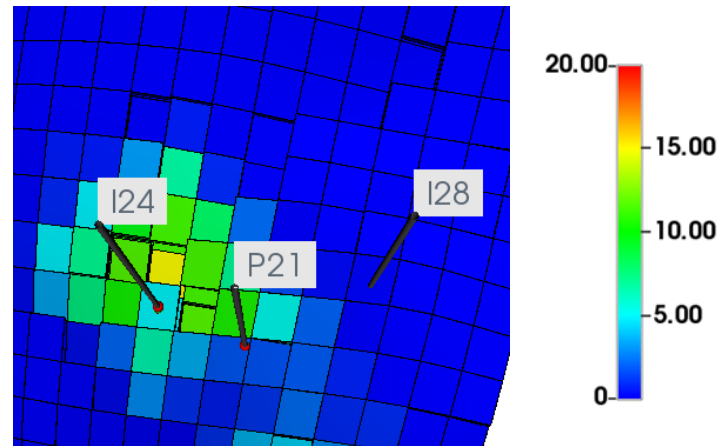


Figure 4-2: Observed gas per unit area - total (meters) in one of the RMs within two years of opening well I24.

Table 4-2 summarizes the results. Figure 4-3 and Figure 4-4a highlight the evolution of the objective functions and the optimized FDP obtained using FFM-PBE, respectively.

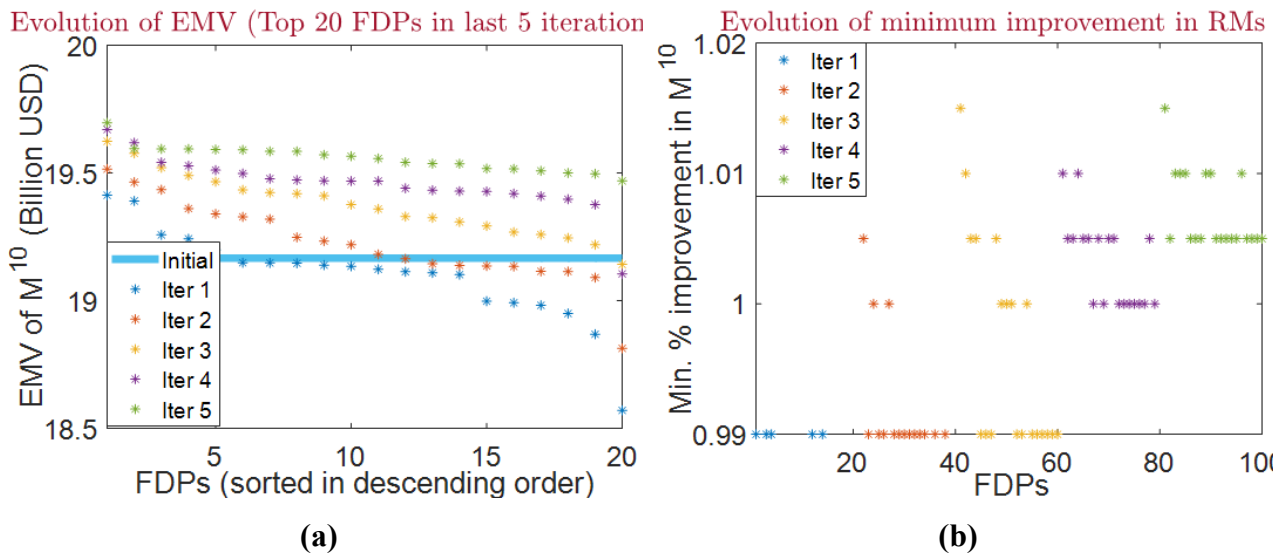


Figure 4-3: Evolution of the (a) EMV of the 10 RMs and (b) the minimum % improvement of individual RMs using the FFM-PBE workflow.

4.4.2 Isolated sector model (ISM)

In ISM workflow, we isolated the S2 and executed three iterations with the M^3 . Subsequently, we implemented five iterations with the isolated S2 of the M^{10} . The optimization process improved the EMV of the M^{10} (with isolated S2) by 21%. A total of 12% was the observed minimum percentage improvement of NPV within this ensemble. We then performed an economic viability test to further improve the FDP, which substantially increased the EMV

of the M^{10} (with isolated S2). Overall, the EMV was improved to 24%, and the minimum percentage improvement of NPV was 15%.

The obtained strategy was implemented in the M^{10} FFM to evaluate its adequacy. **Table 4-2** presents the results. **Figures 4-5** and **4-4b** highlight the evolution of the objective functions and the optimized FDP obtained using FFM-PBE, respectively.

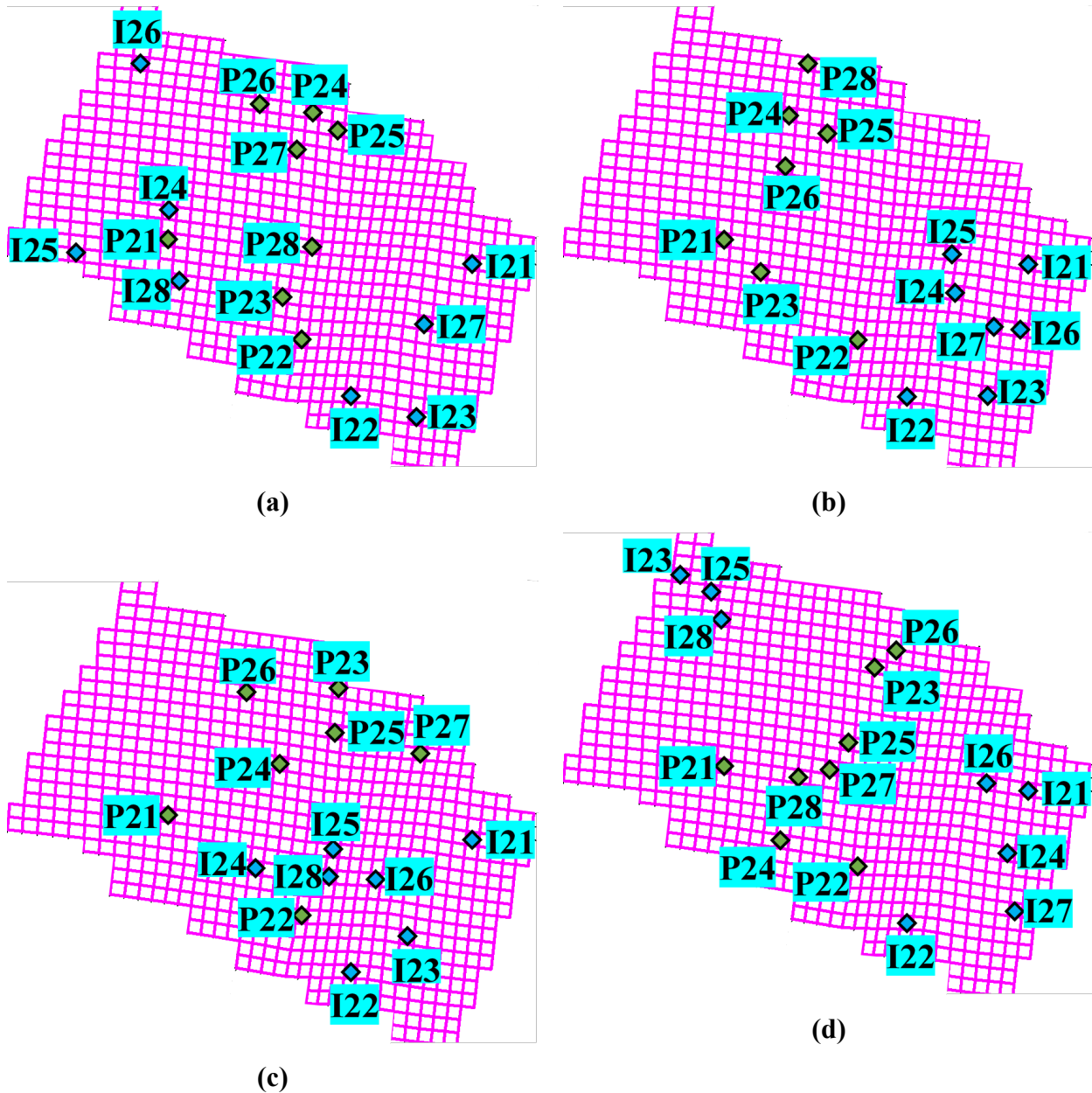


Figure 4-4: Optimal FDP bred by the four workflows (a) FFM-PBE, (b) ISM, (c) FFM-PL-MR and (d) FFM-PL-TR. Note that P21, I21, P22, and I22 have exactly same locations as their positions were considered fixed along with the wells in the remaining sectors.

Table 4-2: Summary of time consumed and results yielded by different workflows ^[1].

			FFM-CL ^[2] with			1	2	3	4
			10 RMs + IDLHC	10 RMs + 2S-IDLHC	3 RMs +IDLHC	FFM-PBE	ISM	FFM-PL-MR	FFM-PL-TR
2S-IDLHC	Step 1	Total Simulations	6000	1800	1800	1800	1800	1800	1050
		Mean Simulation Time (hours)	7.7	7.7	7.7	1.6	1.7	1.6	1.4
	Step 2	Total Simulations	5000	5000	1500	1800	5000	5000	1800
		Mean Simulation Time (hours)	7.7	7.7	7.7	7.7	1.7	1.6	2.3
Adjustments (Intuitive/Economic viability) ^[3]			10	10	10	10	480+ 10	10	10
Total simulations for the workflow			11010	6810	3310	3610	7050	6810	2860
Total time consumed (days)			353	218	106	70	52	46	24
% Time saved ^[4]			0%	38%	70%	80%	85%	87%	93%
Efficiency ^[4]			1	2	3	5	7	8	15
% change in EMV(M^{10})			-	-	-	3.7%	3.4%	2.5%	4.2%
Min. % improvement (M^{10})			-	-	-	2.6%	2.4%	1.4%	1.7%

[1] With the same processing capacity for all the workflows in the same distributed computing system

[2] FFM-CL = Full-field model – Complete lifecycle (i.e., traditional method of performing optimization)

[3] In ISM, 480 simulations were run to evaluate the economic viability (improving S2 results by 14%). All RMs were run once at the end of the optimization process for a final evaluation/adjustment.

[4] Compared to the traditional approach of using 10 RMs with the available IDLHC algorithm proposed by Hohendorff Filho and Schiozer (2018). This method was selected as the authors presented their workflow faster than the well-established genetic algorithm.

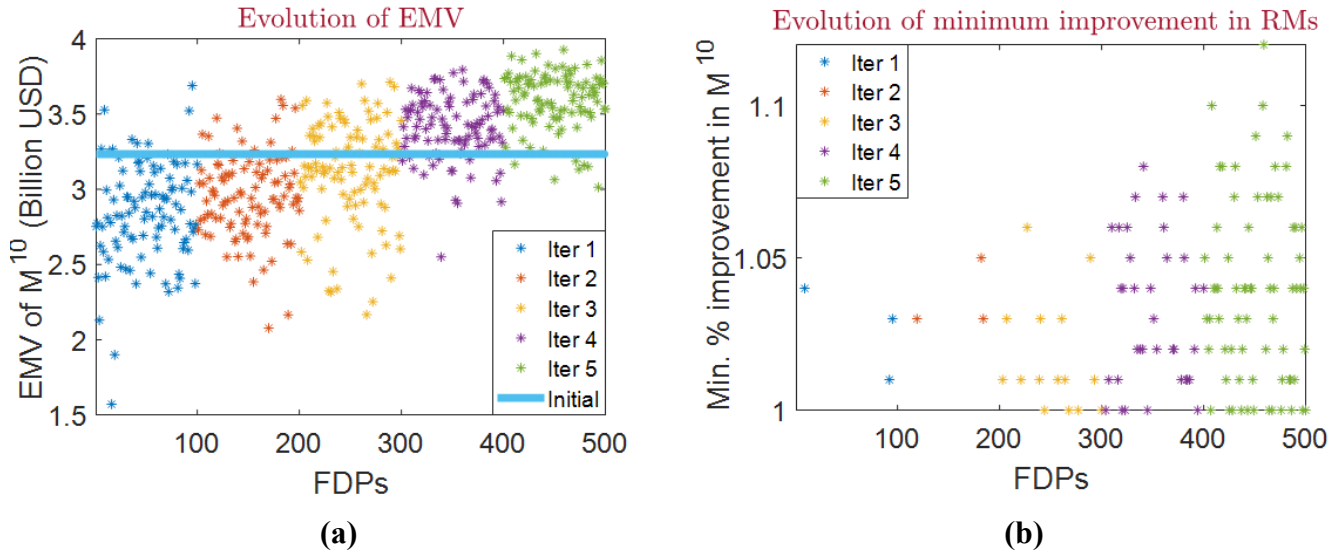


Figure 4-5: Evolution of the (a) EMV of the 10 RMs and (b) the minimum percentage improvement of individual RMs with isolated S2 using the ISM workflow.

As ISM uses the isolated S2, it finds the best setup by placing the injectors as far apart as possible from the producers. Consequently, it places the injectors on the eastern side of the field and the producers on the western side of the field, closer to the crest. While this setup is excellent for the box-type isolated sector model, it certainly hampers the field recovery process, as shown in **Figure 4-10**.

4.4.3 Full-field model – partial life – monetary results (FFM-PL-MR)

Like FFM-PBE, 40% of the field's contractual life was considered adequate in the FFM-PL-MR workflow. We simulated the M^3 and the M^{10} during the first and second steps of the 2S-IDLHC, respectively. At the end of the optimization process, we reviewed the optimized FDP for any potential discrepancy and made intuitive adjustments. Finally, the optimized strategy was simulated for the contractual life in the M^{10} to evaluate its adequacy.

Figures 4-6 and **4-4c** highlight the evolution of the objective functions and the optimized FDP obtained using FFM-PL-MR, respectively. As expected, FFM-PL-MR attempts to place the injectors closer to the producers to maintain pressure and improve sweep efficiency over the defined time frame. **Table 4-2** presents the complete results.

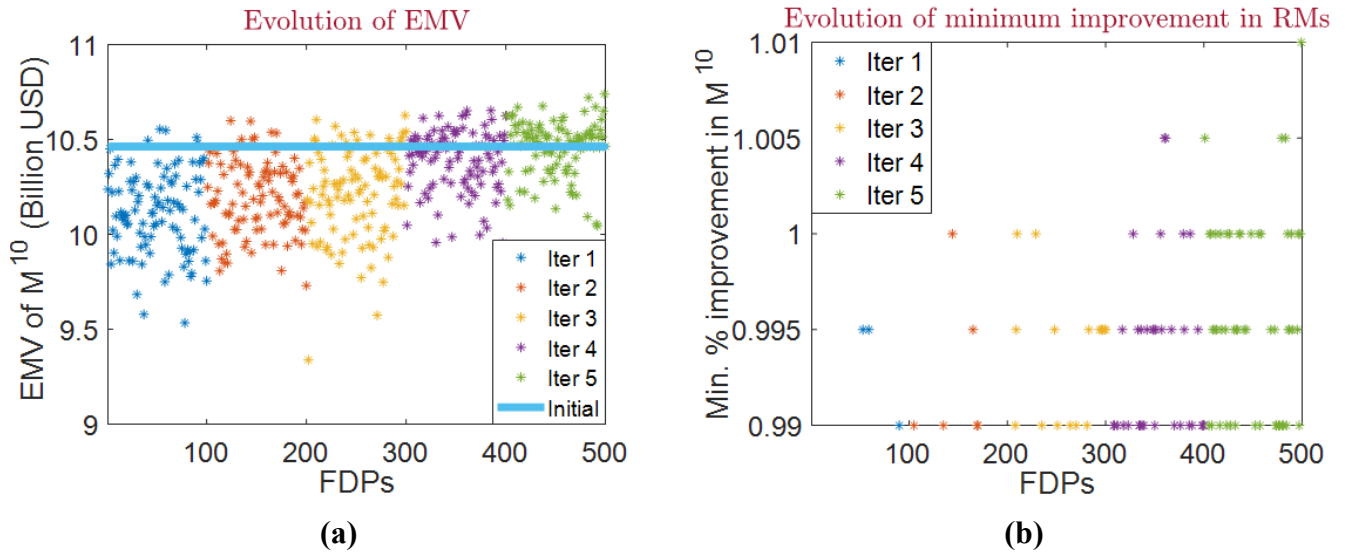


Figure 4-6: Evolution of the (a) EMV of the 10 RMs and (b) the minimum percentage improvement of individual RMs with partially simulated FFMs using the FFM-PL-MR workflow.

4.4.4 Full-field model – partial life – technical results (FFM-PL-TR)

To employ the cluster-based search space reduction for optimization, we initiate this workflow by redefining the search space and constraints:

1. **Define search space and constraints:** A total of 772 grid blocks are valid solution candidates (x) of the problem space (X) in the optimization problem. To extract the best FDPs from a massive number of solutions (a permutation of 12 wells out of 772 locations), we start by defining search space for producers and injectors.
 - **Producers:** The search space for producers is defined based on the movable oil in the vicinity. To approximate movable oil, we discretized the three-phase relative permeability diagram (**Figure 4-7**). Using this and 3D saturation maps at the end of the history period, one can obtain the oil's movability in each grid block at that particular time. We sequentially eliminated the grid blocks with the lowest movable oil within the 9 km², 4.8 km², and 1 km² using a 30% cutoff value (**Figure 4-8a**). Next, we ensured that none of the eligible candidates of the search space is close to the existing wells. A total of 230 eligible candidates (**Figure 4-8b**), roughly covering a third of the sector, were considered adequate for the subsequent step.
 - **Injectors:** To ensure 100% reinjection of the gas produced while curbing the chances of an early breakthrough, we eliminated the solution candidates of the problem space based on the mean horizontal permeability across the vertical depth (**Figure 4-9a**). We also removed the solution candidates, which had a very high horizontal permeability in

one or more blocks across the vertical extent. This step ensured that the injection process would not be inefficient. We also confirmed that none of the eligible candidates of the search space were close to the existing wells in the field. A total of 520 eligible candidates (**Figure 4-9b**) covering roughly 2/3 of the sector were considered adequate for the subsequent step.

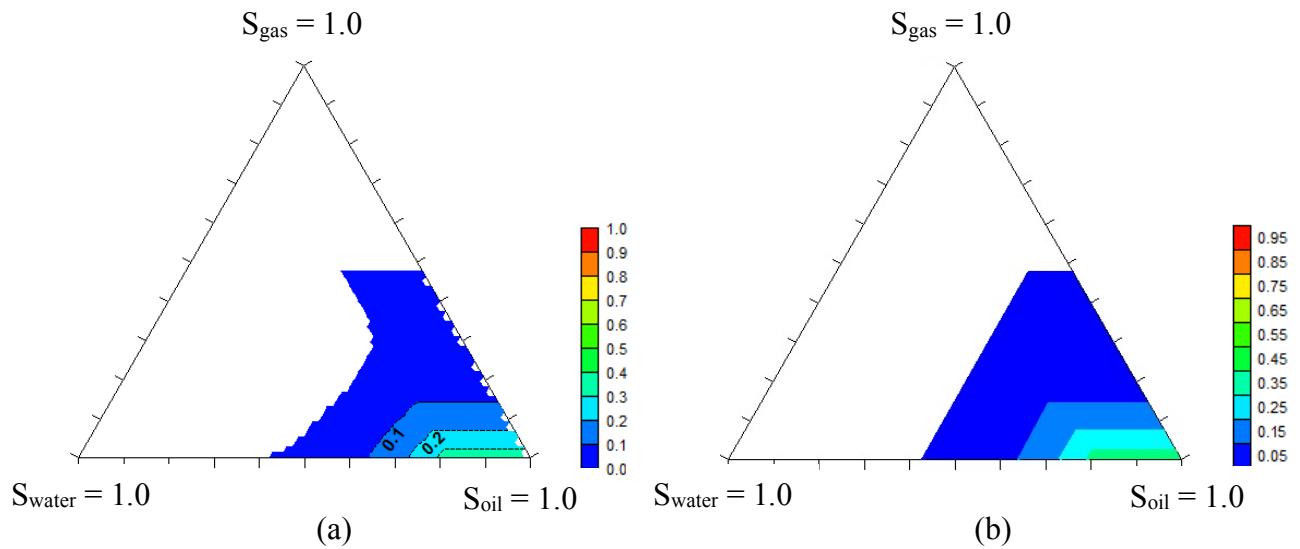


Figure 4-7: An example of the (a) original and (b) discretized three-phase relative permeability diagram.

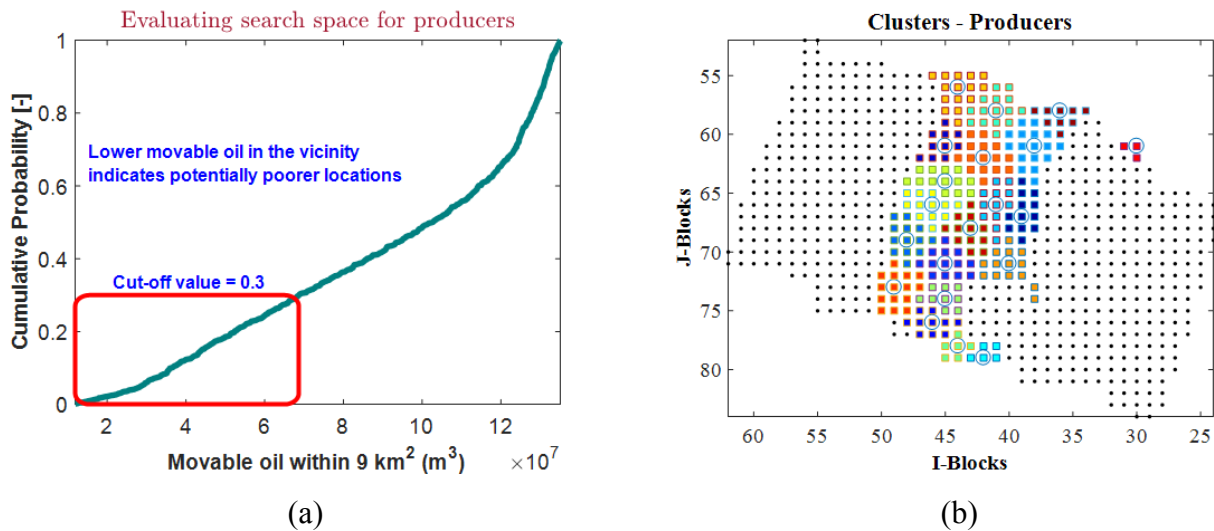


Figure 4-8: (a) An example of reducing problem space by evaluating the movable oil within 9 km² of each grid block and (b) well-defined 230 eligible candidates for selecting producers with defined clusters and centroids.

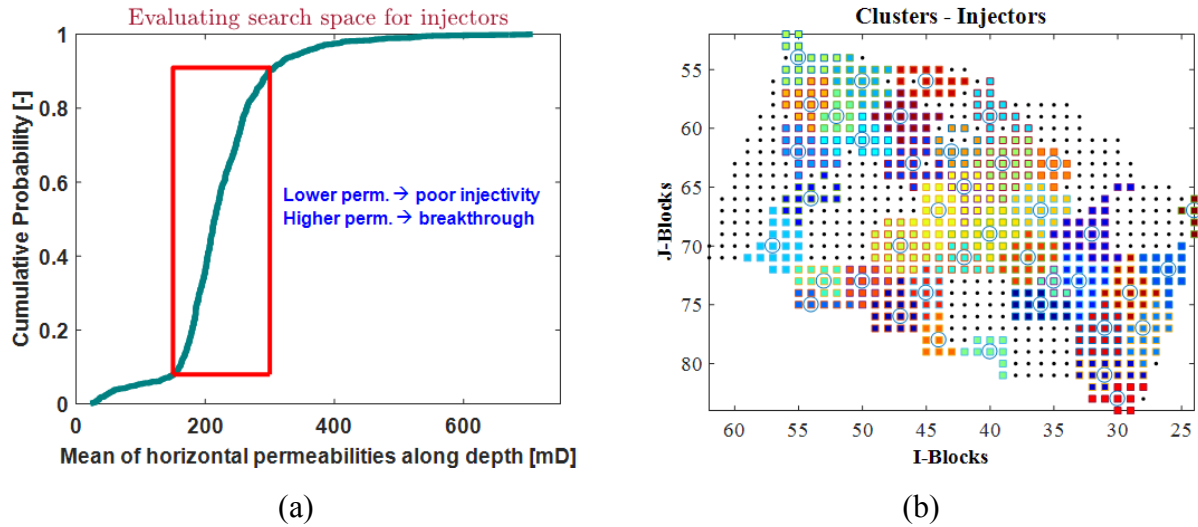


Figure 4-9: (a) Example of reducing problem space by evaluating the mean of horizontal permeabilities across the vertical depth and (b) well-defined 520 eligible candidates for selecting injectors with defined clusters and centroids.

- **Constraints:** The following constraints and simplifications were implemented to improve efficiency:
 - To-be-drilled injectors must be placed at least 1000 meters away from to-be-drilled producers to control the early gas breakthrough.
 - Like previous workflows, 40% of the contractual life was considered adequate for the first step of the 2S-IDLHC algorithm. However, for greater efficiency, we opened all wells at the end of the history period while maintaining WAG cycles.
 - For the second step of the 2S-IDLHC, we used 50% of the contractual life to simulate the field partially. However, we extracted the technical results at the end of both 40% and 50% of the contractual life.
- 2. **Define clusters and centroids:** Once the search space is defined using engineering insights, all eligible candidates are treated equally. At this step, we used them to define 20 and 40 clusters/centroids for the producers and injectors using k-means clustering based on distance (**Figures 4-8b** and **4-9b**). This step forms the base of the subsequent steps to gradually explore each cluster's neighborhood and cover the entire search space.
- 3. **Employ Algorithms 4-1 and 4-2:** We used these centroids as the only available eligible candidates during the first step of 2S-IDLHC. **Table 4-3** defines the technical results and their respective weights used during this process. For calculating the “net flux oil - directional,” we multiplied the net flux oil with its Gini index. Gini index is a statistical

tool to capture the inequality in a frequency distribution. Thus, “net flux oil - directional” improves the EMV by acknowledging the potential oil movement from all directions beyond PL. All grid parameters were calculated for the neighboring area of $\sim 5 \text{ km}^2$. By the end of the first step of 2S-IDLHC, there were only 17 and 18 eligible candidates for producers and injectors, respectively ($\sim 42\%$ reduction of eligible candidates).

Table 4-3: Technical Results and their assigned weights for the simulations with PL = 40% of the contractual life ^[1].

Scalar Parameters ^[2]	Weights	Grid Parameters ^[3]	Weights
Cumulative oil produced	1	Net flux oil - directional	0.15
Gas oil ratio	-0.045	Net Gas in vicinity	-0.25
Water oil ratio	-0.025	Net Water in vicinity	-0.1

^[1] Similar to NPV calculations, the weights are also discounted over time.

^[2] Weights of scalar parameters were selected based on the proportion of oil/water/gas production cost.

^[3] Existing simulations of the M^{10} with initial FDPs were used to estimate a logical set of weights using linear regression.

4. **Fine Tuning:** We employed fine-tuning with the changing PMF of the decreasing centroids. This was performed in two discrete phases during the second step of the 2S-IDLHC:

- **Expansion of the surviving clusters:** We defined three distinct clusters/centroids within the surviving clusters and executed two iterations. Only 39 and 37 eligible candidates for producers and injectors, respectively, withstood by the end of these iterations ($\sim 27\%$ reduction of eligible candidates).
- **Inclusion of complete search space:** Finally, we broke down all surviving clusters (39+37) into individual eligible candidates to perform further fine-tuning. In other words, we considered all possible locations within the surviving clusters during the last three iterations of the process. As we started with an initial ensemble of clusters representing the search space, we can affirm that the entire search space was explored by the end of this step.

Lastly, the optimized strategy was simulated for the contractual life in the M^{10} to evaluate its adequacy. **Figure 4-4d** illustrates the optimized FDP. The FFM-PL-TR attempts to consider the contractual life by placing the injectors to improve the flow over the entire period. Unlike FFM-PBE, it does not try to shut down any existing well and places more wells

in the deeper eastern peripheral to minimize breakthrough. Also, unlike FFM-PL-MR, it distances the injectors from the producers even when we used partial-life-based simulations like FFM-PL-MR.

Nevertheless, it is always possible to optimize the objective function to attain a globally optimal solution, but the main goal of this work is to emphasize practical methodologies to accelerate the optimization problems without affecting the objective function, while keeping in mind that all models are inherently imperfect.

By re-evaluating the optimized strategies, one can observe that all the workflows attempt to place the producers as close to the crest as possible to minimize breakthrough, as shown in **Figures 4-1b** and **4-4**. The injectors, on the other hand, are placed very differently. FFM-PBE tries to improve sweep by placing three injectors on the southwestern side of the S2 near an existing well, P21. The other injectors are placed on the relatively deeper peripheral on the eastern side of the field. Such a setup also helps sweep more oil towards the producers in the S3 (**Figure 4-10**). As we defined minimum inter-well spacing at 400 meters, one can also observe wells being placed nearby in some instances.

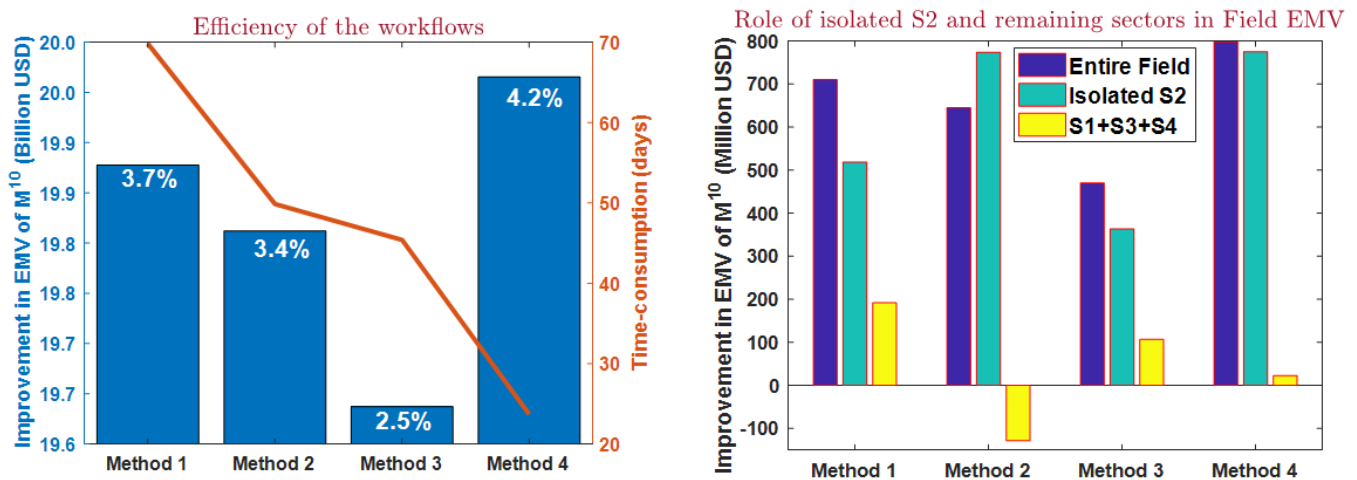


Figure 4-10: (a) Comparing the improvement in Field's EMV (nominal value and percentage) with the time consumption of the workflows and, (b) comparing the improvement in EMV (relative value) and approximating the role of isolated S2 and remaining sectors in entire field improvement.

Table 4-2 summarizes the results and **Figure 4-10** presents the efficiency of the workflows. The improvement appears to be small as we only optimize one sector of the field. This leads to deflated values as we optimize only a quarter of the field to evaluate its impact on the entire field. For example, we obtained a 3.4% improvement in the field's EMV using the ISM workflow. In terms of nominal value, however, a 3.4% increment is equivalent to 650

Million USD. This value is also equivalent to a substantial 24% improvement in the isolated S2.

4.5 Discussion

In the previous sections, we defined and implemented four workflows to expedite the FDP optimization process. In this section, we discuss the advantages and disadvantages of the workflows to establish their applicability in different situations. As the optimization process is more pertinent for revising the FDP with continuously accrued information over time, it is vital to discuss the workflows in that context too. Thus, we compare and evaluate all the workflows to recognize their practicality for revising FDPs with the closed-loop field development and management workflows.

4.5.1 Full-field model – Propagation of best experiments (FFM-PBE)

The FFM-PBE can expedite the process fivefold using FFM simulations while considering all temporal and spatial boundary conditions. The newly introduced concept of "propagation of best experiments" in this workflow also outperforms some ML-based methods in reducing the number of simulations (Santos et al., 2020). This quality also renders it fit for optimizing the operational settings of the wells and ICVs throughout the contractual life. However, performing several closed-loop field development/management cycles with this expensive workflow can sometimes render the process unfeasible. For an even more extensive or complicated giant field (Azoug and Patel, 2014), this method may not serve the purpose of FDP optimization. Due to the FFM simulations' impracticality in such instances, one should reconsider the following elements:

1. **Processing power:** Increasing the total number of processors in the distributed simulation environment can reduce the total time consumed.
2. **Representative models:** Reducing the number of RMs would also accelerate the workflow. Such a trade-off, however, comes at the cost of overlooking uncertainty.
3. **Employing cluster-based search space reduction technique for optimization:** This technique can also improve the final solution while reducing the required simulations.
4. Substituting the first three iterations with the FFM-PL-TR ones can also help increase efficiency of the workflow six-fold.

4.5.2 Isolated sector model (ISM)

This workflow made the optimization process sevenfold faster while focusing on the isolated sector itself. At the end of the workflow, we tested the optimized strategy on the FFM simulations.

Nevertheless, this step only helps ensure the final strategy's workability instead of playing any role in its evolution. This inference is best shown by **Figure 4-10b**. As expected, the ISM workflow better optimizes the isolated S2. However, as it fails to acknowledge other sectors, we negatively impact the results for the entire field (as shown by the bar graph in **Figure 4-10b**). It thus requires a better test to generate a more robust FDP from the perspective of the entire field.

Therefore, one of the biggest concerns with the ISM workflow is the negligence of the boundary conditions. Boundary conditions are vital for any physics-based simulation model. While other workflows honor the spatial boundary conditions, ISM downplays its importance by isolating itself from the neighbouring blocks (**Figures 4-10b** and **4-11**). Depending on reservoir characteristics, this can harm the entire field with effects ranging from trivial to significant, as shown in **Figure 10b**.

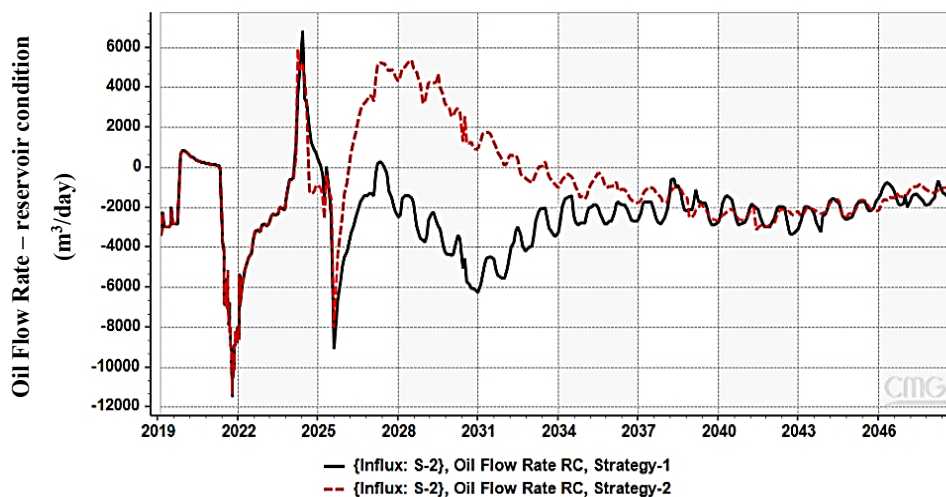


Figure 4-11: Two FDPs (Strategy 1 and Strategy 2) in a single FFM can yield contrasting total oil flow rate (influx) from all sectors surrounding S2. However, the ISM workflow assumes a constant 0 influx at all times as it ignores the boundary conditions.

Such disregard of the boundary conditions also makes the optimized strategy insensitive to any changes outside the isolated sector. New intermittent information acquired and assimilated in the adjacent sectors during closed-loop field development/management will not affect the ISM's final strategy. Even if the well placement or operational settings were very different outside the isolated sector, these would still have zero impact on the final strategy obtained using the ISM workflow. Likewise, the referred insensitivity also invokes misinformed decisions. The workflow also does not serve the purpose of optimizing the

decision variables across the entire field. Optimizing the FDP for the entire field using this method would be more time-consuming and questionable than other workflows.

Using **Algorithm 4-2**, this workflow can become more than twice as efficient and therefore very helpful for defining an initial FDP. However, the gaps discussed above still make it a poor workflow for closed-loop field development and management methodologies, especially in developing the entire field. Nevertheless, one can thoroughly test the workflow's sensitivity to ponder its use. As the location of development wells generally has greater impact than their operational settings, this workflow may still be applicable to revise FDPs in the management and revitalization phase of a particular sector.

4.5.3 Full-field model – partial life – monetary results (FFM-PL-MR)

Apart from the boundary conditions, time is another inevitable part of the optimization process. Regardless, this workflow attempts to only use partial simulations to define FDPs for the longer run.

Firstly, one must adequately propose the partial time to control the trade-off between time consumed and results. The partial life must capture a significant part of the total NPV and include the field's response to the most critical spatial boundary conditions (e.g., wells and operational settings). We used 40% of the contractual life in the presented result as it covered ~55% of the total NPV of the RMs, while expediting the optimization process eightfold. However, it fails to capture the newly drilled wells' response in the second development phase of S2 to a large extent, as those wells were only opened in the penultimate year before the end of the 40% contractual life (**Table 4-1**). This lack is one reason for its poor performance in terms of objective function. To obtain better results with this workflow, while improving the efficiency nine-fold, we recommend using at least 60% of the contractual life combining **Algorithms 4-1** and **4-2**.

Most importantly, this workflow yields a very intuitive FDP (**Figure 4-4c**) that only boosts the monetary value over the partial life without considering the contractual life (**Figure 4-12**). The workflow in itself is incapable of capturing the field's non-linear response for the residual term. This indifference is why such shorter simulations cannot be relied upon for approximating FDPs for the contractual life. One can also notice the passive evolution of the EMV (**Figure 4-6**), which derive from the fact that limited solutions exist for the mid-term optimization (which also helped yield the best solution over the partial life, as shown in **Figure 4-12a**).

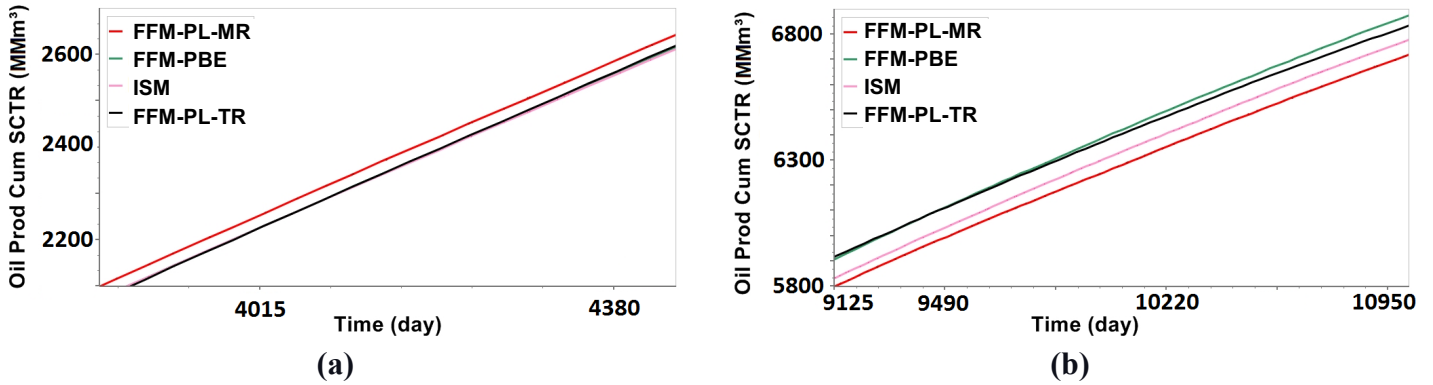


Figure 4-12: Cumulative oil production with the optimized FDPs yielded by the four workflows for (a) mid-term (~2 years before the partial life of 40%) and (b) long-term (5 years before the contractual life). The best FDP for the mid-term (obtained with FFM-PL-MR) becomes the poorest candidate in the long run.

As suggested above, this workflow is unfit for closed-loop field development and management, despite being efficient. Such partial objective functions are more apt for integration with the contractual life to yield a multi-objective and robust strategy over both the short- and long-term (van Essen et al., 2011). However, we included this approach for two reasons:

1. To mitigate the common misconception; improving the financial results for the partial life also implies a continuous improvement for the contractual life.
2. To generate benchmark results for comparing FFM-PL-TR; this comparison is essential to underscore the importance of intermediate technical results for efficient optimization process, even when one disregards time.

4.5.4 Full-field model – partial life – technical results (FFM-PL-TR)

Due to the drawbacks presented in the previous subsection, engineers hardly consider partial simulations for optimizing the complete lifecycle's objective function. For this reason, we introduced the FFM-PL-TR workflow to overcome those drawbacks and enthruse confidence in such partial simulations for efficient optimization. Aside from introducing shorter simulations for approximating the FDP for the contractual life, we introduced a new optimization technique in this workflow. Cluster-based search space reduction technique for optimization can help evaluate a giant problem space efficiently using both gradient-based and gradient-free algorithms.

The scalar technical results attempt to mimic the NPV for the partial life (Table 4-3). We assigned their weights using the cumulative production/injection and the cost of commodities up to the partial life. In other words, using scalar technical results alone would

have had generated results like the ones obtained using the FFM-PL-MR workflow. This ineptitude is where the grid-based technical results come into play. This set focuses on the field's residual life (**Figure 4-12b**), but the weights must be carefully assigned to meet the field's objectives. Using the ten initial simulations with the original FDP, a regression model was used to derive a logical ensemble of weights and mimic the contractual life of NPV. Continuous improvement of these weights with each iteration would definitely help obtain better FDPs.

Our results also indirectly implied two things: The selection of RMs is still a vulnerable process (**Table 4-4**) that needs to be improved for closed-loop field development and management. Besides that the objective function of Method 4 needs further improvement to make it even more risk-averse.

Unlike the last two chapters, we did not implement the optimized strategies in the reference case (or “true field”). This refraining is mainly because the results in the reference case do not dictate the final recommendation for the best technique among the four proposed methods. The main focus of this work was to improve the EMV of the simulation models only rather than the results in the reference case. Nonetheless, we stress that one can improve the results in the reference case by working on the likelihood of success over the ensemble and risk-informed procedures, among other steps.

Table 4-4: Results obtained after implementing optimized strategies in M^{52} .

Objective functions evaluated for M^{52}	Method 1 FFM-PBE	Method 2 ISM	Method 3 FFM-PL-MR	Method 4 FFM-PL-TR
EMV of the ensemble	3.3%	2.9%	2.2%	3.4%
Minimum % improvement	0.6%	-0.4%	-0.8%	-4.1%

Finally, a stepwise increment of the partial life will help optimize the financial objectives via operational settings of wells and ICVs of the entire field throughout its contractual life. Though it might consume more time, it would still be the most efficient among the other proposed or even existing workflows.

A globally optimal solution is one of the targets of optimization. However, all reservoir models are inherently imperfect (Oliver and Alfonzo, 2018; Rammay et al., 2019; Neto et al., 2020; Loomba et al., 2021). Thus, the likelihood of the final solution being a global one in the ensemble (and the actual field) is very low (**Table 4-4**). This axiom, in turn, signifies that one

needs to reduce time on optimization and focus more on reservoir/fluid characterization to address disparities.

From that perspective, we proposed four workflows to improve efficiency while approximating a good FDP that works well for the entire ensemble (M^{10}). Having an efficient workflow, one can develop giant fields and revise the FDP for complex fields requiring high simulation time. It also paves the way to develop a typical field using high-fidelity models to capture the critical aspects and uncertainties at a relatively finer scale.

Based on the results, we advise using FFM-PL-TR as an excellent replacement for the traditional workflows. Using FFM-PL-TR, one can reduce simulation time and improve the project's objective function. Skeptical about search space definition, we repeated the whole workflow by using the entire problem space as the search space. Again, the FFM-PL-TR workflow outperformed the ISM and FFM-PL-MR workflows. This repetition further strengthened the applicability of this workflow.

Coupling the newly introduced optimization technique from FFM-PL-TR, FFM-PBE would be our second preference. This integration would widen the gap between the results obtained using FFM-PBE and ISM. Though FFM-PBE consumes more time than ISM, this increased gap would be a good reason to use it. This workflow also respects boundary conditions, unlike ISM. Without a proper understanding of the impact of other sectors on the isolated sector, the ISM workflow is quite vulnerable for applications.

Finally, the success of FFM-PL-MR is directly proportional to the simulation time under consideration. Meanwhile, increasing the simulation time comes at the risk of losing efficiency and this trade-off renders it unfit for very time-consuming models.

4.6 Conclusions

This work presents four practical workflows to optimize a field development plan (FDP) efficiently, while considering the probabilistic scenarios to capture uncertainty. Method 1 (FFM-PBE) uses a full-field approach to eliminate the inferior FDPs using an intelligent selection process (PBE). Method 2 (ISM) uses an isolated-sector approach. In Method 3 (FFM-PL-MR), we perform the optimization using only the monetary value of the partial life of the field. As an alternative, Method 4 (FFM-PL-TR) uses a cluster-based search space reduction technique to analyze the technical results and predict the non-linear response of the field. The optimized FDP was always implemented in the full-field model (FFM) with complete field-life at the end of all methods to ensure good decisions.

The workflows were proposed to aid the FDP optimization for time-consuming models (e.g., giant fields, higher fidelity models, and compositional models) and typical fields. We implemented the workflows in a giant benchmark field with a very expensive full-field model (FFM) to understand their advantages and disadvantages. The relevant conclusions are listed below:

- The presented workflows can expedite the FDP optimization process 5 to 15 times. We achieved similar results to traditional workflows by running 36-74% less simulations.
- Full-field model – partial life – technical results (FFM-PL-TR) is a good replacement for conventional full-field simulations. We observed the best improvement in the objective function using FFM-PL-TR.
- The technical results obtained with the partial life-based simulations can contribute information for approximating FDPs. At the same time, this study emphasizes that intermediate results can be used for efficiency in the optimization process. FFM-PL-TR workflow improved the efficiency of the FDP optimization process 15 times while using 74% less simulations.
- The newly proposed cluster-based search space reduction technique for optimization eliminates the worst candidates of the problem space faster to improve the field objective functions.
- Although the full-field model – propagation of best experiments (FFM-PBE) workflow provided the second-best results in terms of the objective function, it can still be very time-consuming. Enhancing this workflow with the cluster-based search space reduction and other proposed workflows would help make it more attractive for practical applications.
- The presented isolated sector model (ISM) workflow is slightly less time-consuming than the FFM-PBE workflow, but the results are relatively inferior.
- Full-field model – partial life – monetary results (FFM-PL-MR) workflow is as fast as the ISM workflow but yields the lowest improvement among all workflows. Due to its total disregard for the contractual time, this workflow is only best suited for a quicker evaluation of the initial FDP.
- Finally, model error is an inherent component within the simulation models. As such, this research promotes the idea of developing a field with risk-averse techniques and select an appropriate FDP efficiently that works for the entire ensemble.

Acknowledgments

This work was conducted with the support of Libra Consortium (Petrobras, Shell Brasil, Total Energies, CNOOC, CNPC) and PPSA within the ANP R&D levy as "commitment to research and development investments" and Energi Simulation. The authors are grateful for the support of the Center for Petroleum Studies (CEPETRO-UNICAMP/Brazil), the Department of Energy (DE-FEM-UNICAMP/Brazil), and the Research Group in Reservoir Simulation and Management (UNISIM-UNICAMP/Brazil). Also, a special thanks to CMG and Schlumberger for the software licenses.

Nomenclature

List of Abbreviations

2D	Two-dimensional space
2S-IDLHC	Two-step iterative discrete Latin hypercube
3D	Three-dimensional space
CL	Contractual life
EMV	Expected monetary value
EOR	Enhanced oil recovery
f_c	Cut-off frequency
FDP	Field development plan
FFM	Full-field model
g	Eligible candidates
\mathbb{G}	Search space
IDLHC	Iterative discrete Latin hypercube
ICV	Inflow control valve
ISM	Isolated sector model
LHS	Latin hypercube sampling
ML	Machine learning
MOFO	Multi-objective function optimization
MR	Monetary results
M	Ensemble of scenarios
n	Total number (time-steps, representative models, etc.)

NPV	Net present value
OF	Objective function
P	Probability value
PBE	Propagation of best experiments
PL	Partial life
PMF	Probability mass function
RM(s)	Representative model(s)
S2	Sector-2
TR	Technical results
TR	Vector of technical results
U3-22	UNISIM-III-2022 simulation model
W	Weight matrix
WAG	Water alternating gas
x	Solution candidates
\mathbb{X}	Problem space
Superscript	
0	Initial value
i	Number of FDP/RMs
T	Transpose
Subscript	
k	Index of RM

5 Revising Field Development Plan of a Giant Field Under Uncertainty Using Accrued Information

Authors:

Ashish Kumar Loomba

Vinicius Eduardo Botechia

Denis José Schiozer

Abstract

A field development plan (FDP) is fraught with uncertainties. Its optimization is critical for successfully developing an oil and gas field using the accrued information over time. However, computational expense and heterogeneities, among other factors, can render such tasks infeasible for complex and giant fields considering the time to implement decisions. To tackle this inadequacy, we present an efficient and risk-informed closed-loop field development (CLFD) workflow for recurrently revising the FDP using the accrued information. CLFD is a feedback-based field development process that assimilates the accrued information within the models to improve decision-making processes. To make the process more efficient, we integrated multiple concepts of machine learning, an intelligent selection process to discard the worst FDP options and a growing set of representative models (RMs). These concepts were combined and used with a recently introduced optimizer to efficiently explore the search space of decision variables. Unlike previous work, we also added the execution time of the CLFD workflow and worked with more realistic timelines to confirm the utility of a CLFD workflow. Given the importance of data assimilation and new well-logs in a CLFD workflow, we also worked with rigorous conditions without a reduction in uncertainty attributes. The proposed CLFD workflow was implemented on a benchmark analogous to a giant field with extensively time-consuming simulation models. We demonstrated that the presented workflow can improve the efficiency of the CLFD workflows by >85% compared to the previously validated workflow. The results underscore that an ensemble with as few as 100 scenarios is sufficient to gauge the geological uncertainty, despite working with a giant field

with highly heterogeneous characteristics. Finally, we also presented some acute insights and potential pitfalls of a CLFD workflow. As with the development of a real field, we also present problems related to data assimilation. These observations are critical to providing the necessary recommendations for the practical application of a CLFD workflow. To summarize, we present a validated, efficient, and risk-informed CLFD workflow for revising FDPs to optimize the objective function of an oil and gas field.

Keywords

Efficiency; Field development plan; Giant field; Optimization; Machine Learning; Partial simulations; Predictive analytics; Propagation of best experiments; Reservoir simulation; Time-consuming models; Uncertainties

5.1 Introduction

Drilling wells in an oil and gas field is an inevitable step for extracting natural resources. As it is a cost-intensive process, geoscientists and engineers must drill wells at limited and calculated locations to improve the predefined objective function of the FDP. However, each well perforates only a few square feet of the total formation. With a limited number of wells, one can extract information from only a few square kilometers. Thus, reservoir formation is largely unknown as the ratio of the volume of drilled area to the entire reservoir is negligible. It is thus vital to work with uncertainty to make the best decisions for the FDP.

Incorporating uncertainty allows the operators to embrace the situation more competently and mitigate the risk of failure. It is common to appraise a field to extract new information. Assimilating such information is helpful to update the uncertainty quantification and further improve decision-making under uncertainties. However, obtaining new information during the appraisal phase also comes at an exorbitant cost. Therefore, most decisions relevant to the FDP (number, locations and types of wells, operational settings, and other decision variables) are made using the information before drilling the first development well. Consequently, this process yields a sub-optimal FDP (Loomba et al., 2021).

With this in mind, numerous workflows have been developed to revise FDP under uncertainty and improve the objective function of the project. Closed-loop field development (CLFD) (Shirangi and Durlofsky, 2015; Morosov and Schiozer, 2016; Hidalgo et al., 2017; Kim et al., 2018; Loomba et al., 2021) is one such workflow. CLFD is a feedback-based field

development process that uses data on newly drilled wells and their production over time. Such new wells and their well-testing results, among other sources of information, provide new insights into the fluid flow and reservoir characteristics. CLFD systematically accrues and assimilates such information in multiple phases to update reservoir scenarios. Finally, these scenarios are used to optimize the project's objective function by revising the FDPs.

In Chapter 3, we described the limitations of all prior studies on CLFD. We highlighted that ambiguity in results, limited tests on field-scale models, and incomplete explanation of the evolution of uncertainties are some of the shortcomings of prior studies. We attempted to bridge the gap by validating their risk-informed workflow on two examples. We also addressed the importance of improving the field rather than the simulation models. However, the workflow is very time-consuming and unrealistic for practical applications. We generated 500 petrophysical images to perform data assimilation before selecting representative models (RMs). We also simulated 1600 scenarios per RM during the optimization process. But, unlike theoretical studies, even a single reservoir model of an actual oil and gas field can consume long hours for simulation (Volz et al., 2008; Litvak and Angert, 2009; Azoug and Patel, 2014). It is thus infeasible to simulate tens of thousands of full physics-based simulations using the CLFD workflow of Chapter 3. The study also presumed that CLFD workflow does not require any time for its execution, like previous studies.

To summarize, current workflows are infeasible for a realistic oil and gas asset while completely discounting the critical decision-making period. We therefore present a workflow to enthrone confidence in CLFD for practical applications. This work aims to introduce an efficient CLFD workflow to maximize the benefits of developing a giant and heterogeneous field, using a pragmatic time frame. Unlike most theoretical studies, we work on an extensively time-consuming model. A machine learning (ML) assisted optimization process is also presented in this work to predict the behavior of the partially simulated scenarios. We use it to demonstrate that partial simulations can be used to predict the field's behavior and drastically reduce computational time.

5.2 Objectives

Identifying the gaps in the literature, this article presents a unique case study. We implement an efficient and risk-informed CLFD workflow in rigorous conditions to expose pitfalls and guidelines for its applications. While the general objective of this work is to recurrently revise FDP optimization under uncertainty, the specific objectives are listed below:

1. Present an efficient CLFD workflow for practical applications. As a CLFD workflow consists of multiple steps, it is important to strike a balance to ensure that uncertainty quantification and assessment are done effectively.
2. Validate the workflow on a giant benchmark field, with extensive time-consuming physics-based simulation models. As most studies only use simple synthetic models, it is essential to validate the workflow on a time-consuming and field-scale example to understand its utility.
3. Introduce an ML-assisted technique to accelerate optimization process. Unlike conventional methods, we present the advantage of using intermediate results obtained by running simulations over partial life to optimize the project's objective function. We also use the newly proposed cluster-based learning and evolution optimizer or CLEO (Appendix C) algorithm to explore the problem space intelligently for such complex applications.
4. Introduce a routine for working with multiple approved scenarios to maximize the likelihood of success and expedite the CLFD workflow. We use the concepts of propagation of best experiments and increasing RMs with iterations for the same.
5. Establish the benefit of a CLFD workflow by including its execution time and working with realistic timelines.
6. Revise the FDP without any uncertainty reduction. In other words, data assimilation using historical production data and well-logs are the only components providing new understanding about the reservoir. Such rigorous conditions provide an excellent setup to understand the benefit of data assimilation (DA) process in a CLFD workflow.
7. Discuss the key observations, potential pitfalls of CLFD workflow and provide necessary recommendations for practical applications.

5.3 Methodology

In Chapter 3, we introduced a comprehensive and validated CLFD workflow. The workflow requires a large ensemble of geologically consistent models to work with field uncertainty. We used 500 petrophysical images to assure a reliable coverage of geological uncertainty as the field develops. However, using as many as 500 scenarios can be impractical for real applications, as presented by several authors (Volz et al., 2008; Litvak and Angert, 2009; Azoug and Patel, 2014; Loomba et al., 2022). These facts raise two riveting questions regarding: (a) the number of scenarios and if 500 is the formula for the success of CLFD and (b) how to revise FDP for real applications that are extensively time-consuming.

Ideally, a CLFD workflow must be as efficient as possible as it serves to improve prior decisions during the highly uncertain development phase. Bearing this in mind, we present an efficient and risk-informed workflow to make CLFD workflow viable for real applications. We present a cycle of practical and risk-informed CLFD, as follows:

1. Action: Generate petrophysical realizations to capture the geological uncertainties during this active phase of acquiring first-hand information.
2. Update inputs: Prepare the initial ensemble of scenarios combining updated uncertainty attributes along with geologically consistent petrophysical images.
3. Data Assimilation: Assimilate the noisy production data and minimize its mismatch with the simulated ensemble.
4. Approved Scenarios: Carefully examine the ensemble of posterior scenarios to discard the unlikely scenarios to mitigate their negative impact on the decision-making process.
5. Select RMs and optimize: Efficiently optimize using the concepts of ML propagation of best experiments (PBE) and growing RMs with iterations (see **Algorithm 5-1**). The process uses cluster-based learning and evolution optimizer (CLEO) as the core optimization algorithm. We discuss the critical elements of **Algorithm 5-1** below:

Machine learning (ML) model: An ML model is a program trained with a dataset using one of the countless learning algorithms (for example, linear regression, logistic regression, decision tree, random forest algorithm). A trained ML model can perceive patterns and predict the behavior of a previously unseen dataset.

Table 5-1: List of scalar and grid parameters extracted.

Scalar Parameters	Grid Parameters ^[1]
Cumulative oil produced	Net flux oil (directional)
Gas oil ratio	Net Gas
Water oil ratio	Net Water

[1] Grid parameters are calculated in the vicinity of the wells. We refer readers to Chapter 4 for details.

In this work, we simulate approved scenarios and obtain their net present value (NPV) to prepare the dataset. We extract technical results (**Table 5-1**) from the simulated approved scenarios at different time steps. Structuring this labeled data together, we train our ML model. Such an approach is also known as supervised ML, as we train the ML model by providing it with a labelled dataset.

Algorithm 5-1 - FDP optimization (using CLEO and ML model)

Input: : Problem statement, approved scenarios

Output : Optimized decision variables

Define : Stop criteria

begin

1. Identify problem space, partial life and technical results to be used
2. Using reservoir engineering insights, define search space
3. Define the initial clusters of search space using k-means clustering
4. Select representative eligible candidates for each cluster
5. Simulate approved scenarios to obtain NPV and technical results
6. Make a ML model using extracted data
7. Select r RMs
8. $iter \leftarrow 0$
9. **while** Stop criteria is False **do**
10. Generate n FDPs with the PMF of clusters
11. Use PBE; partially simulate scenarios and extract technical results
12. Predict the NPV using ML model
13. Update PMF of the clusters using best b FDPs
14. **if** Expansion is True **then**
15. Expand the clusters
16. Select representative eligible candidates for each cluster
17. **else**
18. **Break**
19. **end if**
20. Use the best FDP to simulate approved scenarios
21. Update the ML model using new data generated in previous step
22. $iter \leftarrow iter + 1$
23. Update n, r
24. **end while**

end

During each iteration, we simulate the reservoir scenarios over a limited life of the field rather than the complete lifecycle. We extract the technical results for this

partial period and prepare them for the ML model. Our trained ML model predicts the NPV for the lifecycle of the field for this unseen data.

We then use the best FDP in the iteration to simulate the approved scenarios again for the complete lifecycle and extract the labelled dataset. Finally, we update our ML model using this dataset before moving on to the next iteration. The main purpose of using an ML model is to exponentially improve the efficiency of the optimization process.

Propagation of best experiments (PBE): To limit the number of simulations, we introduced the idea of PBE in Chapter 4, which selects the best FDPs over a gradually incrementing subset of RMs within an iteration of the optimization process. Only these selected FDPs are tested with the next subset of RMs. The process is repeated until all RMs have been considered (for more information, the readers are referred to **Algorithm 4-2** in Chapter 4). The main objectives of using PBE are (a) to reduce the total simulations and (b) improve the likelihood of success of the optimized FDP over the ensemble.

Increasing RMs with iterations: We also integrate the concept of growing RMs with each iteration (Wang et al., 2012; Loomba et al., 2022) in conjunction with the risk-averse objective function presented by Chapters 2 and 3. While the former reduces the number of simulations, the latter is a risk-averse approach to maximize the chances of success in the real field.

Cluster-based learning and evolution optimizer (CLEO): In this work, we used CLEO as the core optimization algorithm (Appendix C). CLEO is a user-friendly optimization algorithm that deftly deals with extensive decision variables and problem space.

As we built our workflow on the fundamentals of Chapter 3, we only described the main differences in this work. We direct the readers to Chapter 3 for a better insight into each step. We stress that the workflow presented in Chapter 3 lacks features to make it practical for real field applications. In the next section, we examine these differences and implement the proposed workflow on a giant-field benchmark case. Unlike other studies, we use an extensively time-consuming model to elaborate the indispensable changes made in the complete workflow.

5.4 Application and Results

In this work, we used UNISIM-III, a giant-field benchmark case study (**Figure 5-1**). This synthetic reservoir was created to understand and work with Brazilian pre-salt fields (Chaves, 2018; Correia et al., 2020). The giant field consists of karsts and volcanic rocks, within a carbonate-depositional environment. The benchmark case study includes an ensemble of simulation models (UNISIM-III-2022) to capture uncertainty; and a reference case (UNISIM-III-R) which emulates the “true field”. Such a benchmark case study, with mutually exclusive models, allows engineers and geoscientists to test their methodology. For a detailed explanation of the simulation and reference models, we refer the readers to Correia et al. (2020).

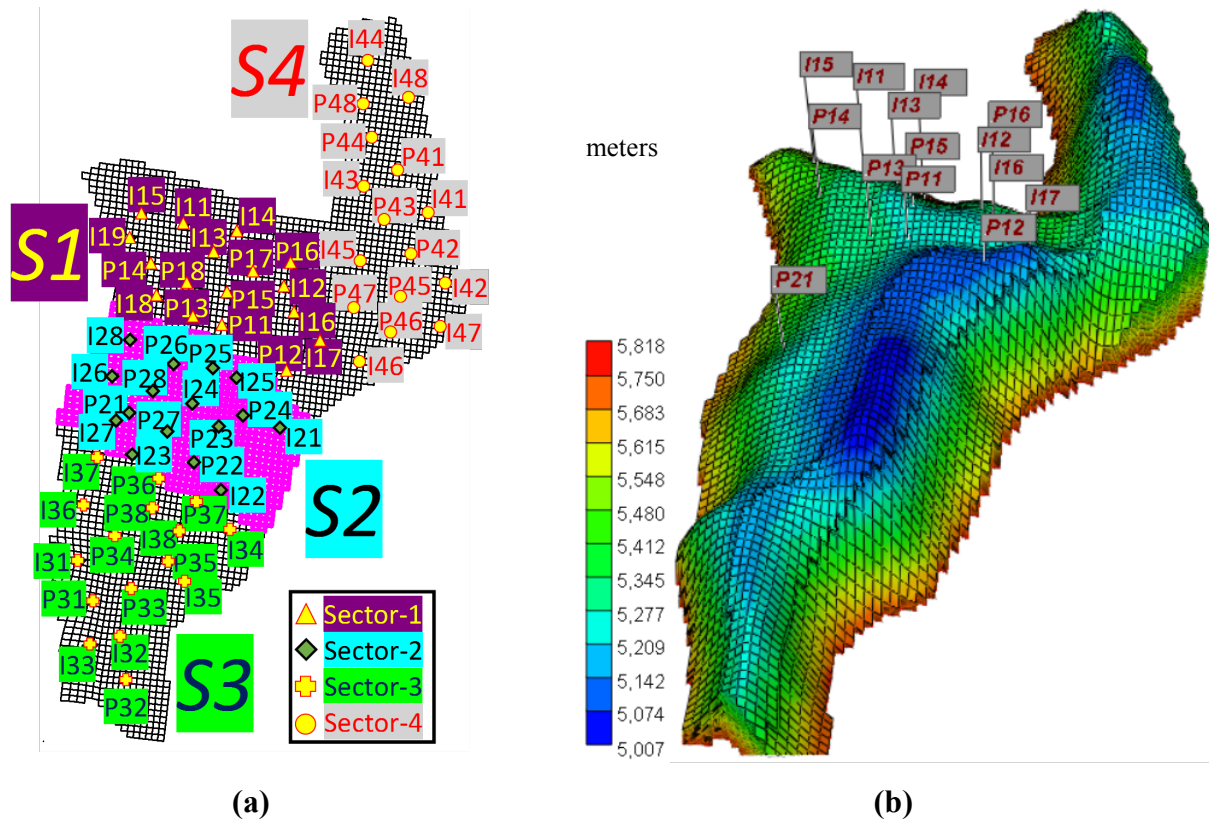


Figure 5-1: (a) UNISIM-III-2022 was divided into four sectors (pink blocks highlight Sector-2) and (b) grid-top map (in meters) of the UNISIM-III-2022 highlighting the field topography (adapted from Chapter 4).

This giant field is divided into four sectors (**Figure 5-1a**) so as to streamline the subsurface operations and sequentially develop the sectors (**Table 5-2**). The sectors communicate with each other and each one corresponds to a production platform. For sustainable development, 100% of the gas produced is re-injected into the reservoir. The authors also defined water-alternating gas for maximizing oil recovery. **Figure 5-1a** shows an

FDP in UNISIM-III-2022 with 33 producers and 32 injectors scattered across the field. Fourteen of these wells (shown in **Figure 5-1b**) were drilled within the first 1219 days of field development.

In this work, we only focus on optimizing the field's net present value (NPV) using the decision variables from sector-2 (S2):

1. Thirteen out of seventeen development wells of Sector-1 are already operational before the first cycle of CLFD (**Table 5-2**).
2. Despite working with limited decision variables from only a quarter of the field (i.e., S2), we worked with full-field models to include the impact of neighboring sectors for making a well-informed decision (Chapter 4). One must note that the locations of the wells of other sectors are considered fixed for all three cycles. Only to-be-drilled wells of S2 are revised using the accrued information over time.
3. Although we are optimizing decision variables of S2, we assimilate newly acquired information (well-logs, production data, etc.) from all four sectors.
4. Since we are working with the entire field, taking one or all sectors for employing CLFD renders little difference, but there is a small difference in execution time. Taking a quarter of the gigantic field (i.e., S2), with limited non-drilled wells as the decision variables only exposes the true merit of CLFD.
5. Sector-2 is the only sector with maximum influence from neighboring sectors (**Figure 5-1a**). Thus, it is a good sector for testing our predictive analytics-based optimization process.

It is also prudent to start with an optimized FDP to gauge the benefit of CLFD workflow. In Appendix C, we assimilated data until $t = 1219$ days to optimize the NPV of the “true field” by 13%, using non-drilled wells (of all four sectors) as the decision variables. We used their optimized FDP as our initial strategy.

Table 5-2 chronologically summarizes the major activities in the field with additional information on the execution of each cycle of CLFD.

Table 5-2: Relevant field activities and information.

Period (days)	Drilling, completion and commission activity in the field ^[1]	Remarks
0-1219	6 producers (P11 ... P16) and 7 injectors (I11 ... I17) in S1; producer P21 in S2	Extended well test performed in S1 in the first year followed an idle 1.4 years
At $t = 1219$, Cycle 0 ^[2] (pre-CLFD) was executed		
1308-2039	4 producers (P22 ... P25) and 4 injectors (I21 ... I24) in S2; 2 producers and 2 injectors in both S3 and S4	
At $t = 1978$, Cycle 1 was executed (revised (i,j) blocks of 7 to-be-drilled wells in S2)		
2039-2315	1 producer (P26) and 2 injectors (I25, I26) in S2; 2 producers and 2 injectors in both S3 and S4	
At $t = 2404$, Cycle 2 was executed (revised (i,j) blocks of 4 to-be-drilled wells in S2)		
2404-2769	2 producers and 2 injectors in both S3 and S4	
2769-3134	2 producers and 2 injectors in S1	All wells drilled in S1
At $t = 3531$, Cycle 3 was executed (revised (i,j) blocks of 4 to-be-drilled wells in S2)		
3592-3957	2 producers and 2 injectors in S2, S3, and S4 each	All wells drilled in S2, S3, and S4
4322	-	~39% contractual life
5053	-	~46% contractual life
11019	-	Field abandonment

[1] We considered a period of 3 months to drill, complete, and commission each well. Only one well per sector is drilled at a given time.

[2] Synonym to pre-CLFD optimization. For details, readers are referred to Appendix C.

In the following subsections, we share our results in further details. In the first subsection, we present the implementation of the methodology discussed in Cycle 1. This subsection is followed by some important observations in Cycle 3. Finally, we discuss the results of all the cycles in the form of a comprehensive table and additional figures.

5.4.1 Cycle 1 of CLFD

The first cycle of CLFD uses the information until the end of the 1978th day (**Figure 5-2**). Provided we used ensemble-smoother with multiple data assimilation or ES-MDA (Emerick and Reynolds, 2013), we limited our work to 100 scenarios. The highlights are provided below:

- We generated 100 images of porosity, permeability and rock-types using 27 well-logs (including 13 new logs from wells drilled after 1219 days).
- Using noisy production data over these 5.4 years, we performed data assimilation for 100 scenarios, combining uncertainty attributes and geostatistical images.
- We approved 44 scenarios from the posterior ensemble of scenarios.
- We used **Algorithm 5-1** to efficiently revise the FDP using the accrued information.

- We executed the optimization process using multiple RMs over ten iterations to improve all 44 simulation scenarios by a median value of 2.3%.

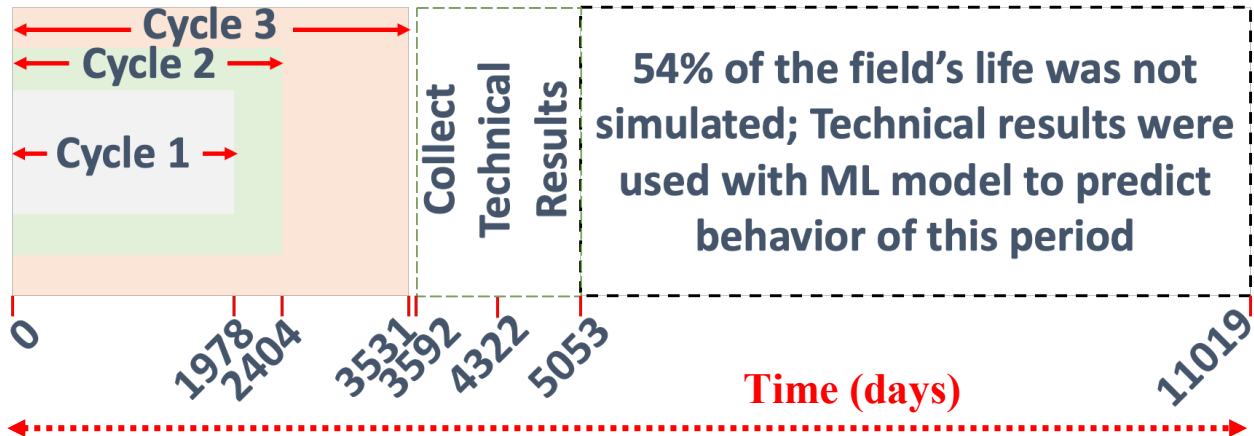
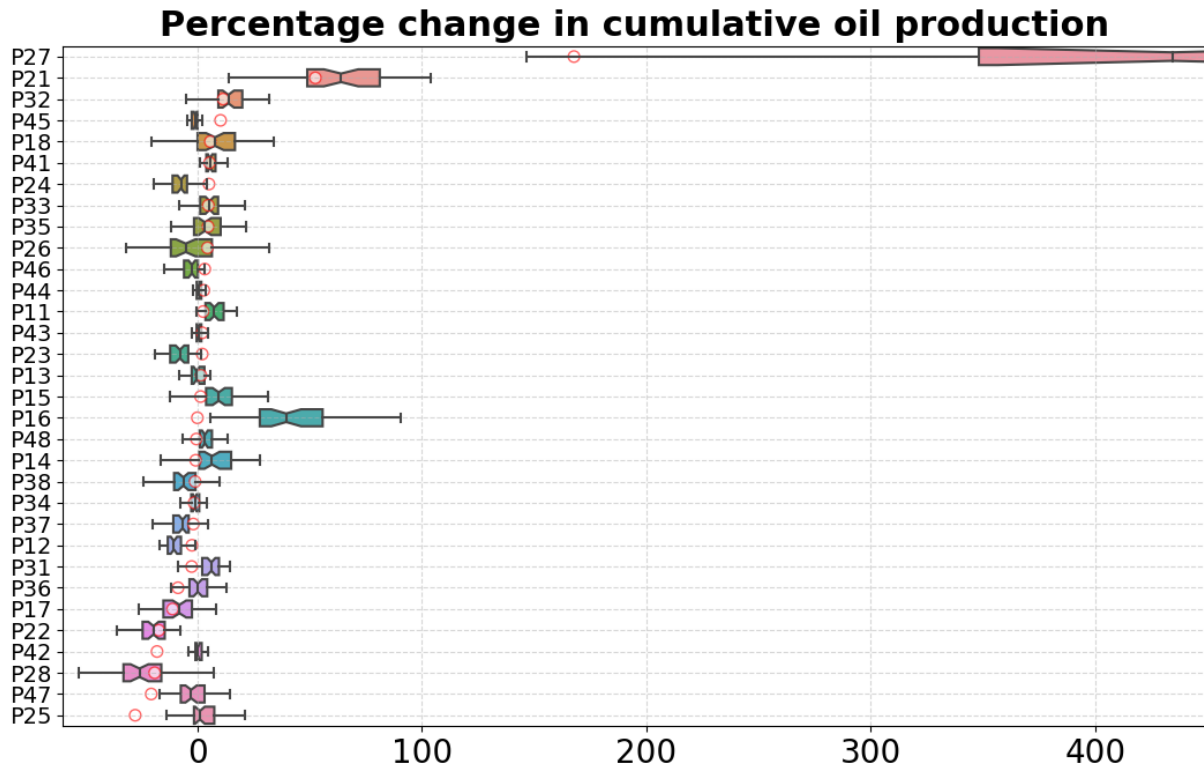


Figure 5-2: Chronology of the CLFD cycles (scaled to dates).

The initial and optimized FDP are illustrated in **Figures 5-6a** and **b**. By implementing the optimized strategy in the reference case, we improved the NPV by 0.8%. Major improvement in oil recovery comes from Sector-3 (1%) and Sector-2 (0.5%). A larger change in recovery factor of Sector-3 demonstrates how the revised decision helped the neighboring sector. Meanwhile, it stresses the importance of working with the entire field rather than isolated models when making a holistic decision for the complete field. We present the percentage change in oil recovery (at the end of Cycle 1) for individual wells in **Figure 5-3**. We observe a similar trend between expected and actual percentage change in cumulative production, with some exceptions (producers P45, P16, P42, P47, and P25). Such differences may occur because of various factors, including the uncertainty attributes, like faults close to such wells, which may or may not compartmentalize the area (see producer P25 in **Figure 5-6b**). It is intriguing to observe how even limited changes made in Sector-2 can affect the wells in Sector-4 (several kilometers away).

It is also vital to maximize the likelihood of success and measure it with the number of improved scenarios, especially when working with huge envelope of uncertainty. In Cycle 1, we improved all the scenarios, which enthruses confidence to implement the optimized strategy in the reference case to obtain successful changes.



[1] To make the graph legible, we truncated the result of producer P27 as the maximum change was observed as high as 1500%

Figure 5-3: Percentage change in cumulative oil production of respective wells at the end of Cycle 1 (the first and second numbers in the well's nomenclature refer to the sector and drilling sequence, respectively). Boxplot and red circles represent the expected and actual % change in cumulative oil production using M_{post}^1 , respectively.

Benchmarking the efficiency of this cycle against the first cycle of Chapter 3, we observed that this workflow is nine folds faster (or 89% more efficient). In **Table 5-3**, we present a simplified comparison to appreciate the results of this work. **Table 5-4** presents detailed results of this cycle, including the total time consumed.

Table 5-3: Estimated time consumed for Cycle 1 using the workflow in Chapter 3 and this article.

# Step	Chapter 3	This work
Action + Update Info	7.5+0.5 days	1.5+0.5 days
Data assimilation	30 days	6 days
Approve scenarios	1 day	1 day
Select RMs + Optimize	243 days ^[1]	22.5 days
Total time	282.5 days ^[2]	31.5 days

[1] Executing 1600 simulations (10 processors/simulation) with 9 RMs using 200 processors with average sim. time of FFM = 8.1 hours.

5.4.2 Practical problems in Cycle 3

Like Cycle 1, we implemented CLFD workflow on subsequent Cycles 2 and 3. However, we came across a notable obstacle in Cycle 3. In this subsection, we expose this critical problem, which resembles practical concerns in the real field development. Some key highlights of this cycle are emphasized below:

- Unlike previous cycles, we assumed that fault transmissibility uncertainty is reduced by this period (9.7 years \cong 32% of the field's life). We therefore used a range of 0 to 0.5 for faults transmissibility across the field (rather than 0 to 1).
- An extremely high gas-oil ratio (GOR) was observed in producer P17 (well from Sector-1) since it started producing (\sim 1.5 years before the execution of Cycle 3). Since the well had been active for a considerable time, we did not consider this observation as an outlier.
- Given that well P17 is drilled in proximity to Sector-2, it is vital to ensure that our models depict this behavior. However, the simulated GOR of the well P17 was perceived to be much lower than the observed GOR (**Figure 5-4**) even after assimilating production data with ES-MDA.

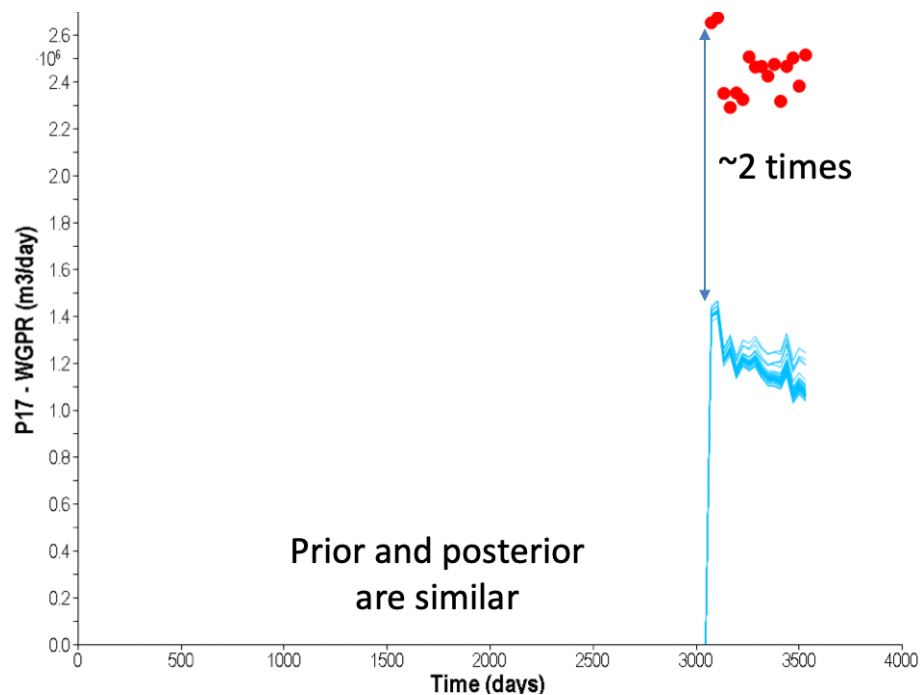


Figure 5-4: For the same oil production, difference in gas production is almost double even after data assimilation (Red dots and blue lines denote the production data of true field and simulated models, respectively).

- Assuming good connectivity between injectors and well P17 as a solution to this problem, we proposed a channel connecting producer P17 and injector I17 to find a workable solution (**Figure 5-5a**).

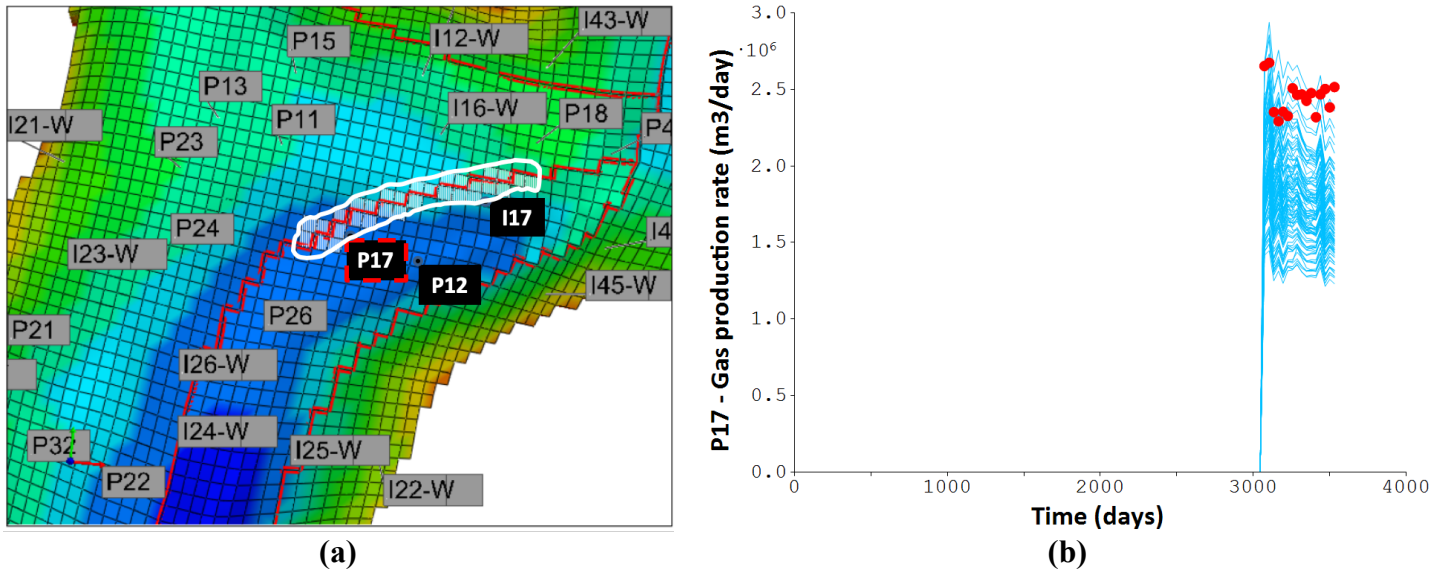


Figure 5-5: (a) Consideration of a thief zone connecting wells P17 and I17, without disturbing the neighboring well P12 and, (b) gas production rate of well P17 after revising data assimilation process.

Poorly history-matched models constrained us to repeat the data assimilation process in this cycle, leading to extra time. To accommodate these necessary changes, time spent on the data assimilation process was commensurate to the optimization process. As such, Cycle 3 took the longest time among the three cycles. In **Figure 5-6**, one can also observe the corresponding changes. Well P27, placed in proximity to the unbeknownst channel in Cycle 2, was moved further away by the end of Cycle 3.

5.4.3 Outcome

Table 5-4 presents detailed results of all three CLFD cycles with the total time consumed. We exhibit the best FDPs obtained at the end of each cycle in **Figure 5-6**. The updated workflow is much more efficient (>85%) than the previously validated workflow.

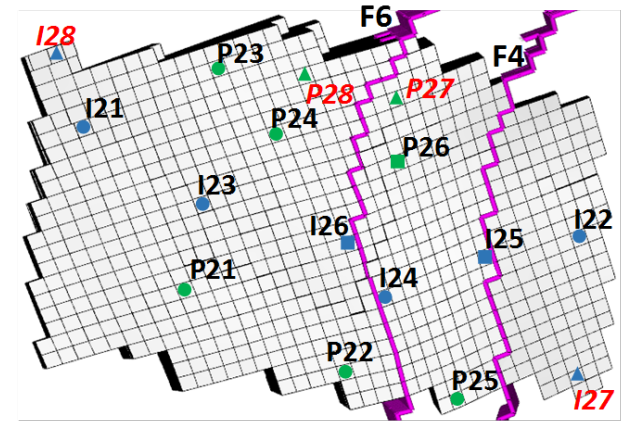
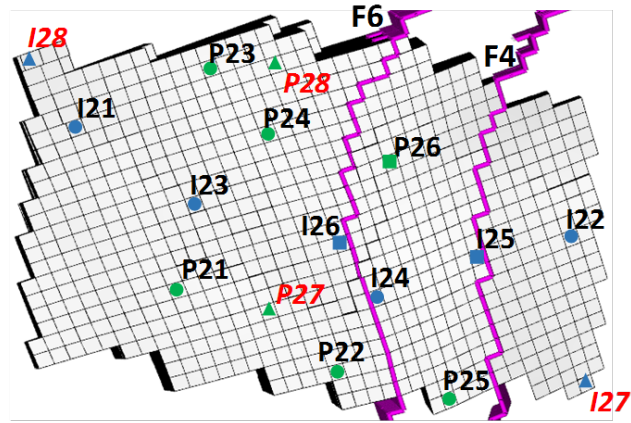
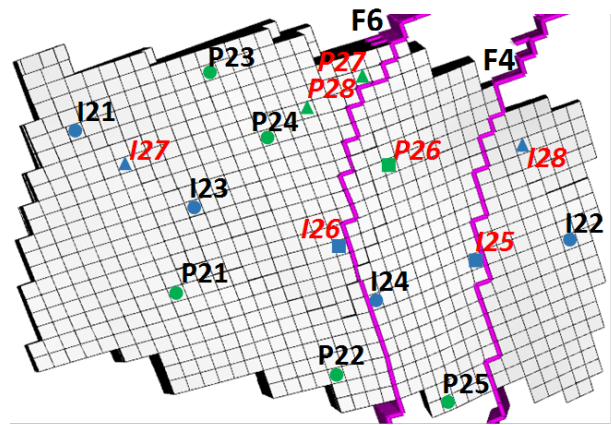
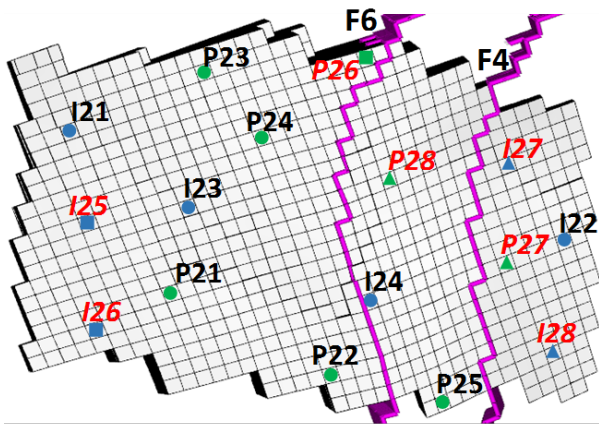


Figure 5-6: From top left and in clockwise direction, the pictures illustrate the evolution of FDP: (a) FDP_0 (initial strategy), (b) FDP_1 (cycle 1), (c) FDP_2 (cycle 2) and, (d) FDP_3 (cycle 3). Faults (F4 and F6), producers and injectors are shown using bold pink, green, and blue, respectively. To-be-drilled wells are highlighted in red italics. Filled circles, squares, and triangles are used to segregate the existing wells and to-be-drilled wells in Cycle 1 and Cycle 2/3, respectively.

Table 5-4: A detailed account of implementation of CLFD.

	Cycle 1	Cycle 2	Cycle 3
Implementation of workflow to revise FDP using simulation models for respective cycles			
Action	Obtained 0+7+3+3 new well logs (from S1, S2, S3, and S4, respectively); Generated M_{prior}^1 using a total of 27 vertical well-logs.	Obtained 0+4+5+5 new well logs (from S1, S2, S3, and S4, respectively); Generated M_{prior}^2 using a total of 41 vertical well-logs.	Obtained 4+0+4+4 new well logs (from S1, S2, S3, and S4, respectively); Generated M_{prior}^3 using a total of 53 vertical well-logs.
Updating inputs	-	-	Range of fault transmissibility was modified from 0-1 to 0-0.5 for all four faults.
Data assimilation	Noisy production data over a period of 1,978 days (18% of the field's life) was used to obtain M_{post}^1 .	Noisy production data over a period of 2,404 days (22% of the field's life) was used to obtain M_{post}^2 .	Noisy production data over a period of 3,531 days (32% of the field's life) was used to obtain M_{post}^3 .
Approved scenarios (AS)	44	48	40
Optimization	FDP ₀ was optimized to obtain FDP ₁ . We used 26 (59% of the AS) scenarios to optimize using 10 iterations of CLEO. Complete ensemble was improved.	FDP ₁ was optimized to obtain FDP ₂ . We used 30 (62.5% of the AS) scenarios to optimize using 7 iterations of CLEO. 94% of the ensemble was improved.	FDP ₂ was optimized to obtain FDP ₃ . We used 24 (60% of the AS) scenarios to optimize using 7 iterations of CLEO. 93% of the ensemble was improved.
Execution time	32 days	27 days	34 days
Range of <i>EVoCL</i>	0.03 to 0.5 Billion USD (0.3 to 5.5%)	-0.04 to 0.18 Billion USD (-0.3 to 1.6%)	-0.03 to 0.16 Billion USD (-0.3 to 1.4%)
<i>EVoCL</i> (for ensemble of AS)	+ 0.25 Billion USD (+2.3%)	+ 0.07 Billion USD (+0.7%)	+ 0.05 Billion USD (+0.5%)
Results obtained by implementing the finalized FDP in UNISIM-III-R (true field) for respective cycles			
\overline{VoCL}	+ 0.08 Billion USD (+0.8%)	+ 0.11 Billion USD (+1%)	+ 0.07 Billion USD (+ 0.7%)

Working with only limited decision variables from a quarter of this giant field, we were able to improve the field's NPV by 0.27 Billion USD (~2.5%) to emphasize the merits of implementing an efficient CLFD workflow. **Figure 5-7a** shows the evolving NPV over cycles. Examining the box plots for all M_{post}^i (set of history-matched simulation models, where 'i' is the number of the cycle), we have:

1. Very high uncertainty in the models at the initial phase of field development.
2. Growing sense of confidence in the evolving ensemble with sizeable reduction in variability.
3. Growing optimism in the evolving ensemble implied by a sharply increasing median NPV compared to the true field's NPV.
4. Assimilating newly accrued information over multiple phases of field development can be beneficial to decrease uncertainty and improve predictive capability.

Figure 5-7b depicts the histogram of changing oil recovery factor at the end of all cycles. Given limited variables were modified to optimize the field's NPV, we also observe limited improvements in individual sectors.

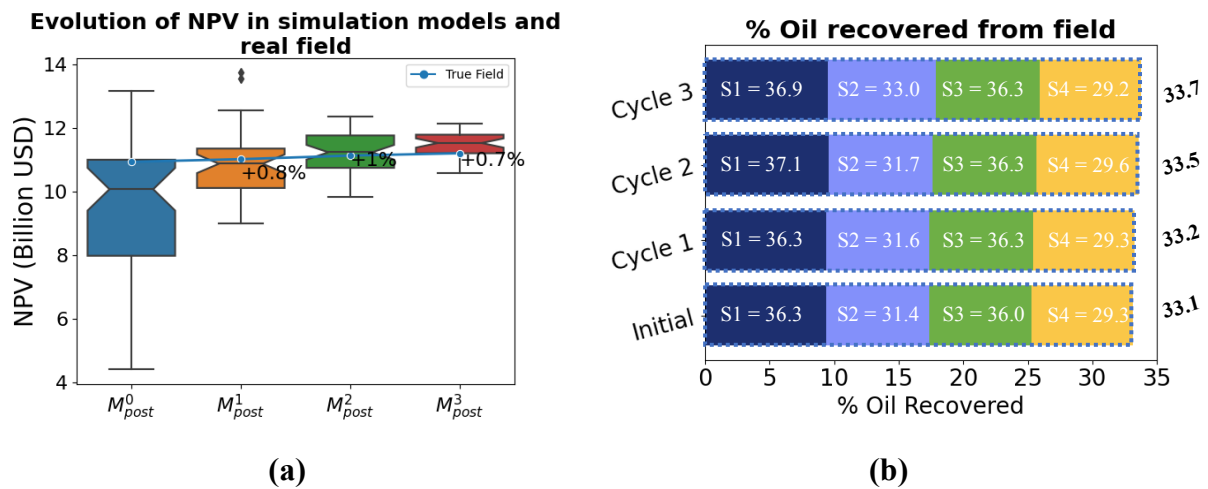


Figure 5-7: Graphs showing the evolution of (a) NPV (M_{post}^i refers to the set of history-matched simulation models, where 'i' is the cycle number) and, (b) oil recovery factor (for each sector) over the cycles.

5.5 Discussion and Recommendations

The main focus of this work is to revise an FDP with newly accrued information using CLFD workflow. We restrict our analysis to its two essential attributes: efficiency and risk-informedness. We also extend our discussion to include (a) its ability to include realistic

timelines for explaining its efficacy in real life, and (b) previously undisclosed observations to enthuse confidence in the workflow.

All previous studies showed CLFD as an integral concept to improve the objective functions over multiple phases. Yet, their workflows are unusable for real field applications due to inefficiency. One of the primary reasons for this drawback is that they only tested their workflows on simple and fast synthetic models (less than five minutes per simulation). In contrast, reservoir models of actual fields can be very time-consuming (Volz et al., 2008; Litvak and Angert, 2009; Azoug and Patel, 2014). **Table 5-5** summarizes the key differences between the workflow presented in Chapter 3 and this article to appreciate one of the key objectives of this work, i.e., efficiency of CLFD.

Table 5-5: Key differences between the workflow presented in Chapter 3 and this article.

# Step	Chapter 3	This work	Remarks
Action	Generated 500 images	Generated 100 images	80% reduction in time
Update info	Generated 500 scenarios with updated info	Generated 100 scenarios with updated info	80% reduction in time
Data assimilation	Performed DA of 500 scenarios using ES-MDA	We performed DA using 100 scenarios	80% reduction in time
Approve scenarios	~50% scenarios approved	~45% scenarios approved	A larger ensemble of approved scenarios is only justified if RMs can be selected without any simulation
Select RMs	Selected 9 RMs; Only these 9 RMs were used for optimization	We selected 3-12 RMs per iteration; different subset of RMs per iteration	Varying RMs helps reduce time and include more scenarios to make better decisions
Optimize	IDLHC was used to optimize well-placement using 1600 experiments per RM	We combined ML model with CLEO algorithm to optimize with 80% lesser simulations	Together with previous step, we achieved >90% reduction in time during optimization process

[1] We compared our work with Chapter 3, where we successfully validated a comprehensive workflow on two case studies.

In a CLFD workflow, results propagate from one step to another. One must be mindful of the quality of these results to avoid failure of the complete workflow (see Chapter 2). On this note, drastically improving the efficiency using only one of the steps can mislead the outcome. Thus, only tweaking the number of scenarios is also insufficient as optimization is the most demanding step in the workflow. A long optimization process can render the CLFD workflow unfeasible for time-consuming applications.

Hence, we presented a holistic solution to make the workflow more efficient (>85%). Using this efficient workflow, we recurrently revised the FDP of an extensively time-consuming model in a month, a much acceptable timeframe. We reduced the ensemble size to improve the efficiency of the CLFD workflow (**Table 5-5**) until approving scenarios. For maximizing the likelihood of success and improving the efficiency of the final steps, we combined multiple concepts with CLEO as the core optimization algorithm.

The quality of being risk-informed is equally critical in a CLFD workflow. Adding to the discussion of Chapter 3, we present some insights for practical implementation of a risk informed CLFD workflow:

- **Action:** The depositional sequence plays a dominant role in the recovery process. Hence, one should construct the ensemble of geostatistical images using multiple geologically consistent scenarios.

Considering efficiency, the number of geostatistical realizations generated and used for subsequent steps is another concern. In Chapter 3, we used 500 realizations in their work, asserting that a large ensemble is necessary to capture the geological uncertainty. However, using as many as 500 realizations to develop a time-consuming model can be impractical. As such, this work uses only an ensemble of 100 realizations to work with time-consuming models while honoring the need for a large ensemble. Despite using an 80% smaller ensemble on a highly heterogeneous and giant field fraught with various complexities, our revised workflow worked. This fact boosts confidence in using 100 realizations rather than 500. At the same time, it raises the question regarding the apt size of the ensemble for a successful understanding of geological uncertainty. Depending on the complexity, one can further adjust the size of this initial ensemble.

- **Update inputs:** In this work, we revised the FDP without including any direct information (Loomba et al., 2021) to test the workflow in a challenging environment (**Table 5-4**). Regardless, this step is key to reducing uncertainty during the field's

development phase. One should estimate the impact of all unknown uncertainties. Accordingly, this knowledge can be used to make an informed decision for subsequent steps. For example, one should focus to approve the scenarios that include more impactful uncertainty attributes. Such a risk-informed step bolsters the likelihood of success of the final outcome, particularly when one improves all scenarios.

- **Data assimilation:** Theoretical studies fail to highlight that several subsea processing activities are involved to separate the extracted commodities. While the total hydrocarbon extracted from the field is measured more accurately after such processes, the well production data is bound to suffer with higher noise. Also, depending on the availability of gauges, only limited well parameters (for example, total liquid rate and bottom-hole pressure) may be available to perform data assimilation. It is therefore important to include more subjective knowledge of the field to improve the data assimilation process under such complications.

In practice, one does not know the true reservoir characteristics of an oil and gas field. But using a benchmark case gives us the advantage of studying the "true answer" in a controlled environment after executing all three cycles of CLFD. We also revisited the problem of DA in Cycle 3 (see **Figure 5-4**). Re-evaluating the uncertainty parametrization, we realized that non-mapped fractures running along the fault were the primary reason for the observed discrepancy. This observation highlights the following:

1. Unknown uncertainty attributes can cause mismatched production data.
2. As the reference case was built independently of the simulation model, it is common to encounter differences. Such differences helped us demonstrate problems from real life situations.
3. Such non-mapped fractures only ran along the fault (within a close proximity). However, as the scale of the reference and simulation models is quite different, simulation models are not able to capture this behavior, even after DA. With the large differences in the scale, it is quite unrealistic to portray this behavior accurately as the DA cannot identify such instances. We can affirm this further based on the results obtained, despite using channel to mimic the faults (**Figure 5-5a**). In that instance, we observed that it was still difficult to perform DA with lower mismatch.
4. Presenting a functioning workflow under such strenuous conditions enthruses confidence in the concept of CLFD as well as our workflow.

As learned from Cycle 3, a better DA technique is also required to work with a much larger noise and, without experiencing any collapsing uncertainty attributes. To improve DA in such problematic instances, one could also use local grid refinement in addition to new uncertainty parameterization to understand the mismatched area better. Given that solutions are based on the knowledge and experience of the engineer, we believe that the presented solution is subject to further improvement based on aptitude, time, and motivation. As the focus of this work is CLFD, we limit our discussion on this topic.

- Approving scenarios to select and optimize RMs: In this work, we used reservoir engineering insights alongside the CLEO algorithm. One of its benefits in the CLFD workflow is that it helps prevent drilling a well in an unproductive region by using the data of the approved scenarios. These insights also help mitigate the need for correctional steps, like flexibility of drilling (FoD – Chapters 2 and 3). Meanwhile, to improve reservoir engineering insights, we need better ways to include the impact of different factors, like faults. For example, if we have a sealing fault close to the well, we need better techniques to incorporate this information and use zero oil flux from that direction.

We also reiterate the necessity to maximize the likelihood of success over the approved scenarios to ensure success in the "true field". Maximizing the expected monetary value (EMV) of the RMs alone does not endorse its success in the "true field". One must maximize the percentage improvement in the EMV as well as the scenarios improved. Using a growing set of RMs in conjunction with a risk-averse objective function is a good way to efficiently reach that objective.

There are perceived similarities between the concept of (a) growing RMs with iteration and, (b) propagation of best experiments (PBE). As such, we provide a description of their similarities and dissimilarities in **Table 5-6**. In short, both frameworks supplement rather than substitute each other.

As Appendix C highlights, one can achieve a globally optimal solution with simulation models. But, as model error is always prevalent, the solution may be far from a globally optimum solution when applied in a real case. As such, we endorse using predictive analytics to make the optimization process faster. For a better prediction model, one could also use a more detailed feature matrix and effective

learning algorithms. Learning feature importance to pick the best features for the feature matrix is another important step to improve the prediction model.

Table 5-6: Difference between growing RMs over iterations and Propagation of best experiments.

Growing RMs over iterations	Propagation of Best Experiments (PBE)
Similarities	
Both improve efficiency of the optimization process	
Both work with multiple realizations	
For a given subproblem, total number of realizations are fixed	
Dissimilarities	
It solves a series of subproblems , with increasing RMs	It works with only one optimization subproblem
Number of realizations are increased as we advance from one subproblem to the next	Number of realizations are increased within the subproblem only
It was designed to handle as many realizations as possible , irrespective of how many of them are actually being improved	PBE was developed to obtain a solution which improves all realizations within the subproblem
It runs all simulations within a subproblem; thus, it does not improve efficiency within a subproblem	PBE runs only a selected simulation; thus improving efficiency within a subproblem
This framework has a high overall efficiency as it steers all subproblems (Wang et al., 2012)	The efficiency of PBE (as a standalone) is relatively lower as it only acts as a supplementary tool within a subproblem

Depending on the size of the field, number of processors, average simulation time per model, and other computational capabilities, it can take weeks to months to revise the FDP. Nevertheless, one must ensure that FDPs can be revised within a realistic time frame. For a practical implementation of the workflow, it is also vital to include decision-making time as delays in oil production can directly impact the NPV and, at times, render the changes in FDP useless. As none of the previous works included this decision-making period, we included it to exhibit the practicality of our workflow. While, roughly 30 days were required by all the cycles for revising FDP, we added an extra 30 days to include the unforeseen managerial and

engineering decisions. This extra buffer period also serves to explain the benefit of CLFD workflow in case of additional unexpected delays.

The execution time of the workflow also raises the concern of it being a continuous process. Assuming that it takes 30 days to simulate the whole CLFD workflow, the only additional information at this point, in most of the cases, would be a single noisy production data per well. As this additional information may not be value-additive, we stress that CLFD requires deliberate planning to maximize its value.

In addition, the number and size of cycles are two independent variables of CLFD. Although all authors highlight the benefit of increasing the number of cycles in CLFD, they overlook mentioning that this behavior is more in line with the value of money. Using many cycles increases the number of controls over the initial period (which more heavily impacts NPV than the later ones). One must also increase the number of cycles cautiously. Doing this can be disadvantageous in certain cases. For example, in the presented example, no new well logs are acquired between 1219-1756 days. In other words, no new spatial and temporal information is acquired for the to-be-developed Sectors 2, 3, and 4, so ill-informed decisions may be taken, which can arbitrarily lead to success or failure. On the other hand, cycle size depends on the quantity of information it puts forward. So, for a successful implementation of CLFD (with adequate size and number of cycles), we recommend that one should carefully recognize the amount of information, time consumed by CLFD workflow, objective function, and time of executing the workflow, among other things.

Finally, we highlight some key observations. Updated ensemble of each cycle demonstrated similar characteristics (see **Figure 5-8**):

1. **Reduction in volatility:** Decreasing coefficient of variation highlights the lower dispersion around the mean NPV. For a given FDP, we observed sharply decreasing standard deviation in evolving data-assimilated ensemble.
2. **New information reduces uncertainty:** Increasing minimum and decreasing maximum values led to a continually decreasing range of NPVs. Unrealistically optimistic and pessimistic values were ruled out from subsequent ensembles.
3. **Growing optimism:** For a given FDP, we observed the median NPV always starting less than true value in the initial ensemble and ending up over the true value in the final ensemble, as shown in **Figure 5-8**. This observation suggests that the ensembles are evolving to become more optimistic. This is an intriguing behavior provided that the initial and final ensembles were built with data of 18% and 32% of the field's life,

respectively. Though it is difficult to infer with current knowledge, **Figure 5-8** also raises a pivotal question about the possibility of the true NPV falling outside the range of predicted NPV using new models built on newly accrued information.

4. **Improved forecast:** Despite growing optimism and large uncertainty reduction, the actual value of the field always falls within the bracket of simulated models. This boosts confidence in the predictive capability of evolving ensembles. At the same time, this does not necessarily mean that an individual cycle would always induce a positive change as it depends on the percentage of scenarios improved, among other things.

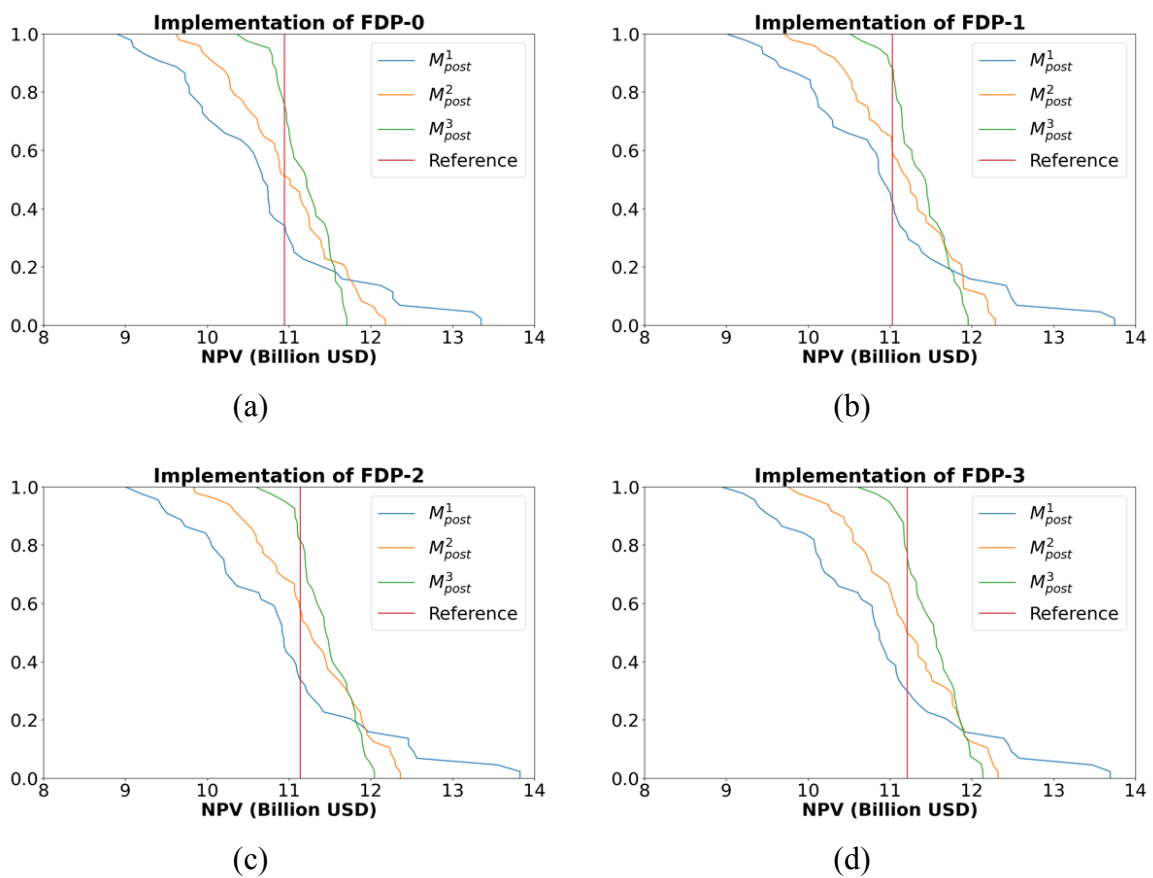


Figure 5-8: (a) FDP₀, (b) FDP₁, (c) FDP₂ and, (d) FDP₃ in M^1_{post} , M^2_{post} , M^3_{post} and reference case.

In this work, we only use a few wells (within a sector) as decision variables to optimize the objective function (NPV) of the entire field. Thus, it is understandable that the improvements are not very large in percentage as the decision variables in other sectors that play a critical role in the field behavior are not altered. At the same time, this unique set-up helps us expose the benefit of CLFD as a consequence of limited changes on the giant field's NPV. This setup also helps indicate the benefits of the ML-assisted CLFD workflow more clearly. The results also demonstrate the benefit of new information coming in the form of

noisy production data. Even without updating new inputs in the simulation model during the earlier cycles, one can observe an ample change.

Similar to Chapter 3, we also mitigated any bias in the optimization process by starting with an optimized strategy from the beginning. Given the large amount of uncertainty and dearth of information, this FDP is not good enough for updated scenarios. At the same time, the optimized FDPs from later cycles are not the best for initial ensembles. This highlights that the initially optimized strategy was good enough for the provided information at that point of time and lack of adequate information in the early phase of development can mislead to suboptimal decisions.

With the passage of each cycle, one expects the new information to reduce uncertainty (also seen in **Figure 5-8**). However, this reduction should be moderate rather than drastic. For practical implementation of a CLFD workflow, we recommend using performance indices to ensure model variability. Descriptive statistics and image processing can be used to measure the variability at each phase of the cycle and maintain diversity in models. This step is essential to embrace key insights and differences from multiple scenarios. Maximizing the likelihood of success over such a variable ensemble would guide the geoscientists and engineers to select a more robust FDP.

5.6 Conclusions

By identifying the research gaps in closed-loop field development (CLFD), we presented an efficient and risk-informed workflow to make robust decisions while evaluating risks and grasping systematic insights. We list the main contributions of this work in this section.

Without an efficient workflow, it can be exorbitantly time-consuming to develop a field-scale example. Thus, we presented an efficient workflow (>85%) for realistic and field applications. We achieved this feat using multiple factors. We demonstrated that an ensemble of as low as 100 scenarios is sufficient to capture the geological uncertainty. We used an ML model and employed a simple learning algorithm for the optimization process. Unlike conventional methods, we extracted intermediate technical results and used them to (a) understand the unseen pattern and (b) forecast the final objective function. We introduced a routine for working with multiple approved scenarios to expedite the CLFD workflow and maximize the likelihood of success, and we also integrated the concept of propagation of best experiments. We also used the newly proposed cluster-based learning and evolution optimizer algorithm to explore the problem space intelligently.

We tested this workflow on a highly heterogeneous and giant field. This benchmark case manifests an extremely challenging environment with spatial and temporal complexity. It is a perfect testing ground for investigating the proposed workflow. To study the impact of CLFD and affirm its proper functioning, we also worked with limited decision variables in a quarter of a giant field and considered practical timelines. Within this controlled environment, we improved the NPV by 0.2 Billion USD (2%) to demonstrate the functioning of the CLFD workflow in complex conditions.

Apart from working with a giant field, we also worked with a realistic timeline. Unlike previous work, we established the benefit of the workflow by including its execution time and buffer period to stress that CLFD works in a delayed environment. Meanwhile, the results indicate that deliberately planning can be beneficial for the successful implementation of CLFD.

As presented, it is usual to encounter problems while minimizing the mismatch between observed and simulated data during the data assimilation process. While there is a degree of subjectivity in the data assimilation process, one must conduct experiments while restricting the total time for a cycle of CLFD and covering uncertainty. Yet, based on the controlled experiments, assimilating data using noisy production data provided a good understanding of the reservoir.

While the evolving ensemble improved the forecasts with reduced volatility, we also observed growing optimism in the models. In our work, we also observed that FDP is quite sensitive. Small changes seemed to affect wells even several kilometers away. One should be wary of such behavior while performing data assimilation or optimization processes.

Talking about potential pitfalls, lack of diversity, or poorly selected subsets of reservoir scenarios for the optimization process can impact the outcome of the workflow. Although reservoir engineering insights helped us drill the wells in productive regions, one could drill the wells in unproductive zones in some rare cases. We must stress that the initial strategy proposed at the beginning of development is more likely to have wells in unproductive zones than the later ones. One must select the CLFD workflow carefully to maximize the value of the closed loop. Inefficient workflows can engender unnecessary delays.

To summarize some of the recommendations for practical applications, one must maximize the likelihood of success using a risk-averse objective function. One should strive to generate and approve a diverse set of scenarios while considering the sensitivity analysis of uncertainty attributes. Being wary of reservoir features and possibly non-mapped uncertainties

can also be helpful for better predictions. In this sense, the use of information sources, such as time-lapse seismic, can help us better understand reservoir characteristics. Finally, spending more time to improve the quality of models, rather than spending extra time on the optimization process, would be an ideal way forward to generate robust outcomes.

Acknowledgments

This work was conducted with the support of Libra Consortium (Petrobras, Shell Brasil, Total Energies, CNOOC, CNPC) and PPSA within the ANP R&D levy as "commitment to research and development investments" and Energi Simulation. The authors are grateful for the support of the Center for Energy and Petroleum Studies (CEPETRO-UNICAMP/Brazil), the Department of Energy (DE-FEM-UNICAMP/Brazil), and the Research Group in Reservoir Simulation and Management (UNISIM-UNICAMP/Brazil). Also, a special thanks to CMG and Schlumberger for the software licenses. The authors would also like to acknowledge the contribution of Vinícius de Souza Rios (Equinor/Brazil).

Nomenclature

List of Abbreviations

CLFD	Closed-loop field development
CLEO	Cluster-based learning and evolution optimizer
DA	Data assimilation
EMV	Expected monetary value
ES-MDA	Ensemble-smoother with multiple data assimilation
FDP	Field development plan
FoD	Flexibility of drilling
GOR	Gas-oil ratio
IDLHC	Iterative discrete Latin hypercube
ICV	Inflow control valve
LHS	Latin hypercube sampling
ML	Machine learning
<i>M</i>	Ensemble of scenarios
NPV	Net present value
PBE	Propagation of best experiments
PMF	Probability mass function
RM(s)	Representative model(s)

S1/2/3/4 Sector-1/2/3/4

WAG Water alternating gas

Superscript

i Cycle

Subscript

i # of FDP (1, 2, 3 ... etc.)

post Ensemble posterior to DA

prior Ensemble prior to DA

6 Conclusions

This thesis presents efficient, comprehensive, and improved closed-loop field development (CLFD) workflows to obtain risk-informed decisions. We begin the work by addressing the existing pitfalls in the existing workflows. Exercising this knowledge, we developed a risk-informed CLFD workflow and validated it using two case studies. Given that practical applications can be time-consuming, we presented four methods to optimize considerably faster while considering the probabilistic scenarios to capture uncertainty. Finally, we integrated all findings to obtain an efficient and risk-informed CLFD workflow, validated using a giant field with time-consuming models. We summarize the key contributions of this thesis below:

1. This thesis emphasizes the functioning of the concept of model-based CLFD.
2. We presented two risk-informed workflows. While the first workflow is comprehensive and equipped for faster models, the latter is more efficient and applicable for time-consuming and practical applications. Without an efficient workflow, a cycle of the CLFD workflow can be extensively time-intensive, rendering its implementation impractical.
3. We successfully validated the functioning of both workflows in three-dimensional and field-scale benchmark models.
4. We demonstrated that a large ensemble of geologically consistent models is vital for reliable coverage of geological uncertainty. While we used 500 realizations in the initial work, we also tested an 80% smaller ensemble (only 100 realizations) in a highly heterogeneous field to conclude it is adequate for capturing geological uncertainty.
5. We also observed that the quality of the well-logs influences the quality of the ensemble of simulation models (swaying the optimism or pessimism). To preserve good variability of simulation models, one must also pay attention to this factor.
6. We showed that the initial ensemble bred using static information alone struggles to depict the historical period. Hence, it requires the assimilation of dynamic data before using them to make well-informed decisions.
7. We exhibited that the quality and quantity of new inputs in the simulation models play a significant role in the field development process. Quantifying the uncertainty attributes more correctly decreases the information gap, which helps improve the reliability for making better decisions.

8. We identified the need for better data assimilation (DA) process to improve the assessment of uncertainties while considering the existing bias and error in simulation models.
9. It is frequent to observe mismatched production data post-DA process in real life. From the perspective of CLFD, one must be cautious of outliers and conduct appropriate experiments (for instance, mapping new uncertainty attributes) while staying mindful of the execution time of a CLFD's cycle.
10. Using high tolerance values can lead to accepting poorly history-matched scenarios, generating an inferior ensemble of an approved ensemble. Ideally, one must discard the implausible scenarios to mitigate the influence on the optimization process.
11. As presented, the selection of RMs is a vulnerable process that needs to be improved for a CLFD workflow. To select an apt number of RMs, one needs to be wary of the qualitative and quantitative aspects of the approved scenarios, while maintaining proper variability in the unexplored area.
12. Maximizing the likelihood of success of the optimized strategy over the approved ensemble of history-matched scenarios improves the probability of success in the actual field.
13. We introduced a bi-criterion objective function focusing on EMV and individual NPVs of the RMs. Using this objective function, we improved the likelihood of success over the "true field" by maximizing the number of scenarios improved.
14. As the optimization process is the most taxing component of the CLFD workflow, we proposed four methodologies to make it efficient. The presented methodologies expedited the optimization process multiple folds by running fewer simulations. Compared to traditional methods, the proposed workflows also yielded similar results in much less consumed time.
15. We introduced the concept of propagation of best experiments (PBE) and tested it in the framework of CLFD to limit the number of simulations intelligently. As PBE selects the best FDPs over a gradually incrementing subset of RMs, it improves the likelihood of success of the optimized FDP over the ensemble while drastically reducing the total number of simulations.
16. Using a growing set of RMs over the iterations can significantly improve the efficiency of the optimization step while ensuring that a maximum number of approved scenarios are considered for making the final decision.
17. We also presented and implemented a machine learning (ML) model using a simple learning algorithm (linear regression) to improve the efficiency of a CLFD workflow.

18. The technical results obtained with the partial life-based simulations can contribute information for estimating FDPs. At the same time, this thesis emphasizes that intermediate results can be used to improve the efficiency of the optimization process by multiple folds.
19. We introduced the value of closed-loop (VoCL) as a performance index. This index assists the decision-makers in selecting the final strategy while quantifying the benefits. While the expected VoCL is always positive due to the optimization process, actual VoCL can yield a negative result due to poor decision(s).
20. A pragmatic drilling approach must be exercised in the “true field” to emulate the real-time decision-making process. This step avoids drilling “unrealistic wells” as the engineers would not drill in non-reservoir zones in a real-life situation, despite the output of simulation models suggesting otherwise. We proposed flexibility of drilling (FoD) to minimize the chances of drilling a well in non-reservoir zones. However, the presented concept of FoD is only applicable to horizontal wells.
21. Considering real-life challenges, we also worked with a realistic timeline of field development to confirm the practical application of a CLFD workflow. We established the benefit of the efficient and risk-informed workflow by including its execution time and buffer period to stress that CLFD works in a delayed environment. At the same time, the results indicate that deliberately planning can be beneficial for the successful implementation of CLFD.
22. We introduced a systematic framework based on bottom-up analysis to improve workflow for model-based CLFD while evaluating the individual steps and asserting their significance.
23. We demonstrated how the propagation of specious scenarios/outputs leads to an overall bias in the results of CLFD. As CLFD is a cyclical process, one needs to be wary about the results of the preceding step to the input of the next step. Concurrently, we also learned how to mitigate the propagation of misleading outputs.
24. We provided a systematic analysis of the complete workflow to elucidate the evolution of uncertainties and enthruse more confidence in its implementation in field applications.
25. As observed in different forms, all models have a certain degree of accuracy, bias, and error compared to the actual field. The proportion of these three traits varies from the initial until the end of the field development, as new information is acquired and utilized. The actual and assumed similarity between the simulation models drives the results of the CLFD workflow. Consequently, this research promotes the idea of developing a field with risk-

averse techniques and selecting an appropriate FDP efficiently that works for the entire ensemble.

While reservoir studies struggle to predict the reservoir performance adequately due to their inherent characteristic of accuracy, bias, and error, a risk-informed and efficient CLFD provides an ideal opportunity to assimilate new information over specified phases and improve the understanding of the field, which is visible in the form of improved decisions.

7 Suggestions for Future Studies

Based on the methodical observations made throughout this work, some of the potential topics for research are listed below:

1. In Chapter 2, we discussed the role of 3D seismic information in generating more coherent petrophysical images. An image conditioned to good 3D seismic data can always assist in capturing the lateral and longitudinal connectivity of the reservoir within the resolution of the seismic survey. In Chapter 3, we also discussed that constraining the geostatistical images to seismic data can reduce the variability of the images while ensuring geological consistency so that the uncertainties shift more towards the “true field” value. Future studies could address how 3D/4D seismic information impacts the spatial variability of realizations and thus reduce the chances of failure of the optimized FDP and improve the CLFD process.
2. As seen in Chapter 3, we observed qualitative bias in the RMs. Assuming that the approved ensemble of scenarios represents the uncertainty in the field well, ignoring their standard deviation can potentially lead to a negative bias toward risk-informed decision-making. Based on the several other observations made in Chapters 2-4, future research can focus on improving the quality and quantity of the RMs so that we can represent the entire ensemble more efficiently to bolster confidence in the optimized result.
3. In Chapter 3, we discussed how the quality of the well-logs has a dominant and direct influence on geostatistical properties. Future studies could expose how to generate images with good variability, especially when the ratio of the explored and unexplored spatial volume is minute. As hypothesized, better usage of variograms can improve the quality of petrophysical images.
4. All models are imperfect and error-prone. As discussed in Chapter 3, failure to predict the history period properly reveals that good history-matched scenarios (with conditions) do not necessarily mean they “represent” the field. Even if the historical period can be naturally stimulated (without forced conditions) within a reasonable acceptable range, this will already ensure that we do not have fallible scenarios. Consequently, such models can significantly improve our understanding of the field. In conjunction with other observations made in Chapters 3 and 5, future work must focus on developing better data-assimilation techniques to minimize the differences between the predicted and actual properties.

5. Chapter 3 discusses an essential characteristic of a good decision-making process. Typically, it should address alternative solutions to overcome technical hitches in the field development process. Although it might seem that robust optimization can fall short in this area, using selected scenarios for developing alternative solutions side-by-side can come in handy in such vulnerable situations. Therefore, an extension of this work would be to devise better alternatives and demonstrate their benefit from the perspective of CLFD.
6. In Chapter 2, we verified that upscaling was not the main reason for the negative results in Morosov and Schiozer (2016). At the same time, this thesis does not investigate the role of upscaled models on the results of CLFD workflow. It would be intriguing to understand how different fidelity of simulation models can impact the outcome of CLFD. While the conventional wisdom suggests that a higher fidelity model can capture the flow behavior better, it may also imbibe a relatively large model error. More investigation is needed to unravel the impact of the grid size and the fidelity of the models.
7. Some other relevant topics for research are:
 - a. Propose an FoD method for vertical wells.
 - b. To evaluate the quality and the quantity of information accrued over time to make an objective decision of implementing CLFD workflow.
 - c. To find new ways to conduct economic feasibility tests of individual wells in the FDP before its implementation in the actual field, especially in a time-consuming reservoir model.
 - d. To assess the number of geostatistical realizations while considering the complexity of the given field.
 - e. To find ways for guiding the well-scheduling to acquire vital information much earlier to maximize the impact of CLFD. One should also study the benefits of CLFD over the concept of the value of information in such circumstances.
 - f. To recognize a way for selecting the number and size of cycles while considering the amount of information, time consumed by CLFD workflow, and objective function, among other things.
 - g. To develop new performance indices to quantify the benefit of optimized strategy and its probability of success in the actual field, to enthuse confidence in the concept of the CLFD.
 - h. To test a case study that uses geostatistical realizations built using multiple depositional settings.

8. In future studies, one could also examine the impact of the following factors:
 - a. Well-tests
 - b. Higher noise levels in the production data with outliers
9. Future studies can include more control variables to mimic a real field development scenario. Control, placement, type, schedule, and the number of wells, platform, and ICV constraints can be combined to yield better results.

8 References

Ahmed, T. and Meehan, D.N., 2012. Advanced reservoir management and engineering (second edition). Gulf Professional Publishing, Boston. DOI: 10.1016/C2009-0- 64035-6.

Avansi, G.D. and Schiozer, D.J., 2015a. UNISIM-I: synthetic model for reservoir development and management applications. *International Journal of Modeling and Simulation for the Petroleum Industry*, v. 9 (1), pp. 21–30.

Avansi, G. D. and Schiozer, D. J., 2015b. A new approach to history matching using reservoir characterization and reservoir simulation integrated studies. Presented at the Offshore Technology Conference held in Houston, Texas, United States of America, 4-7 May. DOI: 10.4043/26038-MS.

Avansi, G.D., Celio, M. and Schiozer, D.J., 2016. Simultaneous history-matching approach by use of reservoir-characterization and reservoir-simulation studies. *SPE Reservoir Evaluation and Engineering*, v. 19 (4), pp. 694–712. DOI: 10.2118/179740-PA.

Armstrong, M., Ndiaye, A., Razanatsimba, R. and Galli, A., 2013. Scenario reduction applied to geostatistical simulations. *Mathematical Geosciences*, v. 45, pp. 165–182. DOI: 10.1007/s11004-012-9420-7.

Awotunde, A.A. 2014. On the joint optimization of well placement and control. Presented at the SPE Saudi Arabia Section Technical Symposium and Exhibition, Al-Khobar, Saudi Arabia, 21-24 April. DOI: 10.2118/172206-MS.

Azoug, Y. and Patel, H., 2014. Field development plan (FDP) optimization of a giant field for plateau extension and recovery improvement. Presented at the Abu Dhabi International Petroleum Exhibition and Conference, Abu Dhabi, UAE, 10-13 November. DOI: 10.2118/171770-MS.

Badru, O. and Kabir, C.S., 2003. Well placement optimization in field development. Presented at the SPE Annual Technical Conference and Exhibition, Denver, Colorado, United States of America, 5-8 October. DOI: 10.2523/84191- MS.

Beckner, B.L. and Song, X., 1995. Field development planning using simulated annealing - optimal economic well scheduling and placement. Presented at the SPE Annual Technical Conference and Exhibition, Dallas, Texas, United States of America, 22-25 October. DOI: 10.2523/30650-MS.

Bellout, M.C., Echeverría Ciaurri, D., Durlofsky, L.J., Foss, B. and Kleppe, J., 2012. Joint optimization of oil well placement and controls. *Computational Geosciences*. 16, 1061–1079 (2012). DOI: 10.1007/s10596-012-9303-5.

Bittencourt, A.C., 1994. Optimal scheduling of development in an oil field. MS thesis. Stanford University, Stanford, California, United States of America.

Botechia, V.E., Gaspar, A.T.F.S. and Schiozer, D.J., 2013. Use of well indicators in the production strategy optimization process. Presented at the SPE EUROPEC, London, United Kingdom, 10-13 June. DOI: 10.2118/164874-MS.

Botechia, V.E., Gaspar, A.T.F.S., Davolio, A., Avansi, G.D. and Schiozer, D.J., 2018. Investigation of production forecast biases of simulation models in a benchmark case. *Oil & Gas Science and Technology - Rev. IFP Energies Nouvelles*, v. 73, pp. 1–12. DOI: 10.2516/ogst/2018014.

Chaves, J. M. P., 2018. Multiscale approach to construct a carbonate reservoir model with karstic features and Brazilian pre-salt trends using numerical simulation. Presented towards partial fulfillment of the Master's thesis, University of Campinas, Campinas, Brazil.

Chierici, G.L., 1992. Economically improving oil recovery by advanced reservoir management. *Journal of Petroleum Science and Engineering*, v. 8 (3), pp. 205–219. DOI: 10.1016/0920-4105(92)90034-X.

Correia, M., Botechia, V., Pires, L., Rios, V., Santos, S., Rios, V., Hohendorff, J., Chaves, M. and Schiozer, D., 2020. UNISIM-III: Benchmark case proposal based on a fractured karst reservoir. Presented at the ECMOR XVII, 14-17 September. DOI: 10.3997/2214-4609.202035018.

Cullick, A.S., Narayanan, K., Gorell, S.B., 2005. Optimal field development planning of well locations with reservoir uncertainty. Presented at the SPE Annual Technical Conference and Exhibition, Dallas, Texas, United States of America, 9-12 October. DOI: 10.2118/96986-MS.

Dezfuli, H., Maggio, G., & Everett, C. (2010a, May). Risk-informed decision making: Application to technology development alternative selection. In *4th IAASS Conference: Making Safety Matter* (No. HQ-STI-10-055).

Dezfuli, H., Stamatelatos, M., Maggio, G., Everett, C., Youngblood, R., Rutledge, P., ... & Guarro, S. (2010b). *NASA risk-informed decision-making handbook* (No. NASA/SP-2010-576-Version1. 0).

Dige, N. and Diwekar, U., 2014. Efficient sampling algorithm for large-scale optimization under uncertainty problems. *Computers & Chemical Engineering*, 115(2018): 431–454. DOI: 10.1016/j.compchemeng.2018.05.007.

Dorfman, R., 1979. A Formula for the Gini Coefficient. *The Review of Economics and Statistics*, 61(1), 146-149. DOI: 10.2307/1924845.

Emerick, A.A. and Reynolds, A.C., 2013. Ensemble smoother with multiple data assimilation. *Computers & Geosciences*, v. 55, pp. 3-15. DOI: 10.1016/j.cageo.2012.03.011.

Emerick, A.A., Silva, E., Messer, B., Almeida, L. F., Szwarcman, D., Pacheco, M.A.C. and Vellasco, M.M.B.R., 2009. Well placement optimization using genetic algorithm with nonlinear constraints. Presented at the SPE Reservoir Simulation Symposium, The Woodlands, Texas, United States of America, 2-4 February. DOI: 10.2118/118808-MS.

Evensen, G., 2007. Data assimilation: the ensemble kalman filter. Springer, Berlin. DOI: 10.1007/978-3-540-38301-7.

Forouzanfar, F. and Reynolds, A., 2014. Joint optimization of number of wells, well locations and controls using a gradient-based algorithm. *Chemical Engineering Research and Design*, 92(7), 1315–1328. DOI: 10.1016/j.cherd.2013.11.006.

Gaspar, A.T.F.S., Avansi, G.D., Santos, A.A.S., Hohendorff Filho, J.C.v. and Schiozer, D.J., 2015. UNISIM-I-D: benchmark studies for oil field development and production strategy selection. *International Journal of Modeling and Simulation for the Petroleum Industry*, v. 9 (1), pp. 47–55.

Gaspar, A.T.F.S., Barreto, C.E.A.G. and Schiozer, D. J., 2016. Assisted process for design optimization of oil exploitation strategy. *Journal of Petroleum Science and Engineering*, v. 146, pp. 473–488.

Hanea, R.G., Casanova, P., Hustoft, L., Bratvold, R.B., Nair, R., Hewson, C., Leeuwenburgh, O. and Fonseca, R.M., 2017. Drill and learn: a decision making workflow to quantify value of learning. In: Presented at the SPE Reservoir Simulation Conference, Montgomery, Texas, United States of America, 20–22 February. DOI: 10.2118/182719-MS.

Hartigan, J.A., and Wong, M.A., 1979. Algorithm AS 136: A K-Means clustering algorithm. *Journal of the Royal Statistical Society. Series C (Applied Statistics)*, 28(1), 100–108. DOI:10.2307/2346830.

Hidalgo, D.M., Emerick, A.A., Couto, P. and Alves, L.D., 2017. Closed-loop field development under geological uncertainties: application in a Brazilian benchmark case. Presented at the Offshore Technology Conference, Rio de Janeiro, Brazil, 24–26 October. DOI: 10.4043/28089-MS.

Hohendorff Filho, J.C.v., Maschio, C. and Schiozer, D.J., 2016. Production strategy optimization based on iterative discrete Latin hypercube. *Journal of the Brazilian Society of Mechanical Sciences and Engineering*, v. 38, pp. 2473–2480. DOI: 10.1007/s40430-016-0511-0.

Hohendorff Filho, J.C.v. and Schiozer, D.J., 2018. Integrated production strategy optimization based on iterative discrete Latin hypercube. Presented at the ECMOR XVI, Barcelona, Spain, 3–6 September. DOI: 10.3997/2214-4609.201802213.

Hidalgo, D.M., Emerick, A.A., Couto, P. and Alves, J.L.D., 2017. Closed-loop field development under geological uncertainties: Application in a Brazilian benchmark case.

Presented at the Offshore Technology Conference held in Rio de Janeiro, Brazil, 24-26 October. DOI: 10.4043/28089-MS.

Iman, R.L., Helton J.C. and Campbell, J.E., 1981. An approach to sensitivity analysis of computer models: Part I - introduction, input variable selection and preliminary variable assessment, *Journal of Quality Technology*, 13(3): 174-183, DOI: 10.1080/00224065.1981.11978748.

Isebor, O.J., Ciaurri, D.E. and Durlofsky, L.J., 2014a. Generalized field-development optimization with derivative-free procedures. *SPE Journal*, v. 19 (5), pp. 891–908. DOI: 10.2118/163631-PA.

Isebor, O.J., Durlofsky, L.J. and Ciaurri, D.E., 2014b. A derivative-free methodology with local and global search for the constrained joint optimization of well locations and controls. *Computational Geosciences* v. 18 (3–4), pp. 463–482. DOI: 10.1007/s10596-013- 9383-x.

Janiga D., Czarnota, R., Stopa, J., Wojnarowski, P. and Kosowski, P., 2017. Performance of nature inspired optimization algorithms for polymer Enhanced Oil Recovery process. *Journal of Petroleum Science and Engineering*, 154: 354-366. DOI: 10.1016/j.petrol.2017.04.010.

Jansen, J.-D., Douma, S.D., Brouwer, D.R., Van den Hof, P.M.J., Bosgra, O.H. and Heemink, A.W., 2009. Closed- loop reservoir management. Presented at the SPE Reservoir Simulation Symposium, The Woodlands, Texas, United States of America, 2-4 February. DOI: 10.2118/119098-MS.

Jansen, J.D., Fonseca, R.M., Kahrobaei, S., Siraj, M.M., Van Essen, G.M. and Van den Hof, P.M.J., 2014. The egg model – a geological ensemble for reservoir simulation. *Geoscience Data Journal*, 1(2): 192–195. DOI: 10.1002/gdj3.21.

Kennedy, J. and Eberhart, R., 1995. Particle swarm optimization. Proceedings of ICNN'95 - International Conference on Neural Networks, 4: 1942–1948. DOI: 10.1109/ICNN.1995.488968.

Kim, J., Kang, B., Jung, H. and Choe, J., 2018. Closed-loop field development optimization with well type conversion. Presented at the 80th EAGE Conference and Exhibition, Copenhagen, Denmark, 11-14 June. DOI: 10.3997/2214- 4609.201801194.

Kim, J., Yang, H. and Choe, J. 2020. Robust optimization of the locations and types of multiple wells using CNN based proxy models. *Journal of Petroleum Science and Engineering*, 193 (2020). DOI: 10.1016/j.petrol.2020.107424.

Litvak, M.L., and Angert P.F., 2009. Field development optimization applied to giant oil fields. Presented at the SPE Reservoir Simulation Symposium, The Woodlands, Texas, United States of America. 2-4 February. DOI: 10.2118/118840-MS.

Loomba, A.K., 2015. Well trajectory optimization. MSc thesis, Delft University of Technology, Delft, The Netherlands.

Loomba, A.K., Botechia, V.E. and Schiozer, D.J., 2020. Bottom-up analysis to unravel potential problems and emphasize the impact of individual steps in closed-loop field development. Presented at the Offshore Technology Conference, Houston, Texas, United States of America, 4-7 May. DOI: 10.4043/30776-MS.

Loomba, A.K., Botechia, V.E. and Schiozer, D.J., 2021. Application of risk-informed closed-loop field development workflow to elucidate the evolution of uncertainties. *Journal of Petroleum Science and Engineering*, 197 (2021). DOI: 10.1016/j.petrol.2020.107960.

Loomba, A.K., Botechia, V.E. and Schiozer, D.J., 2022. A comparative study to accelerate field development plan optimization. *Journal of Petroleum Science and Engineering*, 208 (Part D). DOI: 10.1016/j.petrol.2021.109708.

McKay, M. D., Conover, W. J., and Beckman, R. J., 1979. A comparison of three methods for selecting values of input variables in the analysis of output from a computer code. *Technometrics*, 21: 239–245. DOI: 10.2307/1268522.

Meira, L.A.A., Coelho, G.P., Santos, A.A.S. and Schiozer, D.J., 2016. Selection of representative models for decision analysis under uncertainty. *Computers & Geosciences*, v. 88, pp. 67–82. DOI: 10.1016/j.cageo.2015.11.012.

Meira, L.A., Coelho, G.P., Silva, C.G., Schiozer, D.J. and Santos, A.S., 2017. RMFinder 2.0: an improved interactive multi-criteria scenario reduction methodology. Presented at the SPE LACPEC, Buenos Aires, Argentina, 17-19 May. DOI: 10.2118/185502-MS.

Morosov, A.L., 2016. Evolução do risco durante o desenvolvimento de campos de petróleo. Tese de M.Sc., UNICAMP - Universidade Estadual de Campinas, Campinas, Brasil.

Morosov, A.L. and Schiozer, D.J., 2016. Field development process revealing uncertainty assessment pitfalls. Presented at the 78th EAGE Conference and Exhibition, Vienna, Austria, 30 May - 2 June. DOI: 10.2118/180094-MS.

NASA, 2008. *Agency risk management procedural requirements* (No. NPR 8000.4A). Technical report, Office of safety and mission assurance (NASA), Washington, DC. Available at https://nodis3.gsfc.nasa.gov/displayCA.cfm?Internal_ID=N_PR_8000_004A_&page_name=main.

Nesvold, R.L., Herring, T.R. and Currie, J.C., 1996. Field development optimization using linear programming coupled with reservoir simulation - Ekofisk field. Presented at the SPE European Petroleum Conference, Milan, Italy, 22-24 October. DOI: 10.2118/36874-MS.

Neto, G.M.S., Davolio, A. and Schiozer, D.J., 2020. 3D seismic data assimilation to reduce uncertainties in reservoir simulation considering model errors. *Journal of Petroleum Science and Engineering*, v. 189, pp. 1–12. DOI: 10.1016/j.petrol.2020.106967.

Nwachukwu, A., Jeong, H., Pyrcz, M. and Lake, L.W., 2018. Fast evaluation of well placements in heterogeneous reservoir models using machine learning. *Journal of Petroleum Science and Engineering*, 163: 463–475. DOI: 10.1016/j.petrol.2018.01.019.

Oliver, D.S., He, N. and Reynolds, A.C., 1996. Conditioning permeability fields to pressure data. In: Presented at the 5th European Conference on the Mathematics of Oil Recovery, Leoben, Austria, 3-6 September. DOI: 10.3997/2214- 4609.201406884.

Oliver, D.S., Reynolds, A.C. and Liu, N., 2008. Inverse theory for petroleum reservoir characterization and history matching. Cambridge University Press, Cambridge. DOI: 10.1017/CBO9780511535642.

Oliver, D.S. and Alfonzo, M., 2018. Calibration of imperfect models to biased observations. *Computational. Geosciences*, v. 22 (1), pp. 145–161. DOI: 10.1007/s10596-017-9678-4.

Onwunalu, J.E. and Durlofsky, L.J. 2010. Application of a particle swarm optimization algorithm for determining optimum well location and type. *Computational Geosciences*, 14: 183–198 (2010). DOI: 10.1007/s10596-009-9142-1.

Pettan, C. and Stromsvik, J.F., 2013. The Peregrino challenge: how to keep reliable models while drilling eight wells per year. Presented at the Offshore Technical Conference, Rio de Janeiro, Brazil, 29-31 October. DOI: 10.4043/24522-MS.

Rammay, M.H., Elsheikh, A.H. and Chen, Y., 2019. Identifiability of model discrepancy parameters in history matching. Presented at the SPE Reservoir Simulation Conference, Galveston, Texas, United States of America, 10-11 April. DOI: 10.2118/193838-MS.

Sarma, P. and Chen, W.H., 2008. Efficient well placement optimization with gradient-based algorithms and adjoint models. Presented at the SPE Intelligent Energy Conference and Exhibition, Amsterdam, The Netherlands, 25-27 February. DOI: 10.2118/112257-MS.

Sarma, P., Chen, W.H. and Xie, J., 2013. Selecting representative models from a large set of models. Presented at the SPE Reservoir Simulation Symposium, The Woodlands, Texas, 18–20 February. DOI: 10.2118/163671-MS.

Santos, D.R., Fioravanti, A.R., Santos, A.A.S. and Schiozer, D.J., 2020. A machine learning approach to reduce the number of simulations for long-term well control optimization. In: Presented at the SPE Annual Technical Conference and Exhibition, United States of America, Denver, 27-29 October. DOI: 10.2118/201379-MS.

Schiozer, D.J. and Mezzomo, C.C., 2003. Methodology for field development optimization with water injection. Presented at the SPE Hydrocarbon Economics and Evaluation Symposium, Dallas, Texas, United States of America, 5-8 April. DOI: 10.2118/82021-MS.

Schiozer, D.J., Ligero, E.L., Suslick, S.B., Costa, A.P.A. and Santos, J.A.M., 2004. Use of representative models in the integration of risk analysis and production strategy definition. *Journal of Petroleum Science and Engineering*, v. 44 (1–2), pp. 131–141. DOI: 10.1016/j.petrol.2004.02.010.

Schiozer, D.J., Santos, A.A.S., and Drumond, P.S., 2015. Integrated model based decision analysis in twelve steps applied to petroleum fields development and management. Presented at the SPE EUROPEC, Madrid, Spain, 1-4 June. DOI: 10.2118/174370-MS.

Schiozer, D.J., Avansi, G.D. and Santos, A.A.d.S.d., 2017. Risk quantification combining geostatistical realizations and discretized Latin hypercube. *Journal of the Brazilian Society of Mechanical Sciences and Engineering*, v. 39 (2), pp. 575–587. DOI: 10.1007/s40430-016-0576-9.

Schiozer, D.J., Santos, A.A.S., Santos, S.M.G. and Hohendorff Filho, J.C.v., 2019. Model-based decision analysis applied to petroleum field development and management. *Oil & Gas Science and Technology – Rev. IFP Energies Nouvelles*, v. 74 (46), pp. 1–20. DOI: 10.2516/ogst/2019019.

Shirangi, M.G. and Durlofsky, L.J., 2015. Closed-loop field development under uncertainty by use of optimization with sample validation. Presented at the SPE Reservoir Simulation Symposium, Houston, United States of America, 23-25 February. DOI: 10.2118/173219-MS.

Silva, L.O.M.D., 2018. Seleção de estratégia de produção robusta com o uso de modelos representativos para campos de petróleo na fase de desenvolvimento. Tese de M.Sc. UNICAMP - Universidade Estadual de Campinas, Campinas, Brasil.

Soares, R.V., 2017. *Influência da técnica de localização do ganho de Kalman no ajuste de histórico de produção*. Tese de M.Sc., UNICAMP - Universidade Estadual de Campinas, Campinas, Brasil.

Soares, R.V., 2017. Use of an iterative ensemble smoother methodology in a history matching and uncertainties assessment process. Presented at the SPE Annual Technical Conference and Exhibition, San Antonio, Texas, United States of America, 9-11 October.

Soares, R.V., Maschio, C. and Schiozer, D.J., 2018. Applying a localization technique to Kalman gain and assessing the influence on the variability of models in history matching. *Journal of Petroleum Science and Engineering*, v. 169, pp. 110–125. DOI: 10.1016/j.petrol.2018.05.059.

Storn, R. and Price, K., 1997. Differential evolution – a simple and efficient heuristic for global optimization over continuous spaces. *Journal of Global Optimization*, 11: 341-359. DOI: 10.1023/A:1008202821328.

Toledo, S., Avansi, G.D. and Schiozer, D., 2017. Updating reservoir simulation models with well test information for reduction of uncertainties in early field development. Presented at the SPE EUROPEC, Paris, France, 12-15 June. DOI: 10.2118/185865-MS.

van Essen, G., Zandvliet, M., Van den Hof, P., Bosgra, O., Jansen, J.-D., 2009. Robust waterflooding optimization of multiple geological scenarios. *SPE Journal*, v. 14 (1), pp. 202–210. DOI: 10.2118/102913-PA.

van Essen, G.M., Van den Hof, P.M.J., Jansen, J.D., 2011. Hierarchical long-term and short-term production optimization. *SPE Journal*, v. 16 (2011), pp. 191–199. DOI: 10.2118/124332-PA.

Volz, R.F., Burn, K., Litvak, M.L., Thakur, S.C., and Sergey S., 2008. Field development optimization of eastern siberian giant oil field development under uncertainty. Presented at the SPE Russian Oil and Gas Technical Conference and Exhibition, Moscow, Russia, 28-30 October. DOI: 10.2118/116831-MS.

Yang, C., Nghiem, L.X., Card, C. and Bremeier, M., 2007. Reservoir model uncertainty quantification through computer-assisted history matching. Presented at the SPE Annual Technical Conference and Exhibition, Anaheim, California, United States of America, 11–14 November. DOI: 10.2118/109825-MS.

Wang, C., Li, G., Reynolds, A.C., 2007. Optimal well placement for production optimization. Presented at the SPE Eastern Regional Meeting, Lexington, Kentucky, United States of America, 11-14 October. DOI: 10.2523/111154-MS.

Wang, H., Ciaurri, D.E., Durlofsky, L.J. and Cominelli, A., 2012. Optimal well placement under uncertainty using a retrospective optimization framework. *SPE Journal*, v. 17 (2012), pp. 112–121. DOI: 10.2118/141950-PA.

Weise, T., 2011. Global optimization algorithms - theory and application. Available online at www.it-weise.de/projects/book.pdf.

Yang, C., Nghiem, L.X., Card, C. and Bremeier, M., 2007. Reservoir model uncertainty quantification through computer-assisted history matching. Presented at the SPE Annual Technical Conference and Exhibition, Anaheim, California, United States of America, 11-14 November. DOI: 10.2118/109825-MS.

Yeten, B., Durlofsky, L.J., Aziz, K., 2002. Optimization of nonconventional well type, location and trajectory. Presented at the SPE Annual Technical Conference and Exhibition, San Antonio, Texas, United States of America, 29 September - 2 October. DOI: 10.2523/77565-MS.

Zakirov, E.S., Zakirov, S.N., Indrupskiy, I.M., Lyubimova, O.V., Anikeev, D.P., Shiryaev, I.M., Baganova, M.N., 2015. Optimal control of field development in a closed loop. In: Presented at the SPE Russian Petroleum Technology Conference, Moscow, Russia, 26-28 October. DOI: 10.2118/176642-MS.

Zandvliet, M.J., Handels, M., van Essen, G., Brouwer, R., Jansen, J.-D., 2008. Adjoint- based well-placement optimization under production constraints. *SPE Journal*, v. 13 (4), pp. 392–399. DOI: 10.2118/105797-PA.

Zio and Pedroni (2012). Panorama des processus décisionnels tenant compte du risque. Numéro 2012-10 des Cahiers de la Sécurité Industrielle, Fondation pour une Culture de Sécurité Industrielle, Toulouse, France (ISSN 2100-3874). Disponible à l'adresse <http://www.FonCSI.org/fr/>.

Appendix A : Concept of Risk-informed Decision-making

In this appendix, we expound on the risk-informed CLFD workflow for decision-making. The concept of risk-informed decisions has been exploited in the process industry and business models for a long time. In 2012, Zio and Pedroni described in detail the risk-informed decision-making approach adopted by the National Aeronautics and Space Administration (NASA) and by the United States (US) Nuclear Regulatory Commission. We used this concept with CLFD workflow in this thesis.

Zio and Pedroni (2012) differentiated between a risk-based and risk-informed decision-making process in their work. The authors defined a risk-based decision-making as: *“A risk-based decision-making process provides a defensible basis for making decisions and helps to identify the greatest risks and prioritize efforts to minimize or eliminate them. It generally does not lead much space for interpretation.”*

As a risk-based process is a strict workflow without room for individual interpretation, Dezfuli et al. (2010a, b) and NASA (2008) defined a risk-informed approach to mitigate performance shortfalls in the outcome. Contrarily to a risk-based process, risk-informed decision-making is a calculated, cautious and contemplative process to “inform” decision-making using a set of key performance indicators, in combination with additional considerations used during a risk-based process (Zio and Pedroni, 2012). Unlike a risk-based decision-making process, the authors stressed that technical information is not the sole basis for decision-making and identified the significance of human judgment in the risk-informed decision-making process. They attributed this to vast uncertainty and gaps in technical information, as well as the intrinsic nature of the decision-making process being a subjective and value-based task.

Reflecting on the previous studies in the niche area of CLFD, this thesis promotes a deliberate implementation of CLFD using a risk-informed and efficient workflow. Rather than an automatic process, the thesis asserts that technical benefits of a CLFD workflow can only be exploited by understanding the true nature of the problem. Technical components (for example: reservoir characteristics, uncertainty attributes and their overall impact, geophysics and geology, fidelity of simulation models, commercial analysis, infrastructure development, etc.) and non-technical components (for example: time-consumption, software knowledge, and its internal parameters’ handling skills, mitigating specious outputs at the end of each step to

thwart the overall negative impact, learning when to modify sub-steps to accomplish overall goals, etc.) must be successfully integrated for each cycle of a CLFD workflow. We list three examples to appreciate the risk-informed nature of the presented work:

1. Data assimilation: History-matching is an ill-posed and inverse problem with multiple solutions. In Chapter 5, we presented a practical problem related to this step (**Figure 5-4**) and its solution based on our subjective interpretation (**Figure 5-5a**). The mean of the simulated output of the problematic well was still lower than the observed output (**Figure 5-4**) even after data assimilation. However, weighing the efficiency, updated models, and subjective knowledge of the associated risk, we decided to continue with the subsequent steps of the CLFD.
2. Approved models: Usually, one picks the best scenarios from the subset of history-matched reservoir models. Based on the analyses in this thesis, we stress that this step must focus on discarding poorer scenarios rather than accepting the best ones (see **Table 3-8**). Furthermore, this step is imperative to reduce the computational cost for the subsequent step (selection of RMs), where one needs to run the ensemble of approved scenarios to select RMs. For instance, in the third cycle of Chapter 3, we saved 423 simulations (see **Tables 3-4** and **3-7**) without thwarting the outcome of CLFD. Similarly, this step improved the efficiency in Chapter 5 by working with a smaller set of approved models for all the cycles, thus saving several months.
3. Improving the results in the reference case: Unlike previous studies, our thesis does not emphasize maximizing the EMV of the RMs. We studied the impact of each step on the subsequent stages and thus understood how to mitigate the specious outputs. In Chapters 2 and 3, we observed the importance of maximizing the likelihood of success over the RMs. **Table 3-9** extended this conclusion and revealed the impact of maximizing the minimum improvement over the RMs on the outcome in the reference case. In Chapter 5, we extended the idea by attempting to maximize the ensemble of approved scenarios rather than just RMs, while maximizing the minimum improvement over this ensemble. Even though some FDPs yielded higher EMV over this ensemble, we did not use them in the reference case as they presented a relatively higher chance of failure.

At multiple stages, the thesis encourages end-users to identify more performance indicators along with the sensitivity analysis to understand the impact of various parameters/steps for improving the final decision using subjective interpretation.

To conclude, cumulative knowledge of the reservoir engineers and geoscientists is fundamental for assimilating technical and non-technical elements for mitigating the risks of failure of the revised decisions or FDP at the end of each cycle (NASA (2008); Dezfuli et al. (2010a, b); Zio and Pedroni, 2012). We promote the idea of a risk-informed workflow to highlight its significance and impact on CLFD. One of the inherent goals of this work is to encourage engineers to use CLFD as a beneficial technique in a more “well-informed” environment rather than push-button automation.

Appendix B : Using “Flux Boundary Option” for Well Location Optimization: A Feasibility Study

B.1 Introduction

In 2019, Computer Modelling Group Ltd. (CMG) introduced the “flux boundary option” in GEM. As CMG explains in their manual:

“It enables writing out of flux boundary conditions from full field run to designated boundaries of a potential reduced run. The reduced runs can then be performed on a smaller set of grid blocks using the flux boundary information written during the full field run.”

In this appendix, we present the feasibility of using the “flux boundary option” for optimizing the NPV of a deterministic reservoir scenario using i^{th} and j^{th} grid blocks of vertical wells as the control variables.

B.2 Objective

We examine the applicability of the flux boundary option (FBO) in terms of its function for performing production strategy optimization in a giant field like UNISIM-III-22 (see Section 4.4).

B.3 Methodology

In this section, we report the methodology followed for studying the feasibility of the FBO:

1. Define the flux boundary in the simulation file(s):
 - a. Define the name and number of the flux-boundary sector using *FLXB-NAMES keyword. This needs to be followed by defining the grid-blocks under the flux-boundary sector using *FLXB-DEF *ALL (or *IJK) keyword. An example:


```
*FLXB-NAMES 'flxb-S2' 1 (*FLXB-NAMES keyword must appear only once)
*FLXB-DEF *ALL
3267*0 2*1 61*0 2*1 56*0 7*1 48*0 15*1 46...and so on.
```
 - b. After defining the flux boundary (required for both full field and reduced simulation models), define the flux type (*FLUX or *PRESSURE) and select the *FLXB-OUT option in the full-field simulation model. An example:


```
*FLXB-OUT (This part is necessary for outputting the flux boundary)
*FLXB-TYPE *FLUX (not a mandatory keyword as *FLUX is default option)
```

c. For the reduced run simulation, these 2 keywords must be replaced with:

**FLXB-IN 'name_of_dat_file.flxb'*

**FLXB-ACTIVE 'flxb-S2'* (multiple flux boundary sectors can be activated simultaneously)

Important notes:

- Changing the NULL blocks definition for the reduced run simulation neither affects the simulation time nor results.
 - Use **SRFORMAT *SR3_IMRF* in the I/O section to obtain the *.sr3, *.irf and *.mrf files in 2019/2020 versions of CMG.
2. Generate .flxb file: After editing and placing the necessary keywords and flux-boundary definition in the full field and reduced simulation model, one needs to run the full field model to generate the *.flxb file.
 3. Run the reduced model with the same strategy and features as the whole model to verify the working of the *.flxb file.
 4. Use the generated *.flxb file to run the reduced field model with a different strategy.
 5. Compare and analyze the results of the reduced field model (with and without FBO) with the full field simulation model. Simulation time, output, and potential problems are the assessment criteria.

B.4 Application and Results

In this section, we discuss the application of the methodology on a simulation model of UNISIM-III-2022 (U3-22). While U3-22 run was considered the full field simulation model, isolated Sector-2 was considered for the reduced field simulation runs. Within reduced field simulation runs, we also have: (1) S2-22F, i.e., the reduced model considering the flux boundary option (FBO) and, (2) S2-22, i.e., isolated Sector-2 model without FBO (**Table B-1**). Two well-location strategies were tested (labelled as Strategy1 and Strategy2). 10 processors were used with GEM 2019.10 in high performance computing (HPC) cluster.

Table B-1: Description and name of the models used in this appendix.

Description of Model	Name
Full Field Model	U3-22
Isolated Sector 2 with FBO ^[1]	S2-22F
Isolated Sector 2 without FBO	S2-22

^[1] One does not need to isolate sector when using FBO

After executing Step#1 of the methodology, we performed the full field simulation of U3-22 model using Strategy1 to obtain the Strategy1.flxb file. Next, we used this file for running the S2-22F with Strategy1 to verify the similarity in results. Simultaneously, we simulated the S2-22 with Strategy1 to compare the results.

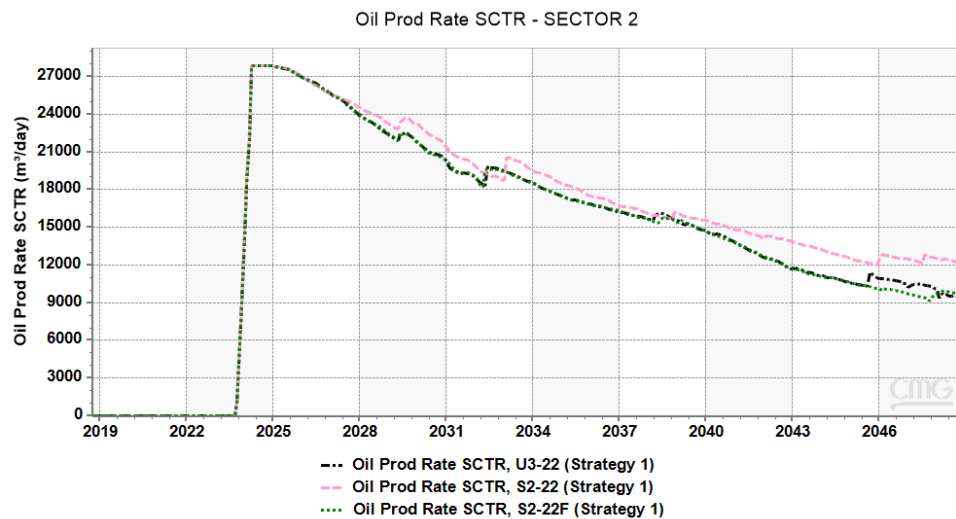
Subsequently, we ran the S2-22F and S2-22 models with Strategy2. One must note that the S2-22F with Strategy2 was run using Strategy1.flxb file as one would use while performing optimization. **Table B-2** compares time consumption by these runs.

Table B-2: Comparing the simulation time for the full field and reduced field model (with original and modified strategy).

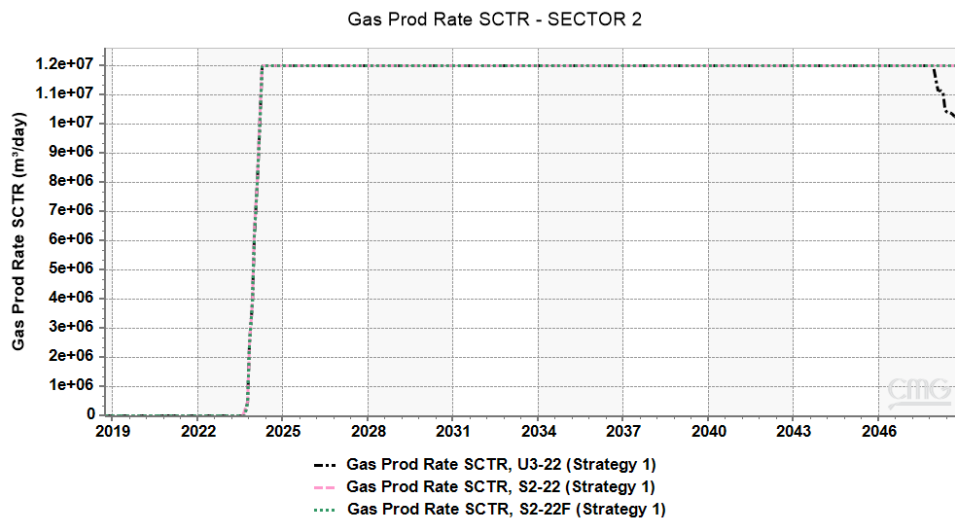
	Strategy 1 (Same as FBO) in			Strategy 2 in		
Simulation time (hrs.)	U3-22	S2-22F	S2-22	U3-22	S2-22F	S2-22
HPC cluster	8.6	3.8	2	8	40*	2.5

* Simulation stopped due to numerical tuning error.

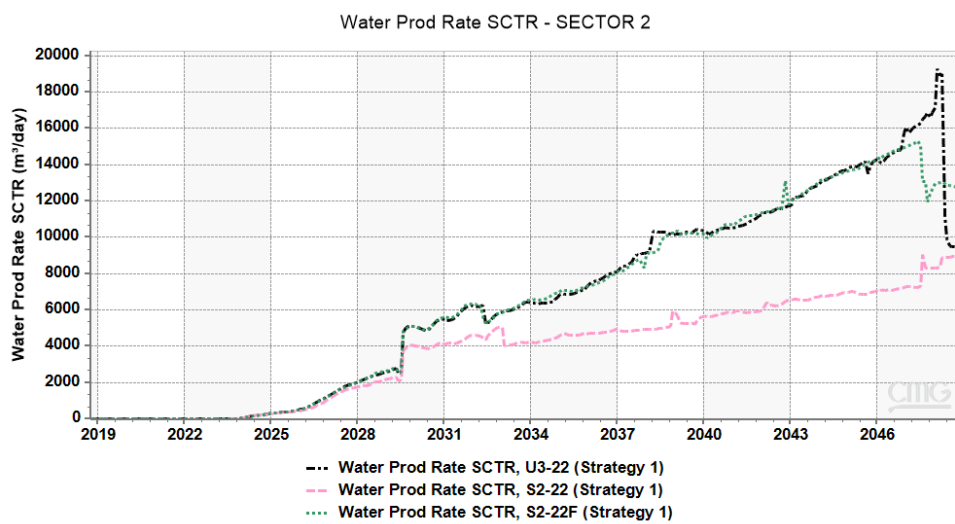
Figure B-1 shows the results obtained after applying Strategy-1 in U3-22, S2-22F and S2-22. The simulated output of S2-22F is similar to U3-22. On the other hand, the output of S2-22 is different as it does not consider the boundary conditions:



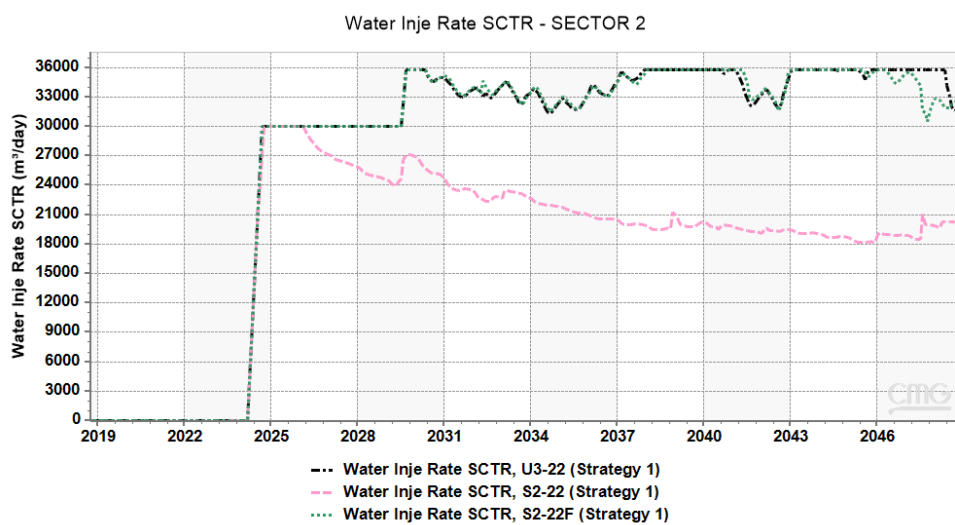
(a)



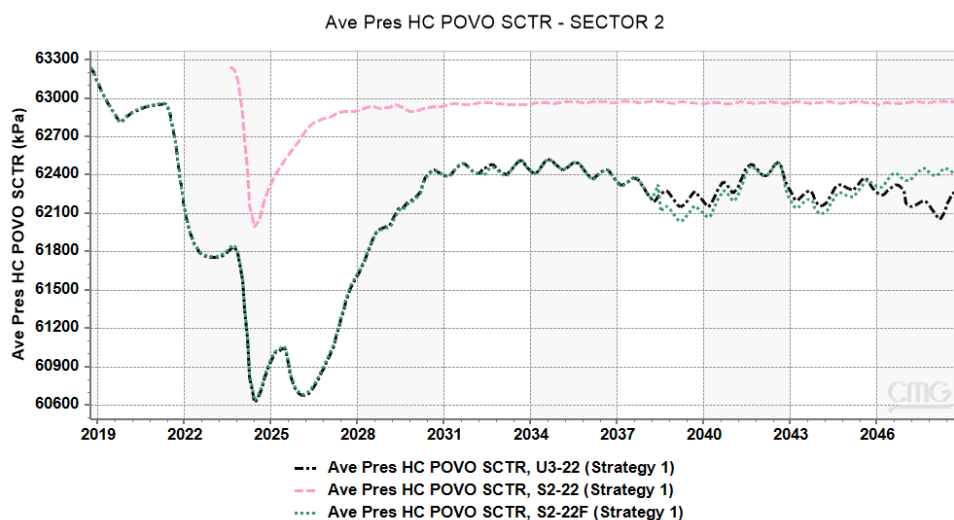
(b)



(c)



(d)

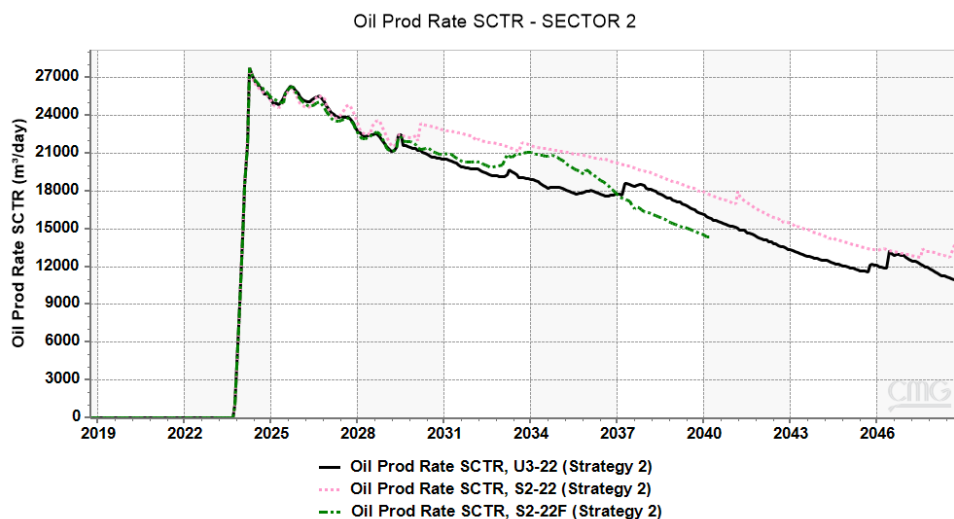


(e)

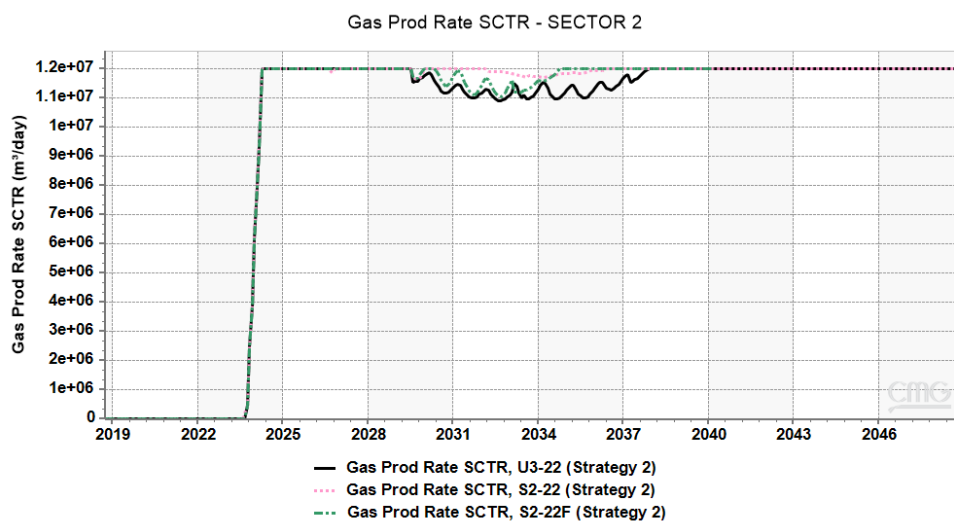
Figure B-1: a) Oil production rate, b) gas production rate, c) water production rate, d) water injection rate and, e) average pressure in Sector 2 after simulating U3-22, S2-22 and S2-22F with Strategy 1.

Gas Production and injection rates were same for the Strategy1, so the latter was not shown in **Figure B-1**. Average pressure was one parameter where higher differences were observed between S2-22 and S2-22F. FBO helped S2-22F (with Strategy1) to imitate the same behavior as seen in U3-22 model (with Strategy1) using 56% lesser time.

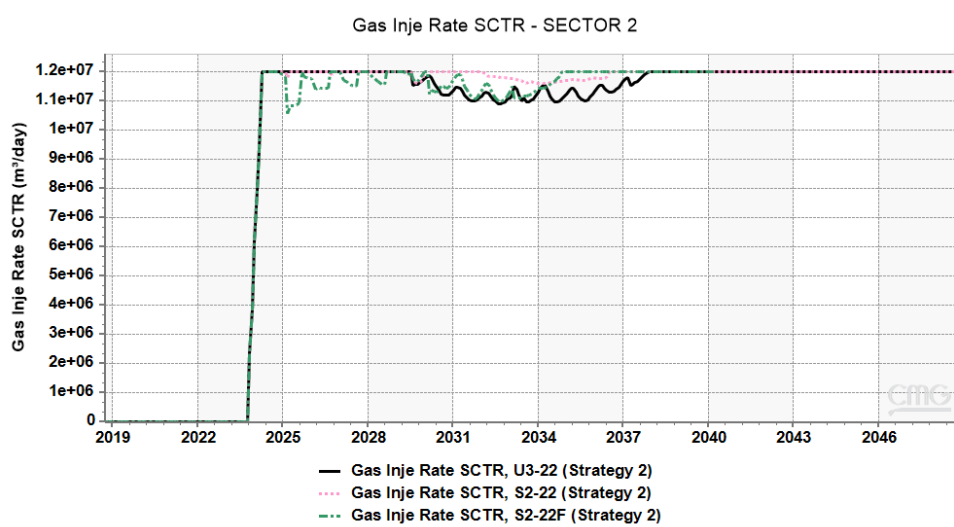
Figure B-2 shows the results obtained after applying Strategy2 in U3-22, S2-22 and S2-22F models.



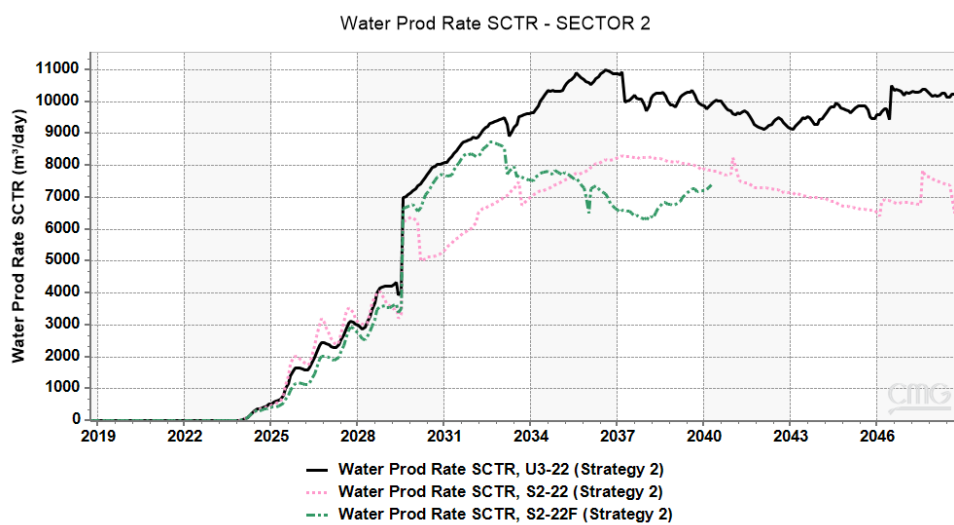
(a)



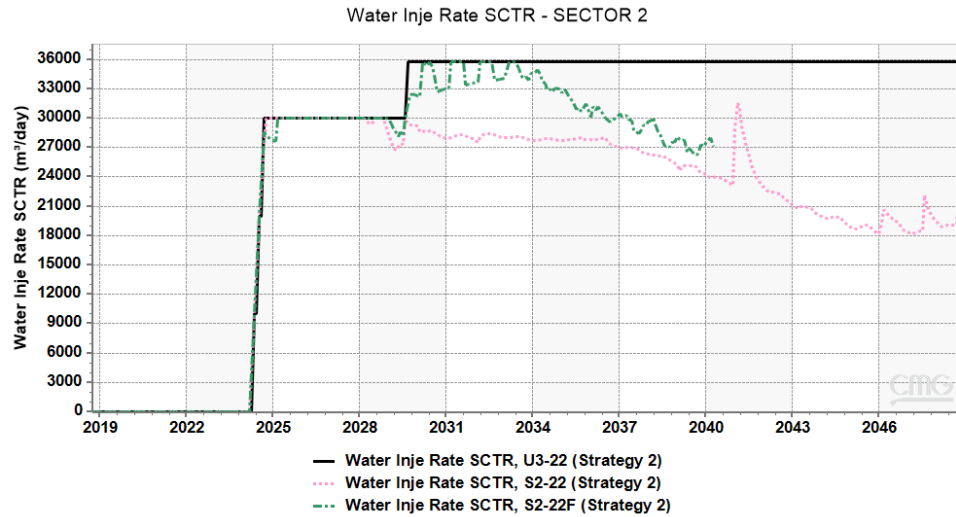
(b)



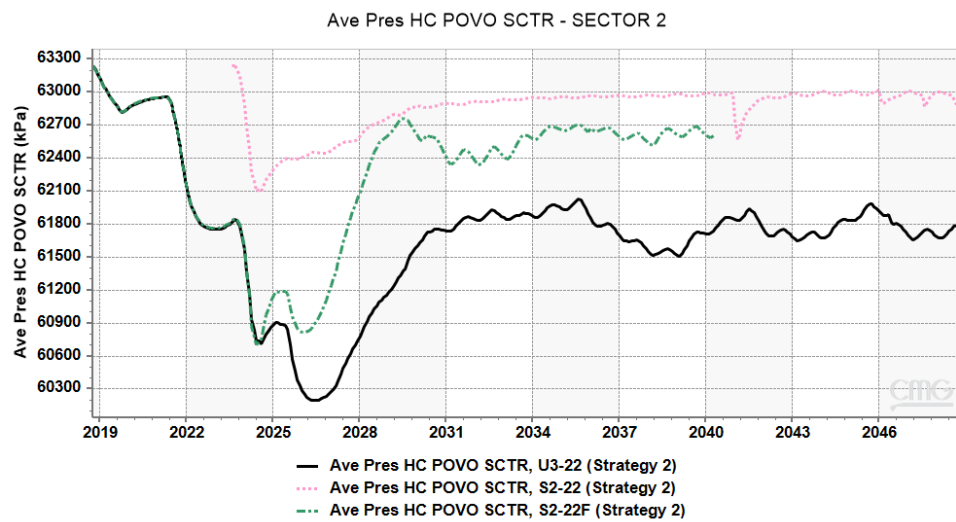
(c)



(d)



(e)



(f)

Figure B-2: a) Oil production rate, b) gas production rate, c) gas injection rate, d) water production rate, e) water injection rate and, f) average pressure in Sector 2 after simulating U3-22, S2-22 and S2-22F (using Strategy1.flxb) with Strategy 2.

The simulated output of S2-22F, S2-22, and U3-22 was observed to be dissimilar when new strategy (Strategy2) was implemented. Due to numerical tuning error, the simulation of S2-22F also failed around the year 2040.

B.5 Discussion

Flux boundary option (FBO) is a tool to perform a reduced field simulation and evaluate the flux-boundary sector. In this appendix, we studied how to exploit this new tool and its feasibility in the field development stage when performing strategy optimization. Below, we discuss a few more observations to deliver a well-informed conclusion on this subject:

1. As **Figures B-1** and **B-2** suggest, performing optimization with S2-22 (i.e., isolated sector without FBO) can yield sub-optimal results for U3-22. S2-22 is prone to bias and tends to exhibit disparity with the full-field model as it does not consider the boundary conditions (same as concluded in Chapter 4).
2. Compared to **Figure B-1**, **Figure B-2** shows a stark difference between the simulation results of U3-22 and S2-22F (both run using Strategy2). Reviewing **Figure B-2**, we can also observe that well-locations had a dominant impact to sway the simulation results of S2-22F closer to the results of S2-22. FBO did not help to imitate the results of the full-field simulation. On the other hand, the results are more similar to the isolated-sector simulation results.
3. In addition, numerical errors can occur when a different strategy (Strategy2) is run with the same *.flxb file. This can lead to multiple problems like incomplete simulations (see **Figure B-2**), convergence errors, extremely long simulation time (see **Table B-2**), etc.
4. Comparing the gas production and injection rates in **Figure B-2 (b and c)**, we notice another discrepancy; S2-22F model was unable to inject 100% gas using *.flxb. Within the same period, both U3-22 and S2-22 models were able to do the same. Thus, it is fair to say that using *.flxb can lead to such errors as well (due to numerical errors/failures).
5. **Figure 4-11** reveals that strategies can have huge and differing impact on inflow behavior. Note that Sector 2 has a positive influx with Strategy2 while it is consistently negative with Strategy1.
6. To justify the use of FBO for optimization, we used Strategy1.flxb to run the reduced simulation model with Strategy2. By doing this, we ignored the influx change that we observed in the U3-22 using Strategy2 (**Figure 4-11**). This makes the use of FBO moot as it will only lead to propagation of uncontrolled uncertainty.
7. For these strategies, the influx from a *.flxb file acts as a noise which needs to be adjusted by cutting timestep. This is corroborated by the large simulation time observed in **Table B-2**. Since this noise is almost zero with the original strategy, we observe a much faster simulation compared to the full field. But, this noise changes with the Strategy2 (**Figure 4-11**) and thus, the simulator is required to cut timestep to adjust pressure and saturation. Due to higher mobility of gas as well as its extensive presence in our models, the saturation changes associated with gas can be more challenging to deal with when there is a huge difference in influx.

We recommend performing a preliminary analysis to determine if FBO can be used for data assimilation. If necessary, this test can be extended to see if it is feasible for control variables optimization. One can also study influx and re-sectorization of flux boundary to reduce time and make this tool attractive, while ensuring the models are completely simulated within a smaller time-frame compared to full-field model.

B.6 Conclusions

“Flux boundary option” is not recommended for performing well-location optimization. It is very important to have the same dates and features in the RUN section of the *.dat file to avoid having a huge simulation time, which cannot be done for a new production strategy.

- FBO replicates field behavior within a good tolerance for the same strategy. Otherwise, it may not replicate field behavior. The simulated output of reduced model (with and without FBO) and full-field model can be dissimilar when new strategies are tested during the optimization process.
- Depending on the influx variation, different sectors of U3-22 may behave differently. With the limited test we performed, we can conclude that it is not appropriate for performing optimization of well-location in Sector-2.

B.7 Remarks

1. To validate the results, we tested different strategies (besides Strategy1 and Strategy2) to confirm the problems observed in this report.
2. FBO does not work with wells drilled on the edge of “flux boundary”. It can strongly affect the solution space unless the “flux-sector” definition is differentiated from the “sector” definition.
3. “Flux boundary” cannot be same as “flux sector”. GEM will crash with an error message.
4. The results were tested using CMG 2019.10 and CMG 2020.10.
5. All simulation files and results are also available for download [here](#).

Acknowledgments

The authors would like to acknowledge the contribution of Luis Carlos Oliveira Pires (CEPETRO-UNICAMP/Brazil) and Juan Alberto Mateo Hernandez (CMG) for validating the results and providing insights on the subject.

Appendix C : Cluster-based learning and evolution algorithm for optimization

Abstract

In this work, we present a cluster-based learning and evolution optimizer (CLEO) for solving optimization problems. CLEO is a metaheuristic algorithm that uses cluster-based manipulation of the problem space during the exploration phase, followed by fine-tuning solutions in the exploitation phase using updated knowledge of the problem space. We propose two approaches based on this new algorithm: one using only Latin hypercube sampling (LHS) and the other using LHS in combination with reservoir engineering insights. In addition to ensuring realistic simulation scenarios, we employed intuitive engineering insights to reveal how empirical knowledge enhances efficiency. Also, we propose simulating the partial life instead of the complete lifespan in the second approach. Technical results obtained at the end of this period are processed and used to find the optimized field development plan (FDP). We conducted both deterministic and probabilistic studies to assess the performance of the proposed approaches for various decision variables, both numerous and restricted. We validated the algorithm by optimizing the FDP for a simple numerical simulation model and a giant field-scale model, and compared our approaches to four well-established optimizers (particle swarm optimization (PSO), differential evolution (DE), designed exploration controlled evolution (DECE), and iterative discrete Latin hypercube sampling method (IDLHC)) in terms of simulation time and objective function results. Overall, the comparison demonstrates the advantages of the newly proposed algorithm.

The results indicate that our first approach performs as well as any well-established optimizer, notably when working with large scale optimization problems. The second approach has slightly lower objective function results than the first one, but it is the most efficient among the compared algorithms, as the best FDP can be obtained by covering as little as 40% of the field's life. This attribute makes it an excellent alternative for developing oil and gas fields, which are fraught with uncertainty and errors in time-consuming simulation models.

Keywords

Optimization; Algorithm; Field development plan; Reservoir simulation; Time-consuming models; Uncertainties; Partial simulations; Predictive analytics; Efficiency; Giant field; Cluster; Decision variables; Gradient-free algorithm; Large scale optimization

C.1 Introduction

In reservoir engineering, one needs to work on numerous optimization problems with multiple decision variables throughout a field's life. These variables constitute a significant part of the FDP, a technical guide that mandates the process of developing the asset. It also has a defined objective function to mathematically represent the overall objective of the field development. Due to diverse and sensitive decision variables in it, optimizing the objective function of an FDP is a challenging task. Thus, manually improving a field's objective function can be a daunting task. This complexity compels geoscientists and engineers to use computer-assisted optimization algorithms for optimizing an FDP.

Optimization algorithms can be classified based on different traits. One way to classify them is based on their numerical approach: gradient-based or gradient-free. Gradient-based algorithms calculate the gradient of the objective function with respect to decision variables to define search direction (Wang et al., 2007; Zandvliet al., 2008; Sarma et al., 2008; Loomba, 2015). The main difference between all gradient-based algorithms is how they use gradients to compute the search direction. Though gradient-based algorithms are less demanding in computational time, they cannot differentiate between global and local optimum. Moreover, it requires intricate coding to obtain gradients from commercial simulators.

In contrast, gradient-free algorithms are easy to use. In theory, these algorithms can converge to the global optimum. However, this outcome comes at a cost of considerably more simulation runs. Several gradient-free algorithms have been presented over time for optimizing an FDP. Genetic algorithm (Yeten et al., 2002; Badru et al., 2003; Emerick et al., 2009), particle swarm optimization (Onwunalu and Durlofsky, 2010), differential evolution (Awotunde, 2014), simulated annealing (Beckner and Song, 1995), and ant colony optimization (Janiga et al., 2017) are a few examples of widely used gradient-free optimization algorithms.

Asides from choosing an apt optimization algorithm, geoscientists and engineers are also challenged by the substantial number of decision variables. Platform constraints, setting and control of inflow control valves (ICVs), and various parameters of a well (e.g., type,

location, operational settings) are a few examples of decision variables. Each decision variable also has its own problem space, ranging from trivial to huge. Due to this additional complexity, it is common to optimize variables either sequentially (Gaspar et al., 2016) or simultaneously (Forouzanfar and Reynolds, 2014). Although sequential optimization may provide a sub-optimal result in some of the simple examples (Bellout et al., 2012), it makes the whole process simpler compared to the latter approach.

Apart from algorithms and problem space, one needs to work with substantial uncertainty as well as inaccuracy. Model error is an inherent component of any simulation model (Oliver and Alfonso, 2018; Rammay et al., 2019; Neto et al., 2020; Loomba et al., 2021). As a result, seeking a global optimum with such models does not imply a globally optimal result in the actual field. Thus, one should strive to improve the quality of models rather than spending an enormous time on the optimization process. This axiom furthers the necessity to have efficient algorithms to optimize an FDP.

In this work, we introduce a metaheuristic optimization algorithm named CLEO, which stands for cluster-based learning and evolution optimizer. It explores and exploits the problem space of decision variables. But, unlike existing algorithms, cluster-based manipulation is used to thoroughly search for the solution. We introduce this derivative-free algorithm to deal with a large problem space and multiple decision variables that impede the joint optimization process. We compare a simple CLEO-based approach with well-established algorithms to show its applicability to simultaneously optimize numerous decision variables. Keeping efficiency in mind, we also introduce another approach that saves a tremendous amount of time and money. We study the use of technical results obtained from partial simulations in this second approach. Using predictive analytics, we provide first-hand evidence of how short-term results can be used to develop long-term field objectives.

We begin this work by outlining the theory of CLEO. Next, we present the two approaches built on the groundwork of CLEO and their pseudocodes. These approaches are first applied to a simple synthetic model with vast and limited decision variables. Deterministic and probabilistic tests are performed to compare them with well-established algorithms. Particle swarm optimization (PSO), differential evolution (DE), iterative discrete Latin hypercube sampling method (IDLHC), and designed exploration controlled evolution (DECE) have been used for comparison. Fast and simple synthetic models are inept at reflecting the true worth of the second approach. Thus, we tested it again on a real and giant-field model to demonstrate the adeptness of the second approach based on partial simulations. Finally, we

discuss the results and recommendations for future work before concluding all significant observations made throughout this work.

C.2 Objectives

The main objectives of this work are:

1. To present a new gradient-free optimization algorithm, CLEO, and its conceptual framework. Unlike existing algorithms, CLEO uses cluster-based manipulation to search the problem space efficiently.
2. To present a simple approach for using CLEO with the Latin hypercube sampling (LHS) technique for sampling (CLEO-M1). This approach is presented for two reasons: (a) to compare the performance of well-established algorithms that use the LHS method and (b) to demonstrate that LHS works sufficiently well.
3. To present a second approach for using CLEO with predictive analytics to optimize more efficiently (CLEO-M2). This approach is presented to work with time-consuming simulation models without compromising the objective functions, considering the model error and uncertainty.
4. To present an in-depth discussion and recommendations for improving CLEO-based approaches to make them more beneficial than existing algorithms.

The next sections describe the concept of the optimization algorithm and introduce two approaches built on the foundation of CLEO.

C.3 Conceptual Framework

It can be challenging to perform an exhaustive search due to a vast problem space and decision variables. This problem is tackled in distinct ways by existing optimizers. Here, we provide a broad picture of our cluster-based learning and evolution optimizer (CLEO) to show how it works and deals with the vastness of problem space and variables.

CLEO is a metaheuristic algorithm that performs efficient exploration by manipulating problem space (**Figure C-1**). First, we define an objective function (y) and problem space (\mathbb{X}) for the given problem statement. However, instead of working with the entire problem space (\mathbb{X}), CLEO groups the solution candidates ($x : x \in \mathbb{X}$) based on their similarities. Each cluster picks a representative solution candidate (x_{rep}) to create a vector of possible solutions (\mathbf{x}). In other words, all clusters are represented by \mathbf{x} and their probability mass function (PMF).

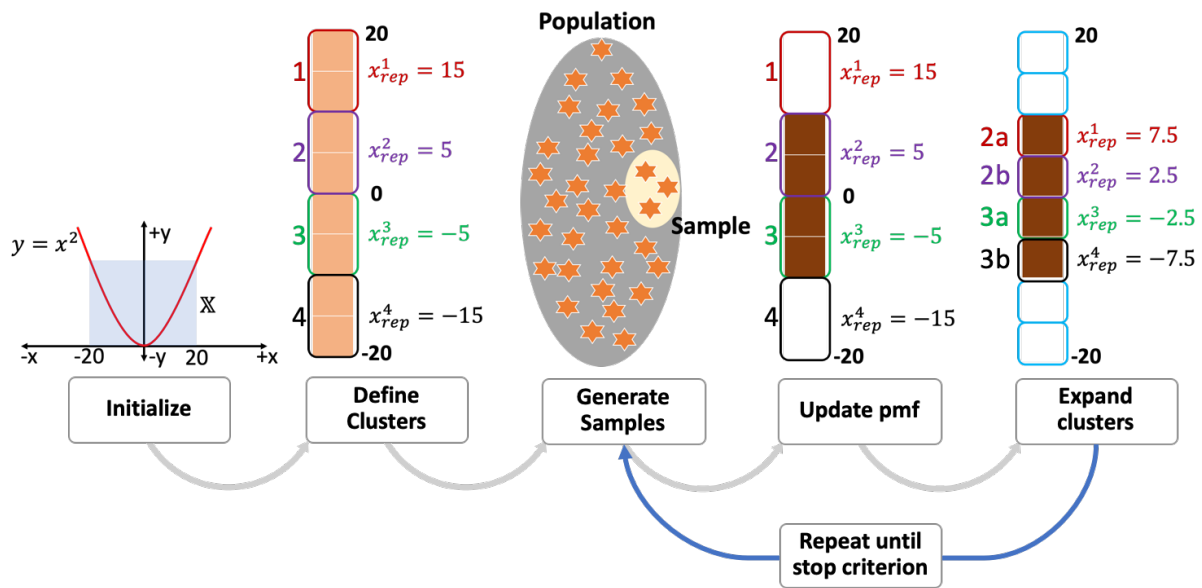


Figure C-1 - A simple optimization problem to illustrate the concept of CLEO.

Employing an appropriate sampling method, CLEO generates a sample only using \mathbf{x} . It is a crucial step to deal with large problem space or decision variables. These samples are used to obtain the corresponding y to evaluate the quality of results. At this stage, CLEO correlates \mathbf{x} and y to update the PMF of each cluster. Using this updated PMF, CLEO gradually starts expanding the existing clusters as well as updating \mathbf{x} . This step assists in exploring the entire problem space as we gradually learn more about each cluster and the nested clusters within it. New samples are generated using the updated PMF, and the objective functions are re-evaluated. The process is repeated until one reaches the stopping criteria (maximum simulation runs or convergence criterion). Thus, learning and continuously evolving the samples by manipulating the clusters lead to exploration of the entire problem space.

Figure C-1 presents a minimization problem with problem space defined by real numbers (\mathbb{R}) between -20 to 20. In this hypothetical example, one can observe that after evaluating the initially defined clusters, we obtained a fair enough knowledge of the problem space so as only to accept $x : \{x \in \mathbb{R} \text{ and } -10 < x < 10\}$. Also, as we are only working with a single decision variable in this example, the number of generated samples equals the number of clusters. In summary, CLEO attempts to optimize the objective function by performing a quick global search and gradual local refinement.

C.4 Methodology

C.4.1 CLEO-Method 1 (CLEO-M1)

As mentioned earlier, sampling technique is the main component of CLEO. While many sampling techniques exist, Dige and Diwekar (2018) conducted experiments to identify the best sampling technique for different variable sizes. However, we restricted ourselves to using the Latin hypercube sampling (LHS) method (McKay et al., 1979 and Iman et al., 1981) in CLEO-M1. This was done for two reasons:

1. A fair comparison with two established optimizers that are based on the LHS method.
2. Establish that LHS works sufficiently well, even with sizable decision variables.

The pseudocode of CLEO-M1 is presented in **Algorithm C-1**. The problem space for each decision variable is clustered based on their similarities. For example, well-controls are grouped solely based on their values, and their respective representative values are selected using Euclidean distance. The benefit of using only representative values is that it drastically reduces the sample size. This is implied from the fact that a larger search space requires a commensurately larger sample to evaluate eligible candidates.

Algorithm C-1 - FDP optimization using CLEO-M1

```

Input:   : Problem statement, simulation models
Output  : Optimized decision variables
Define  : Stop criteria
begin
1. Identify  $\mathbb{X}$ 
2. Define the initial clusters of  $\mathbb{X}$  using k-means clustering
3. Select representative eligible candidate ( $x_{rep}$ ) for each cluster
4.  $iter \leftarrow 0$ 
5. while Stop criteria is False do
6.   Use LHS to generate scenarios with the PMF of clusters
7.   Run the scenarios
8.   Correlate the objective function with the scenarios
9.   Update posterior PMF of the clusters using best  $b$  scenarios
10.  if Expansion is True then
11.    Expand the clusters
12.    Select  $x_{rep}$  for each cluster
13.  else
14.    Break
15.  end if
16.   $iter \leftarrow iter + 1$ 
17. end while
end

```

Using these initial representative values, we create and run the first set of simulation runs. We calculate their respective objective function. The best ones are used to update the PMF of the clusters. One must note that with a larger cluster, in the beginning, CLEO-M1 only attempts to identify and explore the search space. As new clusters are defined within the existing clusters using the updated PMF, the algorithm gradually starts fine-tuning solutions.

C.4.2 CLEO-Method 2 (CLEO-M2)

Working with the entire problem space can be unrealistic, particularly when dealing with time-consuming physics-based simulations. Meanwhile, reservoir engineering insights (REIs) are always available to help math-based optimizers. Thus, we use such REIs in CLEO-M2.

One can evaluate the whole problem space based on reservoir engineering concepts. This allows the engineers to use REIs in multiple forms to eliminate unfeasible solution candidates from the problem space (\mathbb{X}). While REIs can be subjective and vary with experience, they can be easily quantified and implemented to boost the efficiency of the optimization process. Five simple examples of REIs are listed here:

1. Avoid drilling producers in non-pay zone to boost production.
2. Select the problem space for producers based on the amount of movable oil in its neighborhood.
3. Avoid scheduling wells at a much later phase to make them economically feasible.
4. Using a feasible upper and lower bound of tubing head pressure (THP)/bottom-hole pressure (BHP) to define the well-operational settings.
5. Eliminating unfeasible values which may lead to unintentional fracking or lowering the reservoir pressure below the bubble-point pressure.

Using such REIs, one can define a search space (\mathbb{G} : $\mathbb{G} \subseteq \mathbb{X}$) with eligible candidates (g). A smaller search space (\mathbb{G}) prepared by eliminating unnecessary candidates helps to explore the optimal solutions faster.

One can also add empirical constraints to ensure that the generated samples are adequate. For example, inter-well distance and unique values can be used during well-placement optimization. Such constraints ensure that only a feasible reservoir scenario is generated using quality-controlled samples, unlike other optimizers.

Asides from using REIs and LHS in this method, a different idea is presented in CLEO-M2 (**Algorithm C-2**). In this method, instead of using the complete field's life-cycle period in the simulation, we propose using only a partial life for optimization, in which only a part of

field's timeline is run. However, as using the partial life can yield a suboptimal FDP, we also use an additional tool to perform predictive analytics. Predictive analytics denotes using intermediate results obtained at the end of the partial life to predict the best FDP for the complete life.

In this work, we used a regression model to perform predictive analytics and mimic the objective function of the optimization problem. The regression model can be built using the accrued information over the partial life and comparing it with the objective function of the optimization problem (considering the complete life). This regression model is used to address a multi-objective function (MOF), which needs to be maximized in CLEO-M2.

Algorithm C-2 - FDP optimization using CLEO-M2

Input: : Problem statement, simulation models
Output : Optimized decision variables
Define : Stop criteria
begin
1. Identify \mathbb{X} , partial life and technical results to be used
2. Using REI, define \mathbb{G}
3. Define the initial clusters of \mathbb{G} using k-means clustering
4. Select \mathbf{g}_{rep} for each cluster
5. Prepare regression model using already simulated models
6. Define multi-objective function using technical results and regression model
7. $\mathbf{iter} \leftarrow 0$
8. **while** Stop criteria is False **do**
9. Use LHS to generate scenarios with the PMF of clusters
10. Run the scenarios
11. Correlate the MOF with the scenarios
12. Update posterior PMF of the clusters using best \mathbf{b} scenarios
13. **if** Expansion is True **then**
14. Expand the clusters
15. Select \mathbf{g}_{rep} for each cluster
16. **else**
17. **Break**
18. **end if**
19. $\mathbf{iter} \leftarrow \mathbf{iter} + 1$
20. **end while**
end

For instance, a MOF for a simple black-oil model with only two fluids (oil and water) can be built using scalar and 3D grid values at the end of the partial life. Scalar values can entail cumulative production of commodities, while grid values can consist of the 3D saturation maps. The primary purpose of scalar and grid properties is to maximize the objective function until and beyond the history period, respectively.

In summary, CLEO-M2 replaces the complete life-cycle with partial life, and uses the MOF instead of the initially defined objective function of the problem. One must note that due to this trade-off, CLEO-M2 is not adequate to find globally optimal solution (at least in its currently presented form). However, it enjoys the employment of a simple regression model to drastically improve the efficiency of the optimization process without having any significant impact on the final solution.

C.5 Application and Results

We applied the proposed methods to three different examples. In Cases I and II, we applied the methods on a simple synthetic model. In Case III, we used a giant-scale benchmark case to establish the applicability and benefit of CLEO-M2 in real applications.

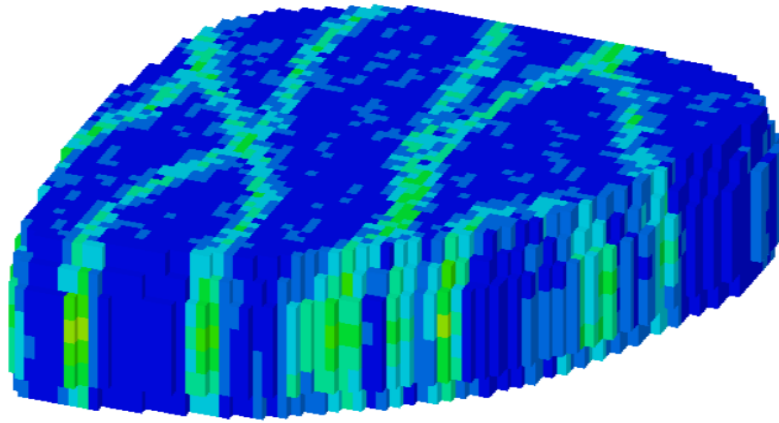


Figure C-2 - 3D synthetic Egg model for Case I.

Case I: Deterministic test with numerous decision variables

We first applied CLEO-M1 to a simple 3D reservoir model, i.e., the Egg model (Jansen et al., 2014). It is a channelized reservoir model with no aquifer and gas cap (see **Figure C-2**). It is composed of 25.2k grid blocks with a dimension of $8 \times 8 \times 4 \text{ m}^3$. Only 18.5k blocks are active. The initial reservoir pressure is 40 MPa. Four producers and eight water injectors are being used to produce this 4 km deep oil reservoir over 3,600 days.

We set the placement and controls of all the 12 wells as the decision variables. A total of 372 decision variables were obtained, composed of x and y positions of the 12 wells, and their BHPs every 120th day. The optimization problem is to maximize the net present value (NPV) using 372 decision variables by identifying an optimal FDP within a vast problem space (3,600 for well-positions and 21 for operational settings). The problem statement is defined as follows:

$$\max_{\mathbf{u}_{1:K}} \mathcal{J}(\mathbf{y}_{1:K}(\mathbf{u}_{1:K})) \quad \text{C-3}$$

$$\mathcal{J}(\mathbf{y}_{1:K}(\mathbf{u}_{1:K})) \stackrel{\text{def}}{=} \sum_{k=1}^K \mathcal{J}_k(\mathbf{y}_k) + \sum_{i=1}^{N_{inj}+N_{pr}} r_i \quad \text{C-4}$$

$$\mathcal{J}_k(\mathbf{y}_k) = \left[\frac{\sum_{m=1}^{N_{inj}} r_{w,inj} \cdot (N_{wi,m})_k + \sum_{n=1}^{N_{pr}} \left(r_{w,pr} \cdot |N_{wp,n}|_k \right) + \left(r_{o,pr} \cdot |N_{p,n}|_k \right)}{(1+d)^{t_k/\tau}} \right] \times \Delta t_k \quad \text{C-5}$$

where \mathcal{J} is the objective function (i.e., NPV) and depends on output vector (\mathbf{y}), which in turn is a function of the decision variables (\mathbf{u}). **Equations C-4** and **C-5** provide a detailed description to compute \mathcal{J} over the discrete time series ranging from 1 to K . We calculate the discounted objective function (\mathcal{J}_k) by multiplying cumulative injection (N_{wi}) and production (N_{wp} and N_p) of the commodities (oil and water) with their respective net cost ($r_{w,inj}$, $r_{w,pr}$ and $r_{o,pr}$) for each discrete time-step k , with a discount rate of d for the reference time τ . The cost of all injectors (N_{inj}) and producers (N_{pr}) is included by summing their construction costs (r) when they are drilled in the reservoir ($t=0$ in Case I and II).

We defined clusters and selected a representative value for each cluster. **Figure C-3** presents the initial centroids defined using the problem space for producers. As we do not use REIs in CLEO-M1, same clusters and centroids are used for injectors.

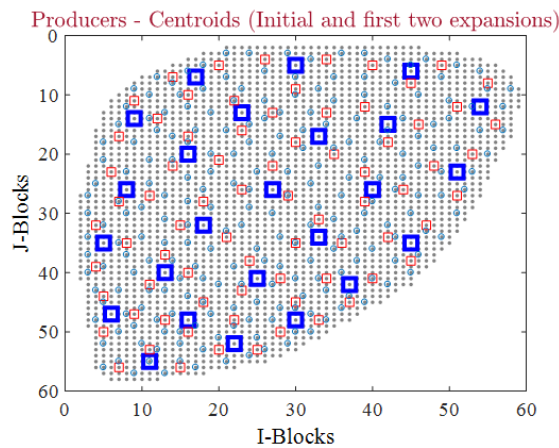


Figure C-3 - Initial, first and second phase centroids for selecting producers (blue, red and teal squares, respectively).

Figure C-4 presents the initial centroids of the producers' BHPs (in MPa). The initial centroids of the injectors' BHPs are 1,000 kPa higher than the ones presented in this figure.

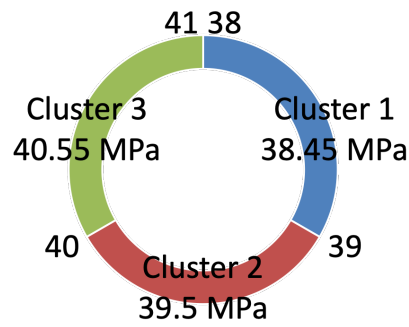


Figure C-4 - Initially, 21 operational settings for the producers were divided in 3 clusters (in MPa).

We used four well-established optimizers to work on this optimization problem. Besides CLEO-M1, we optimized using:

1. Particle swarm optimization, PSO (Kennedy and Eberhart, 1995) with:
 - a. Population Size = 50
 - b. Inertial weight = 0.7298
 - c. Cognition component (C1) = 1.49618
 - d. Social component (C2) = 1.49618
 - e. Treating discrete values equally probable
2. Differential evolution, DE (Storn and Price, 1997) with:
 - a. Population Size = 50
 - b. Crossover rate = 0.8
 - c. Scaling factor = 0.5
 - d. Treating discrete values equally probable
3. CMG's designed exploration & controlled evolution, DECE (Yang et al., 2007) with well-defined internal parameters set by CMG.
4. Iterative discrete Latin hypercube sampling method, IDLHC (Hohendorff Filho et al., 2016) with:
 - a. Population Size = 100
 - b. Cut-off = 20%
 - c. Treating discrete values equally probable

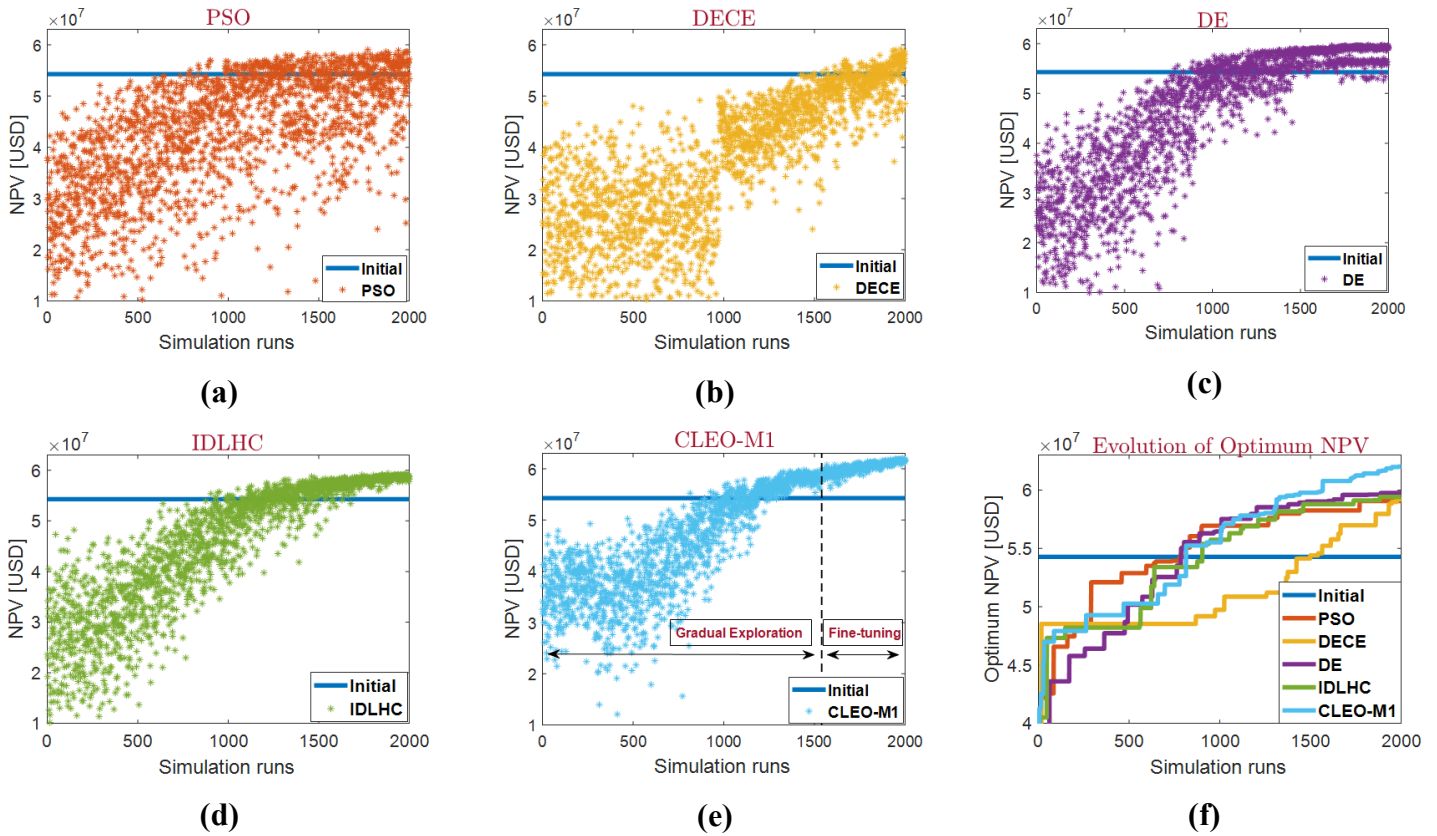


Figure C-5 - Evolution of NPV using (a) PSO, (b) DECE, (c) DE, (d) IDLHC and, (e) CLEO-M1 and finally, (f) comparing their evolution of the optimum NPV (stop criterion = 2000 simulations).

Figure C-5 presents the evolution of the objective function (NPV) for each test. CLEO-M1 starts the process with a gradual exploration and learning phase (**Figure C-5e**). However, it ends providing the best solution compared to other optimizers. Around the 800th run, DE and PSO start to catch up with it to provide better FDPs. Despite this, CLEO continues to constantly evolve FDPs to supersede all results by the end of the 1300th run. The fine-tuning step boosts this NPV growth (**Figure C-5f**).

Figure C-6 shows the total oil per unit area maps at the time of breakthrough (t_{BT}), at $t = 2520$ days (70% of the field's life), and $t = 3600$ days (final time) for the initial FDP and optimized FDPs obtained using all optimizers. All optimized FDPs try to maximize sweep before the breakthrough by optimizing the wells and their BHPs. One can observe that even though waterflooding is critical in the model, early breakthroughs can thwart oil recovery. This fact can also be inferred from **Figures C-7** and **C-8**. We show that all the optimized FDPs improve the recovery factor by controlling the injection rates, lowering the average reservoir pressure, and thus, delaying breakthrough and/or minimizing water production.

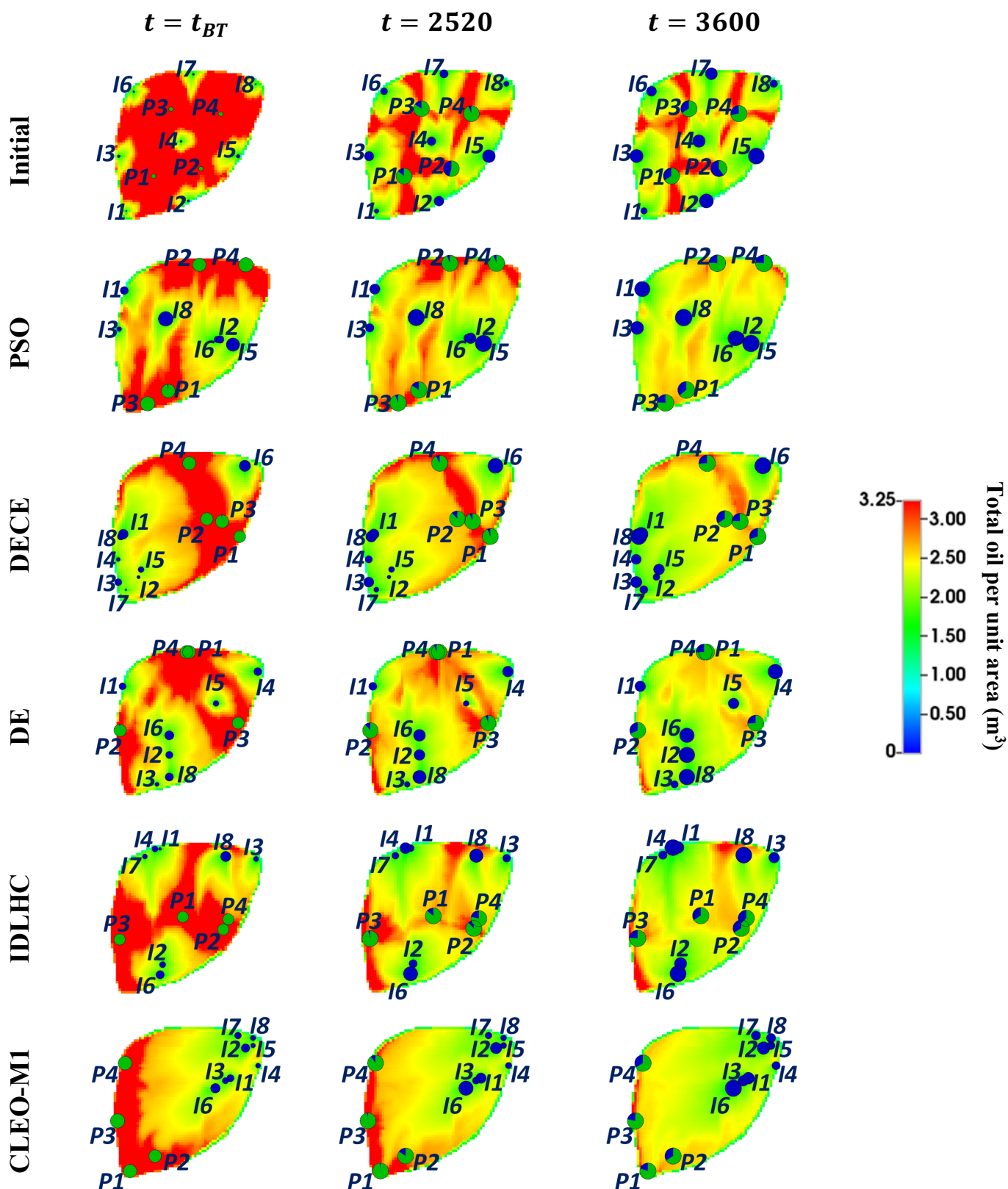


Figure C-6 - Observed total oil per unit area (m³) using the initial and optimized FDPs. The bubbles represent the cumulative oil (green) and water (blue) produced from each well, and their varying sizes is proportional to the total amount of production.

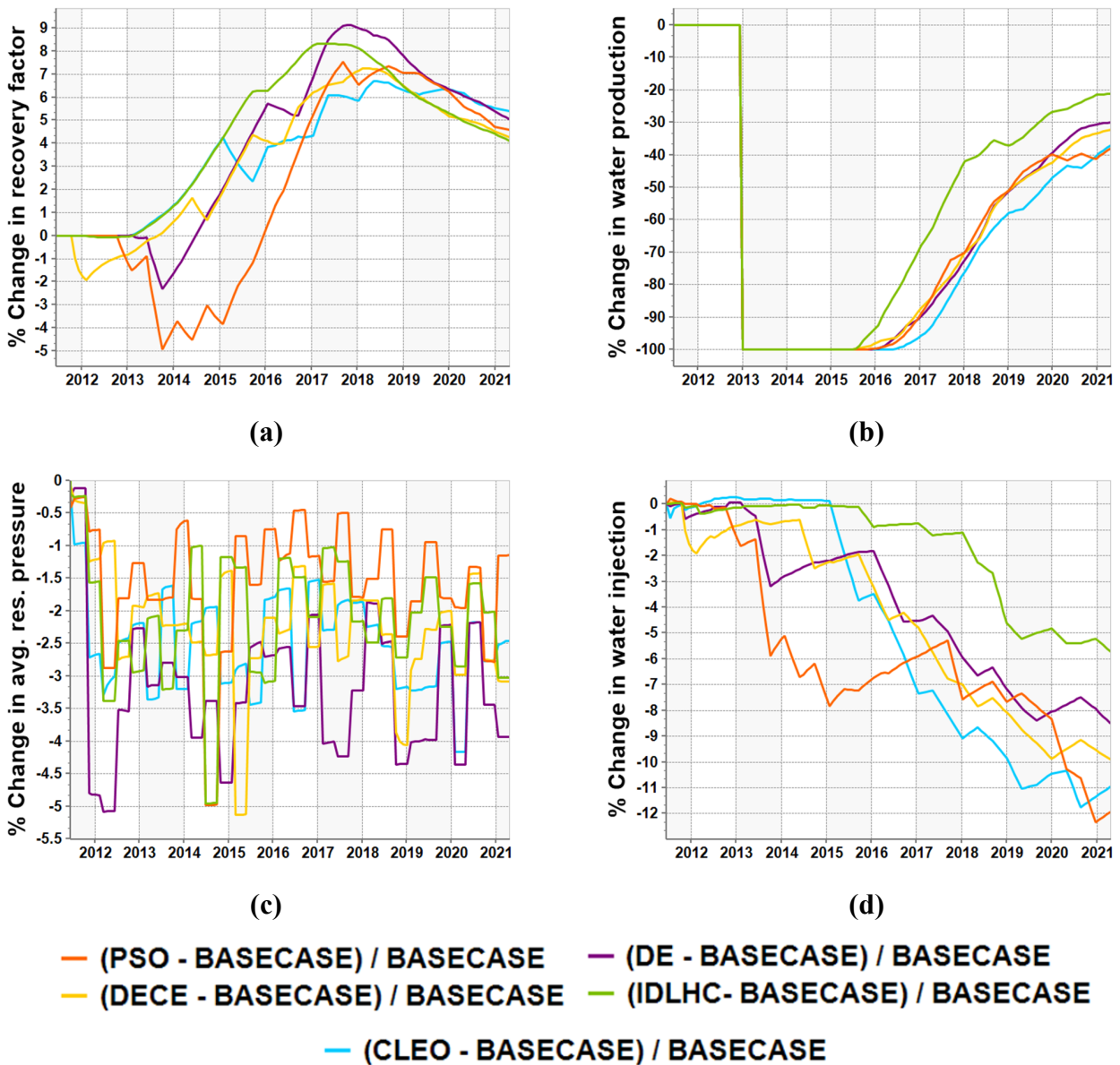


Figure C-7 - % change in (a) recovery factor, (b) cumulative water production, (c) average reservoir pressure and, (d) cumulative water injection compared to the initial FDP.

Figure C-8 shows a few wells and their initial and CLEO-optimized operational settings and dependent outputs. Unlike the initial FDP, all wells have their BHPs adjusted to improve their productivity. Even though the CLEO-optimized Producer 4 is the worst amongst others, it still delays the breakthrough by at least a year. On the other hand, the remaining CLEO-optimized producers extend the production plateau and delay the breakthrough by a much larger margin. The optimized injectors operate with multiple stops for a much-controlled sweep.

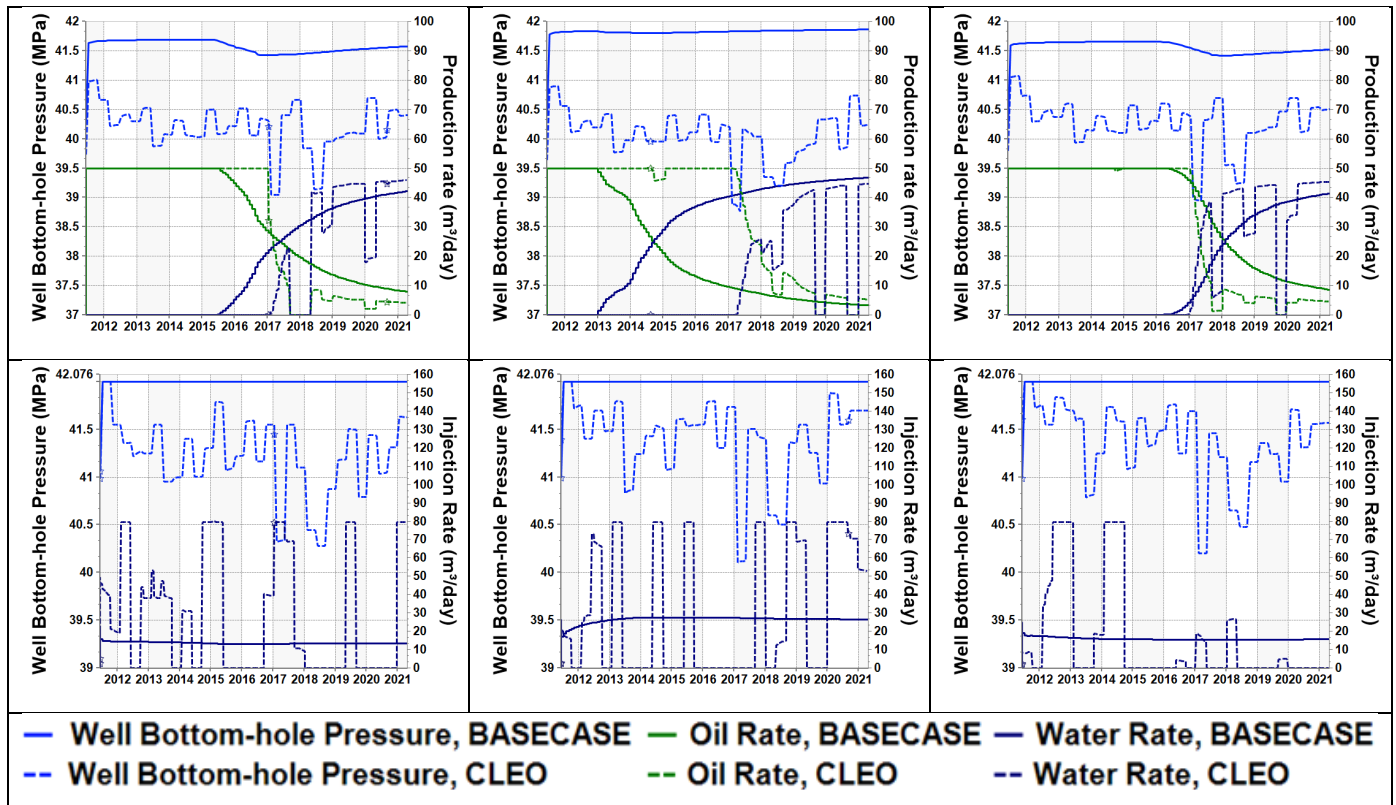


Figure C-8 - Initial and optimal control settings for Producers 1, 2 and 4 (top, left to right) and Injectors 1, 4, 8 (bottom, left to right) as obtained using CLEO-M1.

Table C-1 summarizes the results obtained in Case I using all the optimizers. CLEO-M1 provides the best FDP compared to other well-established optimizers in Case I.

Table C-1 - Summary of Results (Case I) when optimized using stop criterion = 2000 simulations.

Parameters	Optimizers				
	PSO	DECE	DE	IDLHC	CLEO-M1
Final NPV (MM USD)	59.1	59.2	59.8	59.4	62.0
% NPV improvement	8.8%	9.1%	10.1%	9.5%	14.2%
Oil recovery factor (%)	53.5	53.3	53.7	53.2	54.6
Cum. water prod. (MMm ³)	0.171	0.187	0.194	0.218	0.187
Cum. water inj. (MMm ³)	0.629	0.643	0.653	0.673	0.654

The process was also repeated until 4000 iterations for the other optimizers to observe their best outcomes (see Table C-2).

Table C-2 – Testing the repetitiveness of all algorithms in Case I.

Parameters	Optimizers				
	PSO	DECE	DE	IDLHC	CLEO-M1
Minimum NPV (MM USD)	59.2	58.6	60.4	60.0	62.0
Maximum NPV (MM USD)	60.4	59.5	60.9	61.7	62.1
Mean NPV (MM USD)	59.9	58.9	60.6	60.8	62.0
Approximate simulations run until convergence	4000	4000	4000	4000	2000

Case II: Stochastic test with limited decision variables

Having established that a CLEO-based optimizer works well as any established optimizer in the deterministic study, we take a step further to investigate the performance of CLEO-M1 in a stochastic environment (see **Figure C-9**). We also optimized the problem using DE and IDLHC in Case II to benchmark the performance of CLEO-M1 again, while using limited decision variables. We used DE and IDLHC as these algorithms provided the second and third best results in Case I (with extensive decision variables and problem space). However, the main goal of this probabilistic study is to use CLEO-M2 and validate its performance against the two optimizers mentioned above.

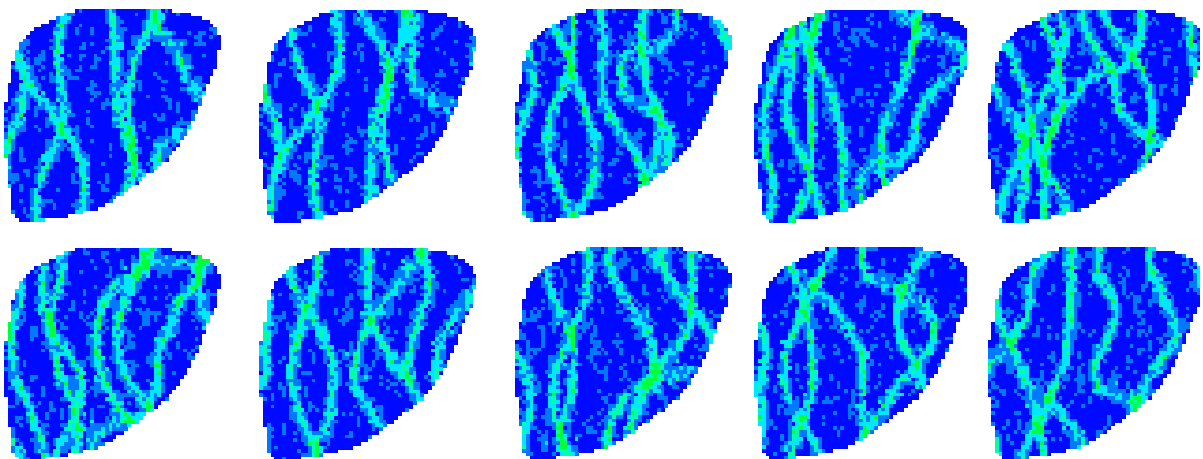


Figure C-9 - Ten egg models with completely different channels (bird's-eye view) to highlight the challenge of optimizing a channelized reservoir. A probabilistic optimization becomes a necessity to mitigate a biased solution obtained using a deterministic model.

The optimization problem in Case II can be described as following:

$$\max_{\mathbf{u}_{1:K}} \sum_{j=1}^{RMs} \mathcal{J}(\mathbf{y}_{1:K}(\mathbf{u}_{1:K})) \times P(j) \quad \text{C-6}$$

where $P(j)$ denotes the probability of occurrence of the j^{th} Egg model to compute the expected mean of the objective function (\mathcal{J}) as described by Equations C-4 and C-5. In other words, our aim is to maximize the expected monetary value (EMV) of the ten Egg models in Case II. However, as we use predictive analytics in CLEO-M2, we used multiple linear regression (MLR) to obtain MOF for the problem statement in Case II:

$$\max_{\mathbf{u}_{1:K_{PL}}} \sum_{j=1}^{RMs} \mathcal{J}_{MOF}(\mathbf{y}_{1:K_{PL}}(\mathbf{u}_{1:K_{PL}})) \times P(j) \quad \text{C-7}$$

$$\mathcal{J}_{MOF}(\mathbf{y}_{1:K_{PL}}(\mathbf{u}_{1:K_{PL}})) \stackrel{\text{def}}{=} \sum_{k=1}^{K_{PL}} \frac{\boldsymbol{\beta}^T * \mathbf{TR}}{(1 + d)^{\Delta t_k / \tau}} \quad \text{C-8}$$

where \mathcal{J}_{MOF} is the discounted MOF of each RM calculated at discrete time steps ($1 \dots K_{PL}$). \mathbf{TR} is a vector of normalized technical results obtained by executing simulation over partial life and $\boldsymbol{\beta}^T$ is the transposed slope coefficients for each technical result. Existing simulations of the ten models with the initial FDP were used to estimate a logical set of weights (Table C-3) using MLR (Loomba et al. 2022).

Table C-3 - Technical Results and their slope coefficients (Case II).

Scalar Parameters	Slope coefficients	Grid Parameters	Slope coefficients
Cumulative oil produced	1	Net flux oil - directional	0.7
Water oil ratio	-0.035	Net water in vicinity	-0.6

We selected weights of scalar parameters based on the proportion of commodities cost at the end of partial life. Once these weights were set, the weights for the grid-based parameters were estimated. We used Pearson's correlation coefficient to identify the best weights for the grid-based parameters (Figure C-10).

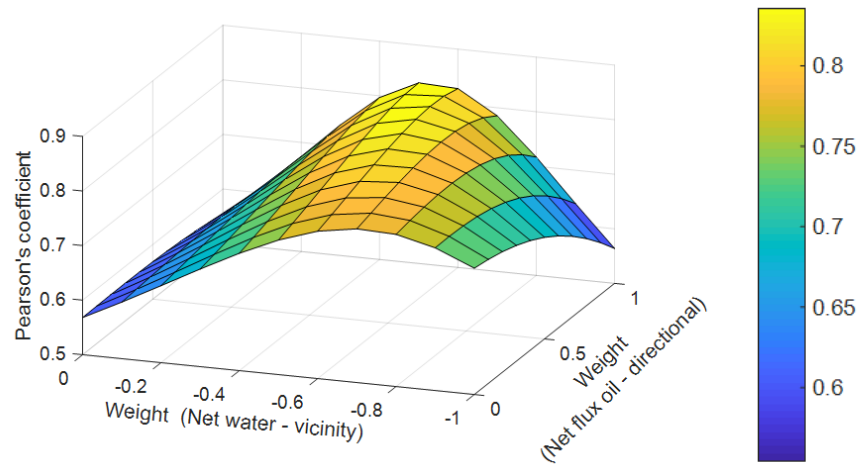


Figure C-10 - A 3D plot to estimate the weights of the grid parameters.

To work with CLEO-M2, we started by reducing the unwanted solution candidates using REIs:

- Placing an injector where one or more blocks along depth have extremely high horizontal permeabilities can lead to an inefficient sweep. We observed that the maximum horizontal permeability in the seven vertical blocks for each solution candidate ranged from 200 to 9900 mD. Based on this fact, we discarded 25% of the blocks with extreme values (**Figure C-11a**).
- We noted the mean horizontal permeability of the seven layers for the remaining solution candidates (160-2400 mD). To mitigate early water breakthrough, we eliminated the grid blocks with higher mean horizontal permeabilities (**Figure C-11b**).

As this synthetic channelized model has a flat top and equally saturated blocks across the whole field, we did not exclude any solution candidates from the problem space of producers. The BHPs of the producers and injectors were maintained lower than the fracture pressure. In a more realistic case, it would be pertinent to set a lower bound for BHPs based on the bubble point pressure of the reservoir.

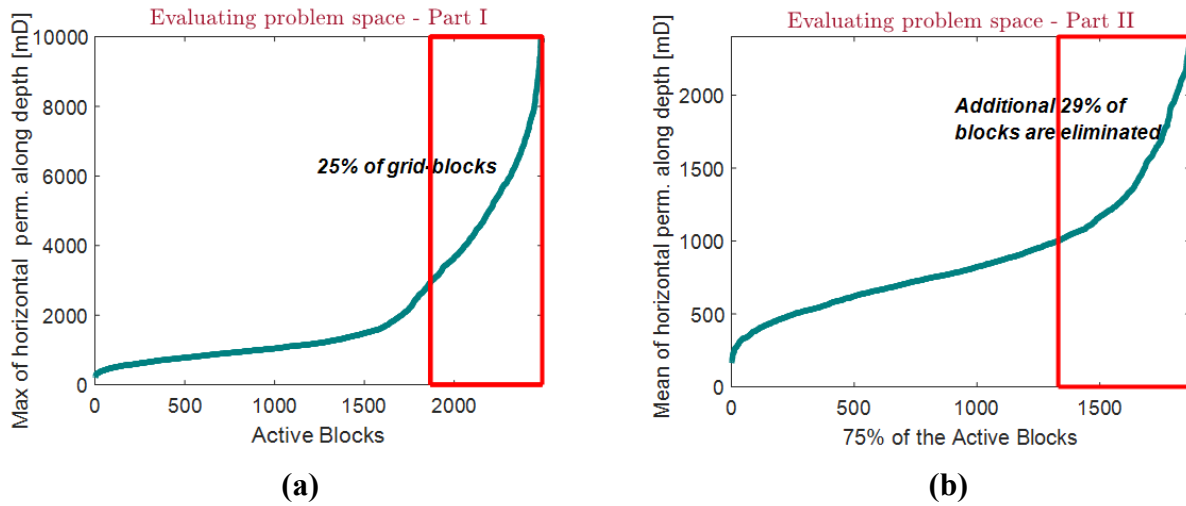


Figure C-11 - (a) 25% of the active blocks were deleted by assessing the maximum of horizontal permeabilities along the depth of each candidate space. (b) An additional 29% of the remaining blocks were considered inadequate as they had a higher mean permeability along depth compared to the other blocks.

In CLEO-M2, we set the partial life equal to 40% of the complete life (simulated 1440 days out of 3600 days). This makes the process highly efficient (as proven in Case III), while encompassing all major events as well as contributing a major chunk (>50%) to the field's objective function. Four technical outputs (**Table C-3**) obtained over three discrete time-steps ($t = 720, 1080$ and 1440) were used to evaluate the MOF presented in **Equation C-7**. While the scalar parameters are self-explanatory, we obtained net flux oil directional by multiplying net flux oil in the vicinity of the producers with their Gini coefficient (Loomba et al. 2022). Net water in the vicinity was estimated by subtracting connate water volume from gross water volume in the neighborhood of the producers.

Using **Algorithms C-1** and **C-2**, we proceeded further to optimize the decision variables in Case II using CLEO-M1 and CLEO-M2, respectively. Also, we used DE and IDLHC to benchmark their performance in this stochastic environment. **Figure C-12** presents the evolution of the objective function (EMV) for each test. Theoretically, one would not obtain the EMV evolution for CLEO-M2 as only partial simulations are run. However, to understand the process, we simulated all the simulations over their complete life to get the graph presented in **Figure C-12c**.

CLEO-M1 performs as well as the established DE optimizer (**Figure C-12e**) again. For a method that runs all models for only 40% of the complete life, CLEO-M2 also performs well in identifying reasonable solutions by the end of the simulation runs. The fine-tuning process

is relatively poor in CLEO-M2 compared to CLEO-M1. This shortfall can be amended by reforming the MLR model, and discussed in more details in the subsequent section.

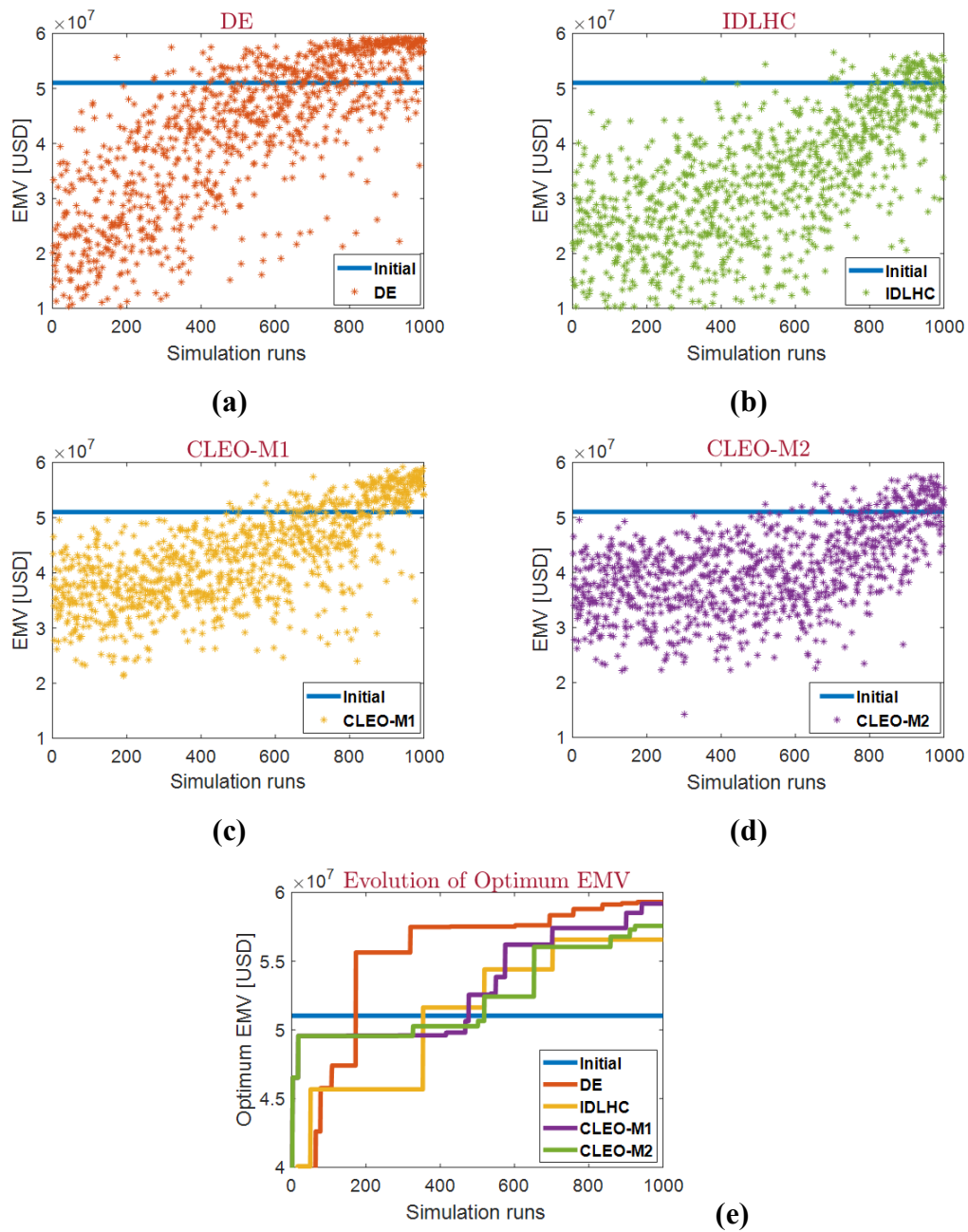


Figure C-12 - Evolution of EMV using (a) DE, (b) IDHC, (c) CLEO-M1 and, (d) CLEO-M2 and finally, (e) comparing their evolution of the optimum EMV (stop criterion = 1000 simulations).

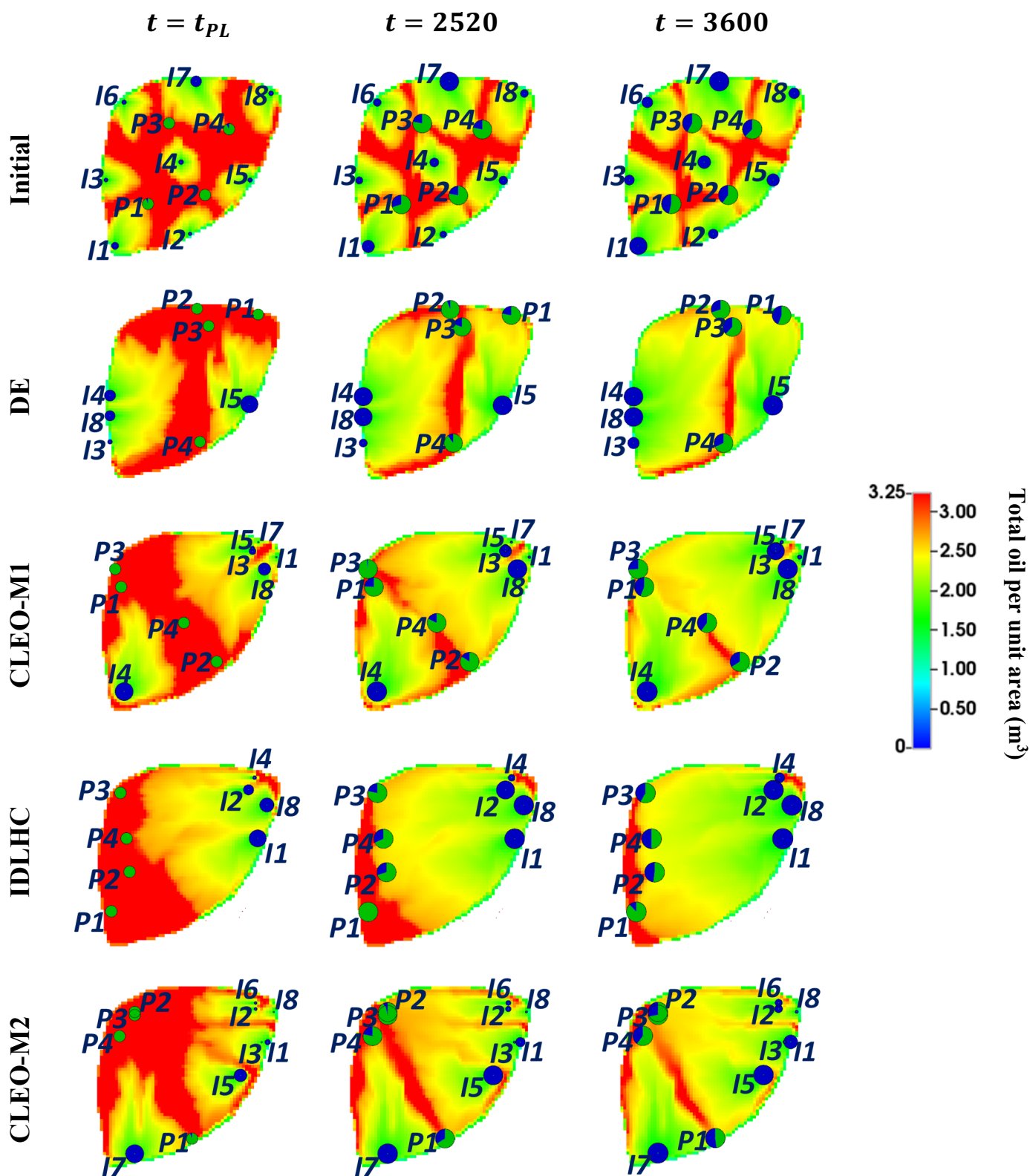


Figure C-13 - Observed total oil per unit area (m^3) in the 5th petrophysical realization using the initial and optimized well-placements. Well bubbles represent the cumulative oil (green) and water (blue).

Figure C-13 shows the oil per unit area (total) maps at different times; t_{PL} (or 1440 days), $t = 2520$ days (70% of the field's life), and $t = 3600$ days (final time). Similar to Case I, we observe that waterflooding is quite critical in the Egg model. This validates the requirement of a higher negative slope coefficient for the net water in the vicinity (**Table C-3**). On the other hand, a higher slope coefficient for the net flux oil – directional is difficult to justify using these graphs as early breakthroughs completely impede the recovery process. However, one can note that changes in oil saturation are minimal over the last 30% of the field's contractual life.

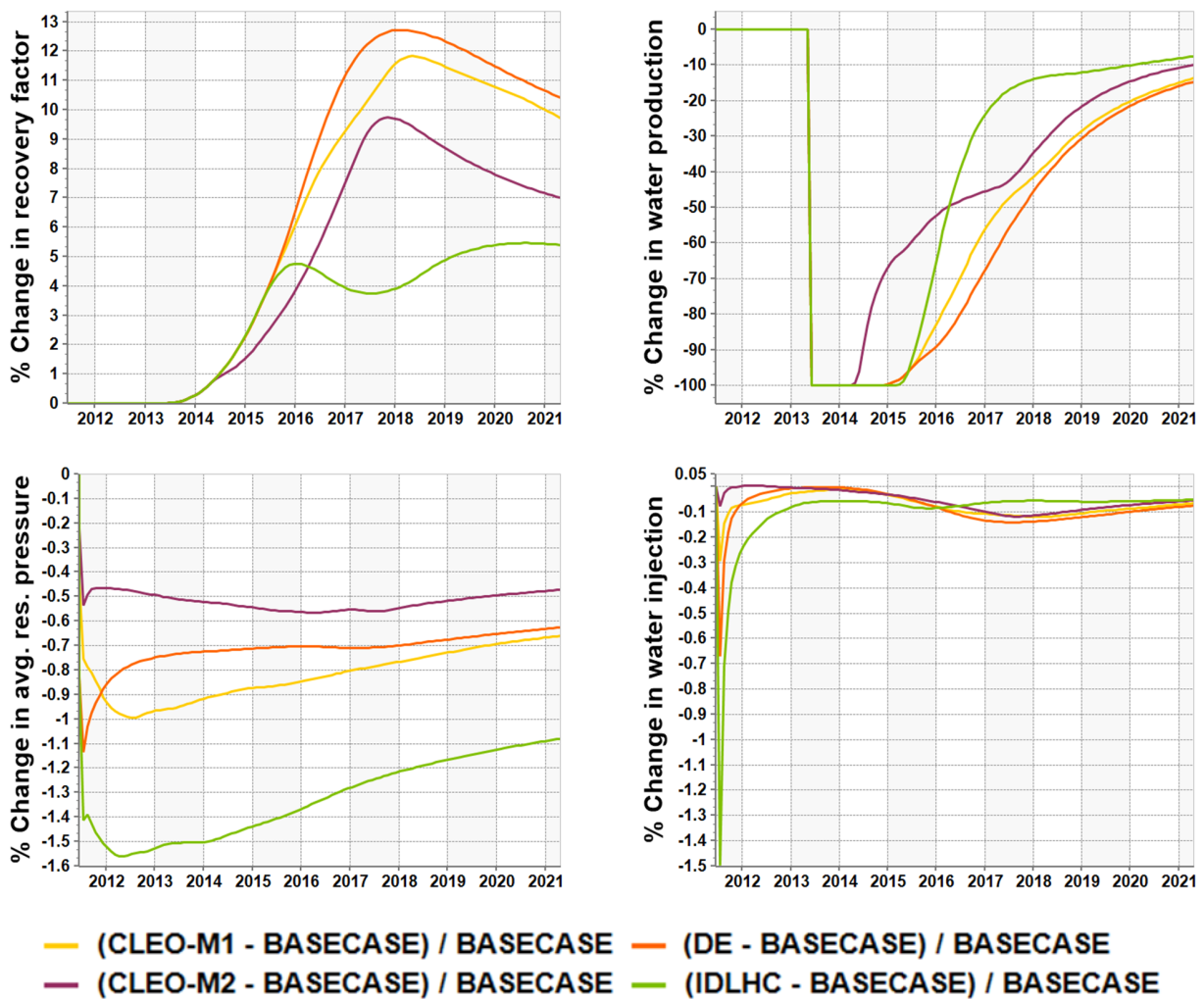


Figure C-14 - (From top left in clockwise direction) % change in recovery factor, cumulative water production, cumulative water injection and average reservoir pressure compared to the initial FDP (as observed in the 5th petrophysical realization).

In **Figure C-14**, we present the impact of optimized FDPs on the field recovery process. We observe a dominant impact of well placement in Case II to minimize the water

breakthrough and subsequent production, unlike Case I, where well-controls played a prominent role.

Table C-4 - Summary of Results (Case II) when optimized using stop criterion = 1000 simulations.

Parameters	Optimizers			
	DE	IDLHC	CLEO-M1	CLEO-M2
Final NPV (MM USD)	59.3	56.6	59.2	57.6
% NPV improvement	16%	11%	16%	13%
% Field life simulated	100%	100%	100%	40%
Oil recovery factor (%)	53.6	52.6	53.3	52.0
Cum. water prod. (MMm ³)	0.255	0.264	0.258	0.269
Cum. water inj. (MMm ³)	0.714	0.714	0.714	0.714

Table C-4 summarizes the results obtained in Case II using all the optimizers. We observed the optimizers improving the objective function between 8.8 to 14.2% (**Table C-1**) in Case I. The minimum NPV improvement was just 62% of the best result. In Case II, we observe CLEO-M1 and DE performing equally well. CLEO-M2, on the other hand, improves the objective function by 13%. This improvement is equivalent to just 80% of the best result observed in Case II. However, we derived this result just using 40% of the field's life to make the optimization process efficient (**Figure C-15**).

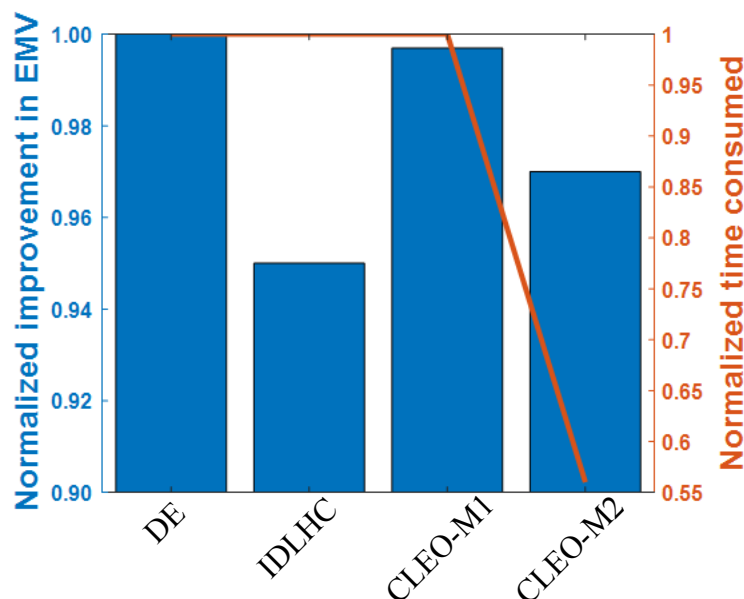


Figure C-15 - Normalized improvement in EMV versus total normalized time consumed (stop criterion = 1000 simulations).

The process was also repeated for the optimizers to observe their best outcomes until convergence (see **Table C-5**).

Table C-5 – Testing the repetitiveness of all algorithms in Case II.

Parameters	Optimizers			
	DE	IDLHC	CLEO-M1	CLEO-M2
Minimum NPV (MM USD)	58.2	57.7	59.7	57.6
Maximum NPV (MM USD)	60.6	59.0	60.6	58.2
Mean NPV (MM USD)	59.8	58.2	60.2	57.8
Approximate simulations run until convergence	1400	1865	1370	1000

Case III: Application on a giant-field benchmark case

In previous cases, we demonstrated the working of both approaches. Yet, it is challenging to validate the true benefit of CLEO-M2 using a simple synthetic model. Thus, we optimize a time-consuming and giant-scale model in Case III using CLEO-M2. We used a set of simulation models representing a giant field under the name of UNISIM-III-2022. Like a typical Brazilian pre-salt reservoir, these models are highly heterogeneous with karsts (Correia et al., 2020). Composed of a total of 2.3MM blocks, each simulation takes more than 8 hours. Consequently, it is impractical to run thousands of simulations using conventional optimization algorithms.

A topographic map of the field with already-drilled wells is shown in **Figure C-16**. With 33 injectors and 32 producers planned to be drilled across the four sectors of the field, each well needs to be drilled at least three blocks apart. Of these 65 wells, 14 wells have already been drilled, leaving 51 wells to be optimized.

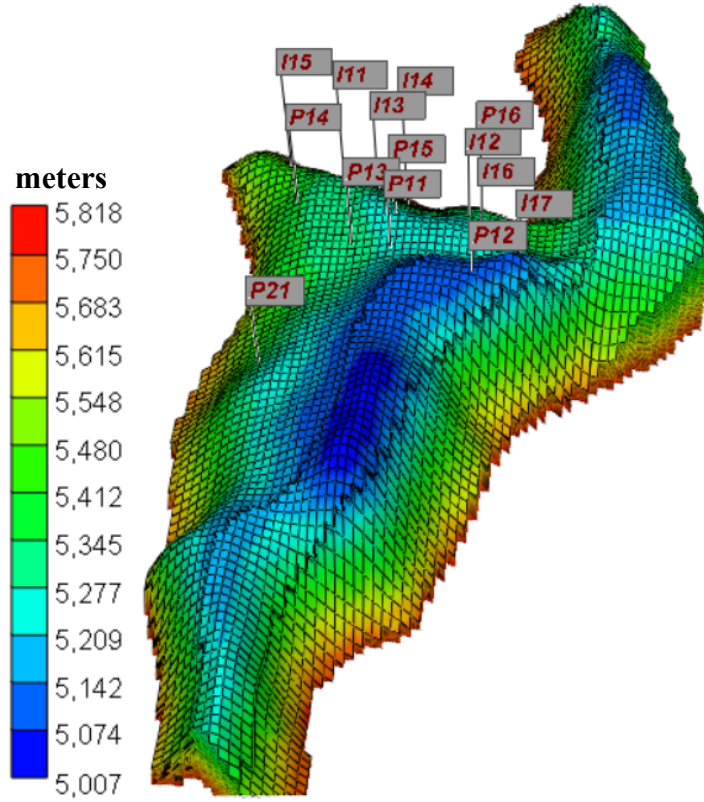


Figure C-16 - A 3D grid-top map of the UNISIM-III-2022 highlighting the field topography (in meters) and the 14 wells already drilled.

A total of 102 decision variables were obtained, composed of discrete x and y locations of to-be-drilled wells. **Equation C-6** describes the optimization problem. To include the challenges of a real field, we use a more comprehensive description of the discounted objective function (Loomba et al., 2021):

$$J(\mathbf{y}_{1:K}(\mathbf{u}_{1:K})) = \sum_{k=1}^K \left\{ \left[\frac{[(R - RT - ST - OPEX) \times (1 - T)] - CAPEX - AC}{(1 + d)^{t_k/\tau}} \right] \times \Delta t_k \right\} \quad \text{C-9}$$

In **Equation C-9**, gross revenue, corporate tax rate, royalties and social taxes are denoted by R , T , RT and ST , respectively. $CAPEX$ and $OPEX$ stand for capital and operational expenditures, respectively. Abandonment costs are denoted by AC .

Alike Case II, we define search space using REIs. We defined the search space for producers by measuring the amount of movable oil in the neighbourhood. To simplify its estimation, we discretized the three-phase relative permeability diagram (**Figure C-17b**). One can use the oil's movability around each grid block using this discretized value and 3D saturation map to calculate movable oil at a given time-step k . Next, we sequentially eliminated

the grid blocks with the lowest movable oil within the 9 km² (± 7 blocks), 4.8 km² (± 5 blocks), and 1 km² (± 2 blocks) to ensure that the selected grid-blocks are a subset of a productive zone. Keeping the efficiency of injectors in mind, we defined their search space the same way as in previous examples. Once the search space was defined for both injectors and producers, we defined clusters and selected a representative value for each cluster.

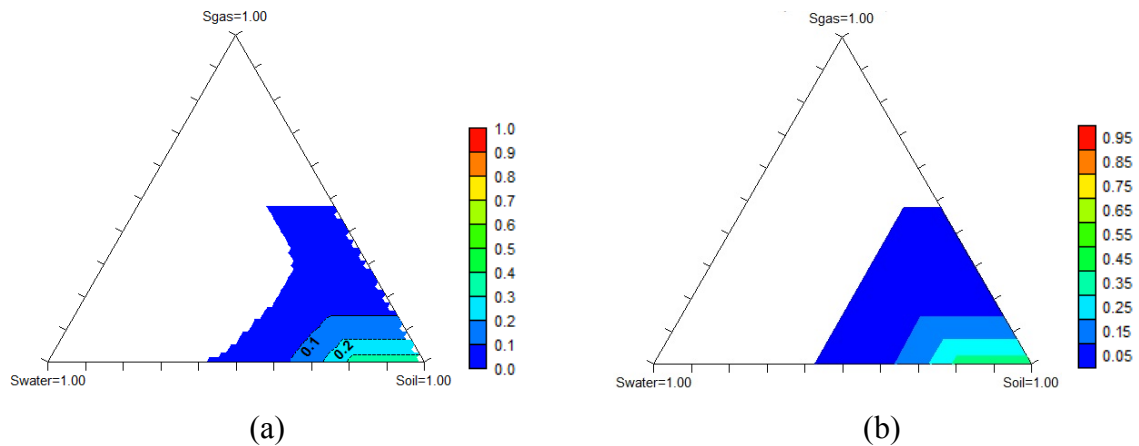


Figure C-17 - An example of the (a) original and (b) discretized three-phase relative permeability diagram (Chapter 4).

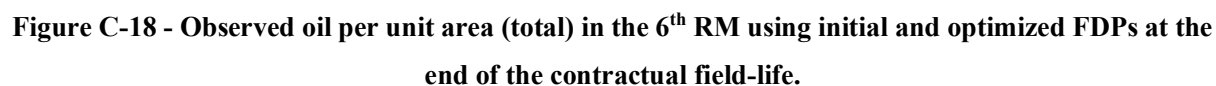
Production data of 1,219 days was used to get history-matched models. To use CLEO-M2, we set the partial life equal to 39% of the remaining complete life (i.e., additional 3,834 days were simulated out of the remaining 9,800 days). This was done for two reasons:

- (a) Ensure average simulation time of the partially-simulated models is less than 2.2 hours. Consequently, this helped us complete the optimization process in ~ 40 days using an ensemble of ten RMs. From an alternative perspective, we saved ~ 120 days by not using the complete life.
- (b) Emphasize that $\sim 40\%$ of the complete life provides acceptable results for optimizing the FDP with a simple MLR model.

Six technical results (**Table C-6**), obtained over three discrete time-steps (every 2nd year prior the end of partial life), were used to evaluate the MOF presented in **Equation C-7**.

Table C-6 - Technical Results and their slope coefficients (Case III).

Scalar Parameters	Slope coefficients	Grid Parameters	Slope coefficients
Cumulative oil produced	1	Net flux oil - directional	0.1
Gas oil ratio	-0.05	Net Gas in vicinity	-0.15
Water oil ratio	-0.02	Net Water in vicinity	-0.05



This field has an anticline structure and light oil with high gas content, requiring the minimization of gas-oil ratio (GOR) to maximize oil production. Despite this, some injectors are placed in relatively higher topographical regions to support the neighboring producers. We

observe this behavior as faults play a pivotal role in the field's production. By compartmentalizing the whole field, they influence the flow across the heterogeneous field (Figure C-18). Yet, we observe that the optimized FDP lowers water production rate and GOR (Figure C-20).

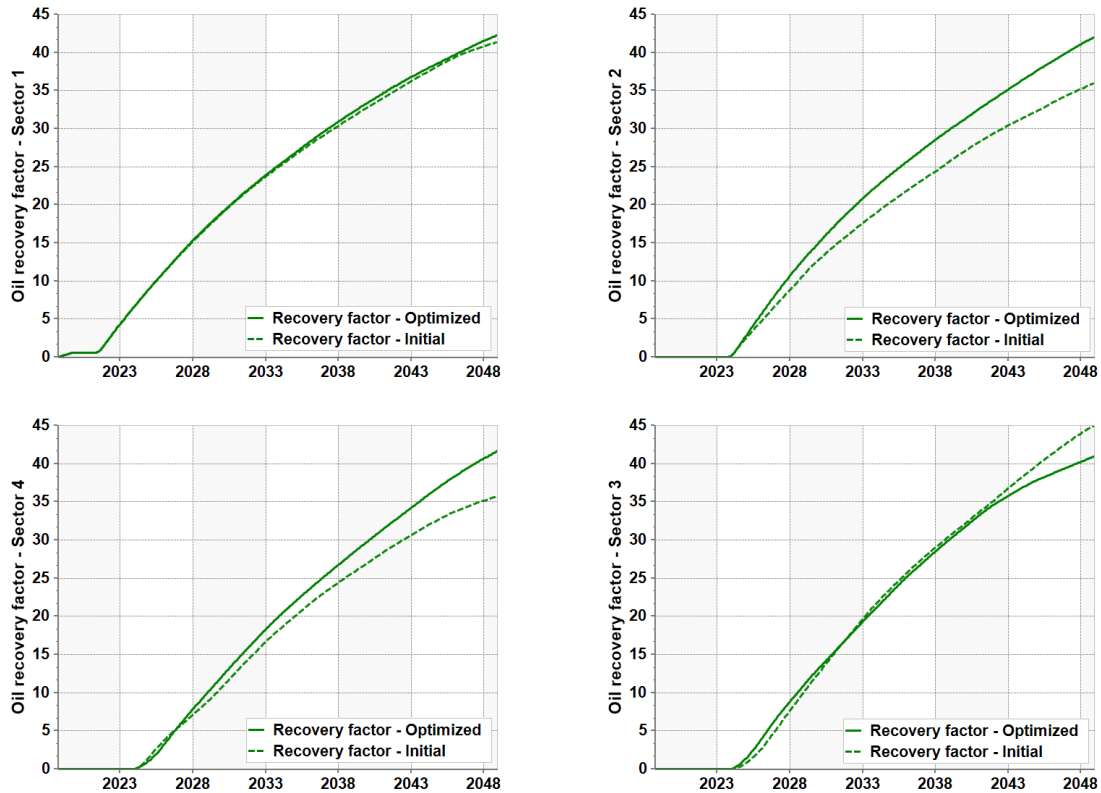


Figure C-19 - Improved oil recovery as seen in the 6th RM for Sector 1-4 (clockwise direction from top left).

Production rates are a function of average reservoir pressure. Most of the time, water is injected to maintain the reservoir pressure and avoid unnecessary gas production. During the initial years of production, we observe the average reservoir pressure being maintained at a slightly lower value than the one obtained using the initial FDP. Yet, it is higher than the bubble point pressure. This, in turn, helps boost the oil production rates as well as cumulative oil production over the initial period. We also observe an improved oil recovery factor in all the sectors except Sector 3. This observation unveils that optimizing the whole field sector-by-sector can be, in some instances, a deterrent for optimizing the whole field.

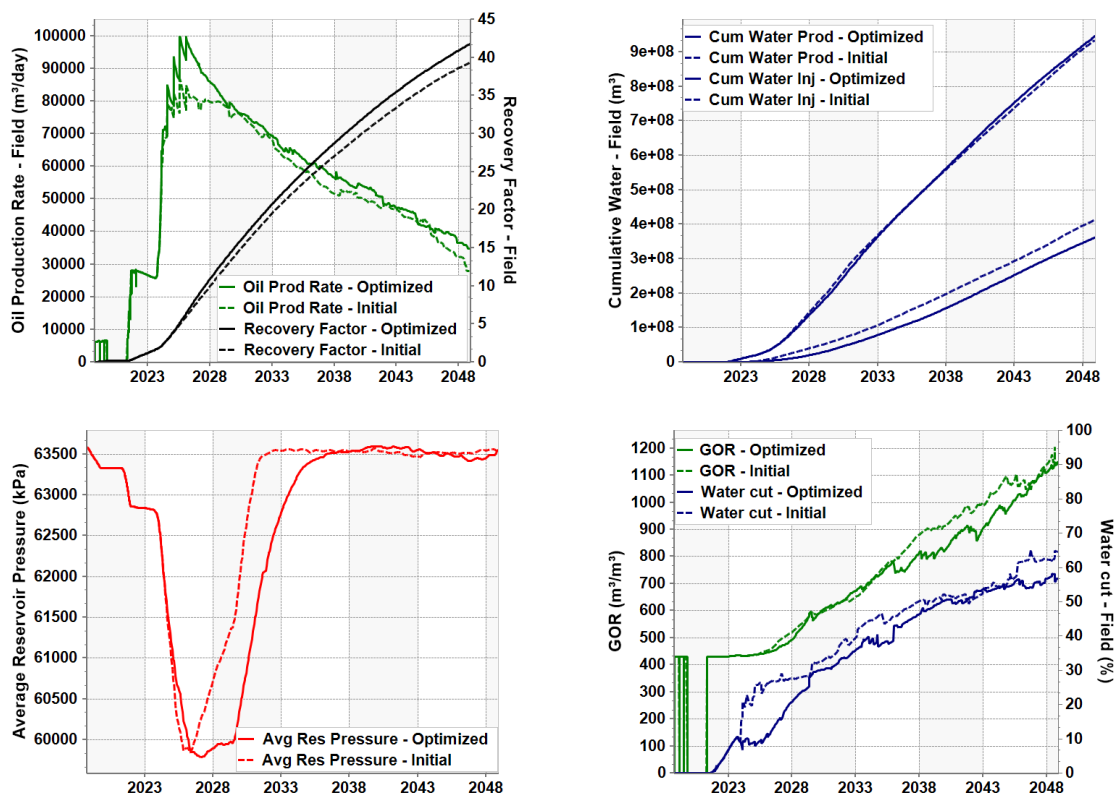


Figure C-20 - Comparing field parameters obtained using the initial and optimized FDP in the 6th RM.

To summarize, 900 scenarios were tested to obtain the best FDP using ten RMs. Not only we saved 120 days using this novel approach, we also improved the EMV of the ensemble of the RMs by 9%, as shown in **Figure C-21**. All the RMs were improved by 3 to 16%, with nominal values improved by 0.5 to 1.9 Billion USD.

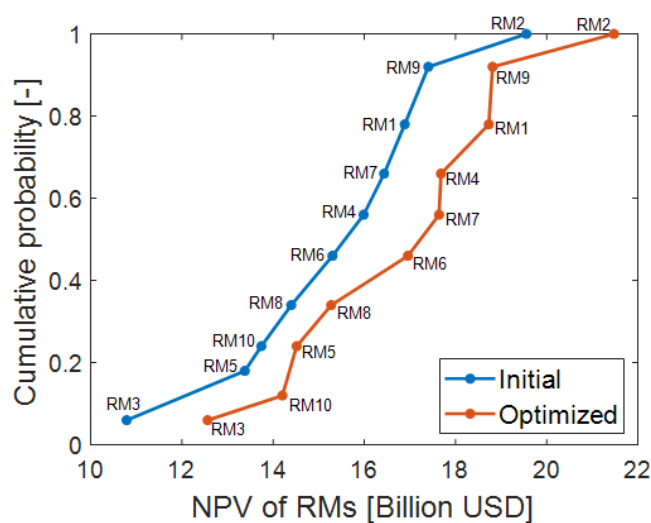


Figure C-21 - Cumulative distribution function with initial and optimized FDP.

C.6 Discussion and Recommendations

In this section, we discuss its strengths and flaws to render a complete view of the subject. We also compare our work with machine learning (ML) based methods and provide recommendations to improve the work for practical applications.

Cluster definition is one of the first steps in our algorithm. One can use any of the myriad of clustering algorithms to group the solution candidates based on their similarities. A subtle but vital benefit of using clusters is that it can reduce the dimensionality of the problem. For example, one can halve the dimensions by assigning X-Y coordinates of a well to a single value. At any point, the minimum number of clusters must be greater than the total number of corresponding and dependent decision variables. For instance, it would be reasonable to have at least n clusters for optimizing the schedule of n wells (drilled one at each unique time).

Even though we can slightly reduce dimensions as discussed, we still need better techniques to deal with huge problem space and decision variables. This is one of the reasons why a CLEO-based approach strongly depends on a sampling method. In this context, Dige and Diwekar (2018) analyzed the best sampling techniques for large-scale stochastic problems. They concluded that LHS-SOBOL is a better technique compared to LHS when dealing with variables > 100 . In our work, we presented LHS as an integral component of both approaches for a fair comparison with DECE and IDLHC. Despite using LHS (**Figure C-22**), we obtained results as good as any well-established optimizer. Thus, one can only infer that using superior methods like LHS-SOBOL can help converge faster and make CLEO-based algorithms even more efficient.

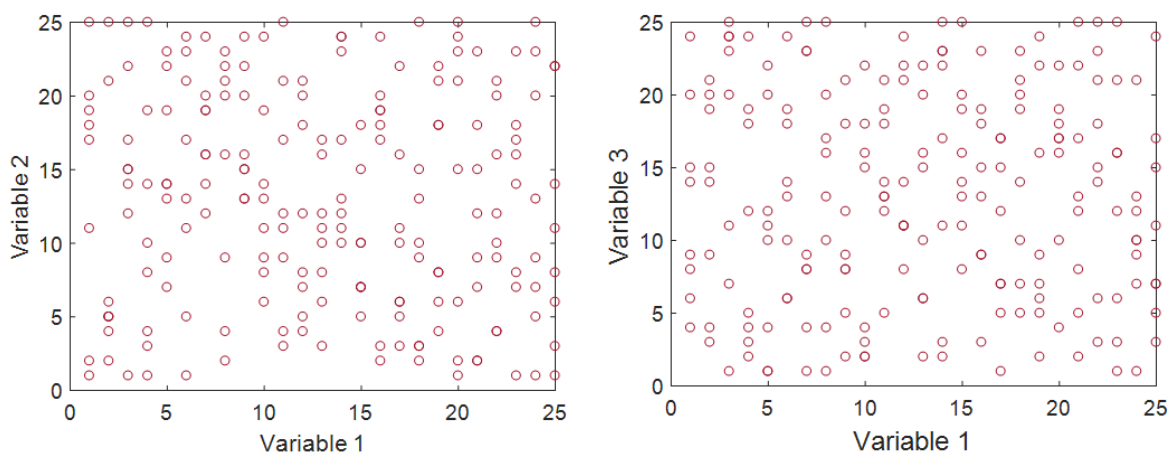


Figure C-22 - 200 samples generated using LHS. Both figures reveal that multi-dimensional samples lose uniformity same as presented by Dige and Diwekar (2018).

On the other hand, simulation models are imperfect (Oliver and Alfonzo, 2018; Rammay et al., 2019; Neto et al., 2020; Loomba et al., 2021). As a corollary, a globally optimal solution obtained from simulation models is only a locally optimal solution in the real field. This fresh outlook should prompt engineers to adopt agile methods that deliver results more efficiently than the existing optimization algorithms. We introduced CLEO-M2 under the same premise.

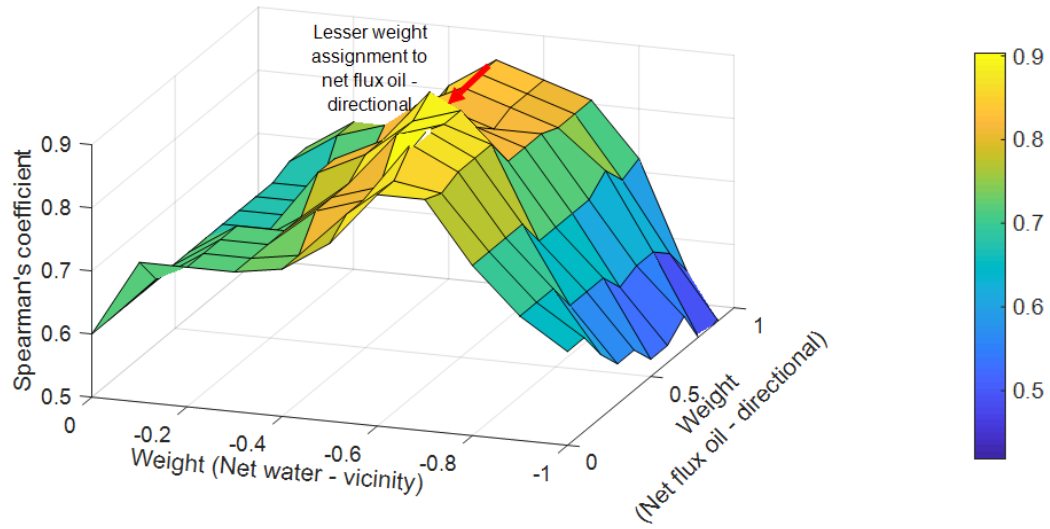


Figure C-23 - A 3D plot to estimate the weights of the grid parameters using the Spearman's rank correlation coefficient.

In CLEO-M2, we used a simple proxy function to replicate the objective function. Such proxy functions lack exactness due to limited data. Even though including more RMs with different FDPs can help improve it, this improvement comes at the cost of more time. We presented simple and perceptive parameters in our work to prepare this proxy. Their weights were ascribed based on the Pearson correlation coefficient (**Figure C-10**). On the other hand, Spearman rank correlation **Figure C-23** serves to provide a rank-based relationship rather than a linear one. For this reason, it can provide a more intuitive set of weights. In short, using a rank correlation method to quantify ordinal association can improve CLEO-M2 further.

CLEO-M2 is not problem-specific. However, as we do not run simulations until the end of the field's life, we must determine a suitable partial time to reap benefits from the predictive analytics. If any key flow behavior occurs beyond the selected partial time, it would hinder the optimization process. At the same time, if the objective function of the project is NPV, latter flow behaviors would only play a trivial role.

Furthermore, running 5-10 best FDPs from the final and, if possible, penultimate iterations can help select a superlative FDP. However, an alternate and better recommendation would be to run RMs with 3-5 FDPs during each iteration. This process can significantly improve the accuracy and reliability of the MLR model to select better FDPs and improve the quality of scenarios being tested in the subsequent iterations.

It is vital to assess the repeatability of the CLEO-based approaches to understand their practical applicability. Increasing the number of samples per iteration or using a more robust sampling technique can ensure repetitiveness. Despite this, we generated samples three times in the first iteration to evaluate the statistics and final PMF before endorsing the repetitiveness of CLEO-based approaches.

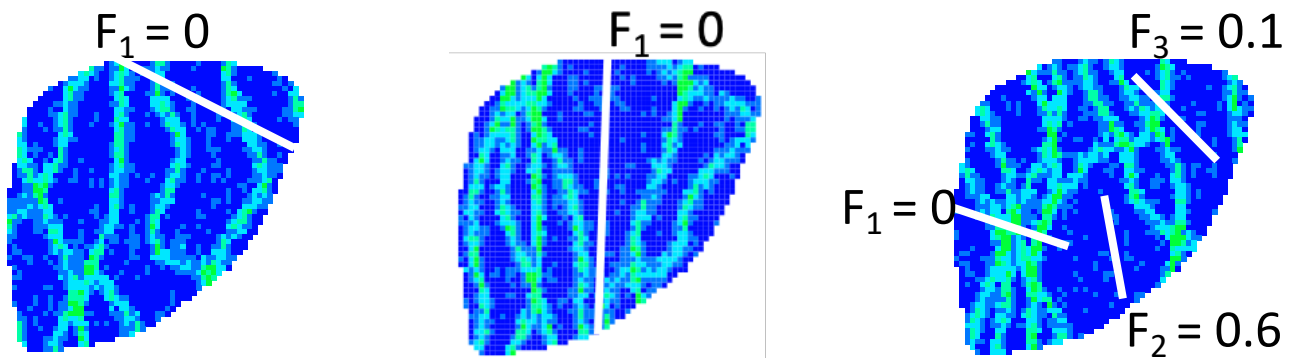


Figure C-24 - Three different scenarios exhibiting faults and their respective transmissibility values. For the same well locations, varying uncertainties compels for better quality and quantity of data to improve prediction using data-driven techniques.

To summarize, CLEO-M1 is a classic optimization method. We only used physics-based simulation models to optimize an FDP with CLEO-M1. With increasing computing power and the volume of data, data-driven optimization methods have gained prevalence these days (Nwachukwu et al., 2018 and Kim et al., 2020). As the name suggests, such methods depend on the quality and quantity of data. The quantity of data is significant since changes as small as one discrete block can significantly impact the outcome. For example, the presence of karsts can drastically impact the flow through subsurface. On the other hand, data quality varies with each iteration, as observed in **Figures C-5** and **C-12**. It also depends on the number of RMs used to build the feature matrix of the ML-based method. For instance, let us assume that three different scenarios exist, as shown in **Figure C-24**. To get a robust result, one would recommend using all scenarios in such a case. Such quintessential situations from real field applications, in turn, increase the number of physics-based simulations. Assuming a time-

consuming model which takes half a day for simulation, it would be ill-advised to run 500×3 simulations to obtain sufficient data for optimizing FDP using data-driven techniques. For the same number of simulations, however, CLEO-M2 can provide an excellent result. It enjoys a perfect balance by partially simulating the full-physics-based model and integrating it with a data-driven technique to predict the nonlinear response of the field.

CLEO-based approaches have an equally broad scope of improvement with REIs and ML algorithms, respectively. One such recommendation would be to use already finished simulations to update ML models to curb the bad scenarios and boost convergence. Lastly, from the perspective of field applications, new methods should always encourage ML to work with time-consuming simulation models that can capture uncertainties at a finer scale.

C.7 Conclusions

Due to a vast problem space and decision variables, it can be challenging to perform an exhaustive search for an optimized field development plan (FDP). In light of this problem, we introduced a new optimization algorithm, CLEO (Cluster-based learning and evolution optimizer). CLEO divides the problem space into large clusters to deal with its size. With each iteration, CLEO keeps learning and updating the probability mass function (PMF). At the same time, all the clusters are gradually expanded to fine-tune solutions. A good sampling technique is another vital component of this algorithm to select a good sample. To sum it up, such a cluster-based manipulation helps to search the problem space deftly.

CLEO offers several advantages. It is user-friendly, easy to code and implement, straightforward, good at handling numerous decision variables and problem space, adaptable and, unique in terms of cluster-based approach for optimization. As it is quite flexible, we introduced two approaches using the conceptual framework of CLEO. Subsequently, we used both these approaches to optimize FDP under different settings.

In Method 1, we presented a simple approach for using CLEO with the Latin hypercube sampling (LHS) technique for sampling. We tested this method in simple synthetic models (Case I and II). Method 1 outperformed well-established algorithms (DE, PSO, DECE, and IDLHC) for huge optimization problems, as seen in Case I. Although we selected LHS for a fair comparison against DECE and IDLHC, a better sampling technique can improve its performance further. We strongly recommend that one should choose the best sampling method depending on the size of decision variables.

Model error is an inherent component of any simulation model. Thus, finding a global optimum with such models does not necessarily mean globally optimal results in the actual

field. For this reason, one should strive to improve models rather than spending an enormous time on the optimization process. Hence, CLEO-M2 was introduced to improve efficiency without hampering the objective functions. We used reservoir engineering insights (REIs) as heuristics to aid the optimization process in addition to simple predictive analytics. We presented this method to optimize an FDP using as low as 40% of the complete life of the field (Case II and Case III). We used predictive analytics in Method 2 to promote the notion that one can even work with intermediate results to identify an FDP on a par with any good algorithm (that uses the field's contractual life).

Although we tested Method 2 on a simple model to validate its performance, a giant field-scale model (Case III) presents the true worth of using Method 2. It made the FDP process 75% more efficient while improving the objective function by 9%. In terms of real-time, 120 days were saved using this novel approach in Case III. At the same time, one needs to include more practical aspects to make Method 2 more reliable and efficient for field applications.

Both the proposed methods have an excellent aptitude for handling huge problem space as well as decision variables. Nevertheless, results obtained using Method 2 will always be less than or equal to those obtained using Method 1. Improving the regression model of Method 2 can boost its predictive capability to provide better results.

Finally, an optimization algorithm only uses mathematics. However, combining it with REIs can reduce the problem space while improving the efficiency of the whole process. For example, one would never drill a well in a low permeability zone. Reducing such zones can indirectly decrease the number of simulations. However, it is crucial to ensure that correct REIs are considered to avoid convergence to suboptimal solutions.

Acknowledgments

This work was conducted with the support of Libra Consortium (Petrobras, Shell Brasil, Total Energies, CNOOC, CNPC) and PPSA within the ANP R&D levy as "commitment to research and development investments" and Energi Simulation. The authors are grateful for the support of the Center for Energy and Petroleum Studies (CEPETRO-UNICAMP/Brazil), the Department of Energy (DE-FEM-UNICAMP/Brazil), and the Research Group in Reservoir Simulation and Management (UNISIM-UNICAMP/Brazil). Also, a special thanks to CMG and Schlumberger for the software licenses.

Nomenclature

List of Abbreviations

3D	Three-dimensional space
AC	Abandonment cost
b	Best scenarios
BHP	Bottom-hole pressure
$CAPEX$	Capital expenditures
CLEO	Cluster-based learning and evolution optimizer
d	Discount rate
DE	Differential evolution
DECE	Designed exploration controlled evolution
EMV	Expected monetary value
FDP	Field development plan
g	Eligible candidates
GOR	Gas-oil ratio
\mathbb{G}	Search space
ICV	Inflow control valve
$iter$	Iteration
J	Objective function
k	k^{th} time-step
LHS	Latin hypercube sampling
M1 / M2	Method 1 / Method 2
MLR	Multiple linear regression
MOF	Multi-objective function
N_{inj}	Number of injectors
N_p	Cumulative oil production
N_{pr}	Number of producers
N_{wi}	Cumulative water injection
N_{wp}	Cumulative water production
NPV	Net present value
$OPEX$	Operational expenditure
$P(j)$	Probability of j

PMF	Probability mass function
PSO	Particle swarm optimization
r_i	Construction cost of the i^{th} well
$r_{o,pr}$	Net oil cost per unit production
$r_{w,inj}$	Net water cost per unit injection
$r_{w,pr}$	Net water cost per unit production
R	Gross revenue
\mathbb{R}	Real numbers
REI	Reservoir engineering insight
RM	Representative model
RT	Royalty tax
ST	Social tax
t	Time
T	Corporate tax rate
THP	Tubing head pressure
TR	Vector of technical results
u	Vector of decision/control variables
x	Solution candidates
x	Vector of possible solutions
\mathbb{X}	Problem space
y	Objective function
y	Output vector (e.g., production and injection rates of wells)
β	Slope coefficients matrix
τ	Reference time
Superscript	
T	Transpose
Subscript	
BT	Breakthrough
k	Time-step
MOF	Multi-objective function
PL	Partial life

Appendix D : License Agreements

Following license agreements grant permission to publish the published manuscripts in this thesis.

D.1 Bottom-up analysis to unravel potential problems and emphasize the impact of individual steps in closed-loop field development



This is a License Agreement between Ashish Kumar Loomba ("User") and Copyright Clearance Center, Inc. ("CCC") on behalf of the Rightsholder identified in the order details below. The license consists of the order details, the Marketplace Order General Terms and Conditions below, and any Rightsholder Terms and Conditions which are included below.

All payments must be made in full to CCC in accordance with the Marketplace Order General Terms and Conditions below.

Order Date	03-Jan-2023	Type of Use	Republish in a thesis/dissertation
Order License ID	1306611-1	Publisher	Offshore Technology Conference
ISBN-13	978-1-61399-707-9	Portion	Chapter/article

LICENSED CONTENT

Publication Title	Offshore Technology Conference (200TC)	Country	United States of America
Author/Editor	Offshore Technology Conference	Rightsholder	Society of Petroleum Engineers (SPE)
Date	01/01/2021	Publication Type	e-Book
Language	English		

REQUEST DETAILS

Portion Type	Chapter/article	Rights Requested	Main product
Page Range(s)	1-19	Distribution	Worldwide
Total Number of Pages	19	Translation	Original language of publication
Format (select all that apply)	Print, Electronic	Copies for the Disabled?	No
Who Will Republish the Content?	Author of requested content	Minor Editing Privileges?	Yes
Duration of Use	Life of current and all future editions	Incidental Promotional Use?	No
Lifetime Unit Quantity	More than 2,000,000	Currency	USD

NEW WORK DETAILS

Title	Risk-informed Closed-loop field development workflow for practical applications	Institution Name	UNICAMP
Instructor Name	Prof. Dr. Denis Schiozer	Expected Presentation Date	2022-12-21

ADDITIONAL DETAILS

Order Reference Number	N/A	The Requesting Person/Organization to Appear on the License	Ashish Kumar Loomba
------------------------	-----	---	---------------------

REUSE CONTENT DETAILS

Title, Description or Numeric Reference of the Portion(s)	Chapter 2	Title of the Article/Chapter the Portion Is From	N/A
Editor of Portion(s)	Ashish Kumar Loomba	Author of Portion(s)	Offshore Technology Conference
Volume of Serial or Monograph	N/A	Issue, if Republishing an Article From a Serial	N/A
Page or Page Range of Portion	N/A	Publication Date of Portion	2021-01-01

SPECIAL RIGHTSHOLDER TERMS AND CONDITIONS

OTC-30776-MS

Marketplace Order General Terms and Conditions

The following terms and conditions ("General Terms"), together with any applicable Publisher Terms and Conditions, govern User's use of Works pursuant to the Licenses granted by Copyright Clearance Center, Inc. ("CCC") on behalf of the applicable Rightsholders of such Works through CCC's applicable Marketplace transactional licensing services (each, a "Service").

1) Definitions. For purposes of these General Terms, the following definitions apply:

"License" is the licensed use the User obtains via the Marketplace platform in a particular licensing transaction, as set forth in the Order Confirmation.

"Order Confirmation" is the confirmation CCC provides to the User at the conclusion of each Marketplace transaction. "Order Confirmation Terms" are additional terms set forth on specific Order Confirmations not set forth in the General Terms that can include terms applicable to a particular CCC transactional licensing service and/or any Rightsholder-specific terms.

"Rightsholder(s)" are the holders of copyright rights in the Works for which a User obtains licenses via the Marketplace platform, which are displayed on specific Order Confirmations.

"Terms" means the terms and conditions set forth in these General Terms and any additional Order Confirmation Terms collectively.

"User" or "you" is the person or entity making the use granted under the relevant License. Where the person accepting the Terms on behalf of a User is a freelancer or other third party who the User authorized to accept the General Terms on the User's behalf, such person shall be deemed jointly a User for purposes of such Terms.

"Work(s)" are the copyright protected works described in relevant Order Confirmations.

2) Description of Service. CCC's Marketplace enables Users to obtain Licenses to use one or more Works in accordance with all relevant Terms. CCC grants Licenses as an agent on behalf of the copyright rightsholder identified in the relevant Order Confirmation.

3) Applicability of Terms. The Terms govern User's use of Works in connection with the relevant License. In the event of any conflict between General Terms and Order Confirmation Terms, the latter shall govern. User acknowledges that Rightsholders have complete discretion whether to grant any permission, and whether to place any limitations on any grant, and that CCC has no right to supersede or to modify any such discretionary act by a Rightsholder.

4) Representations; Acceptance. By using the Service, User represents and warrants that User has been duly authorized by the User to accept, and hereby does accept, all Terms.

5) Scope of License; Limitations and Obligations. All Works and all rights therein, including copyright rights, remain the sole and exclusive property of the Rightsholder. The License provides only those rights expressly set forth in the terms and conveys no other rights in any Works

6) General Payment Terms. User may pay at time of checkout by credit card or choose to be invoiced. If the User chooses to be invoiced, the User shall: (i) remit payments in the manner identified on specific invoices, (ii) unless otherwise specifically stated in an Order Confirmation or separate written agreement, Users shall remit payments upon receipt of the relevant invoice from CCC, either by delivery or notification of availability of the invoice via the Marketplace platform, and (iii) if the User does not pay the invoice within 30 days of receipt, the User may incur a service charge of 1.5% per month or the maximum rate allowed by applicable law, whichever is less. While User may exercise the rights in the License immediately

upon receiving the Order Confirmation, the License is automatically revoked and is null and void, as if it had never been issued, if CCC does not receive complete payment on a timely basis.

7) General Limits on Use. Unless otherwise provided in the Order Confirmation, any grant of rights to User (i) involves only the rights set forth in the Terms and does not include subsequent or additional uses, (ii) is non-exclusive and non-transferable, and (iii) is subject to any and all limitations and restrictions (such as, but not limited to, limitations on duration of use or circulation) included in the Terms. Upon completion of the licensed use as set forth in the Order Confirmation, User shall either secure a new permission for further use of the Work(s) or immediately cease any new use of the Work(s) and shall render inaccessible (such as by deleting or by removing or severing links or other locators) any further copies of the Work. User may only make alterations to the Work if and as expressly set forth in the Order Confirmation. No Work may be used in any way that is defamatory, violates the rights of third parties (including such third parties' rights of copyright, privacy, publicity, or other tangible or intangible property), or is otherwise illegal, sexually explicit, or obscene. In addition, User may not conjoin a Work with any other material that may result in damage to the reputation of the Rightsholder. User agrees to inform CCC if it becomes aware of any infringement of any rights in a Work and to cooperate with any reasonable request of CCC or the Rightsholder in connection therewith.

8) Third Party Materials. In the event that the material for which a License is sought includes third party materials (such as photographs, illustrations, graphs, inserts and similar materials) that are identified in such material as having been used by permission (or a similar indicator), User is responsible for identifying, and seeking separate licenses (under this Service, if available, or otherwise) for any of such third party materials; without a separate license, User may not use such third party materials via the License.

9) Copyright Notice. Use of proper copyright notice for a Work is required as a condition of any License granted under the Service. Unless otherwise provided in the Order Confirmation, a proper copyright notice will read substantially as follows: "Used with permission of [Rightsholder's name], from [Work's title, author, volume, edition number and year of copyright]; permission conveyed through Copyright Clearance Center, Inc." Such notice must be provided in a reasonably legible font size and must be placed either on a cover page or in another location that any person, upon gaining access to the material which is the subject of a permission, shall see, or in the case of republication Licenses, immediately adjacent to the Work as used (for example, as part of a by-line or footnote) or in the place where substantially all other credits or notices for the new work containing the republished Work are located. Failure to include the required notice results in loss to the Rightsholder and CCC, and the User shall be liable to pay liquidated damages for each such failure equal to twice the use fee specified in the Order Confirmation, in addition to the use fee itself and any other fees and charges specified.

10) Indemnity. User hereby indemnifies and agrees to defend the Rightsholder and CCC, and their respective employees and directors, against all claims, liability, damages, costs, and expenses, including legal fees and expenses, arising out of any use of a Work beyond the scope of the rights granted herein and in the Order Confirmation, or any use of a Work which has been altered in any unauthorized way by User, including claims of defamation or infringement of rights of copyright, publicity, privacy, or other tangible or intangible property.

11) Limitation of Liability. UNDER NO CIRCUMSTANCES WILL CCC OR THE RIGHTSHOLDER BE LIABLE FOR ANY DIRECT, INDIRECT, CONSEQUENTIAL, OR INCIDENTAL DAMAGES (INCLUDING WITHOUT LIMITATION DAMAGES FOR LOSS OF BUSINESS PROFITS OR INFORMATION, OR FOR BUSINESS INTERRUPTION) ARISING OUT OF THE USE OR INABILITY TO USE A WORK, EVEN IF ONE OR BOTH OF THEM HAS BEEN ADVISED OF THE POSSIBILITY OF SUCH DAMAGES. In any event, the total liability of the Rightsholder and CCC (including their respective employees and directors) shall not exceed the total amount actually paid by User for the relevant License. User assumes full liability for the actions and omissions of its principals, employees, agents, affiliates, successors, and assigns.

12) Limited Warranties. THE WORK(S) AND RIGHT(S) ARE PROVIDED "AS IS." CCC HAS THE RIGHT TO GRANT TO USER THE RIGHTS GRANTED IN THE ORDER CONFIRMATION DOCUMENT. CCC AND THE RIGHTSHOLDER DISCLAIM ALL OTHER WARRANTIES RELATING TO THE WORK(S) AND RIGHT(S), EITHER EXPRESS OR IMPLIED, INCLUDING WITHOUT LIMITATION IMPLIED WARRANTIES OF MERCHANTABILITY OR FITNESS FOR A PARTICULAR PURPOSE. ADDITIONAL RIGHTS MAY BE REQUIRED TO USE ILLUSTRATIONS, GRAPHS, PHOTOGRAPHS, ABSTRACTS, INSERTS, OR OTHER PORTIONS OF THE WORK (AS OPPOSED TO THE ENTIRE WORK) IN A MANNER CONTEMPLATED BY USER; USER UNDERSTANDS AND AGREES THAT NEITHER CCC NOR THE RIGHTSHOLDER MAY HAVE SUCH ADDITIONAL RIGHTS TO GRANT.

13) Effect of Breach. Any failure by User to pay any amount when due, or any use by User of a Work beyond the scope of the License set forth in the Order Confirmation and/or the Terms, shall be a material breach of such License. Any breach not cured within 10 days of written notice thereof shall result in immediate termination of such License without further notice. Any unauthorized (but licensable) use of a Work that is terminated immediately upon notice thereof may be liquidated by payment of the Rightsholder's ordinary license price therefor; any unauthorized (and unlicensable) use that is not terminated immediately for any reason (including, for example, because materials containing the Work cannot reasonably be recalled) will be subject to all remedies available at law or in equity, but in no event to a payment of less than three times the Rightsholder's ordinary license price for the most closely analogous licensable use plus Rightsholder's and/or CCC's costs and expenses incurred in collecting such payment.

14) **Additional Terms for Specific Products and Services.** If a User is making one of the uses described in this Section 14, the additional terms and conditions apply:

a) ***Print Uses of Academic Course Content and Materials (photocopies for academic coursepacks or classroom handouts).*** For photocopies for academic coursepacks or classroom handouts the following additional terms apply:

i) The copies and anthologies created under this License may be made and assembled by faculty members individually or at their request by on-campus bookstores or copy centers, or by off-campus copy shops and other similar entities.

ii) No License granted shall in any way: (i) include any right by User to create a substantively non-identical copy of the Work or to edit or in any other way modify the Work (except by means of deleting material immediately preceding or following the entire portion of the Work copied) (ii) permit "publishing ventures" where any particular anthology would be systematically marketed at multiple institutions.

iii) Subject to any Publisher Terms (and notwithstanding any apparent contradiction in the Order Confirmation arising from data provided by User), any use authorized under the academic pay-per-use service is limited as follows:

A) any License granted shall apply to only one class (bearing a unique identifier as assigned by the institution, and thereby including all sections or other subparts of the class) at one institution;

B) use is limited to not more than 25% of the text of a book or of the items in a published collection of essays, poems or articles;

C) use is limited to no more than the greater of (a) 25% of the text of an issue of a journal or other periodical or (b) two articles from such an issue;

D) no User may sell or distribute any particular anthology, whether photocopied or electronic, at more than one institution of learning;

E) in the case of a photocopy permission, no materials may be entered into electronic memory by User except in order to produce an identical copy of a Work before or during the academic term (or analogous period) as to which any particular permission is granted. In the event that User shall choose to retain materials that are the subject of a photocopy permission in electronic memory for purposes of producing identical copies more than one day after such retention (but still within the scope of any permission granted), User must notify CCC of such fact in the applicable permission request and such retention shall constitute one copy actually sold for purposes of calculating permission fees due; and

F) any permission granted shall expire at the end of the class. No permission granted shall in any way include any right by User to create a substantively non-identical copy of the Work or to edit or in any other way modify the Work (except by means of deleting material immediately preceding or following the entire portion of the Work copied).

iv) **Books and Records; Right to Audit.** As to each permission granted under the academic pay-per-use Service, User shall maintain for at least four full calendar years books and records sufficient for CCC to determine the numbers of copies made by User under such permission. CCC and any representatives it may designate shall have the right to audit such books and records at any time during User's ordinary business hours, upon two days' prior notice. If any such audit shall determine that User shall have underpaid for, or underreported, any photocopies sold or by three percent (3%) or more, then User shall bear all the costs of any such audit; otherwise, CCC shall bear the costs of any such audit. Any amount determined by such audit to have been underpaid by User shall immediately be paid to CCC by User, together with interest thereon at the rate of 10% per annum from the date such amount was originally due. The provisions of this paragraph shall survive the termination of this License for any reason.

b) ***Digital Pay-Per-Uses of Academic Course Content and Materials (e-coursepacks, electronic reserves, learning management systems, academic institution intranets).*** For uses in e-coursepacks, posts in electronic reserves, posts in learning management systems, or posts on academic institution intranets, the following additional terms apply:

i) The pay-per-uses subject to this Section 14(b) include:

A) **Posting e-reserves, course management systems, e-coursepacks for text-based content**, which grants authorizations to import requested material in electronic format, and allows electronic access to this material to members of a designated college or university class, under the direction of an instructor designated by the college or university, accessible only under appropriate electronic controls (e.g., password);

B) **Posting e-reserves, course management systems, e-coursepacks for material consisting of photographs or other still images not embedded in text**, which grants not only the authorizations described in Section 14(b)(i)(A) above, but also the following authorization: to include the requested material in course materials for use

consistent with Section 14(b)(i)(A) above, including any necessary resizing, reformatting or modification of the resolution of such requested material (provided that such modification does not alter the underlying editorial content or meaning of the requested material, and provided that the resulting modified content is used solely within the scope of, and in a manner consistent with, the particular authorization described in the Order Confirmation and the Terms), but not including any other form of manipulation, alteration or editing of the requested material;

C) Posting e-reserves, course management systems, e-coursepacks or other academic distribution for audiovisual content, which grants not only the authorizations described in Section 14(b)(i)(A) above, but also the following authorizations: (i) to include the requested material in course materials for use consistent with Section 14(b)(i)(A) above; (ii) to display and perform the requested material to such members of such class in the physical classroom or remotely by means of streaming media or other video formats; and (iii) to "clip" or reformat the requested material for purposes of time or content management or ease of delivery, provided that such "clipping" or reformatting does not alter the underlying editorial content or meaning of the requested material and that the resulting material is used solely within the scope of, and in a manner consistent with, the particular authorization described in the Order Confirmation and the Terms. Unless expressly set forth in the relevant Order Confirmation, the License does not authorize any other form of manipulation, alteration or editing of the requested material.

ii) Unless expressly set forth in the relevant Order Confirmation, no License granted shall in any way: (i) include any right by User to create a substantively non-identical copy of the Work or to edit or in any other way modify the Work (except by means of deleting material immediately preceding or following the entire portion of the Work copied or, in the case of Works subject to Sections 14(b)(1)(B) or (C) above, as described in such Sections) (ii) permit "publishing ventures" where any particular course materials would be systematically marketed at multiple institutions.

iii) Subject to any further limitations determined in the Rightsholder Terms (and notwithstanding any apparent contradiction in the Order Confirmation arising from data provided by User), any use authorized under the electronic course content pay-per-use service is limited as follows:

A) any License granted shall apply to only one class (bearing a unique identifier as assigned by the institution, and thereby including all sections or other subparts of the class) at one institution;

B) use is limited to not more than 25% of the text of a book or of the items in a published collection of essays, poems or articles;

C) use is limited to not more than the greater of (a) 25% of the text of an issue of a journal or other periodical or (b) two articles from such an issue;

D) no User may sell or distribute any particular materials, whether photocopied or electronic, at more than one institution of learning;

E) electronic access to material which is the subject of an electronic-use permission must be limited by means of electronic password, student identification or other control permitting access solely to students and instructors in the class;

F) User must ensure (through use of an electronic cover page or other appropriate means) that any person, upon gaining electronic access to the material, which is the subject of a permission, shall see:

- a proper copyright notice, identifying the Rightsholder in whose name CCC has granted permission,
- a statement to the effect that such copy was made pursuant to permission,
- a statement identifying the class to which the material applies and notifying the reader that the material has been made available electronically solely for use in the class, and
- a statement to the effect that the material may not be further distributed to any person outside the class, whether by copying or by transmission and whether electronically or in paper form, and User must also ensure that such cover page or other means will print out in the event that the person accessing the material chooses to print out the material or any part thereof.

G) any permission granted shall expire at the end of the class and, absent some other form of authorization, User is thereupon required to delete the applicable material from any electronic storage or to block electronic access to the applicable material.

iv) Uses of separate portions of a Work, even if they are to be included in the same course material or the same university or college class, require separate permissions under the electronic course content pay-per-use Service. Unless otherwise provided in the Order Confirmation, any grant of rights to User is limited to use completed no later than the end of the academic term (or analogous period) as to which any particular permission is granted.

v) Books and Records; Right to Audit. As to each permission granted under the electronic course content Service, User shall maintain for at least four full calendar years books and records sufficient for CCC to determine the numbers of copies made by User under such permission. CCC and any representatives it may designate shall have the right to audit such books and records at any time during User's ordinary business hours, upon two days' prior notice. If any such audit shall determine that User shall have underpaid for, or underreported, any electronic copies used by three percent (3%) or more, then User shall bear all the costs of any such audit; otherwise, CCC shall bear the costs of any such audit. Any amount determined by such audit to have been underpaid by User shall immediately be paid to CCC by User, together with interest thereon at the rate of 10% per annum from the date such amount was originally due. The provisions of this paragraph shall survive the termination of this license for any reason.

c) *Pay-Per-Use Permissions for Certain Reproductions (Academic photocopies for library reserves and interlibrary loan reporting) (Non-academic internal/external business uses and commercial document delivery).* The License expressly excludes the uses listed in Section (c)(i)-(v) below (which must be subject to separate license from the applicable Rightsholder) for: academic photocopies for library reserves and interlibrary loan reporting; and non-academic internal/external business uses and commercial document delivery.

- i) electronic storage of any reproduction (whether in plain-text, PDF, or any other format) other than on a transitory basis;
- ii) the input of Works or reproductions thereof into any computerized database;
- iii) reproduction of an entire Work (cover-to-cover copying) except where the Work is a single article;
- iv) reproduction for resale to anyone other than a specific customer of User;
- v) republication in any different form. Please obtain authorizations for these uses through other CCC services or directly from the rightsholder.

Any license granted is further limited as set forth in any restrictions included in the Order Confirmation and/or in these Terms.

d) *Electronic Reproductions in Online Environments (Non-Academic-email, intranet, internet and extranet).* For "electronic reproductions", which generally includes e-mail use (including instant messaging or other electronic transmission to a defined group of recipients) or posting on an intranet, extranet or Intranet site (including any display or performance incidental thereto), the following additional terms apply:

- i) Unless otherwise set forth in the Order Confirmation, the License is limited to use completed within 30 days for any use on the Internet, 60 days for any use on an intranet or extranet and one year for any other use, all as measured from the "republication date" as identified in the Order Confirmation, if any, and otherwise from the date of the Order Confirmation.
- ii) User may not make or permit any alterations to the Work, unless expressly set forth in the Order Confirmation (after request by User and approval by Rightsholder); provided, however, that a Work consisting of photographs or other still images not embedded in text may, if necessary, be resized, reformatted or have its resolution modified without additional express permission, and a Work consisting of audiovisual content may, if necessary, be "clipped" or reformatted for purposes of time or content management or ease of delivery (provided that any such resizing, reformatting, resolution modification or "clipping" does not alter the underlying editorial content or meaning of the Work used, and that the resulting material is used solely within the scope of, and in a manner consistent with, the particular License described in the Order Confirmation and the Terms.

15) Miscellaneous.

a) User acknowledges that CCC may, from time to time, make changes or additions to the Service or to the Terms, and that Rightsholder may make changes or additions to the Rightsholder Terms. Such updated Terms will replace the prior terms and conditions in the order workflow and shall be effective as to any subsequent Licenses but shall not apply to Licenses already granted and paid for under a prior set of terms.


b) Use of User-related information collected through the Service is governed by CCC's privacy policy, available online at www.copyright.com/about/privacy-policy/.






c) The License is personal to User. Therefore, User may not assign or transfer to any other person (whether a natural person or an organization of any kind) the License or any rights granted thereunder; provided, however, that, where applicable, User may assign such License in its entirety on written notice to CCC in the event of a transfer of all or substantially all of User's rights in any new material which includes the Work(s) licensed under this Service.


d) No amendment or waiver of any Terms is binding unless set forth in writing and signed by the appropriate parties, including, where applicable, the Rightsholder. The Rightsholder and CCC hereby object to any terms contained in any writing prepared by or on behalf of the User or its principals, employees, agents or affiliates and purporting to govern or otherwise relate to the License described in the Order Confirmation, which terms are in any way inconsistent with any Terms set forth in the Order Confirmation, and/or in CCC's standard operating procedures, whether such writing is prepared prior to, simultaneously with or subsequent to the Order Confirmation, and whether such writing appears on a copy of the Order Confirmation or in a separate instrument.

e) The License described in the Order Confirmation shall be governed by and construed under the law of the State of New York, USA, without regard to the principles thereof of conflicts of law. Any case, controversy, suit, action, or proceeding arising out of, in connection with, or related to such License shall be brought, at CCC's sole discretion, in any federal or state court located in the County of New York, State of New York, USA, or in any federal or state court whose geographical jurisdiction covers the location of the Rightsholder set forth in the Order Confirmation. The parties expressly submit to the personal jurisdiction and venue of each such federal or state court.

D.2 Application of risk-informed closed-loop field development workflow to elucidate the evolution of uncertainties



 Home
  Help ▾
  Live Chat
  Sign in
  Create Account



Application of risk-informed closed-loop field development workflow to elucidate the evolution of uncertainties

Author: Ashish Kumar Loomba, Vinicius Eduardo Botechia, Denis José Schiozer

Publication: Journal of Petroleum Science and Engineering

Publisher: Elsevier

Date: February 2021

© 2020 Elsevier B.V. All rights reserved.


Journal Author Rights




Please note that, as the author of this Elsevier article, you retain the right to include it in a thesis or dissertation, provided it is not published commercially. Permission is not required, but please ensure that you reference the journal as the original source. For more information on this and on your other retained rights, please visit: <https://www.elsevier.com/about/our-business/policies/copyright#Author-rights>

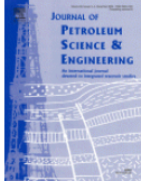
BACK
CLOSE WINDOW

© 2022 Copyright - All Rights Reserved | [Copyright Clearance Center, Inc.](#) | [Privacy statement](#) | [Data Security and Privacy](#)
 | [For California Residents](#) | [Terms and Conditions](#) Comments? We would like to hear from you. E-mail us at customer-care@copyright.com

D.3A comparative study to accelerate field development plan optimization



 Home
  Help ▾
  Live Chat
  Sign in
  Create Account



A comparative study to accelerate field development plan optimization

Author: Ashish Kumar Loomba,Vinicius Eduardo Botechia,Denis José Schiozer
Publication: Journal of Petroleum Science and Engineering
Publisher: Elsevier
Date: January 2022

© 2021 Elsevier B.V. All rights reserved.

Journal Author Rights

Please note that, as the author of this Elsevier article, you retain the right to include it in a thesis or dissertation, provided it is not published commercially. Permission is not required, but please ensure that you reference the journal as the original source. For more information on this and on your other retained rights, please visit: <https://www.elsevier.com/about/our-business/policies/copyright#Author-rights>

BACK
CLOSE WINDOW